Tesis Doctoral

Analysis of gene network branching during optic cup development in zebrafish

Memoria presentada por Lorena Buono para optar al título de Doctora y

dirigida por el Dr. Juan Ramón Martínez Morales

Sevilla, enero de 2020

Programa de Doctorado en Biotecnología, Ingeniería y Tecnología Química (RD: 99/2011)

Acknowledgment

Despite what the title page of this thesis book says, this is a work that has been possible thanks to the co-supervision of both **Juan Ramon Martinez Morales** and **Paola Bovolenta**. We want to thank **Dr. Paola Bovolenta** (CBM, Madrid) immensely. Without her, this thesis would never have existed. Paola is an amazing scientist and an even more amazing woman who should appear as co-director of this work. Unfortunately this was officially not possible only because of merely bureaucratic issues.

This work was supported by the following grants from the Spanish Ministry of Science, Innovation and Universities (MICINN): BFU2017-86339P, BFU2016-81887-REDT, and MDM-2016-0687; as well as Fundación Ramón Areces-2016.

Marine Biological Laboratory (Woods Hole, MA) supported the education and training of the PhD candidate with a scholarship which covered travel costs and registration for the course “Gene regulatory network for development”.

Index

Abstract

Glowing sunflowers in bloom and boulevards of auburn falling leaves. Chilly dawns above the sleeping city and balmy sunsets from the western shore. The smirk of our first crush and the beauty of our mum when she was young. All these images and many more can be perceived by our brain in an instant and kept in our soul for ever thanks to the most fascinating and complex of the senses: the sight.

In all metazoans, sight depends on the intimate relation and combined function of photoreceptors and pigmented cells. These two cell types rise from a pool of common precursors. Unravelling how the gene regulatory networks (GRNs) of these tissues bifurcate into two mutually exclusive developmental programs is an essential step to better understand the molecular basis of retinal degenerative diseases and the branching dynamics of differentiation programs. Here we use the development of the optic cup in zebrafish as a model to explore this biological question, combining RNA-seq and ATAC-seq experiments of different pools of sorted cells derived from distinct domains of the optic cup at several stages of development. This approach allowed us not only to unveil the key specifiers and effector genes operating directly on the morphological and differentiation properties of the eye cells, but also to identify the active cis-regulatory modules orchestrating the specification of its distinct domains. Our results confirm previously known transcription factors as central nodes of the eye GRNs and uncover novel factors playing an unexpected early role in retinal pigmented epithelium (RPE) specification. Further, we untangle how the regulatory dynamics of different transcriptional specifiers harmonize and/or complement each other to carry out the divergent development of the two eye domains. Finally, we tested our findings in human iPSCs differentiating towards RPE cells. This comparison revealed a conserved *consecutio temporum* of transcription factor recruitment along RPE differentiation program, opening new opportunities for the improvement of therapies for retinal degenerative diseases based on cell replacement. Our work is a further step towards the identification of the molecular links between tissue specifiers and effector molecules involved in eye development, many of which will be causative genes for the most common hereditary malformations of the eye.

Key-words: eye development, RNA-seq, ATAC-seq, GRN, transcription factors, cis-regulatory modules

Resumen

Girasoles brillantes en flor y bulevares tapizados de hojas color caoba. Amaneceres fríos sobre la ciudad durmiente y envolventes puestas de sol desde la costa oeste. La sonrisa de nuestro primer enamoramiento y la belleza de nuestra madre de joven. Todas estas imágenes y muchas más pueden ser percibidas por nuestro cerebro en un instante y guardadas en nuestra alma para siempre gracias al más fascinante y complejo de los sentidos: la vista.

En todos los metazoos, la vista depende de la íntima relación y función combinada de los fotorreceptores y las células pigmentadas. Estos dos tipos de células surgen de un conjunto de precursores comunes. Desentrañar cómo las redes de regulación génica (GRN) de estos tejidos se bifurcan en dos programas de desarrollo mutuamente exclusivos es un paso esencial para comprender mejor las bases moleculares de las enfermedades degenerativas de la retina y la dinámica de ramificación de los programas de diferenciación. Aquí utilizamos el desarrollo de la copa óptica en el pez cebra como modelo para explorar esta cuestión biológica, combinando experimentos de RNA-seq y ATAC-seq en diferentes grupos de células purificadas procedentes de distintos dominios de la copa óptica en varias etapas de desarrollo. Este enfoque nos permitió no sólo desvelar los principales especificadores y genes efectores que operan directamente sobre las propiedades morfológicas y de diferenciación de las células del ojo, sino también identificar los módulos cis-reguladores activos que orquestan la especificación de sus distintos dominios. Nuestros resultados confirman factores de transcripción previamente conocidos como los nodos centrales de las GRNs del ojo y descubren nuevos factores que juegan un inesperado papel temprano en la especificación del epitelio pigmentado de la retina (RPE). Además, desciframos cómo la dinámica reguladora de los diferentes especificadores transcripcionales se armonizan y/o complementan entre sí para llevar a cabo el desarrollo divergente de los dos dominios oculares. Finalmente, pusimos a prueba nuestros hallazgos en iPSCs humanas diferenciadas a células RPE. Esta comparación reveló una *consecutio temporum* conservada en el reclutamiento de factores de transcripción a lo largo del programa de diferenciación hacia RPE, abriendo nuevas oportunidades para la mejora de las terapias para enfermedades degenerativas de la retina basadas en el reemplazo celular. Nuestro trabajo supone un paso más hacia la identificación de los vínculos moleculares entre los especificadores de tejido y las moléculas efectoras implicadas en el desarrollo del ojo, muchas de las cuales también serán las causantes de las malformaciones hereditarias más comunes del ojo.

Palabras clave: desarrollo del ojo, RNA-seq, ATAC-seq, GRN, factores de transcripción, módulos cis-reguladores

Introduction

1. Photoreceptors and pigmented cells: the functional unit to sample visual space

1.a. Evolutionary and functional basis of the RPE-photoreceptors tandem

Since the rise of bilateral animals, 450 million years ago, sight has always depended on the close association between photoreceptors and pigmented cells. Photoreceptors are highly-specialized neurons capable of detecting the light and transforming the luminous input into nerve impulse, whereas pigmented cells function as a shading shield protecting photoreceptors. Although all the metazoan structures dedicated to vision exhibit diverse shapes and optical features, all the animal eyes can be traced back to the photoreceptor-pigmented cell basic configuration, defined as the basic functional unit of the ancestral prototypic eye and already present in the cnidarian-bilaterian common ancestor (Letelier, Bovolenta, & Martínez-Morales, 2017)(Fig 1). In the dorsal ocelli of the chordate amphioxus, as well as in the larval eyes of annelids and flat worms, this minimal arrangement allows the detection of the light and represents the most rudimentary example of vision (Arendt, Tessmar, Medeiros de Campos-Baptista, Dorresteijn, & Wittbrodt, 2002; Lacalli, 2004; Rhode, 1992).

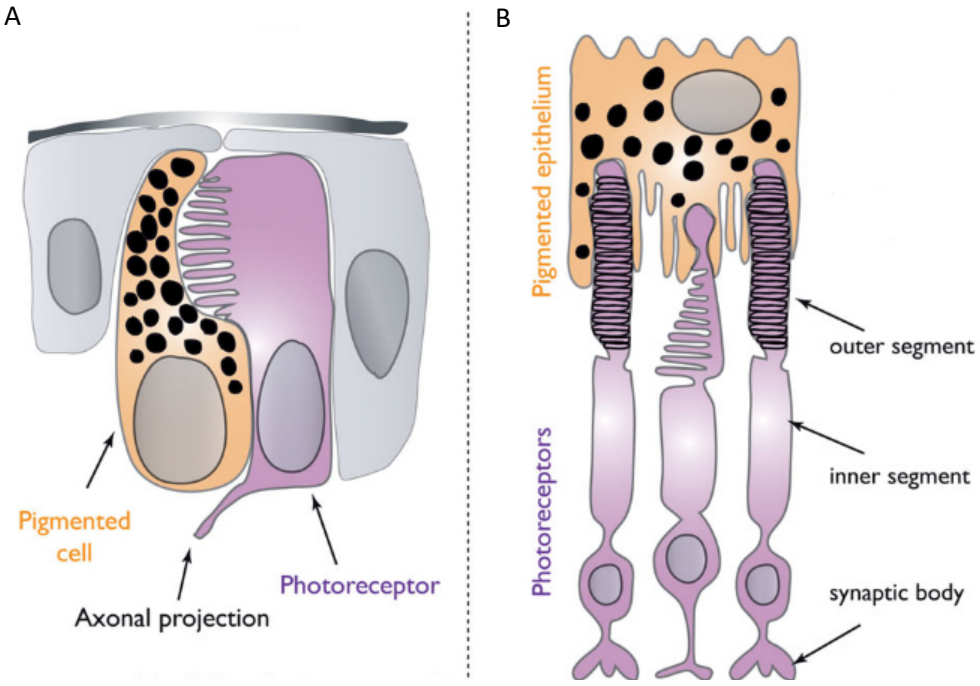

Figure 1. Schematic representation of the evolutionary conserved interaction between pigmented cells and photoreceptors. *The morphology and configuration of pigment cells (orange) and photoreceptors (purple).(A) The larval eye of the annelid Platynereis dumerilii, representing the ancestral configuration of the prototypic eye. (B) The vertebrate retina.* ***From Letelier et al., 2017.***

The photoreceptors are cells particularly susceptible to insults, such as DNA damage, heat-shock response and oxidative stress (Dimitra Athanasiou, Monica Aguilà, Dalila Bevilacqua, Sergey S. Novoselov, David A. Parfitt, 2017). This particular vulnerability is due to their high metabolic rate and their constant exposure to light. It is indeed likely that the crucial protective function for the physiology of photoreceptors played by the pigmented tissue have kept the photoreceptor-pigmented cell association across the whole metazoan evolutionary story. With further additional roles besides its primary one as ocular barrier for scattered light, the retinal pigmented epithelium (RPE) is the vertebrate structure equivalent to the pigmented cell of the prototypic eye (Letelier et al., 2017). The RPE is formed by a monolayer of epithelial cells characterized by the production and accumulation of pigment, such as melanin. It is located between the neural retina (NR) and the choroid, a highly vascularized tissue which serves as connection between the sclera, the eye most external layer, and the photoreceptors in the NR. Apart from photoreceptors, the NR includes also five other cell types: retinal ganglion cells (RGCs), amacrine cells, horizontal cells, bipolar cells and Müller cells (C. Cepko, 2014)(Fig 2).

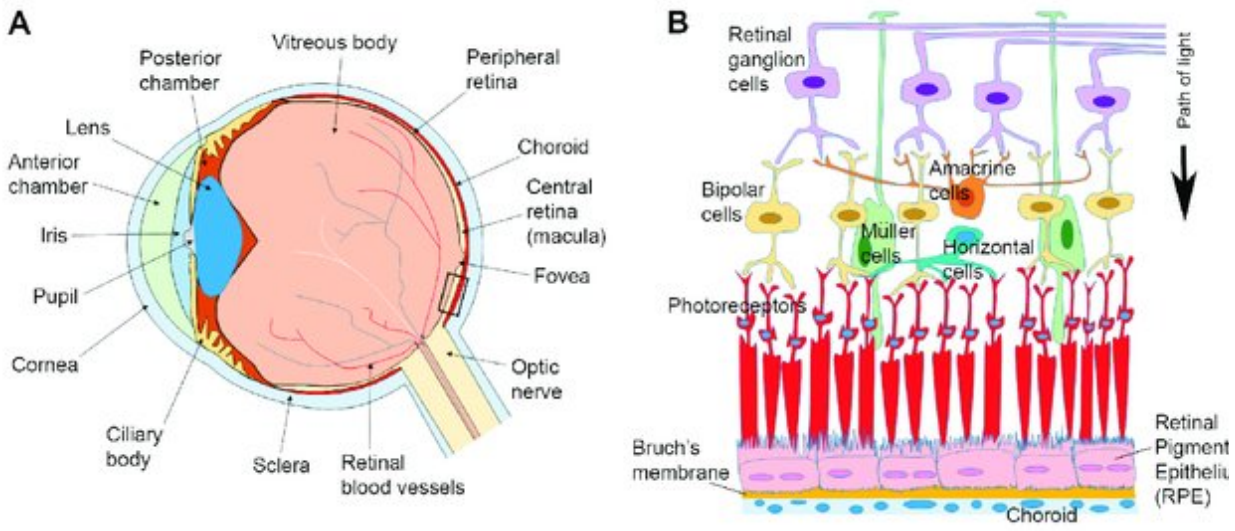

Figure 2. Anatomy of the human eye and arrangement of cells in the retina and associated tissues. *(A) Schematic diagram of the eye in cross-section. (B) Enlargement of the area indicated in box (A) showing relative position of the RPE in relation to other retina cell-types and the choroid. A black arrow indicates the pathway of light.* ***From Keeling et al., 2018.***

Studies in zebrafish revealed that in a significant number of mutants with impaired vision, the affected tissue is the RPE rather than the NR (Neuhauss et al., 1999). The pigmented tissue has been shown

to have a fundamental role not only during the formation of the embryonic optic cup at very early stages, but also later on (Heermann, Schütz, Lemke, Krieglstein, & Wittbrodt, 2015). Once the eye is formed, the RPE constitutes a physical barrier between the NR and the blood vasculature in the choroid, so that the transport of nutrient molecules relies on this tissue. Apart from carrying nutrients, the RPE also secretes several pro-survival growth factors (Letelier et al., 2017). Generally, the loss of trophic sustenance is a frequent event in neurodegeneration and altered levels of growth factors have been found in age-related macular degeneration (AMD), retinitis pigmentosa (RP) and Leber congenital amaurosis (LCA) patients (Kolomeyer & Zarbin, 2014). Numerous studies using animal models for retinal degeneration (RD) demonstrated that the exogenous administration of trophic factors prevents the death of photoreceptors and maintains proper retinal homeostasis (Isiegas, Carolina ; Marinich-Madzarevich, Jorge A.; Marchena, Miguel; Ruiz, José M.; Cano, María J.; Villa, Pedro de la; Hernández-Sánchez, Catalina ; De la Rosa, Enrique J. ; Pablo, 2016; Kimura, Namekata, Guo, Harada, & Harada, 2016; Kolomeyer & Zarbin, 2014; Polato & Becerra, 2015). In addition, the RPE plays a direct role in the phagocytosis of the light-sensitive outer segments of photoreceptors, preventing the accumulation of damaged outer segment membrane which would lead to the degeneration of photoreceptors (Young & Bok, 1969). Finally, the RPE has a crucial function in visual pigment recycling. In brief, in the photoreceptors, the chromophore 11-*cis* retinal is covalently bound to an opsin signalling protein to form a visual pigment molecule. The photoexcitation causes the isomerization of the chromophore 11-*cis*-retinal to all-*trans*-retinal and its release from opsin. Although the production of all-*trans*-retinal is fundamental for activating the photoreceptors and initiating the vision process, neither the opsin nor the all-*trans*-retinal are sensitive to light, so new 11-*cis*-retinal must continuously be provided for photoreceptors to survive and function properly. The conversion of all-*trans*-retinal into 11-*cis*-retinal through a series of enzymatic steps is known as “visual cycle” and it occurs in the RPE. The *trans*-retinal is extruded from the outer segments of the photoreceptors by the transporter *ABCA4* and carried to the RPE by the *IRBP* protein. Once in the RPE, is converted into *cis*-retinal by an enzymatic cascade depending of the functions of *LRAT, RDH5* and *RPE65*. At this point, the freshly reconstituted 11-*cis*-retinal is transported to the sub-retinal zone and then incorporated by the photoreceptors, where it binds with opsins regenerating functional visual pigments to close the cycle (Bertolotti, Neri, Camparini, Macaluso, & Marigo, 2014) (Figure 3).

The anatomical and functional association between the RPE and the photoreceptors is highlighted also by the physical connection between these two cell types: RPE cells have an extremely involuted and expanded apical membrane, with extensions embracing the photoreceptor outer segments called microvilli (Bonilha, 2014; Strauss, 2005). Commonly, a failure in the RPE maintenance and support mechanisms results in photoreceptor degeneration. For instance, mutations altering the function of the factors involved in the visual cycle have been detected in many cases of RP (Ferrari et al., 2011). Recent genetic ablation experiments in zebrafish larvae showed that the loss of the RPE provokes the degeneration of

photoreceptors and that their regeneration is circumscribed only in those regions where the RPE had been previously recovered (Hanovice et al., 2019).

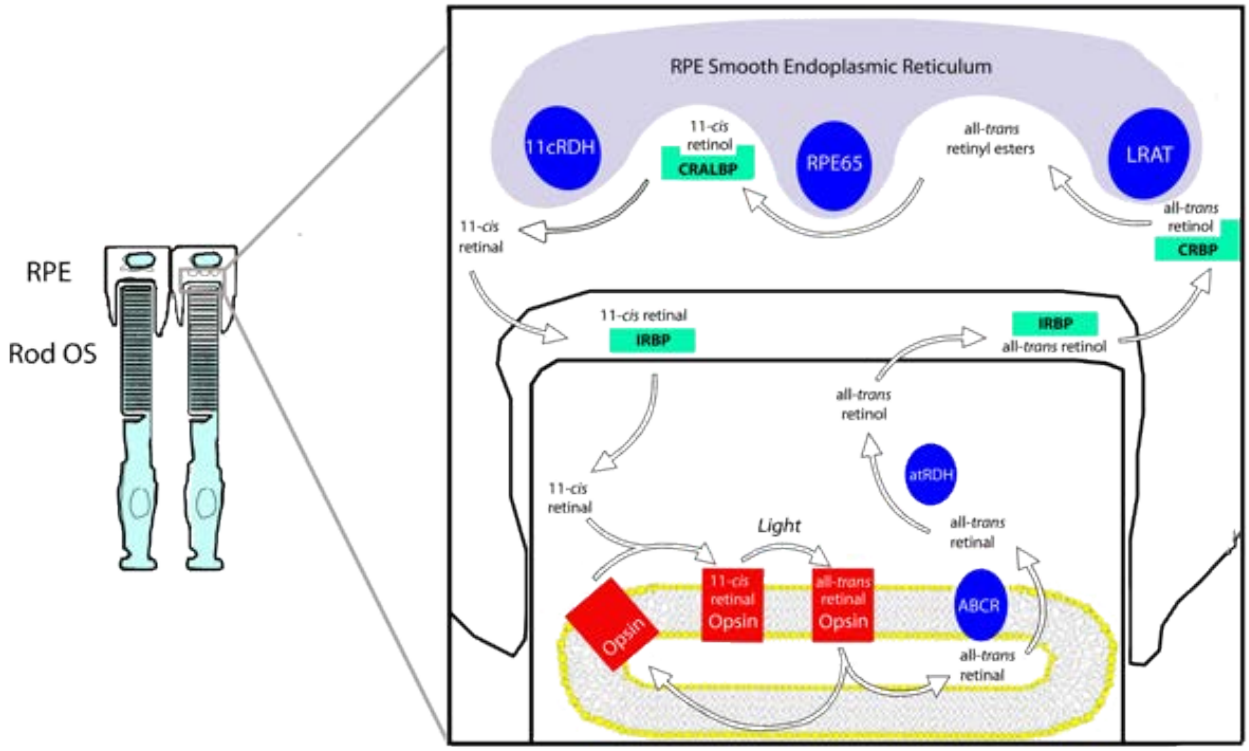

Figure 3. The visual cycle. *The classical visual cycle involves the cycling of retinoids between the photoreceptor outer segments (OS) and the RPE. The visual cycle begins in the outer segment with all-trans retinal's release from the opsin. After reduction to all-trans retinol, the photoproducts cross the sub-retinal space and enter the RPE. Here, 11-cis retinal is regenerated in three enzymatic steps and returned to the photoreceptors. IRBP is thought to transport retinoids through the sub-retinal space.* ***Image by Rosalie K. Crouch (http://photobiology.info/Crouch.html).***

These experiments are representative of what happens in a vast majority of eye degenerative diseases, when the RPE functional disruption causes photoreceptor cell death and *vice versa* (K. Gregory-Evans & Bhattacharya, 1998; Wright, Chakarova, Abd El-Aziz, & Bhattacharya, 2010). Unveiling the principles of the connected developmental mechanisms of RPE and NR will provide a further insight into the understanding of the onset of the retinal dystrophies, which are the most common cause of adult blindness.

1.b. Cell-based therapeutic approaches for degenerative eye diseases

In the present day, there is still no definitive cure for retinal degenerative diseases. However, several therapeutic approaches have proven either to delay their progression or to restore partial photosensitivity. Among others, cellular repopulation is increasingly proving to be a fruitful strategy for RD treatment (Jones, 2017; Yvon et al., 2015). This approach is based on surgical transplantation of retinal cells directly into the patient's affected eye tissue. Cell repopulation can by-pass the prior identification of the mutated genes in the patient, representing an all-encompassing solution to cope with heterogeneity of neurodegenerative diseases. The transplanted cells may either derive from an autologous source (i.e. from the patients themselves), or differentiated from stem cells. Apart from their applications in cell-replacement therapies, stem-cell-derived retinal cells are a good model to study the molecular basis of the neurodegenerative disease and also to test pharmacological compounds (Yvon et al., 2015). Several recent works provided protocols for stem cell conversion into cells with apparently full RPE characteristics (Buchholz et al., 2013; Hazim et al., 2017; Krohne et al., 2012; Maruotti et al., 2013; Rowland et al., 2013; Zhu et al., 2013). Nevertheless, obtaining completely differentiated photoreceptors is proving more challenging. *In vitro* development of proper outer segments represents the principal problem. Presently, due to its simple cell shape, the RPE is the retinal cell type where the majority of the cell repopulation strategies for retinal degeneration focus (Bertolotti, Neri, Camparini, Macaluso, & Marigo, 2014; Nommiste et al., 2017; Ramsden et al., 2013). RPE cells can be differentiated *in vitro* from several stem cell culture, such as human embryonic stem cells (hESCs), umbilical stem cells, foetal stem cells or human induced pluripotent stem cells from somatic cells (hiPSCs) (Ramsden et al., 2013). Indeed, profitable clinical trials have been realized with either hESCs or hiPSCs. However, the transplantation of RPE cells derived from hESCs not only raises ethical issues, but it also requires the administration of immunosuppressant drugs. The employment of hiPSCs could overcome these limitations. RPE cells differentiated in culture from hiPSCs display same characteristics than those derived from hESCs (David E. Buchholz, 2009; Hirami et al., 2009; Osakada et al., 2009). More than that, hiPSCs can be obtained by reprogramming differentiated somatic cells from the same patients using the combination of the TFs Oct4, Sox2, Klf4 and Myc, usually known as 'Yamanaka factors' (Takahashi & Yamanaka, 2006), thus avoiding both ethical and immunological rejection issues. Nevertheless, the autologous hiPSC-derived-RPE transplanted cells retain the mutations which led to the onset of the patient's retinopathy. An effective genetic correction of the diseased cells before transplantation represents the cornerstone aspect for the success of this therapeutic strategy. Recent advances combined patient-derived hiPSCs with genome editing technologies. After molecular diagnosis, the patient-specific gene mutations could be repaired *ex vivo* in hiPSCs and then used for autologous transplant into the affected individual. CRISPR/Cas9 system is an efficient, specific and flexible tool which also allows to target multiple loci simultaneously (multiplex genome editing) (Cong et al., 2013) and this would be an absolute advantage when treating complex multifactorial polygenic diseases. This multiplexing

approach could also be helpful to target apoptotic genes at the same time with the patient-specific disease genes, thus interfering with the disease progression (Letelier et al., 2017). Plus, the therapeutic genome editing mediated by CRISPR/Cas9 maintains the gene expression at physiological levels, avoiding possible adverse effects for gene overexpression induced by exogenous promoters in classical gene therapy procedures (Burnight et al., 2017). Last but not least, a crucial aspect for successful treatment of RD is timing. Photoreceptor or RPE degeneration over time affects other retinal cell layers, so that even interneurons start to degenerate, sweeping away possible effective treatments. Thereby, regardless of the approach, timing is crucial to improve the outcomes (Yu et al., 2017). The period needed to obtain repaired hiPSCs from an RP patient have already been reduced to two weeks thanks to co-delivering protocols of reprograming factors and gene editing constructs (Howden et al., 2015). However, although several protocols for hiPSC differentiation into RPE have been described, they all require more than two months to obtain fully pigmented and functional cells that could be used for surgical transplantation(Brandl et al., 2014; Buchholz et al., 2013; Krohne et al., 2012; Maruotti et al., 2013; Rowland et al., 2013; Singh et al., 2013; Zhu et al., 2013). A deeper insight into the dynamics underlying the differentiation of RPE cells would be instrumental to accelerate the differentiation process. Further, an extensive understanding of the main factors specifying either RPE or retinal neuron progenitor identity would provide new keys to explore the possibility of direct-lineage reprogramming.

2. Vertebrate eye development

2.a. The patterning and morphogenesis of the optic cup

The organogenesis of the vertebrate eye is a complex choreography that involves the integration of inductive signals, activation of genetic programs and morphogenetic movements. Three decades ago, classical lineage tracing studies determined that all the different cell types of the eye arise from a pool of common progenitors (C. E. Holt, Bertsch, Ellis, & Harris, 1988; Turner, 1987; Turner, Snyder, & Cepko, 1990). Eye development begins from an undifferentiated mass of these precursor cells that evaginates bilaterally from "the eye field", a specific region of neuroepithelial cells in the anterior neural plate (Adelmann, 1929): the distal regions expand to form the optic vesicles, while the proximal regions remain narrow and constitute the optic stalks, which are the structures that connect the optic vesicle to the forebrain. In zebrafish, the two optic vesicles are composed by two *back-to-back* neuroepithelial layers equivalent in size, shape and molecular identity: a lateral layer, leaning on to the presumptive lens ectoderm, and a medial layer, in close contact with the underlying mesenchyme. In each optic vesicle, in a frame of few hours these two layers will rotate and differentiate into two different tissues: the lateral layer cells will acquire a bottle-shaped morphology and the whole domain will fold through basal constriction, while the medial layer cells will flatten and the peripheral precursor will move into the lateral domain through the rim. These domains will give rise respectively to the NR and the RPE, forming together a bi-layered cup covering the lens vesicle, which simultaneously invaginates from the surface ectoderm (J. C. Chuang & Raymond, 2002; Eiraku et al., 2011; Fuhrmann, 2010; Kwan et al., 2012; Z. Li, Joseph, & Easter, 2000; Sidhaye & Norden, 2017) (Fig 4). These morphogenetic events are likely orchestrated by the bifurcation of the eye field gene regulatory network (GRNs) into mutually exclusive developmental programs for the NR and RPE. Each of these developmental programs result in distinct cell shapes and functions for the two eye territories. The developmental programs driving the differentiation of both NR and RPE will be illustrated below. However, the specification dynamics determining the initial divergence of their GRNs, as well as the molecular mechanisms driving the acquisition of dissimilar cell shape, are still unclear and poorly explored.

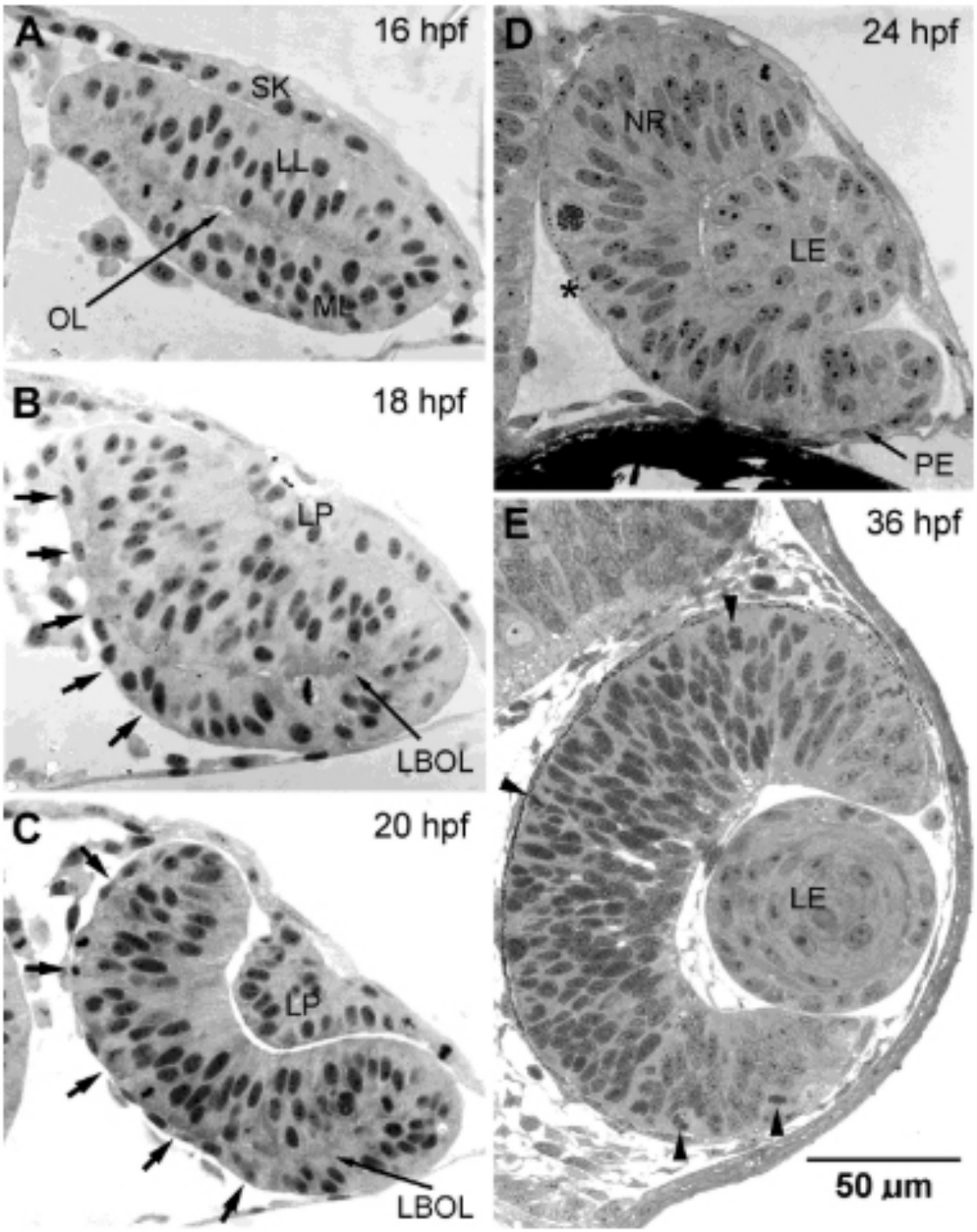

Figure 4. The transformation of the flattened optic vesicle into the eye cup. *(A) 16 hpf. The lateral layer (LL) and the medial layer (ML) were both flat columnar epithelia of nearly equal thickness, separated across the optic lumen (OL) from one another, just deep to the skin (SK). (B) 18 hpf. The dorsal region of the ML has begun to flatten, as cells that were previously columnar have become squamous (short arrows). LBOL: lateral boundary of the optic lumen. LP: lens placode. (C) 20 hpf. The flattening of the dorsal part of the ML extended farther ventrally (short arrows) and the remaining columnar epithelium occupied a smaller part of the ML. (D) 24 hpf. The eye was cup-shaped, as the LL (now the NR) enveloped the LE, and was much thicker than the ML, which was entirely squamous, having lost all its columnar cells. Pigment granules (to the right of *) marked it as RPE. (E) 36 hpf. The NR, RPE, and LE had enlarged, and the NR contained neurons, but mitotic cells (arrowheads) remain.* ***From Li et al., 2000.***

2.b. Molecular insight into the development of the optic cup: The Eye Gene Regulatory Networks

2.b.1. The architecture of Gene Regulatory Networks

The term GRN is used to describe an organized map of interactions between multiple transcriptional regulators and their targets in the cells. They govern gene expression and thus biological processes. In the early 2000s, Erwin and Davidson proposed a GRN model based on three fundamental elements: kernels, input/output (I/O) switches and terminal gene batteries (Davidson & Erwin, 2006). Kernels are represented by the transcription factor (TF) cores situated at the top of the GRN hierarchy. They act as fate specifiers of a restricted cell population, coordinating the activation of a wider number of downstream circuits and effector genes responsible for the morphogenesis, differentiation and function of the cells which will give rise to a particular structure of the organism. Kernel circuits consist of groups of TFs that are highly interconnected and which are usually participating in self-regulatory feed-forward loops that guarantee, in case of activation, the strong implementation of a genetic program. Given their leading position at the top of the GRN hierarchy, kernels tend to be greatly conserved across evolution, for example the heart kernel is extremely conserved from Drosophila to mammals (Wijesena, Simmons, & Martindale, 2017). I/O switches are generally represented by well-known cell signalling pathways, such as *Wnt, Hedgehog, FGFs, TGF-beta* and so on. These pathways function thanks to the coupling between morphogens and receptors, which translates into positional information across the embryo and, hence, activate peculiar TF patterns and biological processes (Domınguez-Cejudo & Casares, 2015). I/O switches may act at different levels of the GRN hierarchy, from activating kernels to inhibiting peripheral sub-circuits responses. They might also be evolutionary conserved, but they are often rearranged to reach distinct purposes in different parts of the organism. Finally, gene batteries are the terminal elements at the periphery of the GRNs. They encode proteins implicated in the biological processes that delineate the diverse molecular and morphogenetic characteristics of the cells. The GRNs are not only represented from transcriptome diversity, but they actually are an interlocking network of TFs, downstream effectors interactions and genomic regions regulating gene expression. These regulatory genomic elements are clusters of several TF binding sequences, which usually correspond to enhancers, although there are other types of DNA control units, such as promoters, silencers and insulators (Fig 5). We refer to all these regulatory DNA regions as “cis-regulatory modules”(Davidson et al., 2002). Usually, each module is at least 300 bps and contains 10 or more binding sites for at least four TFs (Davidson, 2001; Small & Blair, 1992). Each cis-regulatory module interacts with multiple TFs and each TF interacts with multiple cis-regulatory modules. Typically, a particular cis-regulatory module provides a definite pattern of gene expression in space and/or time. Combinations of multiple modules can result in even more complex patterns of gene expression (Gray & Jolla, 1994). The combinatorial activity of the cis-regulatory regions is at least as important as

transcriptional variations of the kernels. Indeed, it has been proposed that mutations affecting cis-regulatory elements like enhancers are the principal motors of evo-devo novelties (Carroll, 2008). Based on this, the detection of TF binding sites (TFBS) in a definite spatio-temporal context and the integration of heterogeneous biological information from transcriptome and cis-regulatory regions may enhance the effectiveness of GRN modeling and prediction of interactions among molecular factors (Mccall, 2010). Several predicted relations among molecular factors have also been confirmed experimentally. This indicated that GRN modeling could be an effective tool for an higher and comprehensive understanding of fundamental events occurring in living organisms, such as developmental processes (Davidson et al., 2002; Huang, He, Sun, & Liu, 2018; Ogundijo, Elmas, & Wang, 2016).

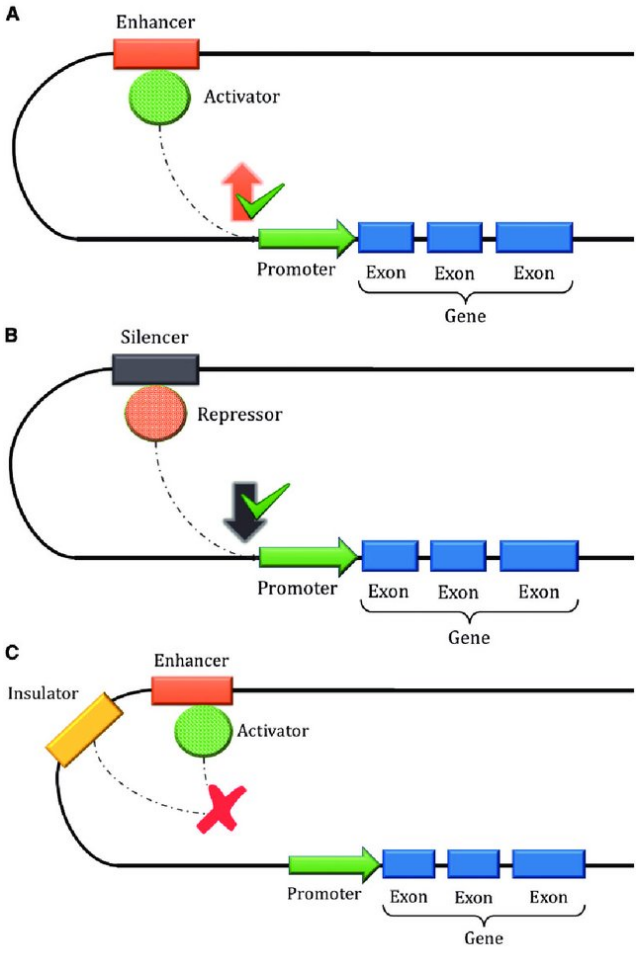

Figure 5. Representation of the effects of cis-regulatory elements. *(A) Enhancers. The enhancer region binds to a protein (activator) that joins to a specific transcription factor binding site in the promoter region, upregulating the target gene. (B) Silencers. The silencer region binds to another protein (repressor) that binds to a specific transcription factor binding site in the promoter region, leading to reduced gene expression. (C) Insulator. The insulator region interacts with the activator protein of an enhancer, blocking its binding to the promoter and inhibiting gene expression. These interactions are highly controlled and dynamic, and modifications to these elements can dysregulate expression and lead to disease.* ***From Rojano et al., 2019.***

2.b.2. The optic cup GRNs

GRNs specifying the eye field

The eye precursor cells in the anterior neural plate got specified as the presumptive eye territory under the influence of the general *Wnt, BMP, Nodal* and *FGF* signalling that patterns the entire nervous system along its antero-posterior axis (Wilson & Houart, 2009). In the middle of the last century, Lopashov and Shroeva demonstrated thanks to classical explant experiments in salamanders that these eye precursors are already committed even before the optic vesicle evagination and will develop as ocular tissue if cultured in vitro (Lopashov & Stroeva, 1964). This multipotent eye state is sustained by a primary GRN operating from the initial stages of the eye field specification. Currently, approximately 200 different genes have been found to regulate the proper eye formation, but the kernel of the network is composed by a restricted number of factors, such as *Rx* (*Rax*), *Pax6*, *Six3*, and *Lhx2*, collectively defined as "eye field transcription factors" (EFTFs)(Zuber, Gestri, Viczian, Barsacchi, & Harris, 2003), which are further deployed for optic cup regionalization and neuronal fate decisions as development progresses (Fuhrmann, 2010; Gregory-evans, Wallace, & Gregory-evans, 2013). Chromosomal lesions affecting EFTFs lead to severe congenital eye malformations, including anophthalmia, microphthalmia and optic fissure closure defects (Fitzpatrick & Heyningen, 2005). Among the EFTFs, especially *Rx2*, *Pax6* and *Six3* were proven to be essential for the eye formation in all the vertebrate models analysed (Sinn & Wittbrodt, 2013). Also in drosophila, the eye specification depends on the genes *eyeless* and *sine oculis,* respectively homologous of *Pax6* and *Six3*, indicating the existence of a conserved hard core of TFs necessary for the development of the eye in bilaterians (Davidson & Erwin, 2006; Wagner, 2007). Although several scientific evidences highlight the EFTFs as central nodes of the complex GRN controlling eye specification, their exact hierarchical relationships remains uncertain. The exogenous expression of a few eye specification genes, such as *Six3* and *Pax6*, is sufficient to induce ectopic development of eye tissue in vertebrates (Chow, Altmann, Lang, & Hemmati-Brivanlou, 1999; Lagutin et al., 2001; Felix Loosli, Winkler, & Wittbrodt, 1999; Zuber, Perron, Philpott, Bang, & Harris, 1999). Hence, it was proven that the miss-expression of *Six3* and *Pax6* triggers the transcription of other eye specification genes. Even if this fact locates both genes at the top hierarchical position of a straight-forward GRN model, probably the network's assembly is way more complex and involves multiple steps of feedback regulation (Juan Ramón Martinez-Morales, 2016). Rather than the expression of *Pax6* and *Six3* alone, the co-expression of EFTF cocktails resulted to function as a much more powerful eye differentiation activator, being sufficient to induce ectopic eyes even outside of the neural tissues (Zuber et al., 2003) and to initiate the eye developmental program into pluripotent cells (Viczian, Solessio, Lyou, & Zuber, 2009). Curiously, these works also evidence that EFTF cocktails' capability to induce the formation of ectopic eyes is mostly dependent on the inclusion of *Otx2* in the mix (Zuber et al., 2003). These data are in line with previous studies demonstrating the crucial function of *Otx* genes during eye

formation (Martinez-Morales, 2003; Matsuo, Kuratani, Kimura, Takeda, & Aizawa, 1995) and with the fact that the ectopic eye induction mediated only by *Six3* or *Pax6* is confined within those domains already expressing *Otx* (Chow et al., 1999; Felix Loosli et al., 1999). Zuber and colleagues attempted to determine the regulatory relationships among the components of the vertebrate eye specification core by comparing the results of their experiments in Xenopus with the model already proposed in Drosophila (Zuber et al., 2003). Through gain and loss of function experiments, some predictions from the Drosophila model were found to be valid also in the vertebrate model. However, despite being suitable as a working model, these findings should be interpreted with caution, as they are purely based on overexpression experiments and some of those assumptions have already been demonstrated to be imprecise. Some experimental discrepancies can also be due to the fact that the exact architecture of the eye GRN somehow differs in different vertebrate groups. Thus, the exact regulatory weight and hierarchical position of EFTFs may vary among different species. For instance in *Rx* mouse mutants, the expression of eye field determinants is affected at very early stages and the eye territory specification is impaired long before optic vesicle evagination (Mathers, Grinberg, & Mahon, 1997; Medina-Martinez et al., 2009; Zhang, Mathers, & Jamrich, 2000), whereas in Xenopus and teleost fish the function of *Rx* does not seem to be essential for the establishment of the eye field, being required only later for the optic vesicle evagination and subsequent eye identity maintenance (Fish et al., 2014; F. Loosli et al., 2001; Felix Loosli et al., 2003; Rembold, Loosli, Adams, & Wittbrodt, 2006). Similarly, in *Lhx2* mutant mice the development of the eye terminate prior the optic cup formation (Porter et al., 1997; Tétreault, Champagne, & Bernier, 2009), while the disruption of the equivalent gene function in zebrafish exhibits a more subtle phenotype, where only the patterning of the ventral forebrain and eye is affected (Seth et al., 2006). An opposite example of functional divergence among vertebrate species regards the TF *ET/Tbx2*, that is an hub of the eye field specification in Xenopus (Zuber et al., 2003). Its loss of function only causes a moderate microphtalmia in mice (Behesti, Papaioannou, & Sowden, 2009). According to the data we have to date, *Six3* may be a possible exception for these phenotypic divergences, since it seems to always hold a leading upstream role during eye specification by suppressing anteriorly the canonical *Wnt* signalling in all the examined species (Carl, Loosli, & Wittbrodt, 2002; Lagutin, 2003; W. Liu, Lagutin, Swindell, Jamrich, & Oliver, 2010; T. Nakayama et al., 2015; Wallis et al., 1999). Even if gene duplication cannot always explain the observed phenotypic discrepancies, there many reported cases in teleost mutants for a given EFTF where the phenotypic differences with mutants in other vertebrate species can be attributed to the presence in the genome of multiple close related paralogues. This is what happens for *Pax6*, whose inactivation in mouse and Xenopus results in an almost total loss of the eye domain (Hill, 1991; Suzuki et al., 2013), but only causes a mild microphtalmia when *pax6b*, one of the two *Pax6* teleost paralogues, is disrupted in zebrafish (Kleinjan et al., 2008).

GRNs specifying the optic cup domains

After the specification of the eye field, signalling molecules coming from the close tissues or the optic vesicle itself act coordinately to restrict the precursors' potentiality. *Shh* and *Nodal* secreted from the CNS midline, *FGFs* from the presumptive lens ectoderm and the retina itself and *BMP* and *Wnt* signals from the extraocular mesenchyme and the dorsal ectoderm pattern the optic vesicle territory into three distinct regions: the NR, the RPE and the optic stalk (Adler & Canto-Soler, 2007; Fuhrmann, 2010; Juan Ramon Martinez-Morales & Wittbrodt, 2009; Steinfeld et al., 2013)(Fig 6A). At the beginning of this process, the early patterning of the vertebrate eye cannot really be considered a tissue compartmentalization in the strict sense of the term, given that various studies reported the relocation of the precursor cell among the distinct domains (C. Holt, 1980; Kwan et al., 2012; Picker et al., 2009). Borders between the eye domains are initially dynamic and based on continuous signalling inputs which maintain tissue identity by coordinating the expression of domain-specific TFs. When the optic cup has completed its folding, eye domains are settled into authentic compartments with well-delimited borders and no cellular blending as a consequence of reciprocal transcriptional repression. For example, the antagonism between *Pax2/Pax6* and *Mitf/Vsx2* play a role in the demarcation of the optic stalk/NR and RPE/NR borders, respectively (Bharti, Liu, Csermely, Bertuzzi, & Arnheiter, 2008; Horsford et al., 2005; Schwarz et al., 2000). Even later on during embryogenesis, these eye territories retain a certain capacity of trans-differentiating into another eye domain (Coulombre & Coulombre, 1965; Guillemot & Cepko, 1992; C. Pittack, Jones, & Reh, 1991; Rowan & Cepko, 2004; Turque et al., 1996; Vogel-Höpker et al., 2000). For example, the perturbation of the *FGF* signalling in mouse or the miss-expression of *Six6* in chick result in RPE-to-NR switch of cell identity (Galy, Néron, Planque, Saule, & Eychène, 2002; Toy, Yang, Leppert, & Sundin, 1998; Zhao et al., 2001). This capacity is lost as the embryo development progresses and the eye domains progressively acquire increasingly diverging physiological and morphological characteristics, such as pigmentation or neuronal identity. In the adult, the competence of the eye cell types for trans-differentiation has been documented only in amphibians (Del Rio-Tsonis & Tsonis, 2003; Fuhrmann, Zou, & Levine, 2014).

Next, we will illustrate the main findings about the GRNs orchestrating the developmental mechanisms of NR and RPE, which are the two principal ocular tissues on which this work focuses.

Neural Retina specification GRN

At the end of optic vesicle evagination, the NR specification program swivel around the homeobox TF *Vsx2*, also called *Chx10*, which was identified as the first determination gene differentially expressed in the presumptive NR layer versus the presumptive RPE layer (I. S. C. Liu et al., 1994). Several studies indicate *Vsx2* as a main factor in the specification of the retinal domain, repressing RPE identity through direct

repression of the TF *Mitf* (Bharti et al., 2008; Horsford et al., 2005; Rowan & Cepko, 2004; Zou & Levine, 2012). Its activity seems to be required also for a correct maintenance of the NR-specific GNR, whose principal regulators are inherited EFTFs, such as *Rx, Pax6, Six3* and *Six6* (Bharti et al., 2012; Fuhrmann, 2010; Medina-Martinez et al., 2009). *FGF* signalling from the presumptive lens plays a determinant role in specifying the NR and repressing the RPE domain. It inhibits the expression of the RPE specifier *Mitf* and stimulates *Vsx2*, thus determining the boundary between the two territories.(Z. Cai, Feng, & Zhang, 2010; Guillemot & Cepko, 1992; Horsford et al., 2005; Hyer, Mima, & Mikawa, 1998; Nguyen & Arnheiter, 2000; Catrin Pittack, Grunwald, & Reh, 1997; Vogel-Höpker et al., 2000). This *FGF* signalling cascade responsible of the NR fate induction seems to operate through the *Shp2/MEK/ERK* pathway (Z. Cai et al., 2010; Galy et al., 2002; Zhao et al., 2001). Interestingly, the RPE-to-NR switch of cell fate produced by *FGF* signalling perturbation does not occur in null mutant mice for *Vsx2* (Horsford et al., 2005). Therefore, *Vsx2* seems to be under the direct control of the *FGF/ERK* pathway and *Mitf* inhibition operated by *FGF* is somehow dependent on *Vsx2* function. Even if some of the peripheral targets of the NR circuit have been inferred by transcriptomic analyses in *Vsx2* knockout animal and cell culture models (Phillips et al., 2014; Rowan & Cepko, 2004), to date the exact hierarchical logics among the core components of the NR specification network (i.e. *Vsx2, Pax6, Six3, Six6* and *Rx*) remain ambiguous.

Retinal Pigmented Epithelium specification GRN

As previously seen for the eye field and NR specification (see previous chapter), species-specific differences in the wiring of the transcriptional networks and inductive signalling have been documented also for the RPE. However, even if with different regulatory weights, in vertebrates the differentiation of the RPE seems to be always dependent on the cooperative active of *Mitf* and the *Otx* family members *Otx1* and *Otx2* (Fuhrmann et al., 2014; Martínez-Morales, Rodrigo, & Bovolenta, 2004). While optic cup morphogenesis occurs, *Otx* genes are restricted from the whole precursors to only the RPE domain (Bovolenta, Mallamaci, Briata, Corte, & Boncinelli, 1997; Lane & Lister, 2012; J. R. Martinez-Morales, Signore, Acampora, Simeone, & Bovolenta, 2001). *Mitf* is a basic helix-loop-helix (*bHLH*) TF that plays a main role in pigmented cell specification, both in melanocytes and RPE (Arnheiter, 2010; Hodgkinson et al., 1993; Steingrímsson, Copeland, & Jenkins, 2004). Also the establishment and maintenance of the eye pigmented cell GRN relies on the inductive molecules secreted by neighbouring tissues, such as activins (member of the *TGF-B* family) derived from the extraocular mesenchyme, as well as *BMPs* and *Wnts* from the surface ectoderm (Hyer, Kuhlman, Afif, & Mikawa, 2003; Müller, Rohrer, & Vogel-Höpker, 2007; Steinfeld et al., 2013). In mouse, *Wnt* signalling has been reported to induce RPE specification through a *β-catenin* dependent process by directly activating *Tcf/Lef* binding sites in both *Mitf* and *Otx* enhancers (Fujimura, Taketo, Mori, Korinek, & Kozmik, 2009; Westenskow, Piccolo, & Fuhrmann, 2009). In chicken, *Wnt* stabilizes the *BMP* mediator *Smad*

through the inhibition of *GSK3β* and this seems sufficient to induce RPE fate. Indeed, when ectopic *BMP* is applied to NR cells, they switch fate to RPE (Steinfeld et al., 2017, 2013). Moreover, *BMP* produced in the extraocular mesenchyme or in the RPE itself helps to maintain *Mitf* expression and downregulate *Pax6* (Müller et al., 2007). In the RPE, activins are also involved in the induction of Mitf and repression of Vsx2 expression (Fuhrmann, 2010). In mouse and chick, but not in zebrafish, *Mitf* loss-of-function impairs the correct specification of the presumptive epithelium, that fails to pigment and develops as a pseudo-stratified neuroepithelium (Bumsted & Barnstable, 2000; Mochii, Ono, Matsubara, & Eguchi, 1998; A. Nakayama et al., 1998; Nguyen & Arnheiter, 2000). On the contrary, *Mitf* overexpression enhances the RPE regulatory network, and in certain genetic backgrounds can induce the trans-differentiation of the NR into pigmented cells (Horsford et al., 2005; Planque et al., 1999). The synergic activity of *Mitf* and *Otx* factors induces the pigmentation cascade interacting directly at the protein level (Lane & Lister, 2012; Martinez-Morales, 2003). Both TFs have been demonstrated to directly promote the expression of melanogenic genes such as *Trp1, Trp2, Tyrosinase* and *Qnr71*, combinatorially binding their consensus motives, CATGTG (M-box) and TAATCC/T (K50-type homeodomain), respectively (Goding, 2000; Martinez-Morales, 2003). Furthermore, it has been reported that *Pax6*, in general mostly associated with the NR regulatory network, is also crucial for the establishment of the RPE identity, together with *Mitf* (Bäumer et al., 2003; Bharti et al., 2012).

More recent studies have also found *Yap* to have an important role during RPE development (J. Y. Kim et al., 2016; Miesfeld et al., 2015). *Yap*, and its paralogue *Taz*, are transcriptional regulators which control several cellular processes, including cell response to mechanical cues (Totaro, Panciera, & Piccolo, 2019). In the optic vesicle of *Yap* conditional mouse mutants, the presumptive RPE layer differentiate as an ectopic NR and the expression of *Otx2* is not detected (J. Y. Kim et al., 2016). In chicken and mouse, the optic vesicle cell capacity to switch their fate in response to GRN perturbation highlights the great potential of these progenitor cells to give rise to any cell type of the eye. Not surprisingly, in certain species and/or at earliest stages of development, eye cells are able to switch their fate during healing processes (Del Rio-Tsonis & Tsonis, 2003). In zebrafish, the ectopic expression of *Yap* in the NR domain results in the differentiation of pigmented cells, but, contrary to what happens in mice, the simple loss of *Yap/Taz* does not results in RPE-to-NR switch of fate, but only in a partial impairment of the RPE (Miesfeld et al., 2015).

Despite the great advances in the last years, our understanding of eye regulatory circuits is still fragmentary and the precise hierarchical relationships among the principal TFs of these networks continue to be ambiguous. In addition, the bifurcation of the eye GRNs into domain-specific developmental programs has a direct impact in the acquisition of the defined cell shape, which is very dissimilar between each domain. Still, very little is known about the transcriptional specifiers and morphogenetic effectors that

drive the rearrangement of the cell shape during the folding of the optic cup. Many of the important nodes of the eye developmental network (e.g. *Pax6, Otx2, Rx, Vsx2*, etc.) have also been identified as essential components of the "coloboma gene network" (Fig 7 B), a group of genes with an high rate of mutation in human families affected by eye abnormalities such as microphthalmia, anophthalmia, and coloboma (MAC) (Gregory-evans et al., 2013; C. Y. Gregory-Evans, Williams, Halford, & Gregory-Evans, 2004). Although this group of diseases represents the preponderant cause of genetic blindness from birth (Porges et al., 1992), its molecular causes are obscure and far from being fully understood. Thus, a deeper insight of the complex dynamics of the eye GRNs would have relevant medical implications.

Even if many of the eye regulatory mechanisms illustrated above were already known before the advent of the Next Generation Sequencing (NGS) technologies, our understanding of the genetic mechanisms driving the differentiation of the ocular tissues have remarkably improved after the onset of a multitude of techniques that allow the systematic interrogation of transcriptional regulation dynamics. In the next subchapter (**2.c. NGS technologies onset: how genome-wide approaches contributed to unravel the eye GRNs**) we will discuss in details the importance and the scope of these findings for the revolution they brought into the field of eye developmental biology. Not least, because taking advantage of the genome wide approach allowed by next NGS technologies, the work presented in this thesis attempts to bridge a gap in our knowledge of the mechanisms driving vertebrate eye development. Main studies using NGS technology to explore the GRN of the developing eye are summarized in Figure 6.

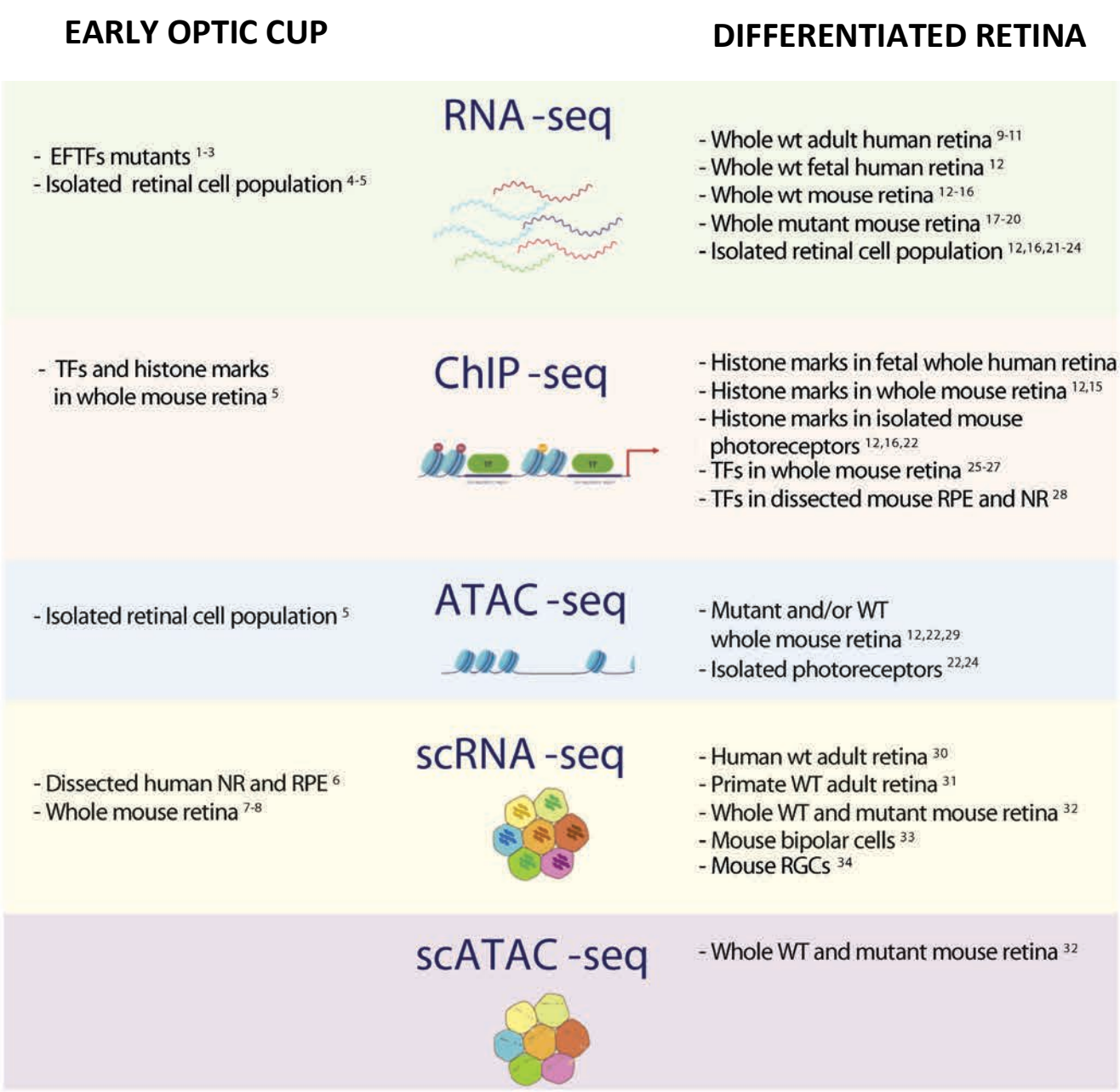

Figure 6. Overview of relevant genome-wide studies focused on eye differentiation using the NGS technologies. *Datasets were catalogued basing on the developmental window they explore, if before (left) or after (right) the retina neurogenesis. References are indicated: [1](Yin et al., 2014), [2](Fish et al., 2014), [3](Diacou et al., 2018), [4](Gao et al., 2014), [5](Zibetti et al., 2019), [6](Hu et al., 2019), [7](Lo Giudice et al., 2019), [8](Clark et al., 2019), [9](Farkas et al., 2013), [10](Li et al., 2014), [11](Pinelli et al., 2016), [12](Aldiri et al., 2017), [13](Krishna et al., 2016), [14](Gamsiz et al., 2013), [15](Grant et al., 2011), [16](Ueno et al., 2016), [17](Brooks et al., 2011), [18](Mustafi et al., 2011), [19](Murphy et al., 2016), [20](de Melo et al., 2016), [21](Kim et al., 2016), [22](Mo et al., 2016), [23](Ueno et al., 2017), [24](Hughes et al., 2017), [25](Popova et al., 2012), [26](Corbo et al., 2010), [27](Hao et al., 2012), [28](Samuel et al., 2014), [29](Ruzycki et al., 2018), [30](Lukowski et al., 2019), [31](Peng et al., 2019), [32](Norrie et al., 2019), [33](Shekhar et al., 2016), [34](Rehaume et al., 2018).*

2.c. NGS technologies onset: how genome-wide approaches contributed to unravel the eye GRNs

2.c.1. *Genome-wide expression profiling of the eye transcriptome*

Systems biology introduced the necessity of studying the interactions among the components of a biological system using a holistic approach. The arrival of high-throughput sequencing technologies made possible to obtain a comprehensive and genome-wide understanding of the cell state at both transcriptional and epigenetic levels, bypassing the limitations and biases of alternative whole genome methodologies, such as microarrays. Since early 2000s, high-throughput sequencing-approaches have been applied to unravel the complexity of the eye regulatory networks and to discover new candidate genes involved in sight diseases. Sanger sequenced ESTs from the embryonic mouse retina (Mu, 2001; J. Yu et al., 2003) revealed a very complex gene expression dynamics, derived from the heterogeneous populations of dividing and non-dividing cells composing the developing eye (C. L. Cepko, Austin, Yang, Alexiades, & Ezzeddine, 1996). SAGE technique also provided a further contribution to the characterization of retinal gene expression both through development as well as in the adult mouse (Blackshaw, Fraioli, Furukawa, & Cepko, 2001; Sharon, Blackshaw, Cepko, & Dryja, 2002). These pioneer experiments of transcriptomic profiling identified a number of genes showing a restricted temporal expression and a substantial proportion of novel transcripts (J. Yu et al., 2003), as well as peculiar isoforms different from those reported previously (Sharon et al., 2002). The developing eye exhibited more transcripts involved in cell structure, gene regulation and protein expression, whereas the adult retina transcriptome showed an enrichment in genes involved in phototransduction and metabolism (J. Yu et al., 2003). Multiple expressed genes fell into putative functional categories not previously associated with retinal development and/or disease (Blackshaw et al., 2001). All these findings highlighted the necessity of an omics approach to unveil new molecular players involved in eye development. These pioneer genome-scale experiments widened the horizons of classical developmental genetics studies and took up the challenge of connecting datasets together to define the architecture of the regulatory networks driving the differentiation and morphogenesis of the eye. As a preliminary statement, it is important to note that the assembly of GRNs is complex and we just started gathering enough information to have a minimal understanding of their architecture. Despite of the advances in the systemic identification of many network nodes and edges, the field is still going through an exploratory phase that follows the pace of recent technological innovations. However, to have an integrative view on the contribution of these different technologies to our understanding of retinal networks, a schematic representation of early and late GRNs will be provided as a parallel thread to the reader (Fig 7 and 8).

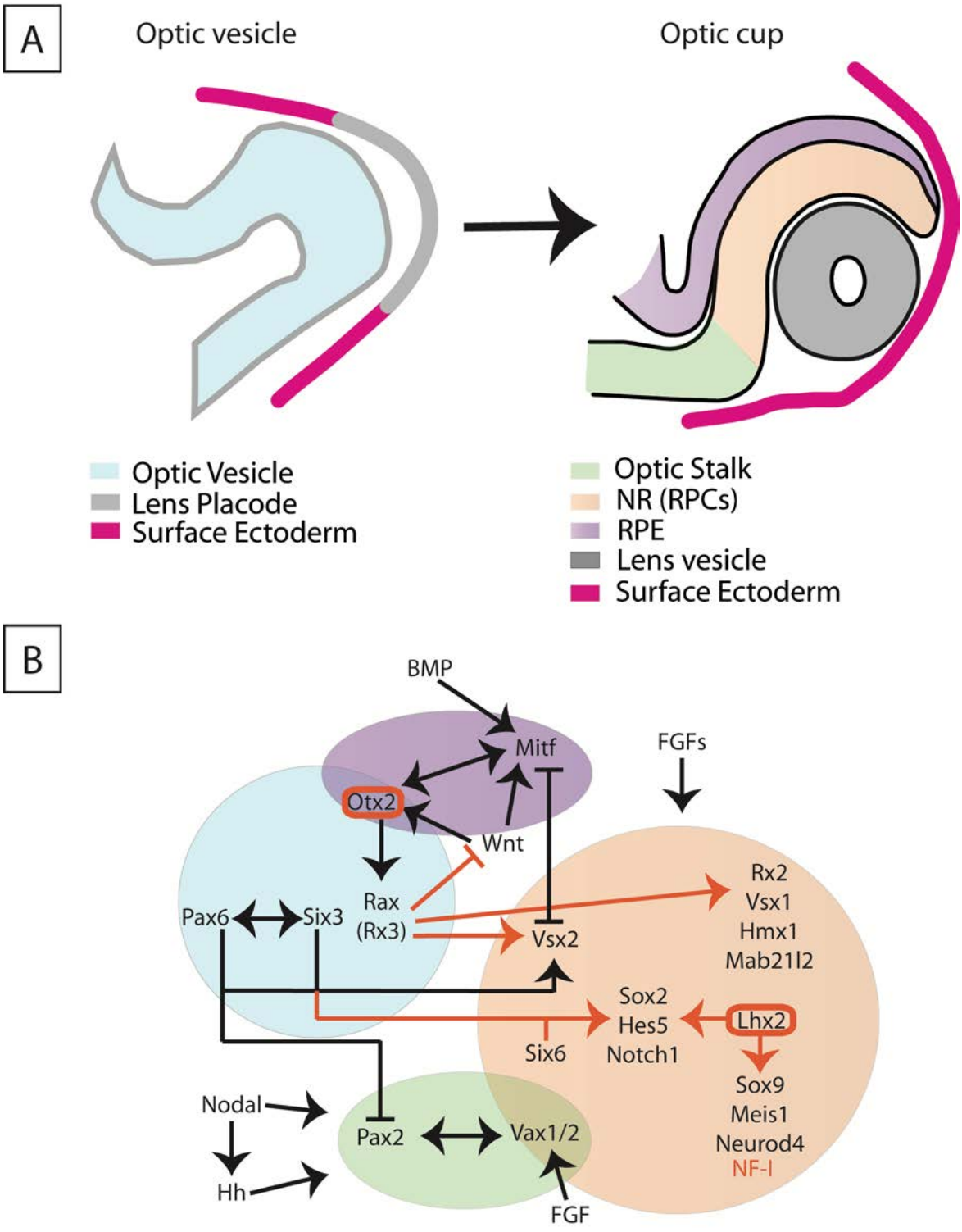

Figure 7. Schematic representation of core GRNs during optic cup patterning. *(A) Early eye morphogenesis. The bilayered optic cup formed by NR, RPE and optic stalk develops from the undifferentiated precursors of the optic vesicle. (B) Core GRNs specifying the distinct domains of the optic cup. Colour code: gene names and arrows in black indicate known regulators and their relationships also confirmed by NGS technologies; gene names and arrows in orange indicate the identification of new regulators and/or their connectivity in NGS studies. Orange boxes around TFs indicate the identification of cis-regulatory modules for a particular TF in ChIP-seq or ATAC-seq studies.*

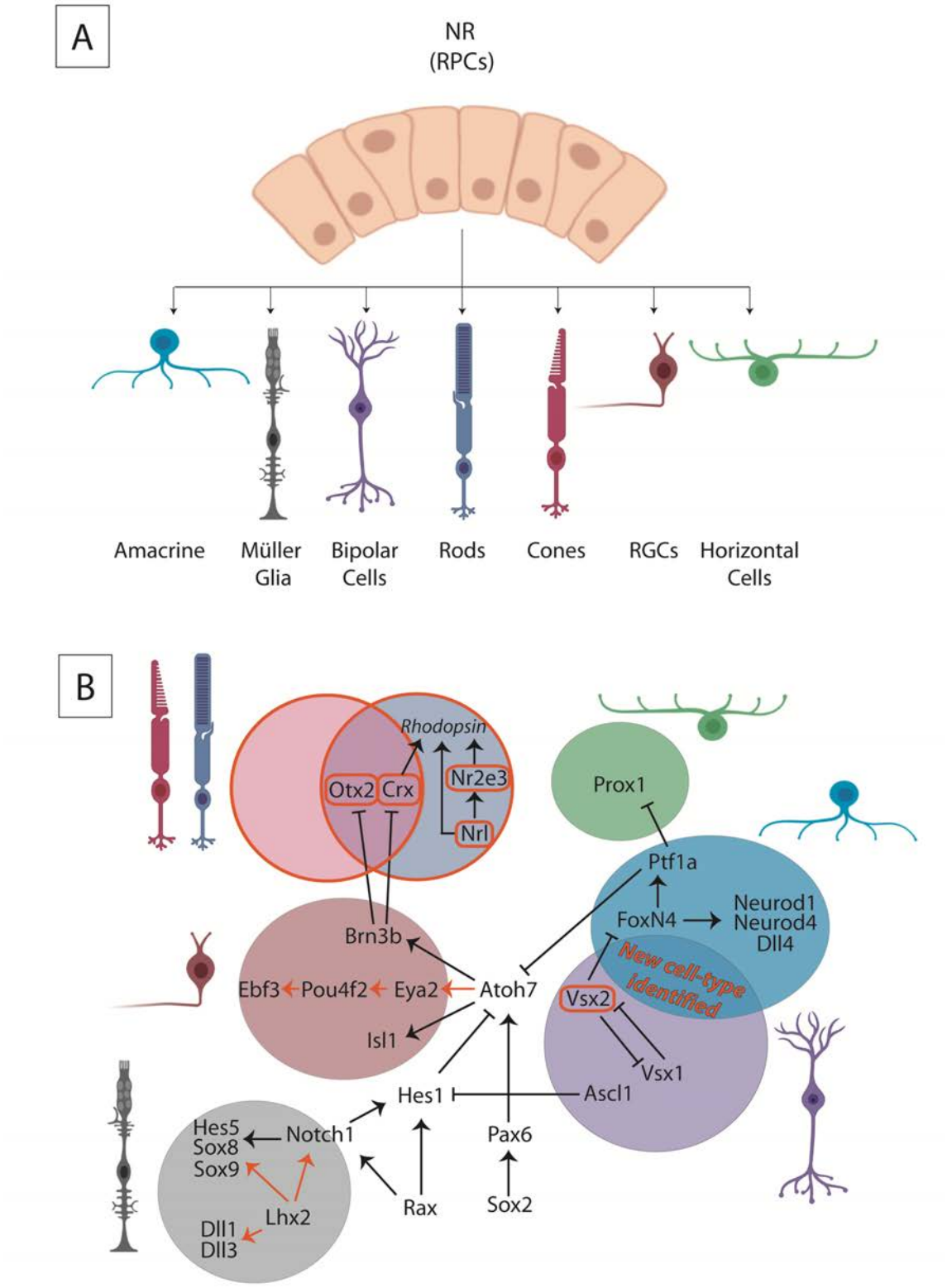

Figure 8. Schematic representation of core GRNs during retina differentiation. *(C) RPCs give rise to seven different retina cell-types. (D) GRNs driving the differentiation of each retinal cell-type. Colour code as in Fig 6 B. The orange frame around cell type indicates the characterization of the cell-type epigenetic marks in ChIP-seq or ATAC-seq studies.*

Over the last decade, the fast development of NGS platforms, such as Roche454, Illumina/Solexa, or Life/APG, among others, revolutionized basic and applied research. These new sequencing technologies produce an enormous volume of sequencing data per run, offering whole-genome coverage at relatively low cost (Metzker, 2010). One of the main applications of NGS is the RNA-seq approach, which enables an unprecedented global analysis of the transcriptome of cells, tissues and organisms. RNA-seq offers a number of important advantages over other methods such as Sanger sequencing of ESTs or expression microarrays, due to its high reproducibility, unbiased detection of transcripts, single nucleotide resolution and quantitative estimation of transcript levels over a large dynamic range of expression (Mortazavi, Williams, McCue, Schaeffer, & Wold, 2008; Z. Wang, Gerstein, & Snyder, 2009). RNA-seq permits not only the detection of variations in gene expression levels, but also identifies alternatively-spliced transcripts, fused genes and mutations, providing a quite complete overview of the cell state. During the last years, RNA-seq has been extensively used as a method of choice to characterize gene expression in retinal development and disease models. Although microarray and SAGE studies had already described the high complexity of the developing eye transcriptome (H. Cai, Fields, Hoshino, & Priore, 2012; Sharon et al., 2002; Yoshida, Yashar, Hiriyanna, & Swaroop, 2002), more recent RNA-seq studies revealed that the eye transcriptome is even more complex than previously reported (Farkas et al., 2013; M. Li et al., 2014). In mouse, it can contain up to 34,000 transcripts (Brooks, Rajasimha, Roger, & Swaroop, 2011) and in humans 65% of all the protein-coding genes are expressed in the retina (Pinelli et al., 2016). This multiplicity could not be appreciated with cDNA microarrays and SAGE, which allow a smaller number of expression profiles being analyzed simultaneously. Additionally, RNA-seq studies shed light onto tens of thousands of novel alternative splicing (AS) and alternative promoter usage events occurring in the mouse retina (Grant et al., 2011; J. W. Kim et al., 2016). Many of the retina genes undergoing AS processes are among the most highly expressed and correlated with retinal disease (Gamsiz, 2013). In mouse photoreceptors, AS involves the frequent inclusion of specific microexons (Murphy, Cieply, Carstens, Ramamurthy, & Stoilov, 2016). Genes that do not alter their expression during retina development are associated with an higher degree of AS compared with those genes undergoing dynamic transcriptional regulation (Krishna et al., 2016). This suggests that AS may act as an alternative post-transcriptional mechanism for gene expression fine-tuning. Despite these encouraging advances, understanding the regulatory roles of AS in retinal development and homeostasis will require further investigation.

Transcriptomic profiling through development has revealed coordinate regulatory waves that recapitulate the stereotyped sequence of cells' birth in the retina. Several reports have characterized a first transcriptional wave related to the differentiation of ganglion, horizontal, cone and amacrine cells; and a second wave associated to the maturation of rod photoreceptors and the differentiation of bipolar and Müller glia cells (Swaroop, Kim, & Forrest, 2010; Zhang et al., 2006; Ueki et al., 2015; Ueno et al., 2017; Wang, Sengel, Emerson, & Cepko, 2014; Zelinger & Swaroop, 2019). A very recent RNA-seq analysis

confirmed a similar transcriptional-waves profile for human retinal samples, and confirmed the existence of a photoreceptor specific splicing program (Mellough, Bauer et al. 2019). Although temporal and spatial gene expression profiles can be used to infer GRN architecture (Yang, Fang et al. 2019), these methods have been scarcely applied to the analysis of retinal networks in vertebrates. Most systemic studies have focused on cell-specific retinal networks (Fig 8), using two main experimental strategies. A first strategy entails the flow cytometry sorting of neuronal populations using cell-specific transgenic lines, as reported for the analysis of *Atoh7* expressing precursors differentiating to retinal ganglion cells (Gao, Mao et al. 2014). An alternative strategy consists in the RNA-seq profiling of mutants in which one of the cell types is selectively absent. This is the case for the analysis of the retinal transcriptome upon *Lhx2* conditional loss, which is essential for Müller glia specification via *Notch* signalling pathway (de Melo, Zibetti et al. 2016). Due to its relevance for understanding the aetiology of retinal degenerative diseases, intensive investigations on cell-specific regulatory networks have focused particularly on photoreceptors and their main GRN nodes, *Nrl* and *Crx*. Transcriptomic analyses of retinal cells in mutant models for these central nodes allow the identification of novel downstream nodes and the definition of relevant edges within the photoreceptors network (Blackshaw, Fraioli et al. 2001, Brooks, Rajasimha et al. 2011, Mustafi, Kevany et al. 2011, Kim, Yang et al. 2016). Beyond gene expression studies, mutant models for key nodes of the retinal GRNs have also constituted a powerful tool for the identification of relevant cis-regulatory modules (see following sections).

Much less investigated are the GRNs underlying the early steps of eye field specification and patterning. A few studies have used a NGS approach, focusing the attention on important nodes of the early network. One of these key regulators is the gene *Rx* (*Rax*), which mutation has been shown to arrest eye development leading to anophthalmia in different vertebrate species (Kennedy et al., 2004; F. Loosli et al., 2001; Felix Loosli et al., 2003; Mathers et al., 1997; Voronina et al., 2004). The impact of *rx3/rax* mutation on the transcriptome has been analysed by RNA-seq in zebrafish (Yin, Morrissey et al. 2014) and Xenopus (Fish, Nakayama et al. 2014). The zebrafish study by Yin and colleagues delineated a model of *Rx3*-regulated genes during early eye morphogenesis. In their work they show that at least one paralogue of all EFTFs appears to be deregulated in the *Rx3* null zebrafish mutants. They assess that *Rx3* promotes optic vesicle morphogenesis and represses brain development via the down-regulation of genes mediating *Wnt* signalling and the enhanced expression of homeodomain EFTFs and retinoid-signalling genes (Yin, Morrissey et al. 2014). Systemic analyses of retinal transcriptomes using mutant mice for other key regulators, such as *Lhx2* (Tetreault, Champagne et al. 2009) and *Six3/Six6* (Diacou, Zhao et al. 2018) also support the notion of a highly interdependent network of EFTFs (Figure 7 B).

2.c.2. Identification of cis-regulatory modules

Understanding the regulatory logic behind gene networks requires much more than examining transcriptome changes. Among other things, it is necessary to characterize the genomic regions targeted by the relevant TFs within the network: the cis-regulatory modules (Davidson et al., 2002). Although cis-regulatory modules were already well known before the onset of NGS technologies, their amount and the actual regulatory power of the non-coding fraction of the genome has been frequently neglected or underestimated before the ENCODE project (ENCODE Consortium, 2012). Since their onset, NGS-based approaches have been used to systematically identify these cis-regulatory modules either studying protein-DNA interactions and histone modifications by ChIP-seq (Barski et al., 2007; Johnson, Mortazavi, & Myers, 2007; Jothi, Cuddapah, Barski, Cui, & Zhao, 2008) or chromatin accessibility through DNase-seq, ATAC-seq and related techniques (J. Buenrostro, 2013; Thurman et al., 2012) .

ChIP-seq combines chromatin immunoprecipitation with massive parallel sequencing and is a useful approach to identify the cis-regulatory modules containing binding sites for a given TF (Park, 2009). Individuating TF binding sites in a definite spatio-temporal context provides critical information for GRN modeling. Thanks to this approach, in the adult mouse eye, it has been shown that the TF *Otx2* binds distinct genomic regions and acts following radically different regulatory logics in two distinct cellular types where it is expressed: the NR and the RPE (Samuel, Housset, Fant, & Lamonerie, 2014). Except for a few exceptions such as the one mentioned above, pioneer attempts of constructing a circuitous GRN in the context of retina development were focused mainly on photoreceptors' specification. In combination with gene expression analyses, ChIP-seq experiments pivoted on the key regulators *Crx* and *Nrl* (Corbo, Lawrence et al. 2010, Hao, Kim et al. 2012, Kim, Yang et al. 2016). *Crx* is an essential regulator of photoreceptor-specific genes for both rods and cones, whereas *Nrl* is the principal transcription factor that determines only the rod photoreceptor cell fate. In *Crx* mutant mice, both rods and cones fail to develop outer segments and eventually die (Furukawa, Morrow et al. 1999, Hennig, Peng et al. 2008, Corbo, Lawrence et al. 2010). *Nrl* null mice lack of rods and their photoreceptors layer is composed only by cones, and conversely *Nrl* ectopic expression in photoreceptor precursors results in a rod-only retina (Mears, Kondo et al. 2001). Corbo and colleagues demonstrated that *Crx* regulates downstream photoreceptor TFs and their target genes binding directly to their regulatory elements. By comparing the *Crx* binding sites in wild type and *Nrl* null mice, they were also able to identify rod- and cone-specific regulatory regions as well as many shared elements (Corbo, Lawrence et al. 2010). A second ChIP-seq study focused on *Nrl* showed a large overlap between *Crx* and *Nrl* peaks, which reinforces the hypothesis of their synergic function in specifying photoreceptor fate (Hao, Kim et al. 2012). Interestingly, although many of the genes identified as *Crx* targets by Corbo and colleagues resulted to be deregulated in the *Crx* null retinas (Livesey, Furukawa et al. 2000), a considerable percentage showed unaltered expression levels. One possible explanation for this

inconsistency could be that other TFs, including *Nrl*, may compensate the loss of *Crx*. Alternatively, individual cis-regulatory modules may have variable regulatory weight in gene transcription, or transcriptional adaptation mechanisms may play a compensatory role (El-Brolosy, Kontarakis et al. 2019).The genome-wide identification of histone modifications by ChIP-seq constitutes a powerful tool to identify potential cis-regulatory modules (Kouzarides 2007). Several studies have revealed detailed dynamic patterns of histone modifications during ocular development. ChIP-qPCR experiments in mouse retinas at distinct stages showed that the levels of H3K4me3, H3K27me3 and H3/H4ac in some of the retina-specific gene loci dynamically and globally changed along development (Watanabe and Murakami 2016), suggesting the importance of the role of chromatin architecture also during the differentiation of the eye. Popova and colleagues analysed the landscape of histone modifications in whole mouse retinas during development, but this time taking advantage of the NGS technology to obtain a genome-wide picture of the chromatin marks H3K4me2 and H3K27me3 (Popova, Xu et al. 2012). In this work the authors described a unique epigenetic signature marking rod photoreceptor-specific genes. The concept of a pattern of histone modifications specific of a particular cell type has also been explored by Ueno and collaborators (Ueno, Iwagawa et al. 2016, Ueno, Iwagawa et al. 2017). They discovered that photoreceptor-specific loci were also marked by H3K4me3. This very specific histone modification pattern was not detected in association with genes specific of other retinal cell lineages (Ueno, Iwagawa et al. 2016). A similar approach highlighted an exclusive function for H3K27me3 in Müller glia cells specification. The authors showed that H3K27me3 is involved in the repression of the Müller glia differentiation program in other retinal lineages (Ueno, Iwagawa et al. 2017). The importance of epigenetic modifications for eye development has been explored in loss-of-function experiments affecting genes that catalyse histone modifications. In the mouse retina, the pharmacological inhibition of the histone deacetylase *HDAC1* and the subsequent increase in H3K9ac and H4K12ac, but not H3K27ac, stopped rod differentiation and maintained the expression of retinal progenitors genes, such as *Hes1* and *Vsx2* (Ferreira, Popova et al. 2017). Similarly, the knock down of *Jmjd3*, a histone demethylase encoding gene specifically expressed in the inner nuclear layer resulted in the loss of a subset of retinal bipolar cells (Iida, Iwagawa et al. 2014).

Finally, a recent work by Aldiri and colleagues used ChIP-seq in eye tissues to map a broad set of histone modifications associated with active or repressive chromatin. Developmental changes in histone marks at the promoters and within gene bodies were correlated with variations in gene expression and chromatin accessibility in this comprehensive study. Combining histones epigenetic state and changes in DNA methylation, they saw that approximately half of differentially regulated genes correlate with at least one kind of epigenetic change. This was especially true for genes involved in neuronal differentiation, rather than for that characteristic of the progenitor status. In this study, the authors identified stage-specific super-enhancers conserved in humans and mice. Interestingly, although DNA-methylation patterns did not show a high rate of conservation across human and mouse retinal development, histone changes

resulted to be strongly conserved, especially the histone modifications associated to the stage-specific super-enhancers (Aldiri et al., 2017)

2.c.3. *Chromatin-accessibility studies*

Although ChIP-seq studies offer a genome-wide analysis of DNA-protein interactions at high resolution, the current standard methods still require abundant starting material. This remains a bottleneck for the acquisition of biologically relevant epigenetic data (Gilfillan, Hughes et al. 2012). In addition, ChIP-seq relies on antibody specificity and sensitivity. Complementary techniques, such ATAC-seq, have been adopted as a valid approach to characterize epigenetic landscapes and identify active cis-regulatory modules, even for small cell populations. ATAC-seq assesses genome-wide chromatin accessibility thanks to an hyperactive mutant form of *Tn5* transposase (Reznikoff, 2008), that inserts sequencing adapters into the open regions of the genome. The tagged DNA regions are then purified, PCR-amplified and sequenced using NGS (Fig 9). This technique captures open chromatin regions, usually trimethylated at H3K4, H3K36 and H3K79. These histone modifications are typically correlated to cis-regulatory modules (Kouzarides, 2007; Lowe, Cuomo, Voronov, & Arnone, 2019). In combination with transcriptomic and functional analyses, the technology allows obtaining a snapshot of the dynamic interactions between TFs and cis-regulatory modules, either through development or during physiological and pathological processes.

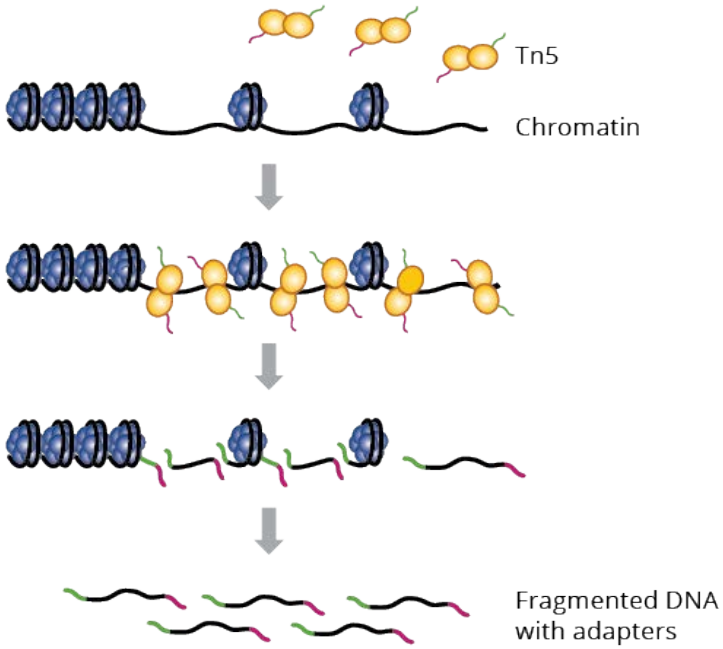

Figure 8. ATAC-seq workflow. *Tn5 inserts Illumina sequencing adapters into native chromatin, in DNA regions that are not protected by nucleosomes, while simultaneously fragmenting the DNA. DNA in open chromatin is therefore adapter-tagged and can be enriched over the background of closed chromatin using PCR followed by quantification via NGS. The accumulation of Tn5 insertion sites is therefore a measure of chromatin accessibility.*

ATAC-seq is a relatively recent technique and so far it has been scarcely used to investigate the mechanisms of retina development. Nevertheless, recent works took advantage of this technology to explore the epigenomic landscape of the retinal tissues in mammals (Mo, Luo et al. 2016, Aldiri, Xu et al. 2017, Hughes, Enright et al. 2017, Zibetti, Liu et al. 2019). In the extensive study of Aldiri et al. they overlapped histone marks from ChIP-seq data with regions of open chromatin defined by ATAC-seq, to characterize cis-regulatory elements dynamics through development. The information derived from ATAC-seq studies, in conjunction with other epigenetic marks, was particularly useful to discriminate among active, poised and polycomb-poised enhancers (Aldiri, Xu et al. 2017). Using a similar multi-omics approach in the developing mouse retina, Zibetti and colleagues searched for enriched binding motifs in open chromatin regions. They identified LHX2 as a main candidate regulator and further investigated its dynamic role in the global control of chromatin accessibility and transcription in murine RPCs (Zibetti, Liu et al. 2019)(Figure 7 B).

ATAC-seq studies have also helped to understand better the unique nuclear architecture of mammalian rod photoreceptors. In nocturnal mammals, rods possess an "inverted" structure with a compact mass of heterochromatin in the centre of the nucleus rather than the characteristic peripheral clumps observed in most cell types. This peculiar configuration is thought to improve visual sensitivity in low-light conditions

conferring singular optical features to the rods nuclei (Solovei, Kreysing et al. 2009, Eberhart, Feodorova et al. 2013). Recent studies have used ATAC-seq to identify thousands of loci selectively closed in rods relative to cones as well as many neuronal types. Analysis of open chromatin regions showed that rod-specific genes are typically regulated by proximal regulatory sequences, while in cones distal enhancers play a significant role in gene regulation (Mo, Luo et al. 2016). Moreover, the analysis of rods and cones epigenomic landscapes revealed a distinct enrichment of TF binding sites, unveiling important differences in the cis-regulatory grammar of these cell types (Hughes, Enright et al. 2017). DNA hypomethylation usually coincides with accessibility and putative regulatory activity in many cell types and tissues (Stadler, Murr et al. 2011, Burger, Gaidatzis et al. 2013). Interestingly, in adult rods a significant percentage of DNA hypomethylated regions are not in active chromatin and do not overlap with ATAC-seq peaks. Many of these regions show hallmarks of regulatory sequences that were active earlier in neuronal development, suggesting that these elements could persist undermethylated due to the particular chromatin architecture in mature rods, thus representing "vestigial enhancers" (Mo, Luo et al. 2016). Notably, both studies observed that the open chromatin profile of photoreceptors lacking the rod transcriptional regulators NRL or NR2E3 is shifted to that of native cones, implying that the activity of these TFs regulates the selective closure of chromatin in rods (Mo, Luo et al. 2016, Hughes, Enright et al. 2017). While NRL and NR2E3 seem to mediate the closure of non-rod-specific-chromatin acting as master regulators, recent data by Ruzycki et al. suggest that *Crx* cannot act as a "pioneer" factor during photoreceptor fate specification. *Crx* seems only capable to act on chromatin regions that have already been "primed" in precursor cells, rather than targeting completely closed cis-regulatory elements to induce de novo chromatin remodeling (Ruzycki, Zhang et al. 2018).

Despite these advances, the ultimate mechanisms that commit RPCs to the photoreceptor lineage are still unclear. Actually, this uncertainty about the precise genetic stimuli triggering terminal differentiation can be applied to any cell population in the retina. The fact that, at a given stage of development, the retinal tissue is a miscellany of proliferating progenitor cells, diverse committed cells and differentiating cells (Cepko 2014) hinders the identification of such pioneering mechanisms. The averaging of signatures derived from multiple retinal populations leads to an imprecise estimation of cell-type-specific transcriptional and epigenetic changes, particularly those depending on the cell environment. For instance, some of the genes harbouring repressive marks appeared to be up regulated in the whole retina but were down regulated when studied in a purified rod population (Aldiri, Xu et al. 2017). Advances in our understanding of eye development and treatment of retinal diseases will require a more comprehensive characterization of the distinct cell types. This should include the profiling of individual cell transcriptomes and epigenetic landscapes.

2.c.4. Single-cell approaches

Recent technological breakthroughs in single-cell sequencing (J. D. Buenrostro et al., 2015; Shapiro, Biezuner, & Linnarsson, 2013) have made it possible to measure gene expression and assess chromatin structure at the single-cell level, thus paving the way for exploring heterogeneity also among eye cells. Since 2009, single-cell RNA-seq (scRNA-seq) can be used to analyze the transcriptomes of a large amount of cells through the use of microfluidics device or other approaches as flow cytometry (Kolodziejczyk, Kim, Svensson, Marioni, & Teichmann, 2015; Macosko et al., 2015b). A recent study concluded that although these different protocols may largely vary in their detection sensitivity (that is in any case lower than in classic bulk RNA-seq) their accuracy in quantification of gene expression is consistently high (Svensson et al., 2017). Moreover, a particular advantage of these methods is the capacity of capturing cells at various developmental stages in a single experiment. ScRNA-seq snapshots of expression data during specification and developmental processes represent a continuum of different states, which need to be temporally ordered by computational methods such as trajectory inference algorithms. These bioinformatic methods are generally referred to as "pseudotime" methods (Trapnell et al., 2014). These methods allow the identification of the cell types at the beginning and at the end of a differentiation trajectory, as well as those cells in the intermediate states. By ordering the cells according to pseudotimes, it is possible to identify the transcriptional changes that accompany developmental processes. This permits the detection of differentiation branching points during developmental continuous paths, the identification of crucial points of cellular decision-making and the assessment of which genes are critical for driving these progressions in order to attempt the reconstruction of GRNs (Griffiths, Scialdone, & Marioni, 2018; Haghverdi, Büttner, Wolf, Buettner, & Theis, 2016; Moignard et al., 2015). A few recent studies have used scRNA-seq to comprehensively characterize cell-specific transcriptomic states throughout eye development. Thanks to scRNA-seq, Clark and colleagues provided a further insight into the NR transcriptomic landscape during mouse development. They profiled more than 100.000 single cells from 10 mouse developmental stages to encompass the full course of retinal neurogenesis, its initiation, variations in developmental competence, specification events and differentiation trajectories of each major retinal cell type (Clark et al., 2019). Their approach identified an evident transcriptional difference between early and late-stage RPCs. Significantly different signatures were also observed between primary and neurogenic RPCs, coinciding with changes in RPC competence. In spite of that they could not detect any clear evidence for molecularly distinct RPC subtypes at individual ages. This promote the idea of a stochastic model of cell fate specification during retina development (Gomes et al., 2011; He et al., 2012). Importantly, Clark and colleagues scRNA-seq approach helped to identify the *NFI* transcription factors as selectively expressed in late RPCs and suggested mechanisms by which they control both RPC fate specification and proliferative quiescence (Clark et al., 2019) (Figure 7 B). ScRNA-seq allowed the deciphering of transcriptional maturation mechanisms also in early born retinal neurons, leading to the disclosure of new interesting

candidate genes that may play a role in the molecular differentiation and connectivity wiring of different subgroups of RGCs (Lo Giudice, Leleu, La Manno, & Fabre, 2019).

Single cell approaches do not only help to identify developmental trajectories in complex cell populations but also to describe rare cell-types that would be impossible to characterize otherwise. Several studies have shown that a majority of the genes that have a weight determining the transcriptional divergence between distinct cell types are detectable already by low coverage RNA-seq (10-50,000 reads per cell) (Pollen, Nowakowski et al. 2014, Heimberg, Bhatnagar et al. 2016). In fact, a more crucial sequencing parameter is the number of sequenced cells. A shallow sequencing of large cell numbers facilitates comprehensive classification more than a deep sequencing of a small number of cells. Recent scRNA-seq studies in human (Lukowski, Lo et al. 2019) and primate (Peng, Shekhar et al. 2019) adult retina provided a reference transcriptome specific for retinal cell type and offered an advanced discrimination of the mechanisms defining the retinal identity. In primate retina, Peng and colleagues distinguished more than 70 cell types, included extremely rare cell types such as intrinsically photosensitive RGCs, which constitute less than the 0.002% of all the retinal cells (Peng, Shekhar et al. 2019). Description of rare cell-types is particularly thorough when purified cell populations are used as starting material for single-cell sequencing. Thus, the analysis of mice RGCs isolated by *Thy1* immuno-panning identified 40 different cell subtypes (Rheaume, Jereen et al. 2018). Interestingly, this number coincides with the number of categories identified by electrophysiological recordings in mice RGCs (Baden, Berens et al. 2016), suggesting an exhaustive identification of cellular subtypes through transcriptomic profiling. In fact, single cell sequencing could also help the identification of novel cell types; for instance single-cell transcriptome sequencing of purified retinal bipolar cells identified 15 bipolar cell types, including all types already known from previous studies and two novel types, one of which has a non-canonical morphology and localization with hybrid bipolar-amacrine features (Shekhar, Lapan et al. 2016)(Figure 8 B).

Finally, divergence among cell-types is associated with TF inter-play with cis-regulatory elements also at single cell resolution. Additional methods that provide information about the genomic DNA modifications and chromatin accessibility have been developed for single cell applications, such as snmC-seq, scTHS-seq and scATAC-seq (Buenrostro, Wu et al. 2015, Cusanovich, Daza et al. 2015, Luo, Keown et al. 2017, Lake, Chen et al. 2018, Preissl, Fang et al. 2018). However, to the date these novel techniques have been scarcely applied. A recent work by Norrie and collaborators took advantage of the integration of scRNA-seq and scATAC-seq with bulk Hi-C data to refine a retinal model of cis-regulatory element interactions, in a cell- and developmental-stage-specific-manner. This combined strategy identified a *Vsx2* super-enhancer with a specific activity in bipolar cells. In mouse, the deletions of this *Vsx2* super-enhancer resulted in the total absence of bipolar neurons, with no impairment of RPCs or Müller glia, where *Vsx2* expression is also required for a proper development of the retina (Norrie, Lupo et al. 2019)(Figure 8 B). These data have set a new milestone remarking the importance of single-cell analyses to spot critical cis-regulatory interactions

in retina differentiation. Additional studies will be required to complete a detailed map of how many and which cis-regulatory elements are actually controlling TF activity in a cell-type and developmental-stage-specific- manner.

Although these technical advances boosted the emergence of many single-cell sequencing projects focused on the NR issues, the initial regulatory dynamics triggering the bifurcation of the eye developmental network into two programs for NR and RPE remain a mostly undiscovered land. Hu and colleagues analyzed 2,421 individual cells of human NR and RPE, covering the developmental window between 5 to 24 fetal weeks (Hu et al., 2019). This study succeeded in the identification of a clear gene expression signature for all major cell populations, recapitulating the stereotyped sequence of cells' birth in the retina, and revealed significant differences between the transcriptomic landscapes of the NR and RPE (i.e. NR-enriched genes were associated to nervous system development, while RPE-enriched genes were related to retinol metabolism). This work provides important information on the temporal gene expression in the developing human tissues, but sample size limited the depth of the conclusions. Additional studies will be required to complete a detailed map of how many and which cis-regulatory elements are actually controlling TF activity in a cell-type and developmental-stage- specific- manner. This is essential information to understand the logic of the avant-garde GRNs driving the early step of the morphogenesis and differentiation of the vertebrate eye.

Objectives

As already mentioned in the Introduction, the dynamics underlying the bifurcation of the optic vesicle progenitors' GRN into two mutually exclusive developmental programs for NR and RPE are far from being unravelled. This thesis work aims to provide a better understanding of the regulatory logics specifying two optic cup domains. Hence, our main objectives are:

1. *To characterize the transcriptome bifurcation of the NR and RPE domains by RNA-seq.*

2. *To explore the cis-regulatory landscape controlling gene expression in the said tissues by ATAC-seq.*

3. *To explore the NR developmental network focusing on vsx1 and vsx2.*

4. *To determine the cytoskeletal remodeling of the NR and RPE during optic cup development.*

5. *To individuate novel components of the eye GRNs.*

6. *To verify to which extent our findings may be applied to human clinical investigation.*

Materials and Methods

1. Wet lab methods

1.a. Fish maintenance

Adult zebrafish (Danio rerio) were maintained under standard conditions according to the procedures already described in Kimmel et al. (Kimmel, Ballard, Kimmel, Ullmann, & Schilling, 1995) and in the Zebrafish Model Organism Database(http://zfin.org; Sprague et al., 2003). AB/Tübingen strains were used both as wild type fish and background to generate the different transgenic and mutant lines. Zebrafish embryos and larvae were kept at 28.5°C in E3 medium (5 mM NaCl, 0.17 mM KCl, 0.33 mM $CaCl_2$, 0.33 $MgSO_4$) supplemented with Methylene Blue (Sigma). In those cases when we wanted to prevent pigmentation, 0.003% 1-phenil-2-thiourea was added to the E3. They were staged according to somite number and morphology (Kimmel et al., 1995). All the zebrafish developmental stages in this study are reported in hours post- fertilization (hpf).
Similarly, WT medaka fish strain iCab was maintained under standard conditions described in Iwamatsu (2004). All the medaka embryos were staged are reported according their morphological features (Iwamatsu, 2004).

1.b. Microinjection

Embryos for microinjection experiments were obtained as it follows: one day prior to microinjection, adult zebrafish were separated according to the sex in two different 3 litre tanks. The following morning, immediately after lights were switched on, males and females were placed together into a 5 litre tanks. New-born eggs were physically separated from the adults by a grid and recollected in E3 medium after a 10 minute mating time. Recollected embryos at one-cell stage were manually injected using a microinjector (Narishige). Glass needles were prepared by horizontally pulling standard capillaries (filament, 1.0 mm, World Precision Instruments) with a P-97 Flaming/Brown Micropipette Puller (Sutter Instrument Company). The volume injected was calculated as 1 nl using a graticule (S1 stage Micrometer, 10 mm/ 0.1 mm, Pyser Optics). The injection was performed in the yolk.

1.c. Transgenic Lines

The Tg(vsx2.2:GFP-caax) line was generated at the Functional Genomic Platform of the CABD (Ana Fernández-Miñan), by fusing the medaka vsx2.2 promoter (before, vsx3) (Martinez-Morales et al., 2009) and GFP-caax, as a reporter protein localizing in the cell membrane. The vector was obtained through Tol2 mediated transgenesis (Kawakami, 2007), in combination with multisite gateway technology (Invitrogen). To this end, the medaka Vsx3 promoter was inserted into a p5E-MCS entry vector and recombined with the Tol2kit vectors pME-EGFPCAAX and p3E-polyA into the Tol2 destination vector (Kwan et al., 2007). The resulting expression pattern for this line is therefore GFP expression in the optic vesicle and later on only in the NR domain membranes.

The Tg(enh1-bhlhe40:GFP) was generated by Rocio Polvillo, a technician in Martinez-Morales' lab, using a cis-regulatory sequence identified by Sergio Salgüero, a former member of the Bovolenta's lab. For this purpose, a genomic map from Jose Luis Gomez-Skarmeta's laboratory showing predictive enhancer and promoter epigenetic marks (Bogdanović et al., 2012) was used. The map allowed the identification of different potential regulatory elements of the bhlhe40 gene, including the promoter and four upstream regulatory sequences. All the selected regulatory regions are inactive at 80% epiboly stage but active at 24 hpf, indicating that they are potentially involved in the activation of bhlhe40 expression in the RPE. Each regulatory region was amplified by PCR with specific primers and cloned using the pCR™8/GW/TOPO® TA Cloning® Kit (Invitrogen). In all cases, the plasmids were checked for enhancer insertion in the 3'->5' direction and then used for Gateway recombination with the ZED vector (Bessa et al., 2009). The Gateway™ LR Clonase™ Enzyme Mix was used for the recombination (Invitrogen). The resulting vectors were injected to generate the corresponding transgenic lines. The F0 adults were individually outcrossed with wild type partners to identify founders. A general analysis of the generated lines was performed using confocal microscopy and the line corresponding to the enhancer 1 was selected as the most accurate RPE reporter. From this point, the subsequent generations of the transgenic line were maintained by in-crossing of siblings.

1.d. Cell cytometry

Taking advantage of the restricted fluorescent signal of specific zebrafish transgenic lines, we used FACS to isolated the different eye populations at different stages of development. Negative fluorescence threshold was set using dissociated cells from a WT embryo (Fig 1). Retinal progenitors at 16 hpf (Fig 2), specified NR at 18 hpf and immature NR at 23 hpf cells were isolated from dissected heads of the tg(vsx2.2:caax-GFP)

(Fig 3). Specified RPE at 18 hpf and immature RPE at 23 hpf cells were isolated from the whole embryo of the tg(enh1-bhlhe40:GFP) (Fig 4). Embryos for cell cytometry experiment were obtained as it follows: one day before, adult zebrafish were separated according to the sex in two different 3-litre tanks. On the following morning, immediately after lights were switched on, males and females were placed together into a 5 litre tanks. New-born eggs were physically separated from the adults by a grid and recollected in E3 medium after a 10 minute mating time. The embryos were left to grow until the desired stage and dechorionated. If using whole embryos, they were placed in deyolking tampon (NaCl 55 mM, 1.8 mM KCl, 1.25 mM $NaHCO_3$; 800 µl of deyolking tampon/ 100 embryos) and vigorously pipetted up and down until the yolk dissolution. The samples were centrifuged for 4 min at 4°C and 300 g. The embryo pellets were resuspended in 1 ml of Danieau's Solution 0.5X (29 mM NaCl, 350 µM KCl, 200 µM $MgSO_4*7H_20$, 300 µM $Ca(NO_3)_2$, 2.5 mM HEPES buffer) and centrifuged for 4 min at 4°C and 300 g. The pellets were resuspended in cold FACSMax Cell Dissociation Solution (AMS Biotechnology, 1 ml/300 embryos). In case of using dissected heads, they were directly resuspended in FACSMax Cell Dissociation Solution without going through the deyolking procedure. The samples were incubated on ice for 20 min with periodic manual agitation. Samples were then centrifuged for 4 min at 4°C and 300 g. The pellets were resuspended again in cold FACSMax (500 µl/300 embryos) and passed twice through a 40 µm cell strainer (Falcon). The mixture of dissociated cells was used for sorting. A FACSAria™ Fusion flow cytometer was used with the help of the CABD Flow Citometry facility. Cells were isolated for their fluorescence signal directly in Trizol for RNA extraction or ATAC-seq tagmentation buffer, depending on the downstream applications.

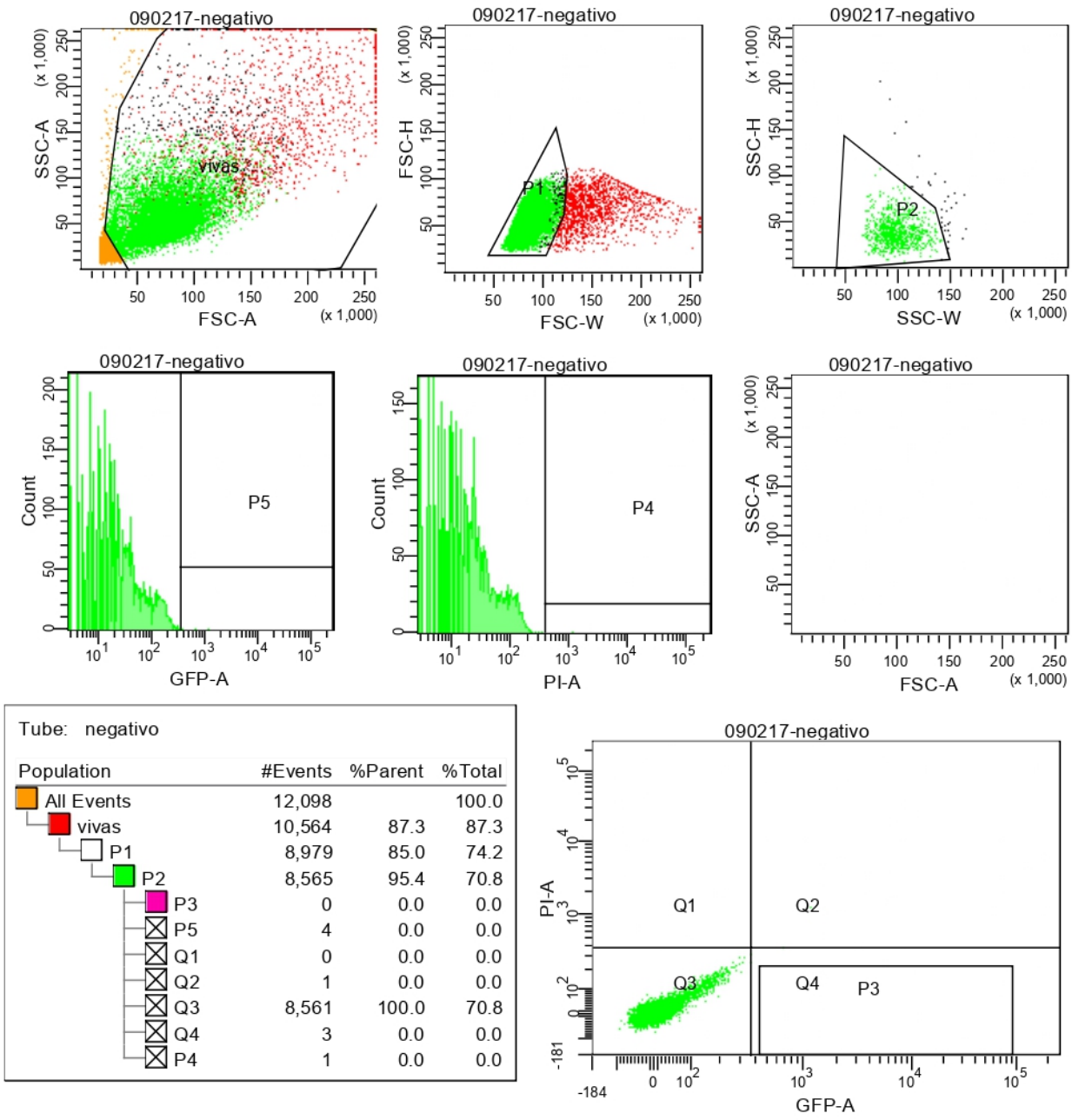

Figure 1. Cell cytometry visualization of GFP-negative dissociated embryos. *FSC indicates cell size, whereas SSC indicates cell complexity. GFP detection of non-specific signal set our fluorescence threshold for following isolation of specific cell population derived from our transgenic lines.*

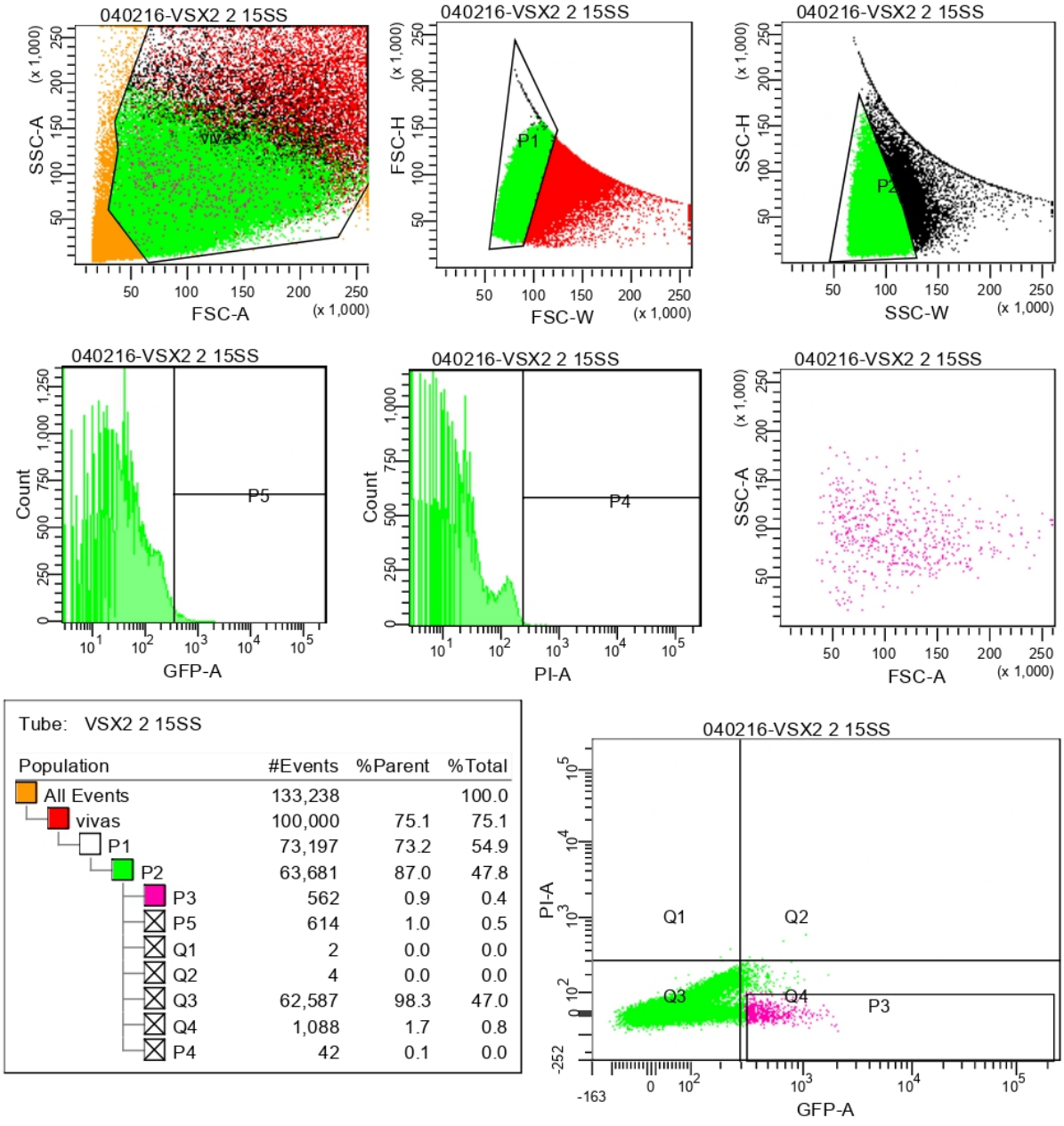

Figure 2. Cell cytometry visualization of eye progenitor cells. *Eye progenitors were isolated using the tg(vsx2.2:GFP-caax) at 16 hpf. We isolated the cells with a GFP-signal exceeding our fluorescence threshold established using a WT embryo (Fig 1). Isolated cells are marked in pink (P3 population).*

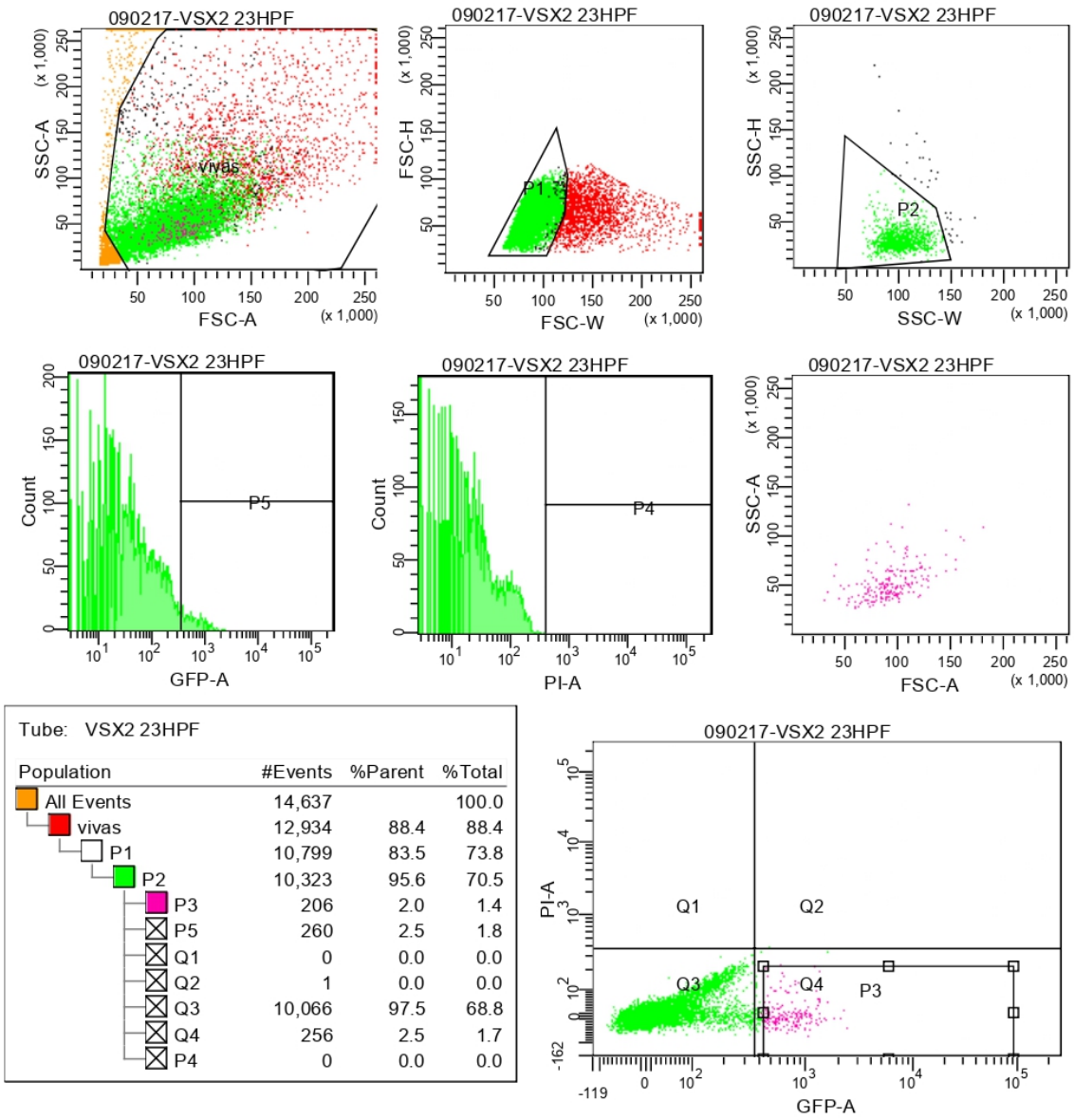

Figure 3. Cell cytometry visualization of NR cells. *NR cells were isolated using the tg(vsx2.2:GFP-caax) at 18 and 23 hpf. In this figure, embryos at 23 hpf were used as example. We isolated the cells with a GFP-signal exceeding our fluorescence threshold established using a WT embryo (Fig 1). Isolated cells are marked in pink (P3 population).*

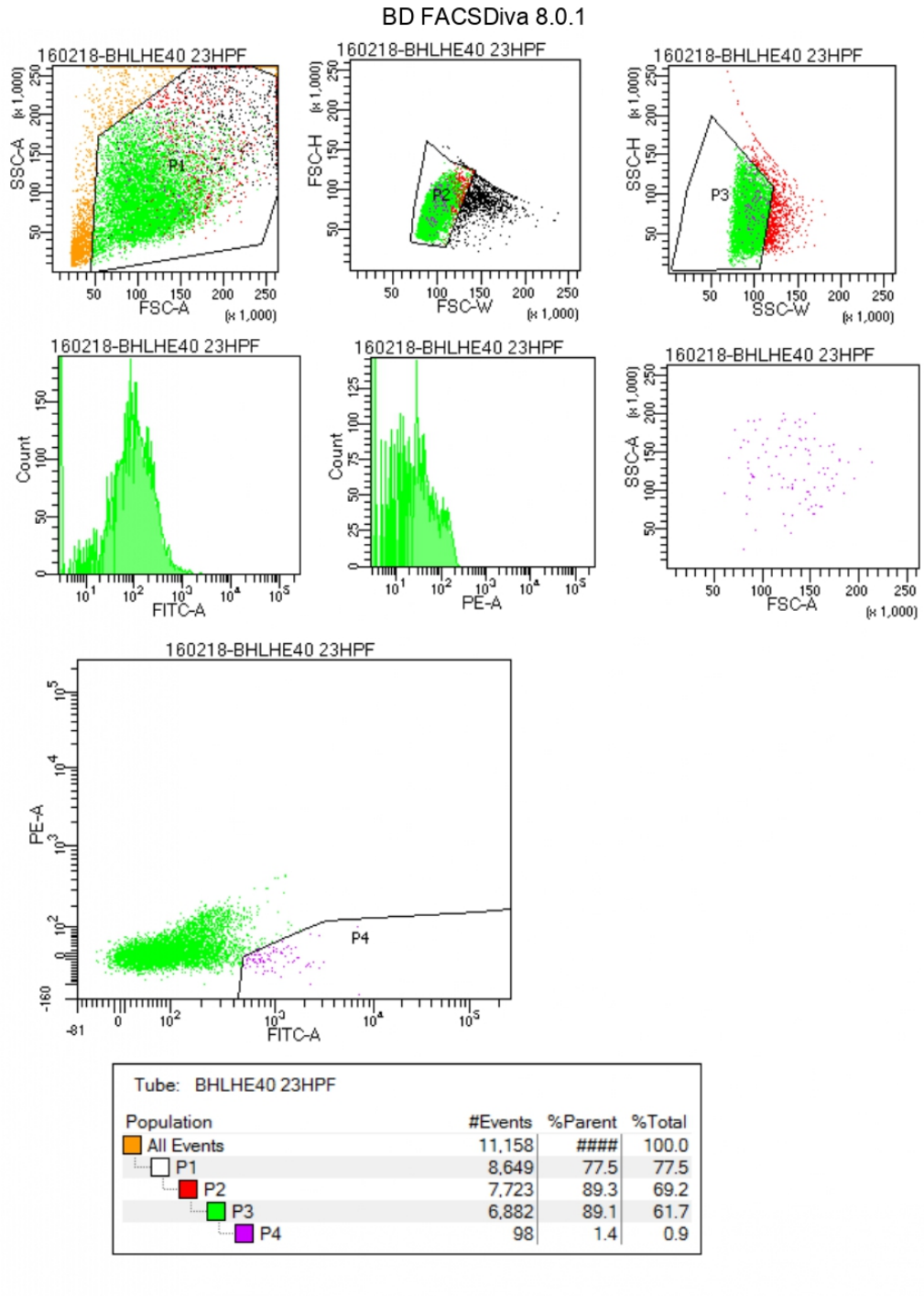

Figure 4. Cell cytometry visualization of RPE cells. *NR cells were isolated using the tg(enh1-bhlhe40:GFP) at 18 and 23 hpf. In this figure, embryos at 23 hpf were used as example. We isolated the cells with a GFP-signal exceeding our fluorescence threshold established using a WT embryo (Fig 1). Isolated cells are marked in pink (P3 population).*

1.e. RNA extraction

Total RNA was extracted using 750 ul TRIzol LS (Invitrogen), a mono-phasic solution of acid phenol and guanidine isothiocyanate, which maintains RNA integrity during sample lysis. After sample harvesting, total volume was adjusted to 1 ml with nuclease free pure water (Invitrogen) and then incubated for 20 min at RT. 200 µl of chloroform (Merck) were added to the samples, that were shacked vigorously and then incubated again for 10 min at RT. Samples were centrifuged at 4°C and 16000 g for 15. This allowed the separation of the sample mixture in an upper aqueous phase containing RNA and a middle interphase and lower organic phase contains DNA, proteins and lipids. The colorless upper phase containing the RNA was transferred to a new RNase-free tube. 500 µl of isopropanol (Merck) and 10 µg of RNase-free glycogen (Thermo Fisher) were added to the aqueous phase, delicately mixed, incubated for 10 min at RT and then centrifuged again at 4°C and 16000 g for 30. The supernatant was discarded, the pellet washed with 1 ml of ice-cold 75% Ethanol (Merck) and centrifuged at 4°C and 16000 g for 5 minutes twice. The supernatant was discarded, the pellet dried for 10 min at RT and then dissolved in RNAse-free water (Invitrogen). Possible DNA contamination was eliminated treating the RNA samples with with TURBO DNAse-free (Ambion). Concentration of the RNA samples was evaluated by Qubit (Thermo Fisher), and then the samples were used for subsequent applications.

1.f. RNA-seq

RNA was extracted from sorted cells and then treated with DNAse as described above. rRNAs were eliminate from the samples with Ribo-Zero® rRNA Removal Kit (Illumina) prior library preparation. Samples were sequenced in SEx125bps reads with an Illumina Hiseq 2500 platform by the sequencing service Fasteris (Geneve, Switzerland). We obtain at least 35 M reads from the sequencing of each library.

1.g. ATAC-seq

5,000 sorted cells in PBS were pelleted by centrifugation at 500 RCF for 5 minutes at 4° C in a pre-cooled fixed-angle centrifuge. All supernatant was removed using two pipetting steps being careful to not disturb the not visible cell pellet. 50 µl transposase Tn5 mixture (25 µl of 2x TD buffer, 2.5 µl of TDE1, 0.5 µl of 1% digitonin, 22 µl of nuclease-free water) was added to the cells and the pellet was disrupted by pipetting. Transposition reactions were incubated at 37°C for 40 minutes in a ThermoMixer with agitation at 300 RPM. Transposed DNA was purified using a QIAgen MinElute Reaction Cleanup kit and purified DNA was eluted in 10 µl elution buffer (10 mM Tris-HCl, pH 8). 1 µl of the eluted tagmented DNA was amplified for

qPCR with modified primers (Table I) and NEBNext® High-Fidelity 2X PCR Master Mix (New England BioLabs) to estimate the number of PCR cycles needed to prepare the library with the following reaction:

Tagmented DNA	1 µl
Primer Fw 5 µM	1 µl
Primer Rv 5 µM	1 µl
Sybr Green 10x	1 µl
NEBNext	5 µl
Nuclease-free H_20	1 µl
---	---
Final Volume	10 µl

98°C	30 s	
98°C	10 s	x 25 cycles
63°C	30 s	
72°C	30 s	
72°C	5 min	
4°C	∞	

After evaluating the optimal number of PCR cycles (usually 1-2 more than the cycle threshold), libraries were amplified with the following reaction:

Tagmented DNA	9 µl
Primer Fw 25 µM	2.5 µl
Primer Rv 25 µM	2.5 µl
NEBNext	25 µl
Nuclease-free H_20	11 µl
---	---
Final Volume	50 µl

72°C	5 min	
98°C	30 s	x (Ct + 1-2 cycles)
98°C	10 s	
63°C	30 s	
72°C	1 min	
4°C	∞	

Primer	**Sequence (5'->3')**
Ad1_noMX	5'- AATGATACGGCGACCACCGAGATCTACACTCGTCGGCAGCGTCAGATG – 3'
Ad2.1	5'- CAAGCAGAAGACGGCATACGAGATTCGCCTTAGTCTCGTGGGCTCGGAGATGT – 3`
Ad2.2	5'- CAAGCAGAAGACGGCATACGAGATCTAGTACGGTCTCGTGGGCTCGGAGATGT – 3'
Ad2.3	5' - CAAGCAGAAGACGGCATACGAGATTTCTGCCTGTCTCGTGGGCTCGGA GATGT – 3'

Table I. Primers used to amplify ATAC-seq libraries

All the libraries were sequenced at the sequencing facility of the CRG (Barcelona, Spain). We obtain at least 100 M reads from the sequencing of each library.

1.h. CRISPR/Cas9

1.h.1. F0 screening

All the sgRNAs were designed using the online tool CRISPscan (https://www.crisprscan.org/ ; Moreno-Mateos et al., 2016) and synthetized following the protocol described by Vejnar et al. (Vejnar, Moreno-Mateos, Cifuentes, Bazzini, & Giraldez, 2016). All the sgRNAs were selected to target the first half of the CDS in exons resulting actually expressed in the eye tissues from our RNA-seq data (trying to avoid the first exon to prevent the usage of an alternative start codon that would produce a possibly functional protein), with an efficiency score > 58 and no predicted off-targets (Table II). Two different sgRNAs were used together to target the same gene. The selected oligo sequence of the sgRNA sequences were purchased from Sigma-Aldrich Oligo Service as DNA molecules (sgDNA). sgDNAs were amplified for PCR and then purified on column (NucleoSpin Gel and PCR clean-up, Macherey-Nagel). The two sgDNAs targeting the same gene were purified together on the same column. Eluted sgDNA concentrations were quantified with Nanodrop 2000. sgRNAs were *in vitro* transcribed using the sgDNA templates with the IVT kit Ampliscribe t7 Flash Transcription (Lucigen). After a 4 h incubation at 37°C, samples were treated with TurboDNAse (Ambion) and then purified through precipitation with sodium acetate and ethanol. The sgRNAs were injected in the zebrafish yolk at 1-cell stage at final concentration of 80 ng/µl together with the Cas9 endonuclease at a concentration of 300 ng/µl. 1 nl of the mixture was injected in each embryo. In the case a target gene had a close paralogue, the sgRNAs targeting both of the paralogues were injected at the same time, adjusting the final concentration of the sgRNA-Cas9 mixture. Phenotype manifestation and penetrance were assessed by careful observation at 24 and 48 hpf.

gene name	**gene ID**	**sgRNA_seq (5'->3')**
mphosh10	ENSDARG00000053912	GGTGGCTTTCGTGGACGAGGCGG
mphosh10	ENSDARG00000053912	GGATTTCGAGGAGGCAGGGGTGG
heatr1	ENSDARG00000099742	GAGGTGCTGGCTCTCCGTCATGG
heatr1	ENSDARG00000099742	GAGGGAGGGCCAATCAGCAAAGG
hells	ENSDARG00000057738	TGGGGCTGCTGTGCTGGCACAGG
hells	ENSDARG00000057738	AGACAGGTTATTCTGGAGGGGGG

nop58	ENSDARG00000104353	AGAGATCTCGATGGGCACAGAGG
nop58	ENSDARG00000104353	GGGCATCAGAAACCAGATGGAGG
mcm5	ENSDARG00000019507	GCGTAACCCTGCAGCCCCGGTGG
mcm5	ENSDARG00000019507	GTGGCGCAGACCAAAGCCAAAGG
dkc1	ENSDARG00000016484	GAGCTGCGACGAGTCCGTTCCGG
dkc1	ENSDARG00000016484	GGGCTGCCTGATCGTGTGTGTGG
cirh1a	ENSDARG00000017675	GGGCCAATCTGGGCCATAACAGG
cirh1a	ENSDARG00000017675	AGAGGGTACGGGACGTCCCGCGG
wdr12	ENSDARG00000003287	GGGGAAGGCTGTGATGACTGTGG
wdr12	ENSDARG00000003287	GAGATCTGCAACCTCGGAGGAGG
ttc27	ENSDARG00000007918	GGAAGTTGCTCTGTTGGCGGTGG
ttc27	ENSDARG00000007918	GTGGCTCCTCTGCTCTTCGGTGG
dhx33	ENSDARG00000051785	GAGGCGGGCATCGGCCGGCAGGG
dhx33	ENSDARG00000051785	GTGTTTGGAGATGTCCCGGCAGG
mcm2	ENSDARG00000102798	GGGCCACACGGTGCGCGAGTGGG
mcm2	ENSDARG00000102798	GAGCGACTGACACTCAGGACAGG
tsr2	ENSDARG00000005772	GTGTGAGCAGGGCAGATTGGCGG
tsr2	ENSDARG00000005772	TGGAGCGTTCAGTCAGCAGAAGG
mif	ENSDARG00000071336	GTGACAGTACATCGCCGTACAGG
mif	ENSDARG00000071336	GTGAGCGAGCAGAGCGCACACGG
fbl	ENSDARG00000053912	GGTGGCTTTCGTGGACGAGGCGG
fbl	ENSDARG00000053912	GGATTTCGAGGAGGCAGGGGTGG
tcf12	ENSDARG00000004714	AGCTTCCAGTGGCGTTCCCTCGG

tcf12	ENSDARG00000004714	GTGGGCGACACCGAGTGTGGCGG
smad6b	ENSDARG00000031763	TGTGCTGCAGGTCAGACCACCGG
smad6b	ENSDARG00000031763	GGGGAAAGTCTTGAGTATGGAGG
vgll2a	ENSDARG00000041706	AGGGGACATCAGTTCGGTGGTGG
vgll2a	ENSDARG00000041706	GTGTATGCGGCTGCAAAATACGG
vgll2b	ENSDARG00000053773	TGGAGCCAGGTAAGCTGATGAGG
vgll2b	ENSDARG00000053773	GAGGTCGGCTCGGGGGAGAGGGG
neurod4	ENSDARG00000003469	TGGCTTTGATTCGGCGGGCACGG
neurod4	ENSDARG00000003469	TGGTTGTGGGCCCAAGTTGGAGG
nr2f1a	ENSDARG00000052695	AGCGCATACTGGCCCGGGTTCGG
nr2f1a	ENSDARG00000052695	GCCGTCCCTGGTGTGGACGGAGG
nr2f1b	ENSDARG00000017168	TGCGGTGGTGCTGATCCACCGGG
nr2f1b	ENSDARG00000017168	TGGCTCGGGTTCGGCTGGTTCGG
tead1a	ENSDARG00000028159	TGTGTCGTTGAAGGATCATACGG
tead1a	ENSDARG00000028159	CGGCAGTGAAAGTGCCGGGGAGG
tead1b	ENSDARG00000059483	GACACCTGCGGGGTAGGGGAGGG
tead1b	ENSDARG00000059483	AGAGGCCGGTCTTACCCCTGCGG
tead3a	ENSDARG00000074321	GATGATCTTTCTGCGGCCACAGG
tead3a	ENSDARG00000074321	TGAAGGGTAGGGTACGGGCTCGG
tead3b	ENSDARG00000063649	TGAAGGTATGCGCTTTCCTGCGG
tead3b	ENSDARG00000063649	GATGGGGGTCGGCCAGAACTGGG
dspa	ENSDARG00000022309	TGGCACGTGACTGGACCTGGAGG
dspa	ENSDARG00000022309	AGGCTGATGCTCAGAGGGTTTGG

wu:fi04e12	ENSDARG00000076673	AGGATCTGAATATTCAGCGGCGG
wu:fi04e12	ENSDARG00000076673	GACGACGGCCTGGAGGAGTGCGG

Table II. sgRNAs used for CRISPR/Cas9 screen

1.h.2. Vsx1/Vsx2 stable lines

Generation of vsx1/vsx2 null stable lines was performed by Joaquin Letelier, a former postdoc in the Martinez-Morales lab. Injected F0 was raised to sexual maturity and then outcrossed with a WT partner to genotype the F1 embryos. This individuated F0 specimens with a mutation for our target genes in the gonads that can be transmitted to the offspring. Various mutant alleles were individuated. In zebrafish, we choose to maintain as -/- stable lines two deletions of 245 and 73 bps, for Vsx1 and Vsx2 respectively. Both deletions eliminate the DNA binding homeodomain of the TFs and also produce a premature stop codon. In medaka, we choose to maintain as -/- stable lines a deletions of 148 bps and a combination of a deletion of 319 and an insertion of 9 bps, for Vsx1 and Vsx2 respectively. The sequences of the sgRNAs used to produce the deletions and the primers to detect the mutation are showed in the tables below (Table III and IV). The double mutant embryos do not reach adulthood, so we obtained double mutant embryos for our analysis from an incross of Vsx1 -/- Vsx2 +/- adults in zebrafish, and from an incross of Vsx1 +/- Vsx2 -/- in medaka.

gene	**gene ID**	**sgRNA_seq (5'->3')**
Vsx1_ZF	ENSDARG00000056292	TAGTTCCTCAAGTTGATGGGAGG
Vsx1_ZF	ENSDARG00000056292	CGTTTACGCGAGAGAAATGCTGG
Vsx1_MD	ENSORLG00000002999	TGTTCTAGAGCATATTGTCTGTTCC
Vsx1_MD	ENSORLG00000002999	GTTAGGGCCTGACCTGGATTCGG
Vsx2_ZF	ENSDARG00000005574	GCTGCCGGAGGACAGAATACAGG
Vsx2_ZF	ENSDARG00000005574	ATTTCTCTGGCGTACACATCCGG
Vsx2_MD	ENSORLG00000022205	TGGGATGATGAGAGTCAAGTTGG
Vsx2_MD	ENSORLG00000022205	GAAAAAAATAACAGAATTGAAGG

Table III. sgRNAs used to generate vsx1 and vsx2 mutant alleles with CRISPR/Cas9 system.

gene	gene ID	Fw_primer (5'->3')	Rv_primer (5'->3')
Vsx1_ZF	ENSDARG00000056292	ATGACTGCCTTTCCGGTGAT	CTGCTGGCTCACCTAGAAGC
Vsx1_MD	ENSORLG00000002999	AACAATAATTTAAAATGCGGAAAAA	GAAACTAAAATCCCATTCAGTGCT
Vsx2_ZF	ENSDARG00000005574	TCGTAATCTTTCCACTGATTCTGAT	TGTTCTAGAGCATATTGTCTGTTCC
Vsx2_MD	ENSORLG00000022205	ATATCACGGGAAATTAAAATGCTC	AAGTCAAATGTGCCATTGTTAGTC

Table IV. Primers used to genotype vsx1 and vsx2 mutant alleles.

1.i. Cell culture

The RPE differentiation starting from hiPSCs was performed by our collaborator Berta de La Cerda (CABIMER, Seville). Human hiPSCs were obtained for reprogramming using non-integrative Sendai virus starting from monocytes deriving from a sample of peripheral blood of a healthy control of age-related macular degeneration (AMD). After a complete characterization including pluripotency markers, karyotype, and differentiation of the three embryonic leaflets, the hiPSCs cell line is considered suitable for use. The cells are maintained in feeder-free conditions, in an adherent culture in covered dish with Matrigel and mTser1 medium in standard incubation at a 37ºC, 5% CO_2 and 20% O_2. Culture medium is changed every two days and cells are passed every 5-7 days, depending on the confluency rate. Dispase is used for gentle dissociation during the passage. The starting point of the experiment (Day 0) is a well of iPS cultured in the described conditions. Then, for the other cell wells the culture medium was changed to RPE differentiation medium (KO DMEM, KSR 15%, Glutamax 2 mM, non-essential aminoacids 0.1 mM, β-mercaptoethanol 0.23 mM, Peniciline/streptomycin). The differentiating cells were harvested directly in Trizol LS (Invitrogen) at day 1, 2, 3, 4, 5, 6, 7, 8, 9 and week 2, 3 and 4 to assess the gene expression of the candidate genes.

1.l. RT-qPCR

One microgram of total RNA, as evaluated by Nanodrop 2000, was reverse transcribed with SuperScript™ IV VILO Mastermix (Thermo Fisher Scientific). Quantitative Real-Time PCR was performed in a CFX96 thermocycler (Bio-Rad) using 20 ng of cDNA (calculated on the basis of the retro-transcribed RNA), 300 nM of each primer and SsoAdvanced Universal SYBR Green Supermix (BIO-RAD). A 2-step thermal protocol with a TaOpt (optimum annealing temperature) of 60 °C was used. Assays were performed in triplicate with a maximal ΔCt of replicate samples ≤ 0.5. Relative expression analysis, corrected for PCR efficiency and normalized respect to reference housekeeping genes was performed with the CFX96 Manager software

(Bio-Rad) for group-wise comparison and statistical analysis. For human samples, HPRT1 and GAPDH were used as housekeeping genes, whereas for zebrafish eef1a1l1 was used.

For primer sequences see table below (Table V and VI).

Human primers:

gene	**gene ID**	**Fw_primer (5'->3')**	**Rv_primer (5'->3')**
OCT4	ENSG00000204531	CTTCAGGAGATATGCAAAGCAGA	TGATCTGCTGCAGTGTGGG
NANOG	ENSG00000111704	GGATCCAGCTTGTCCCCAAA	AGGAAGGAAGAGGAGAGACAGT
RPE65	ENSG00000116745	ACCACCTGTTTGATGGGCAA	AGTGCGGATGAACCTTCTGT
CRALBP	ENSG00000116745	GTCACAACTTGGCCCTGACT	GGTCCATGGTCCTTGGTTGT
TYR	ENSG00000077498	GATTCAGACCCAGACTCTTTTCA	ACGACACAGCAAGCTCACAA
HPRT1	ENSG00000165704	CCCTGGCGTCGTGATTAGTG	TCGAGCAAGACGTTCAGTCC
GAPDH	ENSG00000111640	AGGTCGGAGTCAACGGATTT	TGGAATTTGCCATGGGTGGA
MITF	ENSG00000187098	CCGGGCTCTGTTCTCACTTT	GGAACTGCTGCTCTTCAGCG
OTX2	ENSG00000165588	CCTCACTCGCCACATCTACT	AGTGGAACTTACAGCCTCATGG
BHLHE40	ENSG00000134107	ATTAACGAGTGCATCGCCCA	AGCTCACCAGCTTGTAAACCA
TFEC	ENSG00000105967	GATAAAATCCACTCATTGCTGGTCC	GGGCTTTCTGTAGCTGAGGC
TFAP2A	ENSG00000137203	GAGAGTAGCTCCACTTGGGTG	CCGTCGTGACGGTCCTCG
TFAP2C	ENSG00000087510	GAAGAGGACTGCGAGGATCG	GCTGATATTCGGCGACTCCA
TEAD1	ENSG00000187079	CCATTCCAGGGTTTGAGCCT	GCTTGGTTGTGCCAATGGAG
TEAD2	ENSG00000074219	TCGGAATGAACTGATCGCCC	CCTGGTCCTTCAACTTGGACT
TEAD3	ENSG00000007866	GACCGTACCATTGCCTCCTC	TTGCTGTACGTGTCAGGGTC
TEAD4	ENSG00000197905	GGCACCATTACCTCCAACGA	CAGCTCGTTCCGACCATACA

TCF12	ENSG00000140262	CCATGAAGGCTTGTCCCCAA	GGAGACTAGATTGACAGCCTGG
VGLL2	ENSG00000170162	GCTTTGCTCCGCCTGATGAC	ATAGGCTAGTTTCTGGTGGTAGG
SMAD6	ENSG00000137834	GGGCCCGAATCTCCGC	GGTCGTACACCGCATAGAGG
KRT5	ENSG00000186081	CGAGGAATGCAGACTCAGTG	GCTGCTGGAGTAGTAGCTTCC
KRT4	ENSG00000170477	TCCTTCATCGACAAGGTGCAG	GGGCTCAAGGTTTTTGCTGG
KRT8	ENSG00000170421	CAGCAAATGTTTGCGGAATGAA	AACCAGGCGGAGATCCCTTC
DSP	ENSG00000096696	AGGCTGGAGTACGATGACCT	TAGATGCCTCTAAAGCCTGC
EVPL	ENSG00000167880	CGACTTCCGACTGCTCCATCT	CCAAGTCCTCCAAGGGTGTG
NOTCH1	ENSG00000148400	CTGCCTCTTCGACGGCTTT	AAGTGGAAGGAGCTGTTGCG
NOTCH2	ENSG00000134250	CGAGTGTGTCCCAGGCTATC	CTTCACAGAGTAGGCCCCGA
NOTCH3	ENSG00000074181	GTCTTCCTGGGTTTGAGGGTC	GGGCACTGGCAGTTATAGGT

Table V. Primers used for Real Time q-PCR of human samples.

Zebrafish primers:

gene	**gene ID**	**Fw_primer (5'->3')**	**Rv_primer (5'->3')**
tyr	ENSDARG00000039077	ACGGATACTTCATGGTGCCC	CGCTGACCTGGATCCTGTAAAT
tyrp1b	ENSDARG00000056151	GCCCGTCCAATGGTTCAAAG	GGAGCGCTGTAACCCTCAAT
krt4	ENSDARG00000017624	CTTCGTTGCGGCTCCTATCA	TCCAGGAAGCGCACTTTGTC
krt8	ENSDARG00000058358	TCCGCGCTCAGTATGAAGAC	AAGTTGGCTCGCTGTCCTTT
six3a	ENSDARG00000058008	AAAAACAGGCTCCAGCATCAA	AAGAATTGACGTGCCCGTGT
vsx2	ENSDARG00000005574	GGGATTAATTGGGCCTGGAGG	GCTGGCAGACTGGTTATGTTCC
eef1a1l1	ENSDARG00000020850	TCCACCGGTCACCTGATCTAC	CAACACCCAGGCGTACTTGA

Table VI. Primers used for Real Time q-PCR of zebrafish samples.

1.m. Cryosectioning

Medaka and zebrafish embryos at the appropriate stage for each experiment were dechorionated. The head were dissected and then fixed in 4% (w/vol) paraformaldehyde (PFA, Merck) in 0.1 M phosphate buffer overnight at 4°C or 20 min at room temperature (RT), respectively. Tails were kept for genotyping. Then embryos were washed several times in phosphate buffer saline (PBS) 1X, incubated in 30% sucrose-PBS overnight at 4°C and embedded in OCT-matrix (VWR) in cryomolds, frozen in liquid nitrogen and then kept at -80°C for no more than a week. Cryosectioning was perfomed with a cryostate Leica CM 1850 at 20 µl thickness and dried overnight at RT. Then sections were processed for Phalloidin/DAPI staining.

1.n. Phalloidin/DAPI staining

Slides were dried at RT for at least 3 h, then washed with PBST (0.1% Triton in PBS) 5 times for 5 minutes. After the washes, the slides were incubated with phalloidin solution (1/50 phalloidin-Alexa 488 and 5% DMSO in PBST) at 4°C O/N, covered with parafilm and into a dark humid chamber. Nuclei staining was performed with a 1:1000 DAPI solution in PBST. Then slides were washed twice with PBST. Slides were mounted with a drop of 15% glycerol in PBS. Microscope images were captured immediately with a Leica SPE confocal microscope. 20X objective (+2X zoom) was used for a general view of the retina and a 40X one (+2X zoom) for retinal layers.

2. Bioinformatic Methods

2.a. RNA-seq analysis

After initial quality check with FastQC software (Andrews S., 2010. FastQC: a quality control tool for high throughput sequence data) the files were aligned against zebrafish genome assembly version 10 (danRer10) from Genome Reference Consortium using Tophat v2.1.0 (Trapnell et al., 2013) with the command:

tophat -p 4 -o <output_directory> -G <GTF_file> <genome_index_base> <file.fastq>

After the alignment, output bam files were sorted and indexed using the software Samtools v0.1.19. Transcript abundance and differential gene expression were estimated with Cufflinks v2.2.1 with the following commands:

Abundance estimation

cufflinks -p 4 -o <output_directory> -G <GTF_file> <sorted_file.bam>

Differential gene expression analysis

cufflinks -p 4 -o <output_directory> <GTF_file> -L <condition_A,condition_B> <A_rep1_sorted.bam, A_rep2_sorted.bam, A_rep3_sorted.bam> <B_rep1_sorted.bam, B_rep2_sorted.bam, B_rep3_sorted.bam>

We considered as differentially expressed genes (DEGs) all those variations with FDR < 0.05, if and only the sum of the FPKM of the two condition was ≥ 10. Further statistical analyses and graphical representations were mostly performed using R.

MDS

Multidimensional Scaling Analysis (MDS) was performed using the function *MDSplot* of the R package CummeRbund (Goff, Trapnell, & Kelley, 2019).

Mfuzz

Soft clustering of time-series gene expression data was done for all the transcripts with a variance among the five condition ≥ 3 using the R package Mfuzz with a m = 1.5 (Kumar & Futschik, 2007).

The TF transcript subset was extracted from the total list of genes using the tool "Classification System" of PANTHER (Mi, Muruganujan, Huang, et al., 2019) filtering for the protein class PC00218 (transcription factors). Some TFs were not present in the database, for an annotation issue, and were added to the list by hand (i.e. mitfa, vsx1, vsx2, rx1, rx2, rx3, lhx2b, hmx1, hmx4, sox21a).

The cytoskeleton component subset was obtained retrieving all the genes belonging to GO term "cytoskeleton" (GO:0005856), including all the child and further descendant GO terms, with the R library *biomaRt* (Smedley et al., 2015). The precise list of child GO terms was obtained with the R package *GO.db* (Carlson, 2019).

Heatmaps

All the heatmaps from RNA-seq data were plotted with the R package *pheatmap* (Kolde, 2019) using exclusively the transcripts that resulted to be differentially expressed from the comparison between at least two of our experimental conditions (i.e. PG16vsNR18, PG16vsNR23, PG16vsRPE18, PG16vsRPE23, NR18vsNR23, RPE18vsRPE23, NR18vsRPE18 andNR23vsRPE23). TFs and cytoskeleton components were filtered using the same methodology used for Mfuzz clustering. Prior graphical representation, expression data were normalized for row.

Gene Ontology Analysis

Gene ontology analysis was performed with the online tool GOrilla (Eden, Navon, Steinfeld, Lipson, & Yakhini, 2009) or Panther (Mi, Muruganujan, Ebert, Huang, & Thomas, 2019) using two unranked lists of genes (target and background lists).

2.b. ATAC-seq analysis

Fastq files were aligned against zebrafish genome assembly version 10 (danRer10) from Genome Reference Consortium using an automated pipeline coded in the programming language Perl by Juan J. Tena, a member of the CADB (Santos-Pereira, Gallardo-Fuentes, Neto, Acemel, & Tena, 2019). This pipeline involves the alignment with Bowtie2, the sorting of the output aligned files with Samtools and finally a conversion of the outputs to bed files.

After alignment, peaks were called using the software MACS2 (Zhang et al., 2008) with the following options:

macs2 callpeak -f BED -t <input_file.bed> --outdir <output_directory> -n <output_filename> --extsize 100 --nomodel --shift 50 -g 1464443456

Macs2 output file structure was modified in order to obtain for each peak an identifier name and the correspondent read value in a format that could be used in R for subsequent analyses. Differentially chromatin accessibility was assed using DESeq2, an R package to estimate variance among high-throughput sequencing data (Love, Huber, & Anders, 2014). All chromatin regions reporting a differential accessibility with an adjusted p-value < 0.05 were considered as differentially open chromatin regions (DOCRs).

All the DOCRS have been associated with genes using the online tool GREAT (Hiller et al., 2013) with the option “basal plus extension”. Gene ontology analysis of the genes associated with DOCRs was also performed with GREAT.

De novo motif discovery to calculate the enrichment of particular TF binding sequences in the sets of DOCRs was performed using HOMER (Sven et al., 2010).

Graphical representation of the percentage of DOCRs falling in the different position of the genome was obtain with the R package ChIPseeker (Yu, Wang, & He, 2015) using the function *plotAnnoPie*. The graphical representation of distance from TSS within 3000 bps was obtained with the function *plotAvgProf*.

TF co-occupancy analysis

Top enriched binding motif matrices from the HOMER discovery and binding motif matrices from CISbp database (Weirauch et al., 2014) were used as input for the online tool FIMO (Grant, Bailey, & Noble, 2011) to assess their exact genome position in the DOCRs. Before estimating the rate of TF co-occupancy in same peak among the binding motifs for the different TFs, all the binding motif sequences overlapping for more than 3 bps were eliminated, keeping only the TF binding sequence with the lowest p-value. TF co-occupancy was represented using the online tool *Circo Table Viewer* (http://mkweb.bcgsc.ca/tableviewer/; Krzywinski et al., 2009). Correlation was calculated using the R library *corrplot* (Wei & Simko, 2017).

Activator/repressor cis-regulatory element configuration

For this analysis only the DEGs and the DORCs having a correspondent association between each other were used. The *x* of the cartesian graph represents the log2 of the fold change from the differential expression analysis between the conditions NR 23 hpf and RPE 23 hpf, whereas the y represents the log2 of the fold change from the ATAC-seq data for the same two conditions. The clusters derived from this analysis where used to calculate the number of activator elements and repression elements associated with TFs.

Data Repository

The omics approach used in this thesis work generated a large amount of data poorly suitable to be printed on paper. Main results are always reported in the text, with a reference indicating the main dataset to which they belong. Complete datasets can be found be found as *Appendix* at the following online link:

http://193.147.188.155/lbuo/PhDThesis

Results

1. Eye domain transcriptomic analysis

As already mentioned in the introduction, our current understanding of the mechanisms controlling the bifurcation of the optic vesicle GRN into two distinct and mutually exclusive developmental programs for NR and RPE is still fragmentary. To shed light on this topic, we took advantage of two zebrafish transgenic lines that mark NR and RPE: the tg(*vsx2.2*:caax-GFP) and the tg(enh1-*bHLHE40*:GFP) respectively. These lines allow following the differentiation and morphogenesis of these domains from their initial specification (Fig 1 C).

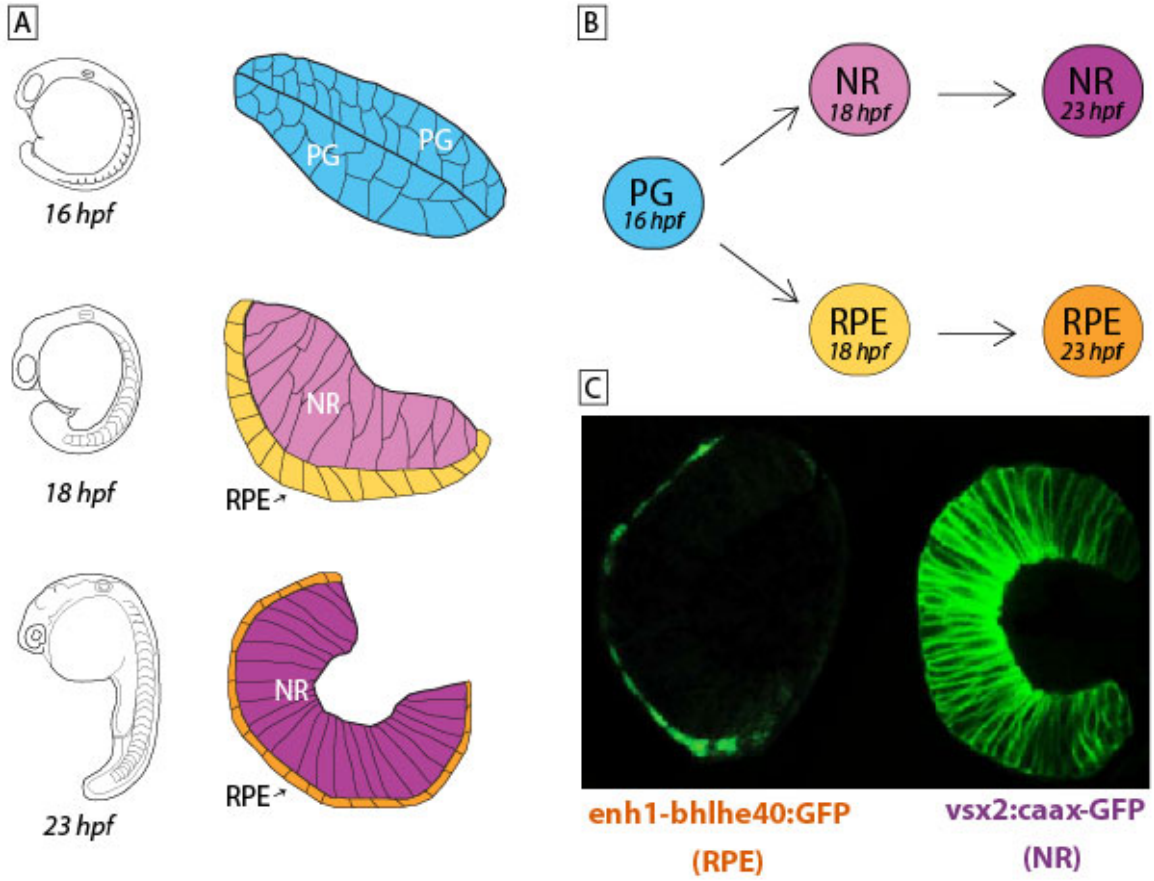

Figure 1. *(A)* ***Morphogenesis of the zebrafish optic vesicle into the optic cup.*** *At 16 hpf the optic vesicle is composed by two layers of undistinguishable and undifferentiated retinal progenitors cells (PG). Both layers are flat columnar epithelia of nearly equal thickness. At 18 hpf the dorsal layer cells (RPE) began to flatten, while the ventral layer cells (NR) acquire a bottle-shaped morphology and fold for basal constriction. At 23 hpf the embryonic eye has completely cup-shaped. The NR is now much thicker and about to start neurogenesis, whereas the RPE has completely lost columnar cells and is entirely squamous. (B) Eye domain cell populations we isolated by flow cytometry. (C) Zebrafish transgenic lines used to mark and isolate the different eye domain populations.*

Vsx2 (*visual system homeobox 2)* is a TF already very well known to be a main player during retina differentiation. It is initially expressed throughout the whole optic vesicle, but after the cell fate splitting of the eye progenitors, its expression gets restricted only to the presumptive NR domain (Gago-rodrigues, 2015). *BHLHE40* (*Basic Helix-Loop-Helix Family member 40*), encodes a light- and hypoxia-induced TF involved in several processes such as differentiation, proliferation and circadian rhythms (Yamada & Miyamoto, 2005). In zebrafish, *bHLHE40* expression is confined to the RPE presumptive domain and, if compared with other known RPE markers, such as *mitf*, *tfec* or *cx43*, its expression is among the earliest (Yao et al., 2006). *BHLHE40* expression pattern makes this gene a proper marker- for the RPE. Sergio Salgüero, a former member of the Bovolenta's lab, analysed different *bHLHE40* cis-regulatory regions and identified specific enhancers modulating the expression of this gene specifically in the RPE, with no interference in the nearby NR or neural tube. They called this cis-regulatory region "enhancer 1" (enh1; for further details see Method section). Coupling these two transgenic lines with flow cytometry technology we isolated five different eye cell populations at different stages of development (Fig 1A-B):

- *optic vesicle eye progenitors (PG) at 16 hpf*, immediately before the optic cup folding, when the two cell layers are still morphologically and molecularly indistinguishable;
- *committed precursors of NR and RPE at 18 hpf,* during the optic cup folding, when the two domains have already started to diverge in shape e molecular identity;
- *immature NR and RPE at 23 hpf*, when the optic cup folding is finishing, the two cell layers have acquired completely different morphology (bottle-shaped for the NR an flat for the RPE) and the neurogenesis of the neural retinal precursor cells (RPCs) is about to start.

The transcriptomic analysis of these different cell populations highlighted thousands of genes significantly modifying their expression during the development from the optic vesicle state (Fig 2A-B; complete tables of DEGs in online Appendix I). Even if the transcript landscape changes are in any case robust, we could appreciate a higher number of transcriptional changes towards RPE differentiation rather than towards NR. Furthermore we calculated the divergence between our experimental conditions by multimensional scaling (MDS) our RNA-seq datasets into a Cartesian space (Fig 2C). In our graphical representation each dimension represents similarity/dissimilarity grade between our samples. This highlights a gradual separation of the transcriptomic landscapes of the NR and RPE from the PG over time. The biggest transcriptomic variations occur between PG at 16 hpf and NR and RPE at 18 hpf (developmental time = 2 hours), when the optic cup has just started its folding and only modest cell shape changes can be appreciated. Later, between 18 hpf and 23 hpf stages (developmental time = 5 hours) we can spot only modest transcriptional variations, that are even smaller in the case of NR. This suggests that both domains, but especially NR, are specified and undergo dramatic transcriptome changes before the optic cup folding begins. Furthermore this happens despite the fact that the architecture of these two tissues is not yet extremely divergent.

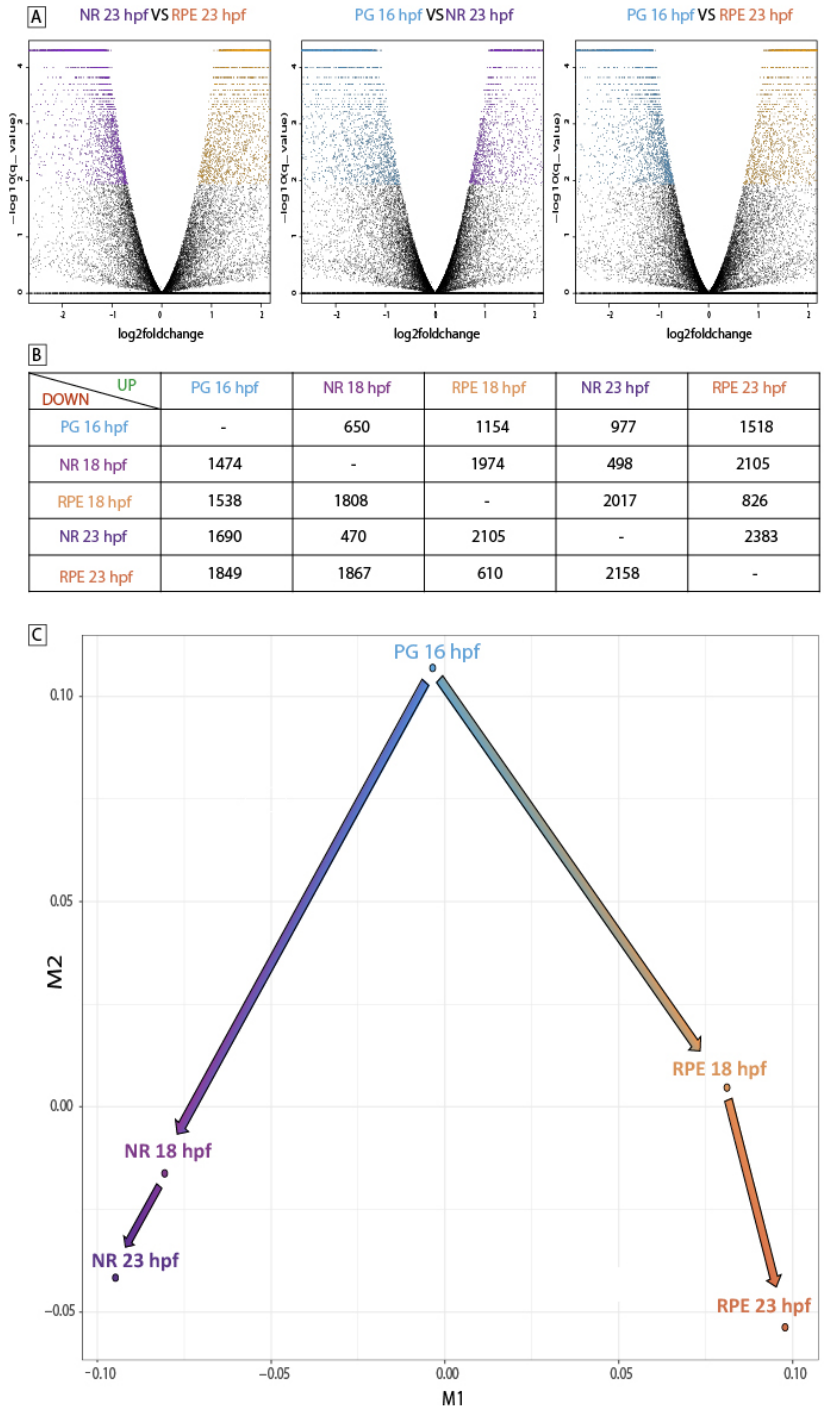

DOWN \ UP	PG 16 hpf	NR 18 hpf	RPE 18 hpf	NR 23 hpf	RPE 23 hpf
PG 16 hpf	-	650	1154	977	1518
NR 18 hpf	1474	-	1974	498	2105
RPE 18 hpf	1538	1808	-	2017	826
NR 23 hpf	1690	470	2105	-	2383
RPE 23 hpf	1849	1867	610	2158	-

Figure 2. Eye domain transcriptome variations during optic cup morphogenesis. *(A) Volcano plots illustrating the transcriptome variations during eye morphogenesis. Each dot corresponds to a gene. Black dots indicate not significant variations, whereas coloured dots point out significant expression variations. (B) Table resuming the number of DEGs (upregulated or downregulated) between each considered condition. (C) MDS of the RNA-seq data from different eye domains at different developmental stages illustrating the grade of divergence among transcriptomic landscapes.*

2. Eye domain cis-regulatory landscape analysis

To gain insight into the architecture of the optic cup GRN, we performed ATAC-seq for NR and RPE at 23 hpf. Sequenced reads can then be used to infer regions of increased accessibility at single nucleotide resolution, mapping the position of cis-regulatory elements (CRE) and TF binding sites (TFBS) (Buenrostro, Giresi, Zaba, Chang, & Greenleaf, 2013). This double RNA-seq/ATAC-seq approach allowed not only the detection of transcriptomic variations, but also the identification of the active cis-regulatory modules linked to the main TFs involved in tissue specification. This cross fire strategy also helped to define hierarchical relationships among the core components of the network.

Our ATAC-seq data detected 238´369 peaks corresponding to accessible (and, thus, somehow active) chromatin. After statistical analysis, a substantial portion of these peaks were found to be differentially open chromatin regions (DOCRs), in other words those regions correspond to cis-regulatory elements (CRE) that are more active in the NR rather than in the RPE, or vice versa. A proportion of 12.6% of all the peaks (30´172 peaks) resulted to be differentially open with an adjusted p-value < 0.05 (Fig 3; complete list of DOCRs in online Appendix II). As already happened for the transcriptome, also the chromatin accessibility landscape registered more variations specific of the RPE, and they showed a higher average fold change (Fig 3B-C).

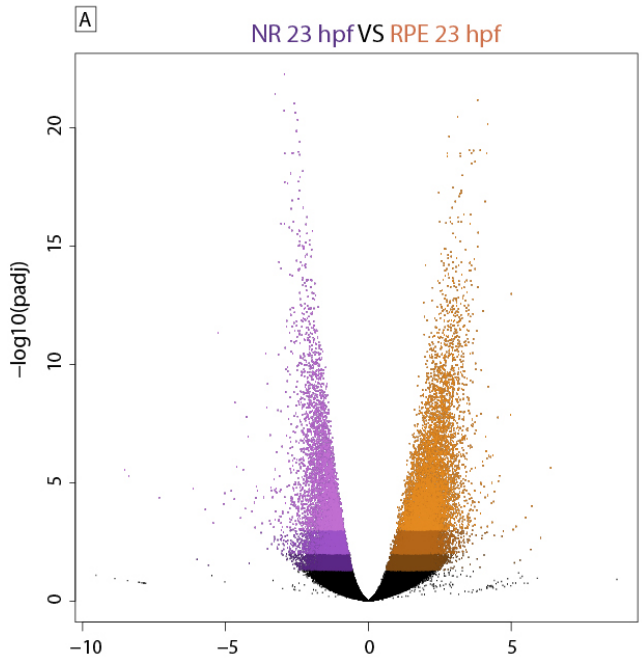

B

adj p-value	DOCRs	NR	RPE
<0.05	30172 (12.6%)	11263	18909
<0.01	19012 (7.9%)	7062	11950
<0.001	11387 (4.8%)	4237	7150

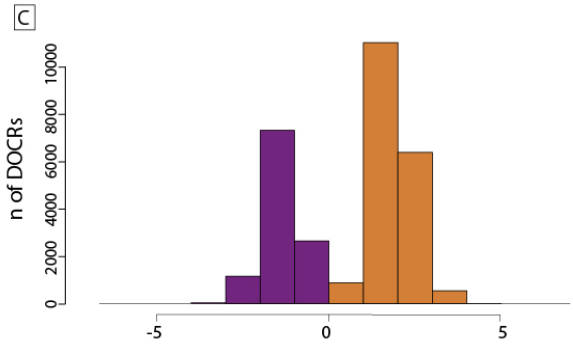

Figure 3. Chromatin landscape changes during optic cup morphogenesis. *(A) Volcano plots illustrating the chromatin accessibility changes during eye morphogenesis. Each dot corresponds to a peak. Black dots indicate not significant variations. Colour shades point out chromatin accessibility changes with different ranges of adjusted p-value (darker: p<0.05; medium= p<0.01, lighter= p<0.001). (B) Table resuming the number of peaks significantly more or less accessible between the two conditions. (C) Histogram illustrating the relations between number of DOCRs and fold change of accessibility.*

Then we examined the distribution of the differentially open chromatin regions in the genome. Even though there is no evident difference in the genome distribution of the whole set of open chromatin regions (OCRs) between NR and RPE, we could appreciate a difference between the disposition of the entire OCRs and the subsets of DOCRs (Fig 4). The genome distribution analysis revealed a decrease of DOCRs in the promoter regions, when compared to the distribution of all the OCRs identified in each domain (NR peaks in the promoter: 11.91% OCRs VS 4.6% DOCRs; RPE peaks in the promoter: 10.03% OCRs VS 3.09% DOCRs).

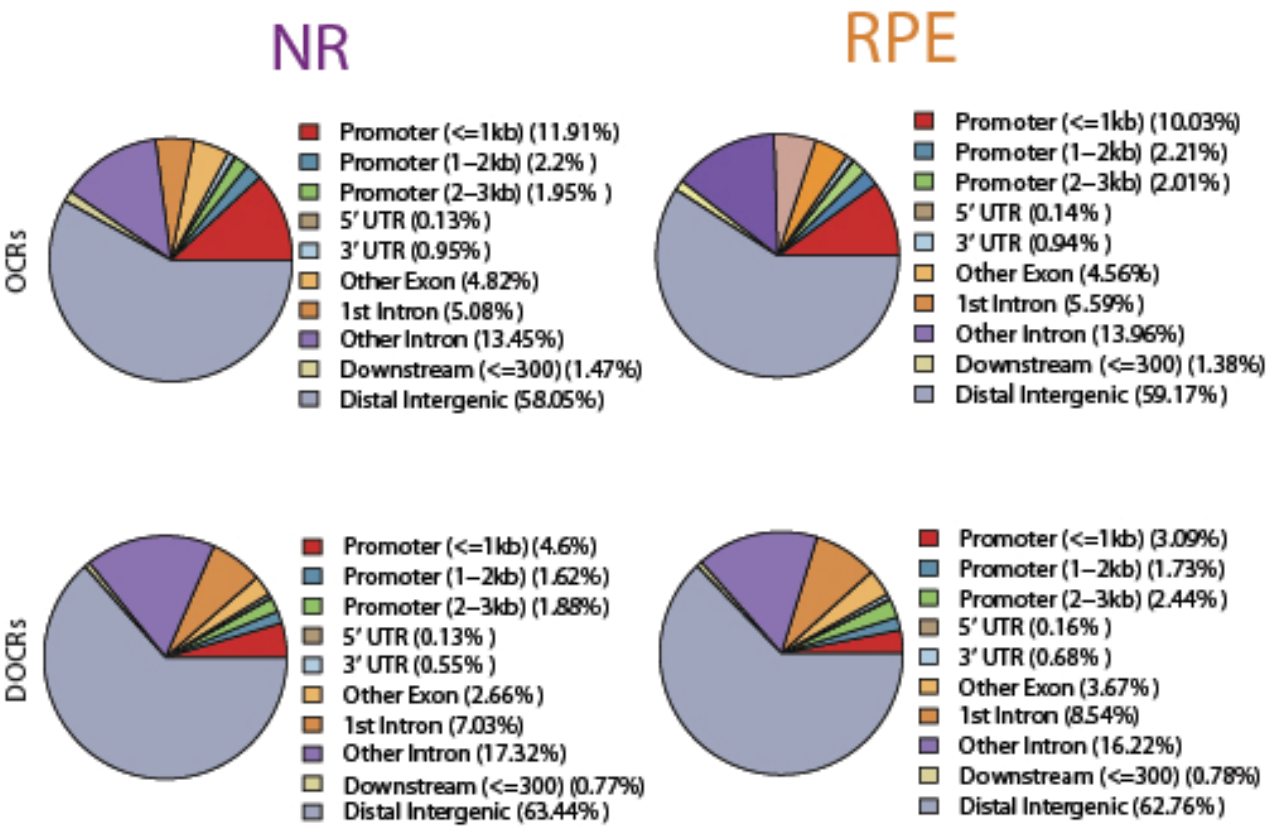

Figure 4. ATAC-seq peak genome distribution. *Pie chart displaying the percentage of peak falling in distinct regions of zebrafish genome. Above, the genome distribution of the whole set of open chromatin regions (OCRs) identified by ATAC-seq in each condition. Below, the genome distribution of the DOCRs.*

The gene ontology analysis of the biological processes linked to genes associated with DOCRs yield results consistent with the type of analyzed tissue. The NR DOCRs were found to be associated with genes involved in nervous system development, neuron differentiation and eye morphogenesis, whereas the genes associated with RPE DOCRs resulted to be implicated in melanocyte differentiation (that also are pigmented cells), epithelial differentiation and migration (Fig 5).

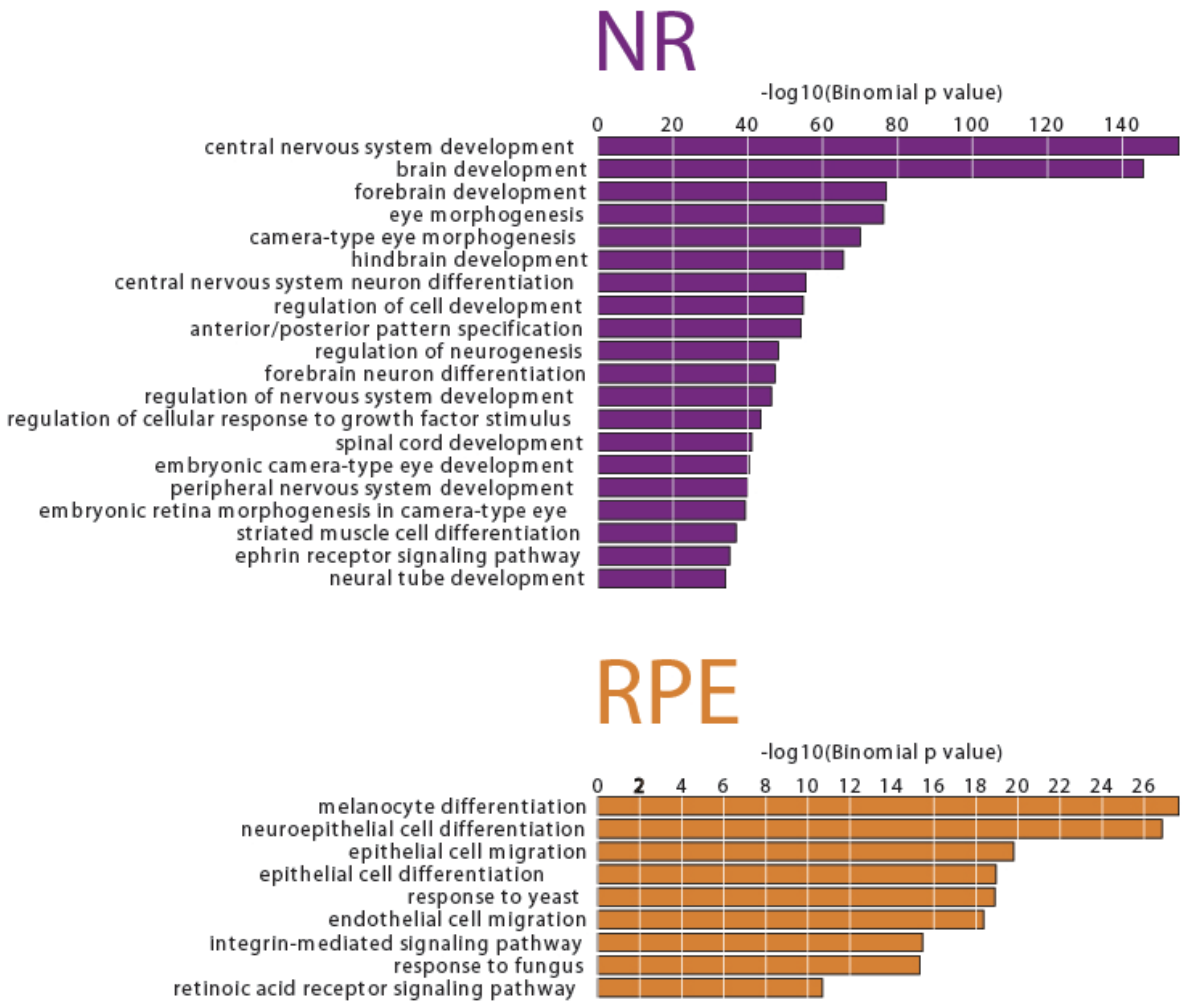

Figure 5. Gene ontology enrichment of the genes associated with DOCRs. *Bar chart showing the GO terms for biological processes enriched in the genes associated to DOCRs. Bar length is proportional to enrichment significance.*

3. Gene expression clustering

Clustering methods are usually applied to reveal regulatory mechanisms underlying gene expression. It is well known that the regulation of gene expression is not achieved by an "on/off" switch, but by a gradual modulation that allows a finer control of gene function. That is why clustering transcript trends across all conditions, rather than one to one comparison, is a more efficient approach when analyzing gene expression dynamics. Clustering can condense the data to a more comprehensible level by subdividing the gene expressions into a reduced number of categories in such a way that genes with similar expression trends fall into the same cluster, whereas genes with dissimilar expression trends fall in different clusters. This approach allows a broad exploration of the data without getting lost among the thousands of individual genes. Frequently, gene expression clusters also tend to be enriched for specific functional or biological process categories. This information may be used to infer unknown roles for genes in the same cluster (D'Haeseleer, 2005). The two most important classes of clustering methods are hierarchical

clustering and partitioning. In hierarchical clustering, each cluster can be subdivided into smaller clusters, producing an agglomerative tree-shaped data structure, also known as dendrogram. Hierarchical clusters are the kind of clusters also used in phylogenetics. On the other hand, partitioning methods produce sharper clusters by subdividing the data into a predetermined and non-overlapping number of groups, without any kind of relationship between them (Fig 6). However, with partitioning methods, establishing how many clusters are actually present in our data is not trivial and it has to be determined "empirically". A common approach is to repeat the clustering with different numbers of clusters, trying to assess the optimal number of clusters to use.

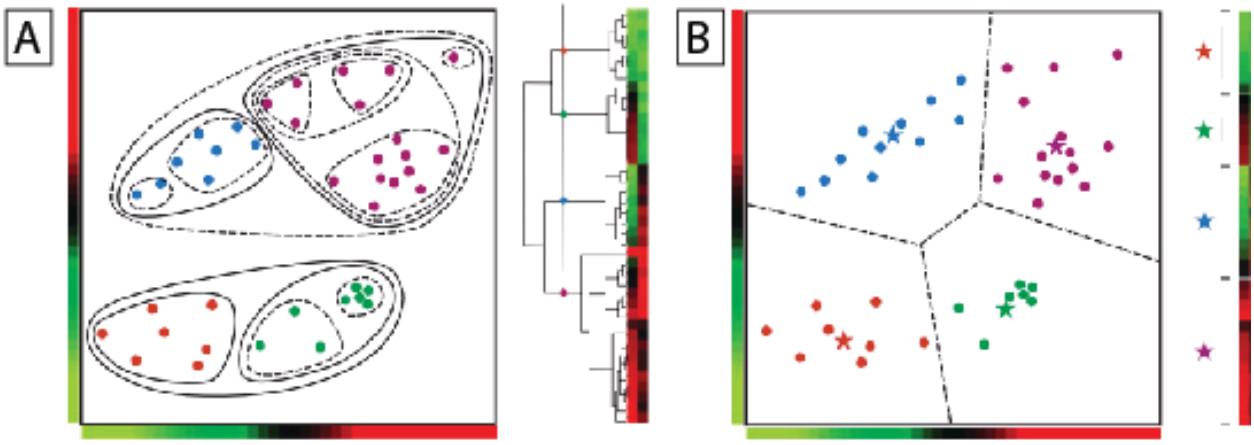

Figure 6. Graphical explanation of the difference between hierarchical and partitioning clustering method. *A simple clustering example with 40 genes measured under two different conditions. The data set contains four clusters of different sizes, shapes and numbers of genes. (A) Hierarchical clustering finds an entire hierarchy of clusters. The tree was cut at the level indicated to yield four clusters. (B) k-means (with k = 4) partitions the space into four subspaces, depending on which of the four cluster centroids (stars) is closest. Adapted from D'haeseleer, 2005.*

To obtain a more exhaustive glance on our datasets we use both hierarchical and partitioning soft clustering for two different classes of genes: TFs and cytoskeletal components. As differentiation and morphogenesis are coordinated phenomena, we wanted to individuate not only the transcriptional specifiers directly responsible of cell fate determination, but also terminal effectors acting during the divergent cell shape remodelling of the NR and RPE. For this last category we focused our attention in genes encoding for cytoskeletal proteins and regulators. With partitioning soft clustering, for both TFs and cytoskeleton components, we discriminated 25 groups of gene expression variation during development from PG towards NR or RPE (Fig 7; tables containing genes belonging to each cluster is in online Appendix III and IV). For TFs, the top three clusters including the highest number of genes (cluster 19 = 53 genes; cluster 11= 48 genes; cluster 21= 45 genes), all refers to TFs upregulated in NR, whereas for cytoskeletal components this tendency appears to be inverted. When considering only the molecules involved in cell

shaping and morphogenesis, the transcripts in the first three bigger clusters are all increased in the RPE (cluster 6= 39 genes; cluster 22= 36 genes; cluster 5= 32 genes).

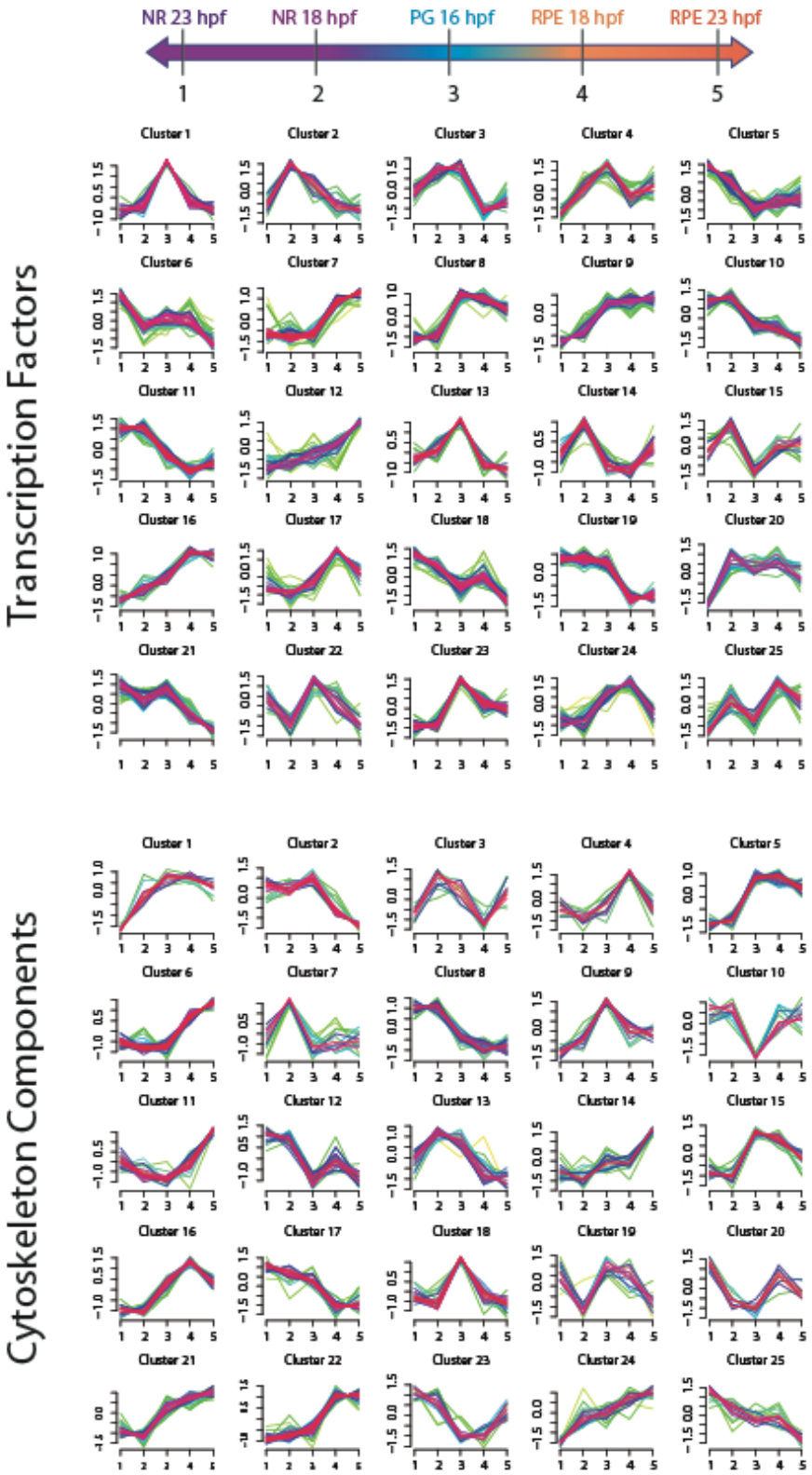

Figure 7. Partitioning clustering of gene expression variations during optic cup development. *Partitioning clustering output (k= 25) showing the expression trends in the distinct domains and stages examined for two classes of genes: TFs (above) and cytoskeleton components (below).*

Classification of differentially expressed TFs and cytoskeletal components involved in the development of the NR vs the RPE is even clearer using the hierarchical clustering approach. We could aggregate all the small sub-groups in 6 big clusters for TFs and 8 for cytoskeletal components (Fig 8; lists of genes belonging to each cluster in online Appendix V and VI).

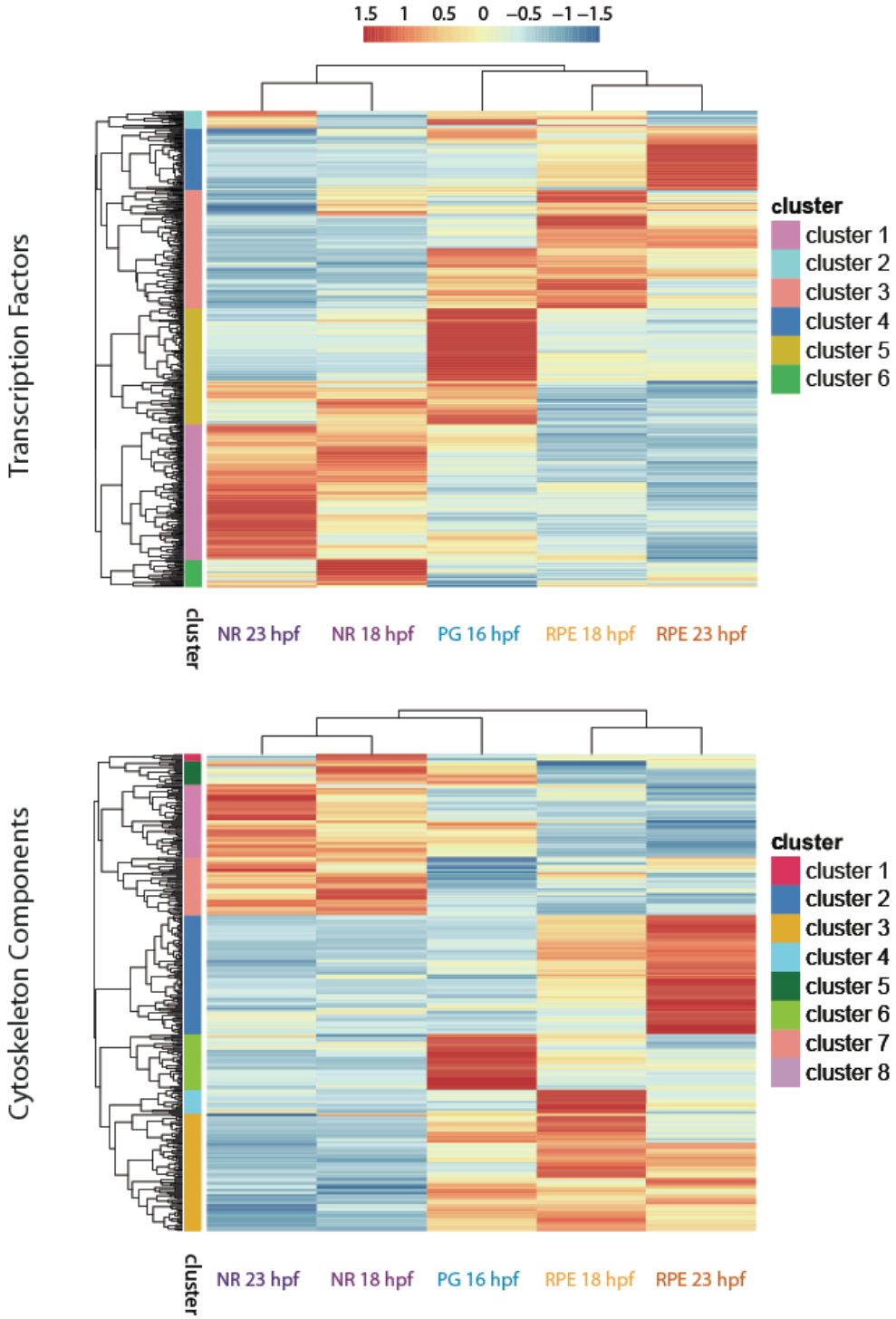

Figure 8. Hierarchical clustering of gene expression variations during optic cup development. *Hierarchical clustering output showing the expression trends in the distinct domains and stages examined for two class of genes: TFs (above) and cytoskeleton components (below).*

Every big cluster can be related to a specific domain and/or stage of the optic cup. With this kind of visualization we cannot appreciate a remarkable difference between the total amount of TFs specific of the NR vs RPE., However, when evaluating the transcript variations of the cytoskeleton molecules, the genes increasing their expression towards the RPE differentiation are a 61% more than in NR (RPE: cluster 2 (90 genes) + cluster 3 (89 genes) + cluster 4 (18 genes) = 197 genes; NR: cluster 1 (55 genes) + cluster 5 (18 genes) + cluster 7 (44 genes) + cluster 8 (5 genes) = 122 genes)(Fig 9). The meaning of these differences will be discussed in a further section.

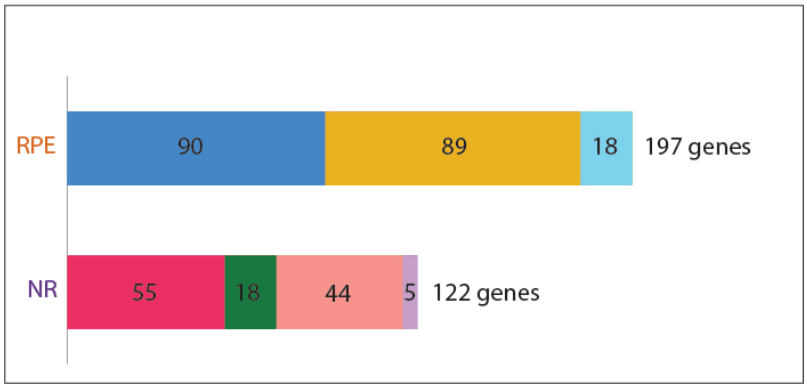

Figure 9. Number of genes belonging to cytoskeleton clusters. *Bar plot indicating the number of genes composing each NR or RPE cytoskeleton cluster. In total, RPE clusters comprise 61% more genes than NR clusters. Colour code reflects Fig. 8.*

Then, we focused our attention on the identity of TFs belonging to different clusters, trying to define precise time windows of expression to infer their hierarchical order of action. Among many other factors (complete list in online Appendix V) we highlighted the presence of significant TF for every cluster:

- *PG 16 hpf (cluster 5)*: *rx3* (which is well known to promote optic vesicle evagination and for being one of the EFTFs (Kennedy et al., 2004; F. Loosli et al., 2001; Felix Loosli et al., 2003; Mathers, Grinberg, & Mahon, 1997; Voronina et al., 2004)), *her* factors (involved in cell and neuronal differentiation (Gaudet, Livstone, Lewis, & Thomas, 2011)) and *foxc, foxd* and *klf* factors (both controlling development, proliferation and growth (Golson & Kaestner, 2016; McConnell & Yang, 2010)) (Fig 10).
- *NR 18 hpf (cluster6)*: *her* factors (also present in PG cluster), *sox19a* and *sox11b*, *vax2* (that controls dorso-ventral patterning of the retina (Schulte, Furukawa, Peters, Kozak, & Cepko, 1999)) and nr2f1b (whose role during retina development has been poorly explored) (Fig 10).
- *NR 23 hpf (cluster1)*: *rx1, rx2, sox2, six3a, six3b, six6b, vsx1, vsx2, hmx1, hmx4 and lhx2b* (all the long- and well-known retina fate specifiers) (Fig 10).
- *RPE 18 hpf (cluster 3)*: *her, foxa, foxi* and *klf* genes (factors belonging to the last three families were present also in PG cluster. *Her* factors, but no *fox* or *klf* factors, were contained also in the NR 18

hpf cluster) *teads and vgll2* factors (effectors and modulators of the Yap/Taz pathway), *grhl* factors, *tcf12, smad2, smad6b*, *tfap2a* and *tfap2c* (Fig 10).

- *RPE 23 hpf (cluster 4)*: *klf* factors (again), *bHLHE40*, *otx2* and *mitfa* (Fig 10).
- *cluster 2:* a small cluster of genes with an expression pattern unrestricted to a specific eye domain (Fig 10).

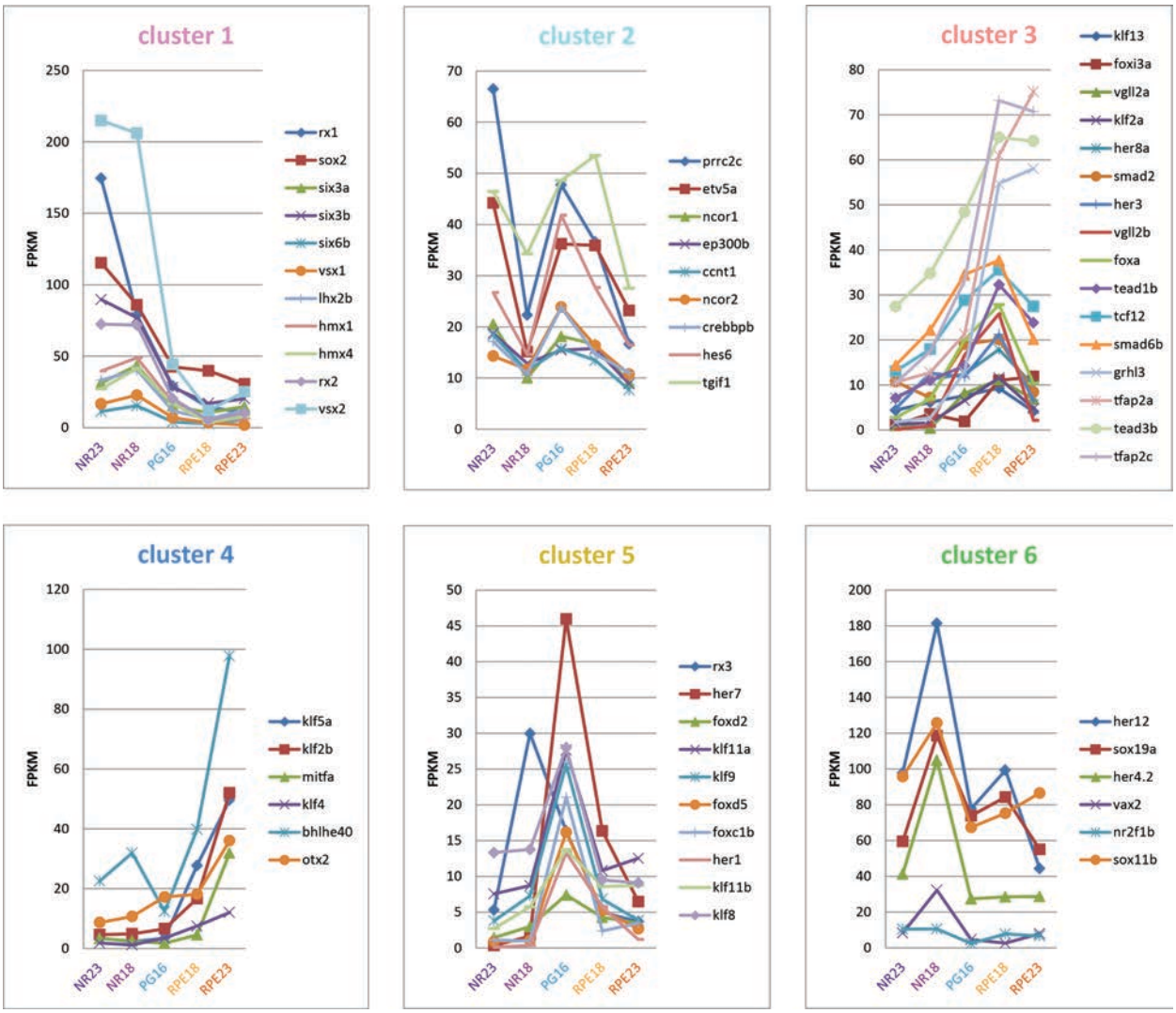

Figure 10. TF cluster gene expression. *Detailed transcript level changes for a group selected TFs in each cluster from Fig. 8.*

The genes included in the NR clusters encompass the majority of the TFs already known to be involved in RPC specification. Most of them started to significantly increase at early stage and the high level of transcript is maintained throughout NR development, peaking at 23 hpf. In contrast, long-known RPE specification genes *otx2* and *mitfa* do not increase at RPE early stage and present no significant changes of the transcript level between PG VS RPE 18 hpf or NR 18 hpf VS RPE 18 hpf. However, cluster 3 TFs such as *tead3b*, *tfap2a* and *tfap2c* started to rise in the RPE already at 18 hpf. Notably, TFs like *tcf12*, *smad6b* and especially *vgll2b* not only peak at 18 hpf, but also rapidly decrease at 23 hpf (Fig 10).

Subsequently, we analysed the content of cytoskeletal component hierarchical clusters by considering the clusters of genes upregulated in PG (*cluster 6*), in NR (*clusters 1, 5, 7* and *8*) or in RPE (*clusters 2, 3* and *4*) and performed a gene ontology (GO) enrichment analysis for the three groups of genes. While the analysis of the list of genes upregulated in PG returns no significant enrichment, the biological process (Fig 11) and cytoskeletal cellular components (Fig 12) enriched in NR are all related to microtubule complex and centrosome organization. This is in agreement with the elongation of the apico-basal axis and the polarization of the microtubules in NR precursors.

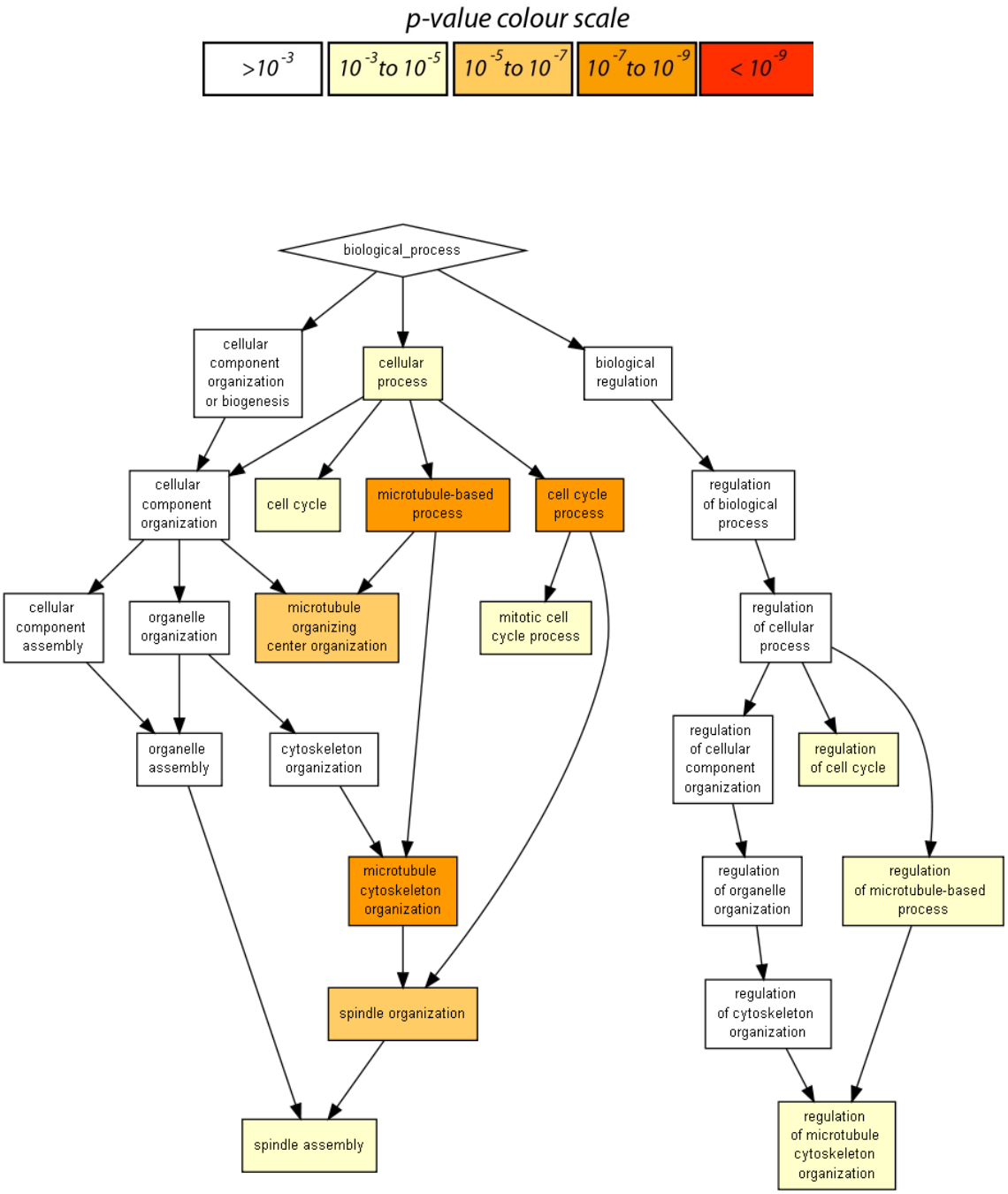

Figure 11. Biological process GO enrichment of genes belonging to cytoskeleton NR clusters.

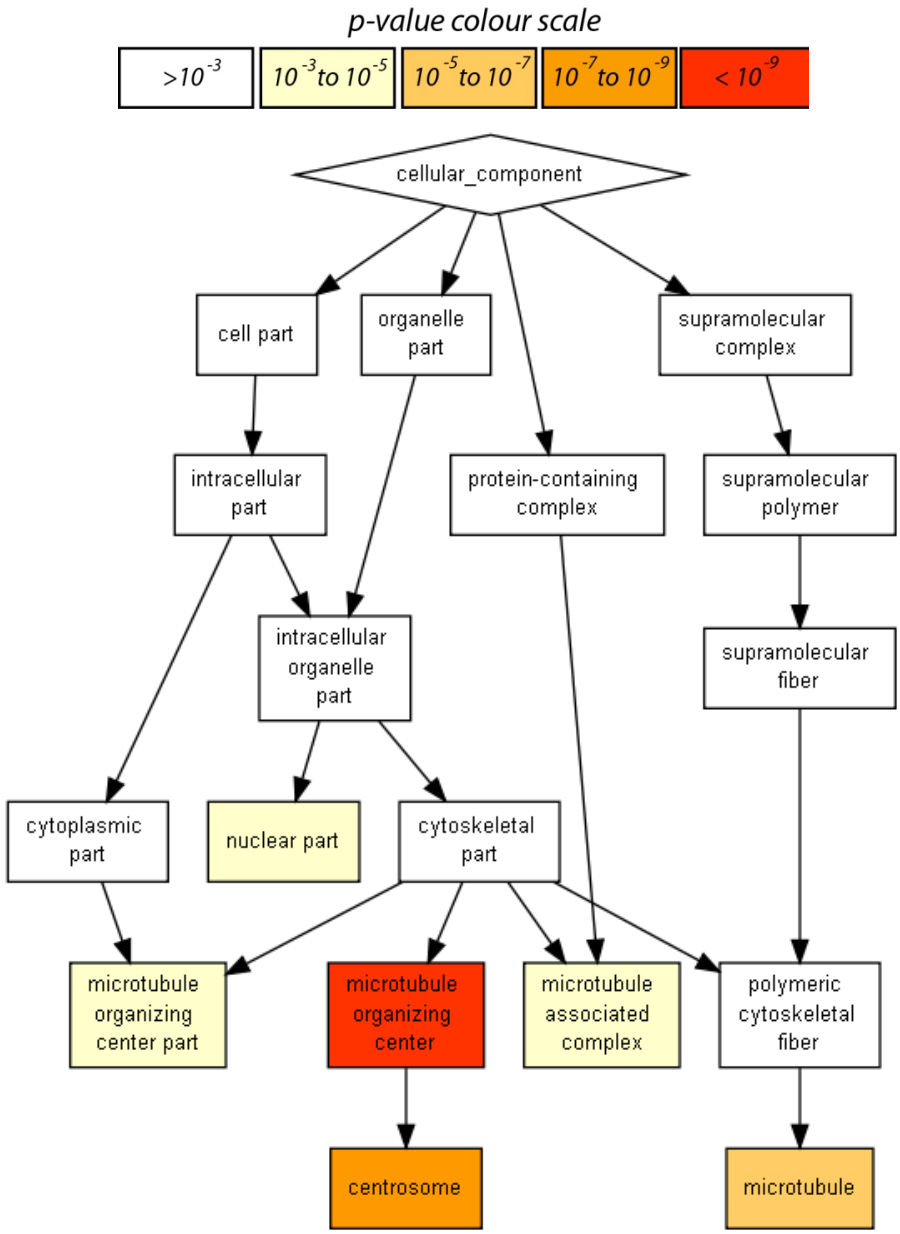

Figure 12. Cellular component GO enrichment of genes belonging to cytoskeleton NR clusters.

On the other hand, the RPE presents biological process enrichment for actomyosin structure organization (Fig 13A) as well as cellular component enrichment for elements of the intermediate filaments (Fig 13B). This intermediate filament weight in the GO enrichment of the pigmented epithelium could be even underestimated due to the large number of keratin genes excluded from the GO analysis software because of database annotation issues (table of excluded genes in online Appendix VII). Keratins are a family of fibrous structural proteins which monomers assemble into bundles to form intermediate filaments (IFs) looping into the desmosome plaques (Wang, Yang, McKittrick, & Meyers, 2016), while actomyosin complex is connected to adherens junction (AJs) (T. Chen, Saw, Mege, & Ladoux, 2018; Hartsock & Nelson, 2008). Desmosomes and AJs join the keratin filament and actin systems of adjacent

cells into a mechanical unit able to bear tensile strength and mechanical force (Hatzfeld, Keil, & Magin, 2017).

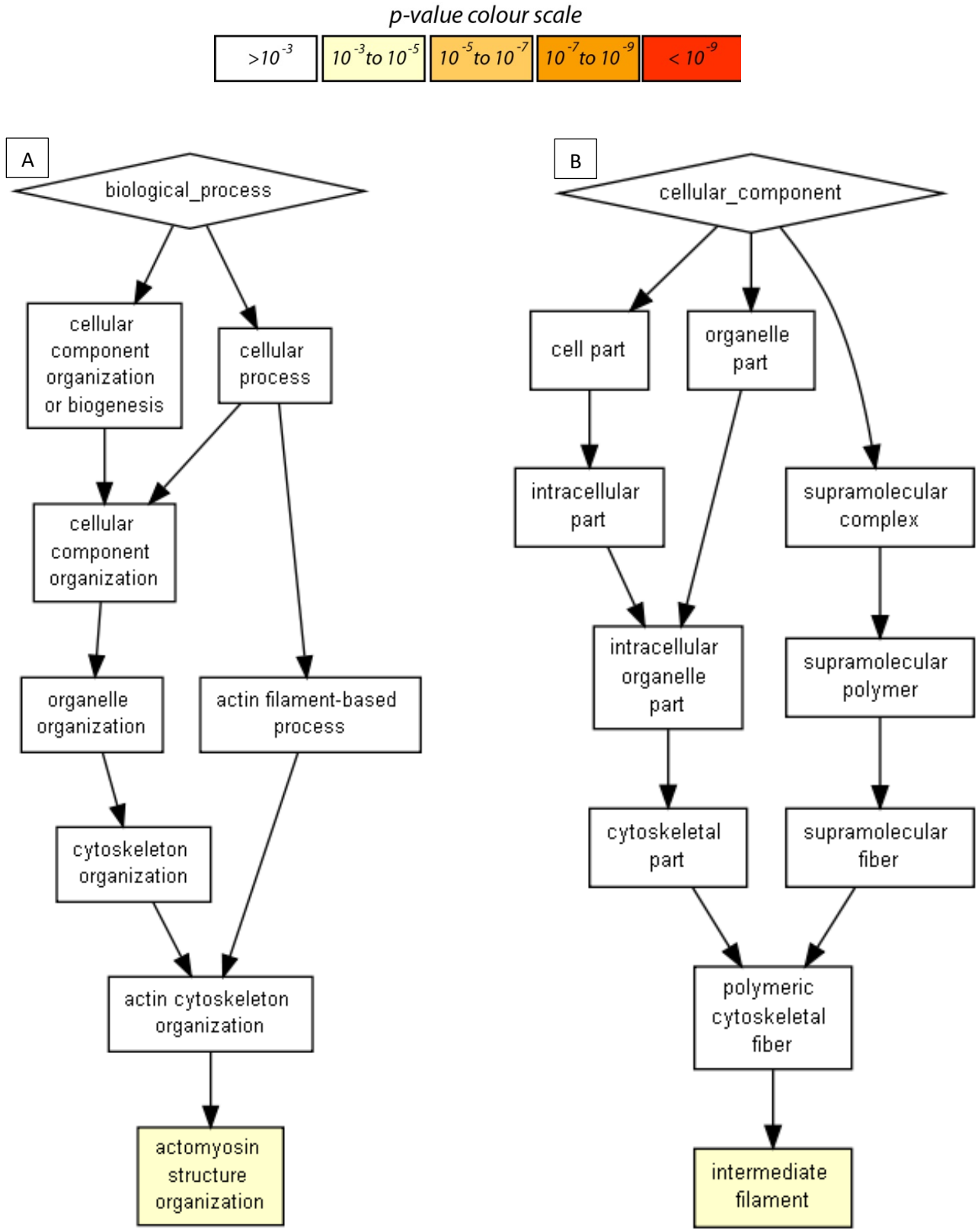

Figure 13. GO enrichment of genes belonging to cytoskeleton RPE clusters. *(A) Biological process GO term enrichment. (B) Cellular component GO term enrichment.*

In addition to the statistical significance determined by the enrichment analysis, a detailed examination showed that both keratins and desmosome components are among the most upregulated genes (i.e. highest fold change and FPKM value) in cells differentiating to RPE (Fig 14).

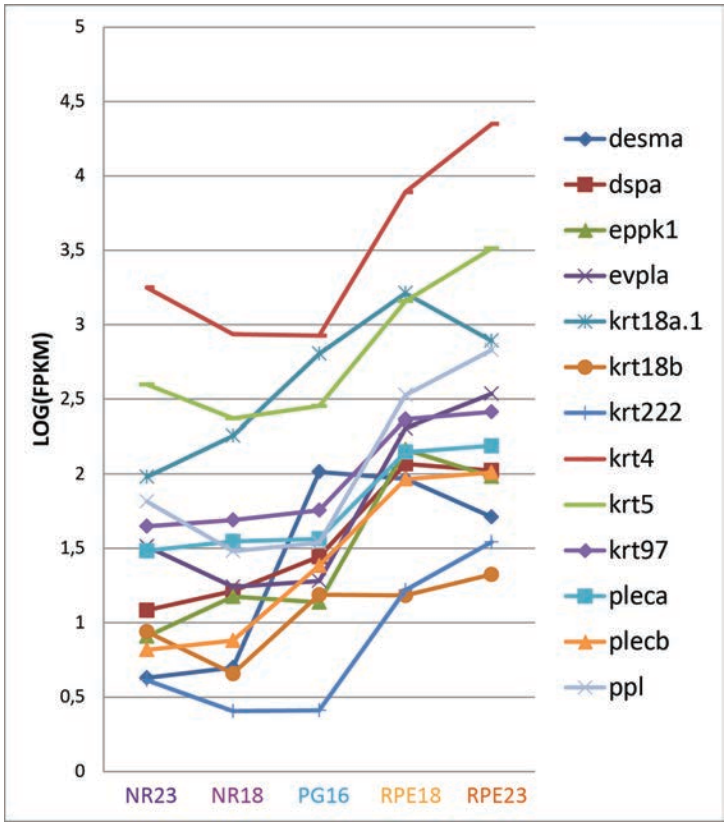

Figure 14. Intermediate filament and desmosome gene expression. *Transcript variations of genes composing intermediate filaments or desmosome during optic cup development. Given the very high expression of some of these genes, expression values are reported as LOG(FPKM).*

4. Relations between transcriptome and chromatin landscape

During development, gene expression patterns are controlled by TF binding to cis-regulatory modules and by the accessibility of these DNA regions in a temporal and domain specific manner. For a high-resolution reconstruction of developmental GRNs, the merely quantification of differential gene expression or assessment of chromatin accessibility alone may be insufficient. The integration of these two datasets can provide a more holistic view of what is occurring within a GRN, because while RNA-seq alone estimates transcript variations but cannot determine direct interactions, ATAC-seq identifies cis-regulatory elements and potential interactions of TFs.

Crossing our RNA-seq and ATAC-seq datasets we obtained a significant overlap between differentially expressed genes (DEGs) and genes associated to differentially opened regions (DOCRs) in NR vs RPE samples at 23 hpf. More in details, 47% of DEGs is associated with at least one DOCR (and,

therefore, an active CRE), and *vice versa* 50% of all DOCRs resulted to be associated precisely with a DEG (Fig 15).

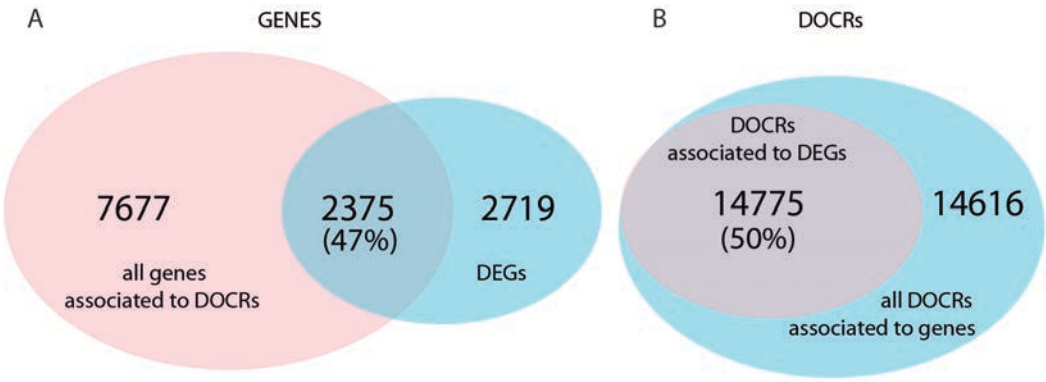

Figure 15. Association between DEGs and DOCRs. *(A) Percentage of overlapping between DEGs and genes associated with DOCRs. (B) Proportion of overlapping between the whole set of DOCRs and only DOCRs associated with DEGs.*

In figure 16 and 17 A show some examples of association between DOCRs and DEGs for marker genes of the NR (*vsx1*, *vsx2* and *six3a*) or RPE (*mitfa*, *tyr* and *otx2*) domains.

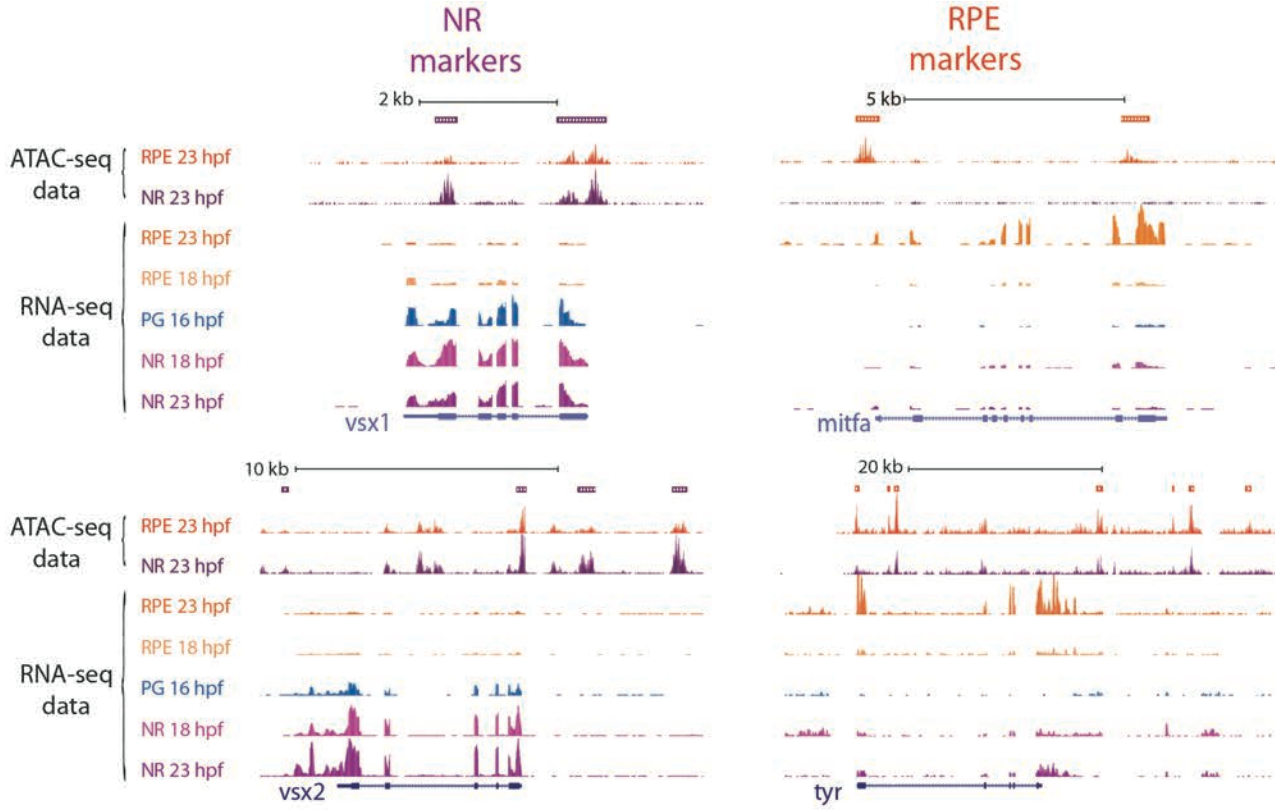

Figure 16. UCSC browser tracks with activator CRE. *Overview of ATAC-seq and RNA-seq tracks of some NR and RPE markers. Bars on the top indicate DOCRs. If purple, the DOCR is more accessible in NR. On the contrary, if orange, the DOCR is more accessible in RPE. In these case all the DOCRs are accompanied by an increasing of transcription of the associated gene in the corresponding tissue.*

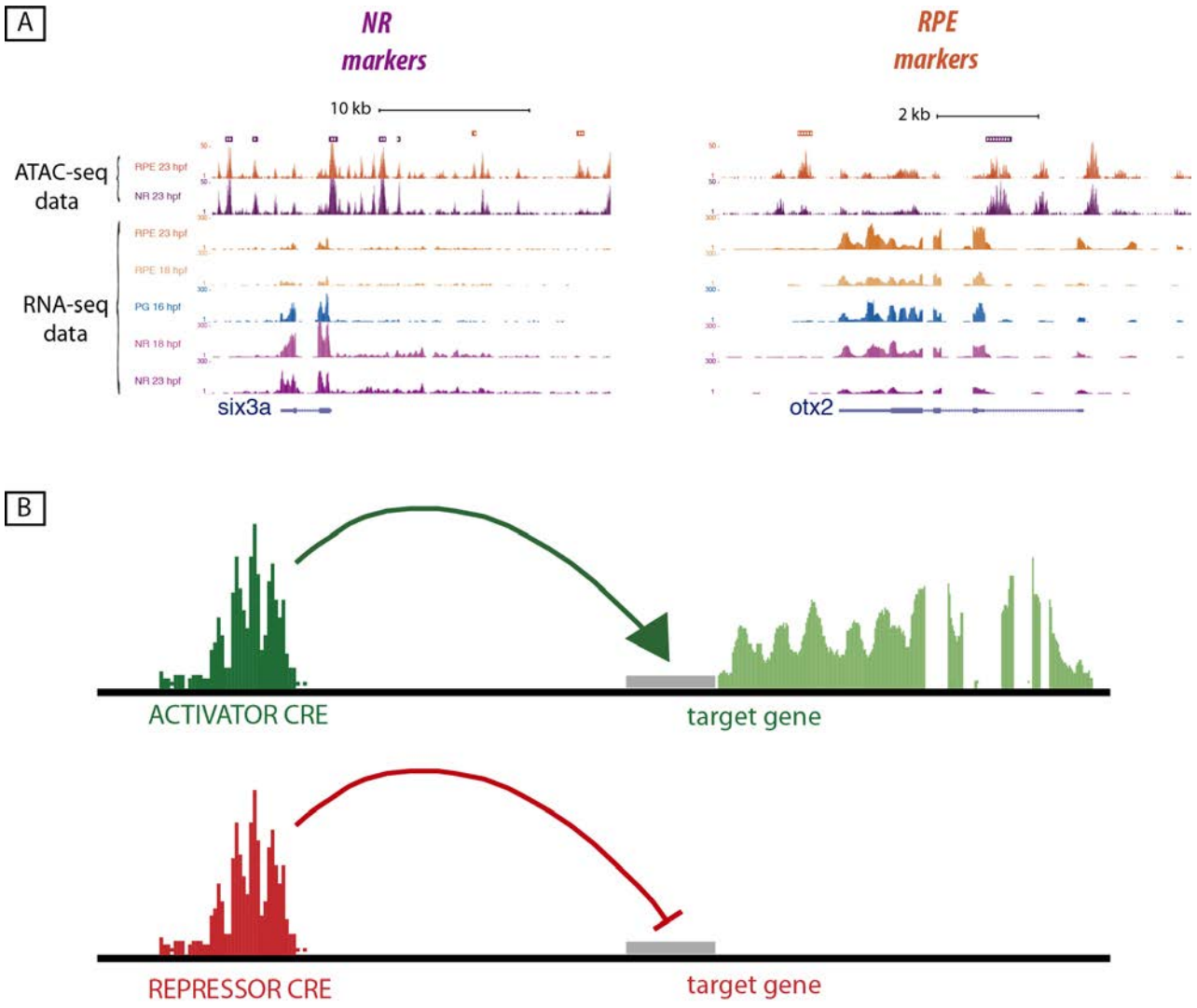

Figure 17. Activator and repressor CRE. *(A) Overview of ATAC-seq and RNA-seq tracks of some NR and RPE markers. Bars on the top indicate DOCRs. If purple, the DOCR is more accessible in NR. On the contrary, if orange, the DOCR is more accessible in RPE. In these case some of the more accessible DOCRs are accompanied by a decreasing of transcription of the associated gene in the corresponding tissue. (B) Graphical explanation of activator and repressor CRE function.*

From the tracks, we can appreciate not only the variations of the transcript levels between tissues (RNA-seq data), but also a concomitant change in chromatin accessibility of the associated CREs (ATAC-seq data). This association between DOCRs and DEGs can be found in the configuration “more accessible DOCR + upregulated gene”, where the CRE is predicted to be an enhancer (Fig 16), or “more accessible DOCR + downregulated gene”, where the CRE is likely to be acting as a silencer (Fig 17). We calculated the number of associated activator and repressor CREs using both all the DEGs and only the subset of differentially expressed TFs (Fig 18).

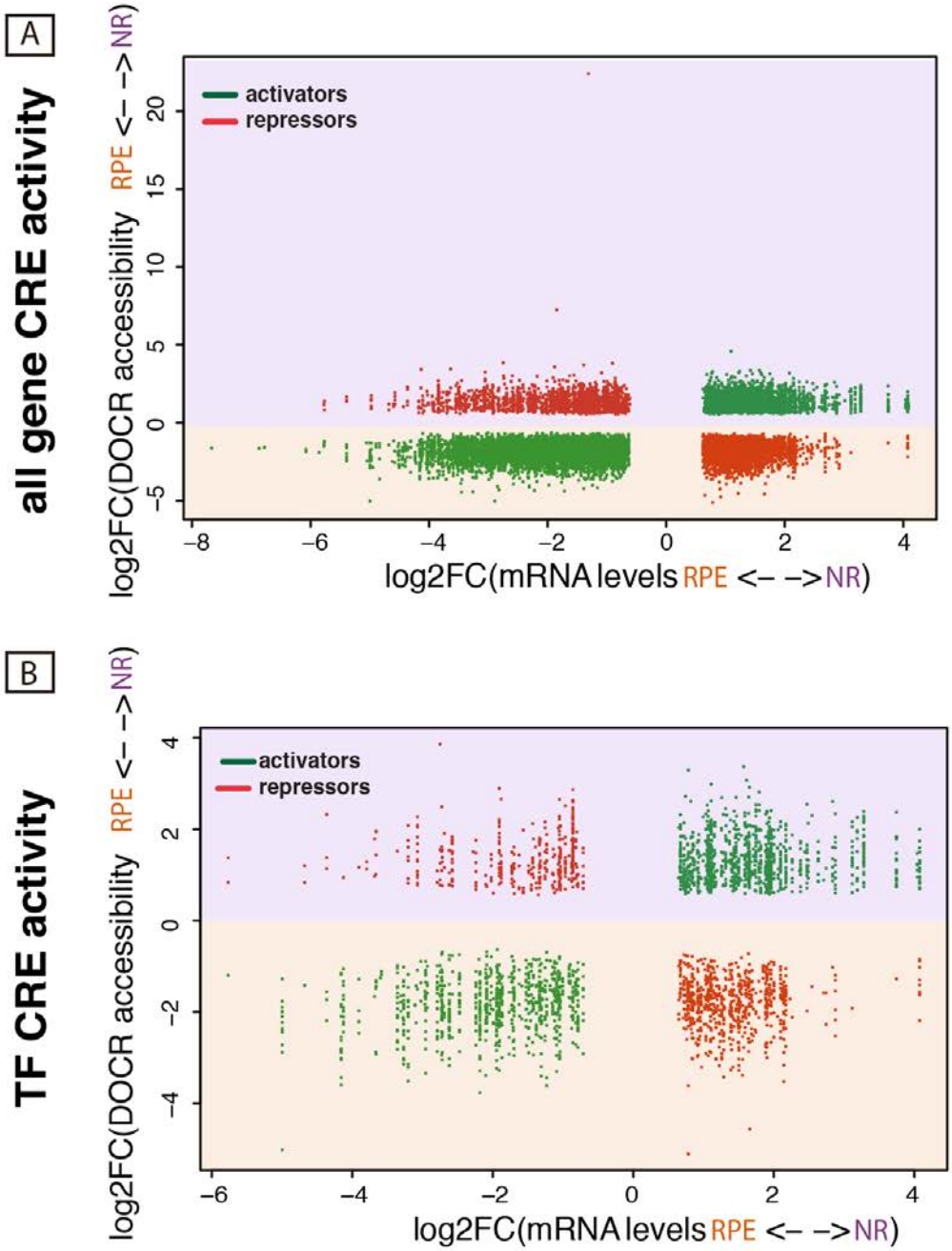

C

	ALL GENES				TFs		
	peaks	genes	peaks/gene		peaks	genes	peaks/gene
NR ACTIVATORS	3434	754	4.55		1174	182	6.45
NR REPRESSORS	1999	552	3.62		388	69	5.62
RPE ACTIVATORS	5984	1119	5.35		869	110	7.90
RPE REPRESSORS	3358	883	3.80		706	173	4.08

Figure 18. CRE configuration in NR and RPE model. *(A) Graph illustrating the functional relations between DEGs and associated DOCRs. (B) Graph illustrating the functional relations between differentially expressed TFs and associated DOCRs. (C) Table resuming the number of activator or repressor CREs associated with all the DEGs or only with the differentially expressed TFs.*

Based on the results of this cross-correlation analysis, we made a number of observations:

- Genes encoding for TFs have a larger number of associated CREs than that other types of genes (on average, 6.01 DOCRs/TF *vs* 4.33 DOCRs/any gene); which suggest higher regulatory complexity.
- Both in NR and RPE, differentially expressed genes are associated more with activators than repressors;
- Regarding TFs, while NR exhibits an activating response stronger than the repressive one (182 *vs* 69 TFs), the opposite happens in RPE. The pigmented tissue shows a very robust repressive cis-regulatory logic, with 173 TFs associated with at least one repressive CREs and only 110 associated with activating ones.

More in details, we examined the quantitative relationship between differentially regulated TFs and type of associated CREs, assigning a precise amount of TFs to the associated number of activating or repressing CREs (Fig 19). Also this kind of analysis confirmed that NR specification program is sustained by the activation of transcriptional regulators, whereas the RPE determination seems to require primarily the repression of the NR-specific-TFs.

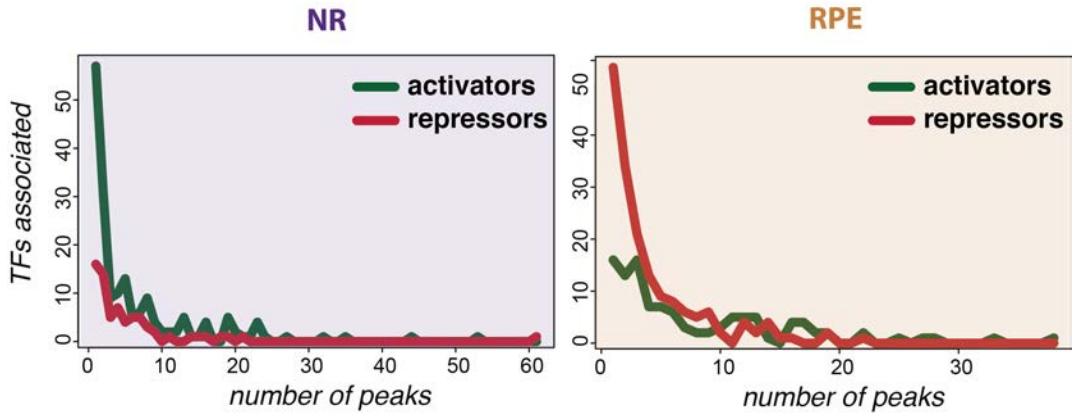

Figure 19. Quantitative association between CREs TFs. *The graphs illustrate the number differentially accessible peaks and of which type (if activators or repressor) are associated to a precise number of differentially expressed TFs.*

Next, we investigated the peak distribution around the transcription start sites (TSS) for both activator and repressor CREs in NR and RPE. In both tissues, activator peaks are distributed closer to TSS than repressors (Fig 20 A). This is not surprising because a fraction of the activator CREs corresponds likely with promoters, while silencers usually obey a longer-range regulatory logic. The statistical analysis of a wider range around TSS, including all the distal DOCRs, confirmed that the distribution of the activator CREs remains more proximal than that of the repressors (Fig 20 B)..

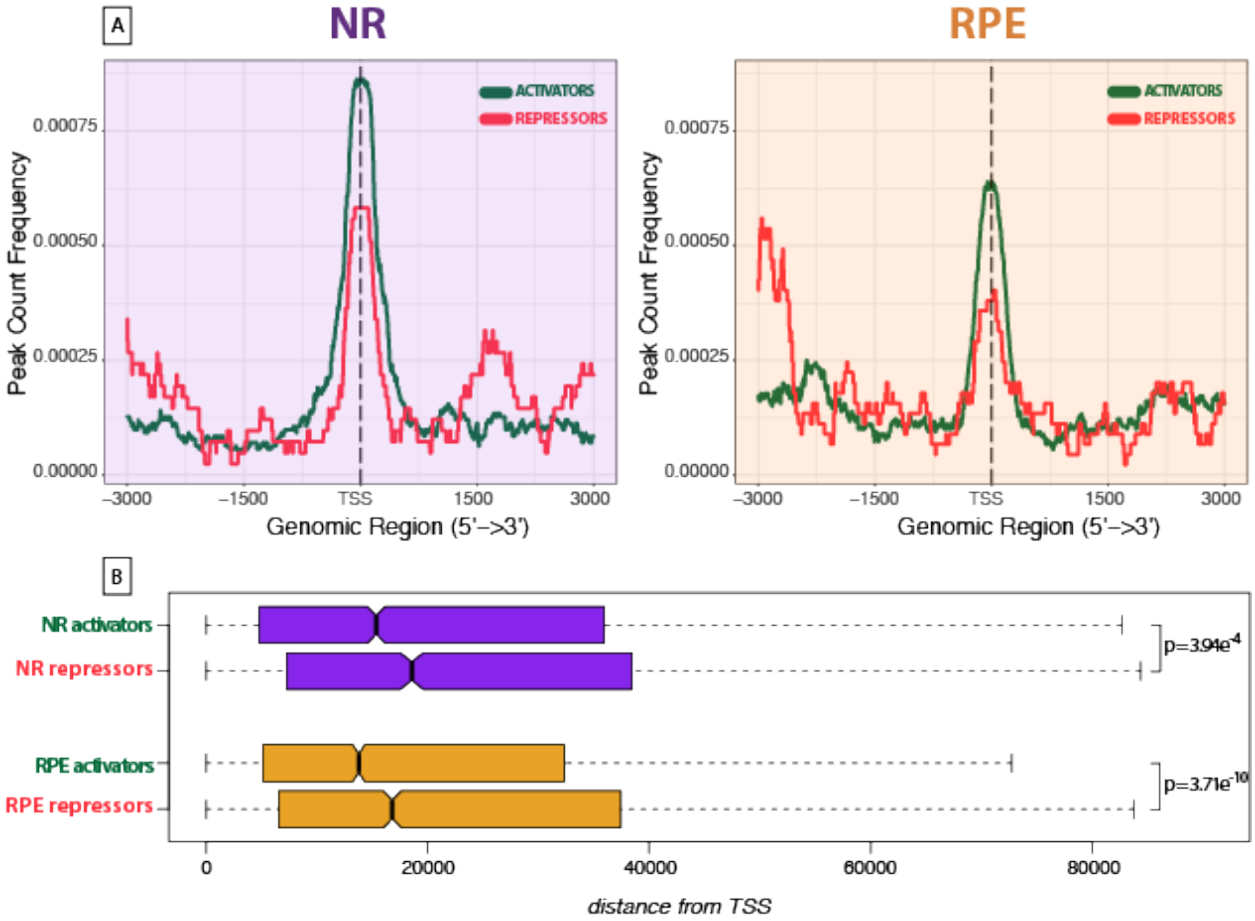

Figure 20. CRE distance from TSS. *(A) Distance from TSS of activator and repressor proximal DOCRs. (B) Average distance from TSS of all the activator and repressor DOCRs.*

5. NR regulatory wiring analysis

Motif enrichment analysis of the NR DOCRs shows a highly significant enrichment for *sox3*, *sox6*, *pax6*, *ror* and the *homeobox* TF binding motifs (Fig 21 A; complete ME analysis in Appendix VIII). The *homeobox* binding motif (5'-TAATT-3') can be bound by *homeodomain* TFs from the K50 PRD-class; such as *vsx1*, *vsx2*, *rx1, rx2*, and *rx3;* and LIM-class, such as *lhx2b*. Since these TFs share an almost identical DNA binding sequence and they are all co-expressed in the NR, it is very likely that they target a partially overlapping set of cis-regulatory modules (Fig 21 B). *Hmx* TFs are expressed in NR and can bind the *homeodomain* as well, but to a slightly different sequence from the one most identified by our motif enrichment analysis. For this reason, they will not be considered in our following investigations.

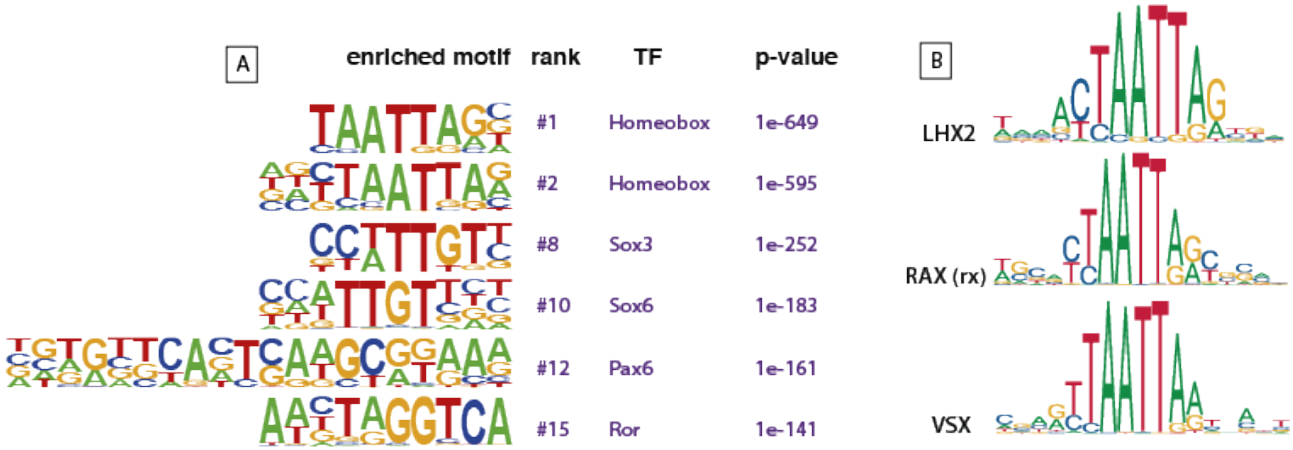

Figure 21. NR motif enrichment analysis. *(A) Representative TF binding motifs enriched in NR DOCRs. (B) Binding motif similarity among TFs of the homeobox family. Mouse Motifs from JASPAR database (http://jaspar.genereg.net).*

In situations like this, with the concomitant expression of different TFs sharing the same DNA binding motif, functional synergy cannot be ruled out. As already mentioned in the introduction, in some cases they might even be able to compensate the loss of another homologous TF. In addition, single TF binding profiles are often not sufficient to dissect complex regulatory networks. To further explore cooperative interactions among TFs during NR specification, we retrieved the individual position weight matrixes (PMW) associated to *homeobox* and *sox* TFs from available databases. Then we used this information to explore their functional synergy in all the NR DOCRs (for more information, see Method sections). Two different approaches were used: calculating the co-occurrence rate of binding sites for two different TFs in the same CREs and estimating percentage of binding sites for different TFs that are located in distinct CREs but associated with the same gene. These analyses revealed an extremely high inter-connectivity degree within the NR GRN (Fig 22).

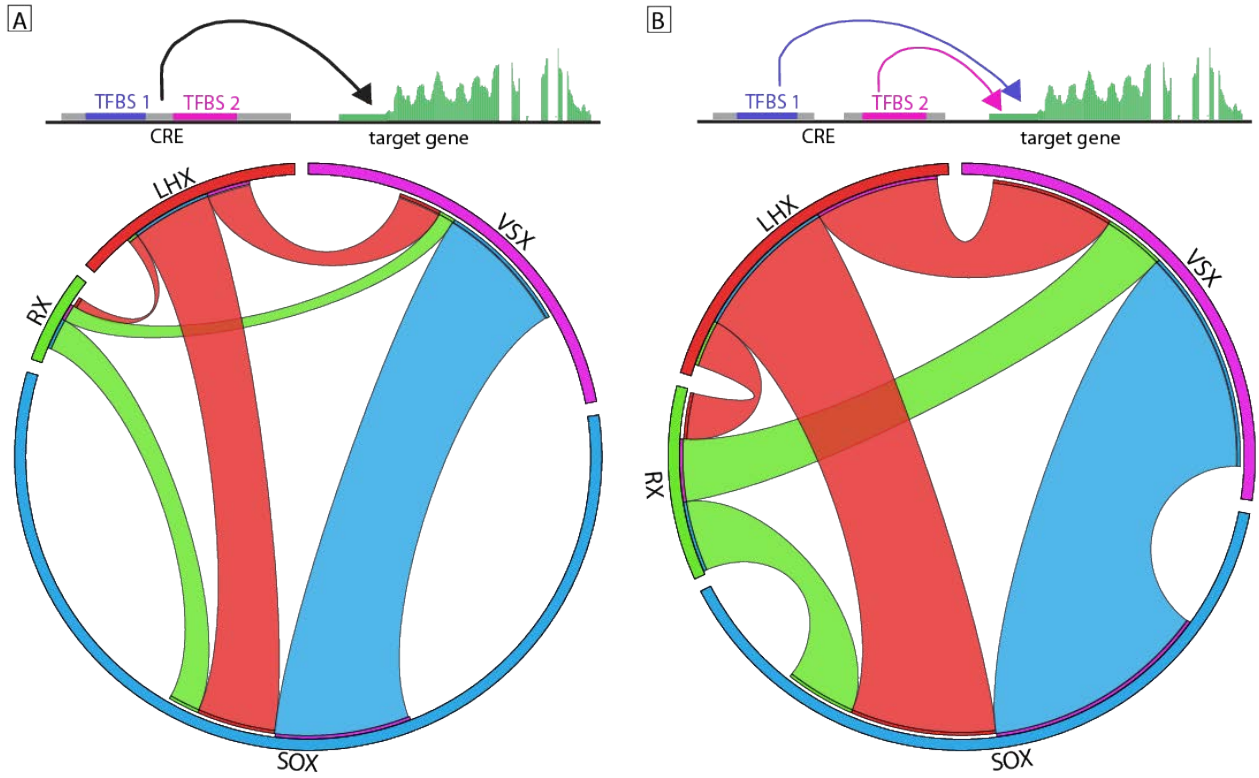

Figure 22. NR TF cooperation. *(A) Circoplot illustrating the co-occupancy rate of TFBS for different TFs in the same DOCRs (B) Circoplot illustrating the degree of cooperation between TFs regulating the same gene from different DOCRs.*

The average co-occurrence rate of different binding sites in the same peak is 29%. When considering specifically the co-occurrence of any *homeobox* binding site with a *sox* binding site, the percentage reaches 53.9%. This combinatorial activity becomes even more pronounced when considering the binding sites in different CREs regulating the same genes. Whereas the cooperation ratio among all the TFs is 53.9% (which is in itself a large percentage), this ratio reaches 88% when the co-occurrence of a *sox* and any *homeobox* TFs is considered. This analysis reveals a remarkably strong cooperative activity of *homeobox* and *sox* factors to drive the NR developmental program (Fig 23 A). When regulating the same gene from different CREs, the homeobox TFs also exhibit an extensive level of cooperation among them, strengthen the hypothesis of a synergistic regulation mechanism to drive the NR differentiation (*lhx/vsx*: 75.1%; *rx/lhx*: 60.4%; *rx/vsx*: 80.3%)(Fig 23 B).

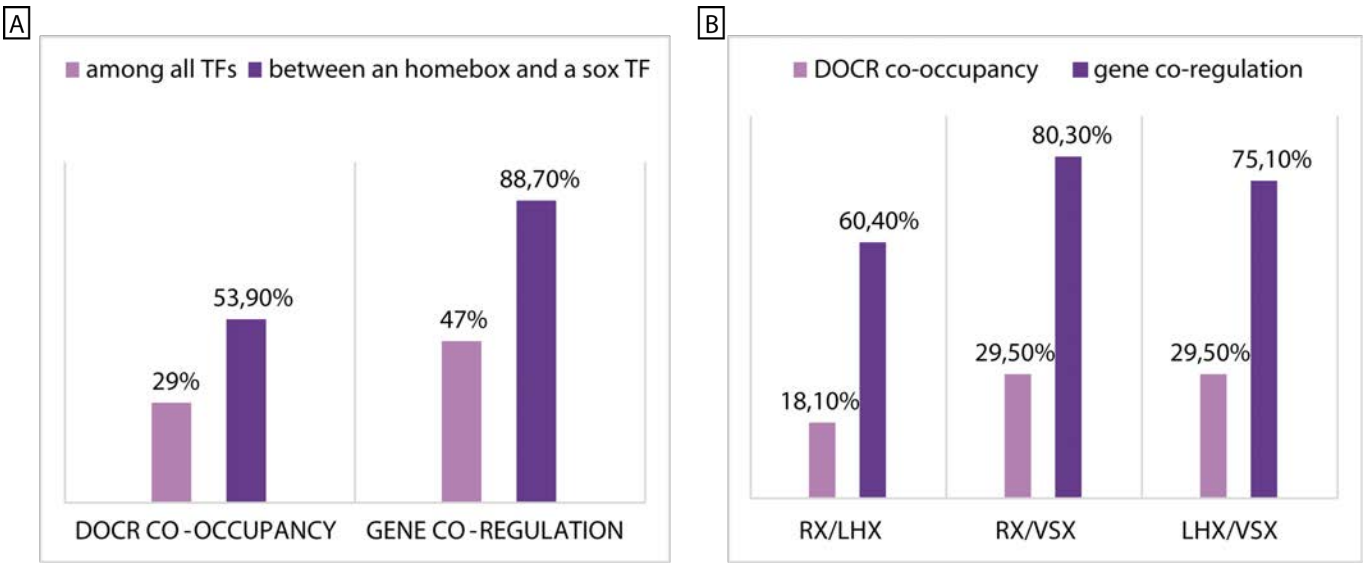

Figure 23. NR GRN redundancy. *(A) Average percentages of cooperativity between NR principal TFs (B) Average percentages of cooperativity within the NR homeobox family TFs.*

We further investigated the role of two of the NR transcriptional hubs, *vsx1* and *vsx2,* in retinal specification in teleosts. Joaquin Letelier, a former member of our lab, mutated both *homeobo*x factors using CRISPR/Cas9 technology in zebrafish and medaka. Several mutated alleles for each *vsx* gene were generated. All the experiments shown in this thesis were performed with stable mutant fish lines exhibiting a deletion of the homeodomain in charge of binding the DNA. In *vsx2* mouse mutants, eye morphology is severely affected, with the RPE invading the NR domain (Burmeister et al., 1996; Horsford et al., 2005; Rowan, Chen, Young, Fisher, & Cepko, 2004). In contrast, the stable zebrafish mutant lines generated in our group for *vsx1* or *vsx2* do not exhibit any kind of aberrant eye morphology (data not shown). However, the double mutants do not reach adulthood and fail to differentiate bipolar cells in the inner nuclear layer (INL) (Fig 24). As a consequence of this retina neurogenesis impairment, the double mutant zebrafish embryos resulted to be blind. Their blindness could be inferred from their darker color due to incapability of adapting to the light (Fig 24 D). This phenomena is called visual background adaptation (VBA), a simple reflex where the zebrafish adjusts the distribution of melanosome in pigment cells in response to changes in the ambient light (Perry, Ekker, Farrell, & Brauner, 2010). Their blindness was later confirmed by electroretinogram recordings, performed in the laboratory of Dr. Stephan Neuhauss (University of Zurich) (data not shown).

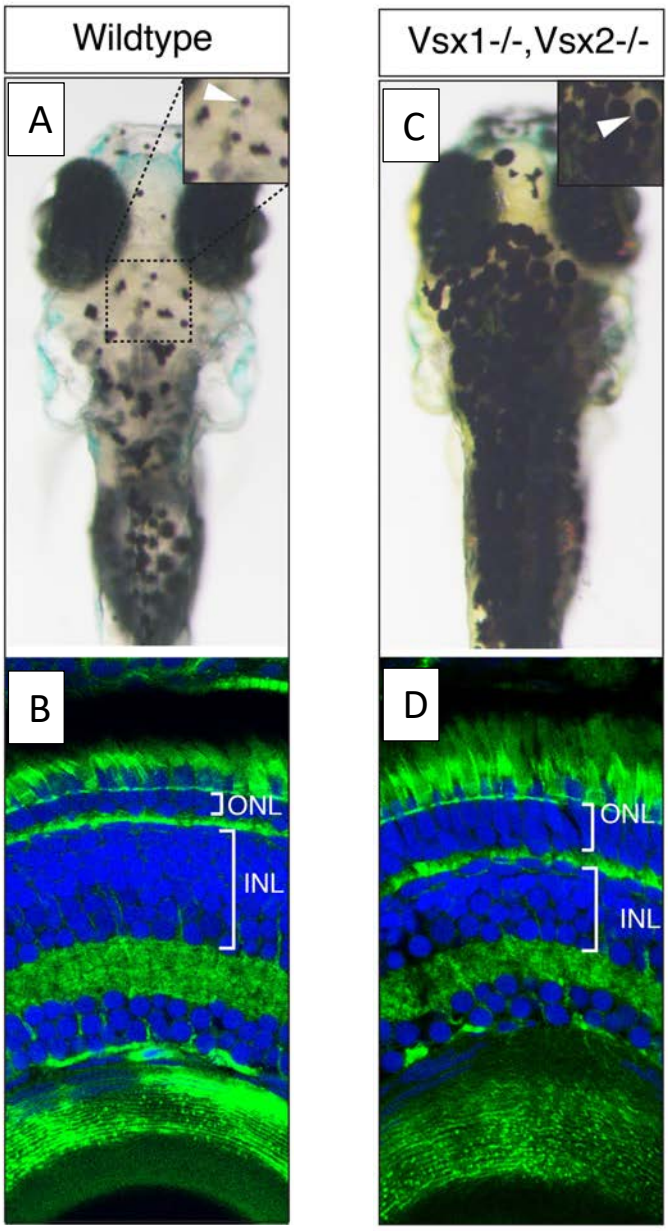

Figure 24. Zebrafish *vsx* mutants. *(A) WT eye morphology and embryo pigmentation pattern at 6 dpf (B) 40X image of DAPI/Phalloidin staining of WT eye at 6 dpf. (C) Vsx1 -/- vsx2 -/- eye morphology and embryo pigmentation pattern at 6 dpf . (D) 40X image of DAPI/Phalloidin staining of vsx1 -/- vsx2 -/- eye at 6 dpf. Image courtesy of Joaquin Letelier.*

Similarly to zebrafish, medaka double mutant embryos for *vsx1 -/- vsx2 -/-* appear WT-like with normal optic cup morphology at stage 23. However, around day 8 they display microphtalmia and aberrant general embryo morphology (Fig 25). The histological analysis of the medaka double mutants revealed that, like in zebrafish, bipolar cells fail to differentiate in the INL. This observation suggests that *vsx1 -/- vsx2 -/-* medakas are also blind.

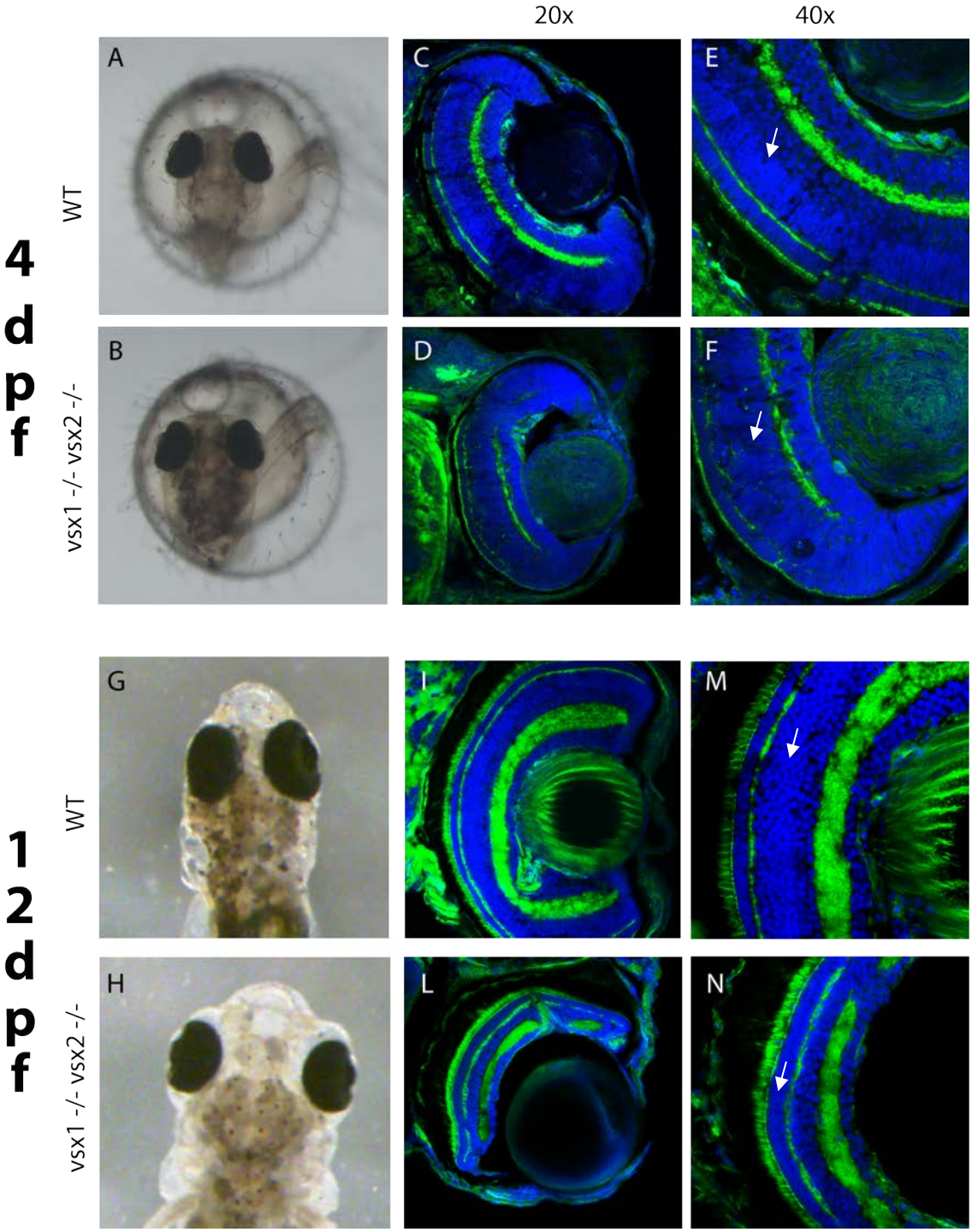

Figure 25. Medaka *vsx* mutants. *(A) WT eye morphology at 4 dpf (B) Vsx1 -/- vsx2 -/- eye morphology at 4 dpf. (C) 20X image of DAPI/Phalloidin staining of WT eye at 4 dpf. (D) 20X image of DAPI/Phalloidin staining of vsx1 -/- vsx2 -/- eye at 4 dpf. (E) 40X image of DAPI/Phalloidin staining of WT eye at 4 dpf. (F) 40X image of DAPI/Phalloidin staining of vsx1 -/- vsx2 -/- eye at 4 dpf. (G) WT eye morphology at 12 dpf (H) Vsx1 -/- vsx2 -/- eye morphology at 12 dpf. (I) 20X image of DAPI/Phalloidin staining of WT eye at 12 dpf. (L) 20X image of DAPI/Phalloidin staining of vsx1 -/- vsx2 -/- eye at 12dpf. (M) 40X image of DAPI/Phalloidin staining of WT eye at 12 dpf. (N) 40X image of DAPI/Phalloidin staining of vsx1 -/- vsx2 -/- eye at 12 dpf.*

To detect the regulatory changes due to the loss of *vsx* factors, and also to explore the possibility of an eventual compensation mechanism to avoid optic cup malformations, we investigate the double mutant *vsx1 -/- vsx2 -/-* zebrafish embryos at 18 hpf using a genome wide approach. RNA-seq analysis revealed modest transcriptomic changes. 1018 genes resulted to be differentially expressed (484 upregulated in the mutant and 534 dowregulated), but only a small portion exhibits changes with a log2FoldChange ± I1.5I (44 upregulated and 38 downregulated)(Fig 26; complete list of DEGs in online Appendix IX). Of these DEGs, only the 5.6% was constituted by TFs (26 upregulated and 31 downregulated; with a log2FoldChange ± I1.5I: 3 upregulated and none downregulated).

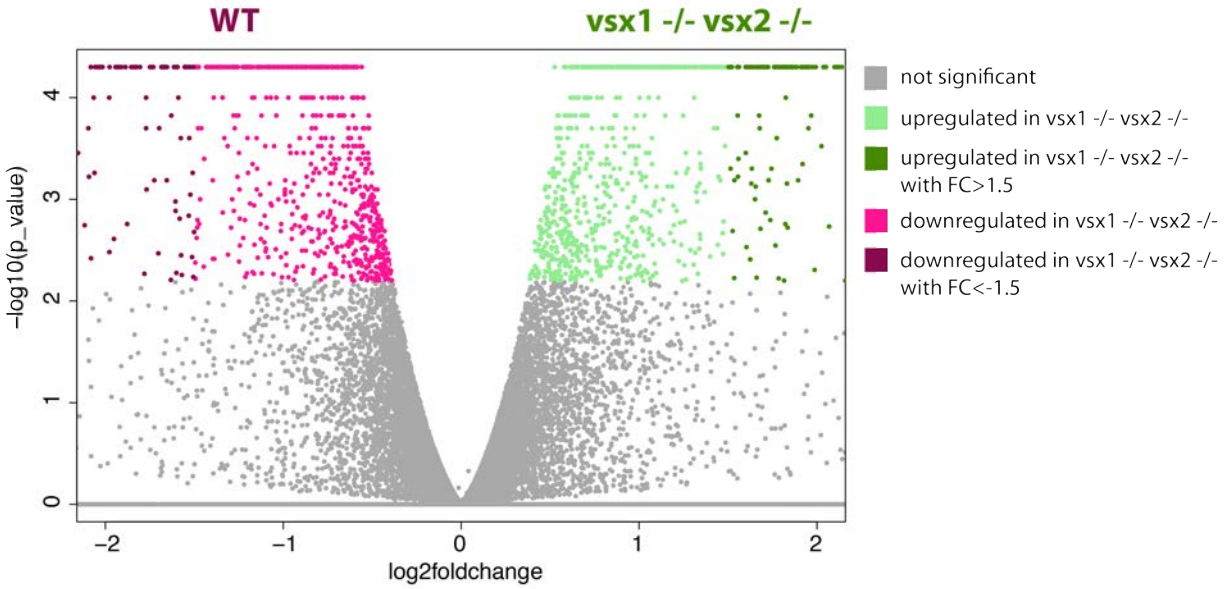

Figure 26. Zebrafish *vsx* mutants transcriptome change. *Volcano plot illustrating the transcriptome variations between WT and vsx1 -/- vsx2 -/- zebrafish embryo head at 18 hpf.*

Only 5 of the TFs known to be involved in eye development resulted to be differentially expressed in the mutant, though with modest fold changes (*sox21a*, *sox21b*, *lhx2b, vax1* and *rx2*; Fig 27 A). We built a small-scale GRN including three of these TFs (*sox21a*, *lhx2b* and *vax1*) and a few other upregulated genes in the *vsx1 -/- vsx2 -/-* double mutants, using literature and database data (Fig 27 B). This GRN model includes 12 genes, 10 of which resulted to be differentially expressed also between the sorted NR- and RPE-cell RNA-seq data at 18 hpf and are therefore involved in optic cup development. Notably, 4 of these genes (*tyr*, *sox10*, *tgfb3*, *tyr* and *scl45a2*) are upregulated in RPE rather than in NR. We calculated that the 21.7% of the genes upregulated in the *vsx1 -/- vsx2 -/-* double mutants are also upregulated in the RPE at the same developmental stage (list of common genes in online Appendix X). This number is probably underestimated because of the "dilution" of the RPE transcriptome signal in the *vsx1 -/- vsx2 -/-* RNA-seq dataset, given

that it was obtained from whole heads and the RPE represents just a small fraction of the tissue input. This result suggests an "expansion" of the RPE molecular identity in the zebrafish double mutants, as already seen in mouse in a more marked morphogenetic manifestation. However, apart from those already mentioned cases, we could not distinguish an evident "retina" signature in the gene ontology of the DEGs in the double mutant. On that account, our transcriptomic data cannot clearly support the idea of a transcriptional compensation mechanism. Alternatively, our RNA-seq analysis suggests that genetic redundancy, provided by synergic TFs, is sufficient to prevent the morphogenetic impairment of the optic cup in zebrafish double mutants.

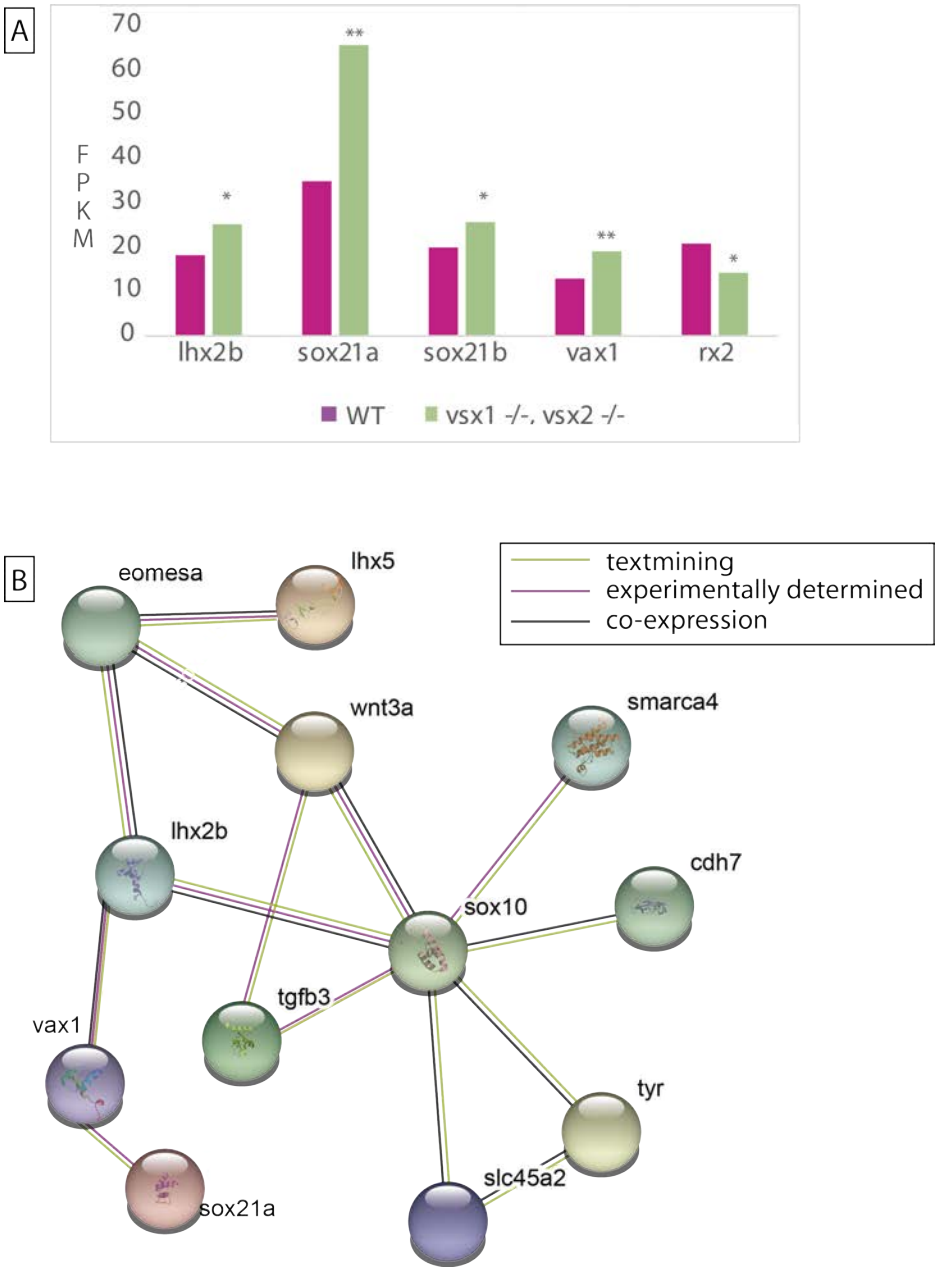

Figure 27. NR GRN changes in vsx1 -/- vsx2 -/- zebrafish. *(A) NR TFs changing expression level in vsx1 -/- vsx2 -/- zebrafish. (A) Small-scale GRN in vsx1 -/- vsx2 -/- zebrafish.*

To further explore the impact of *vsx* gene loss in the architecture of the retinal GRNs, we interrogated the cis-regulatory landscape of the same stage *vsx1 -/- vsx2 -/-* double mutants using ATAC-seq. This approach individuated 1'564 DNA regions with reshaped accessibility (962 DOCRs more accessible in the mutant *vs* 602 less) (Fig 28 A) with considerably high log2FoldChange (Fig 28 B).

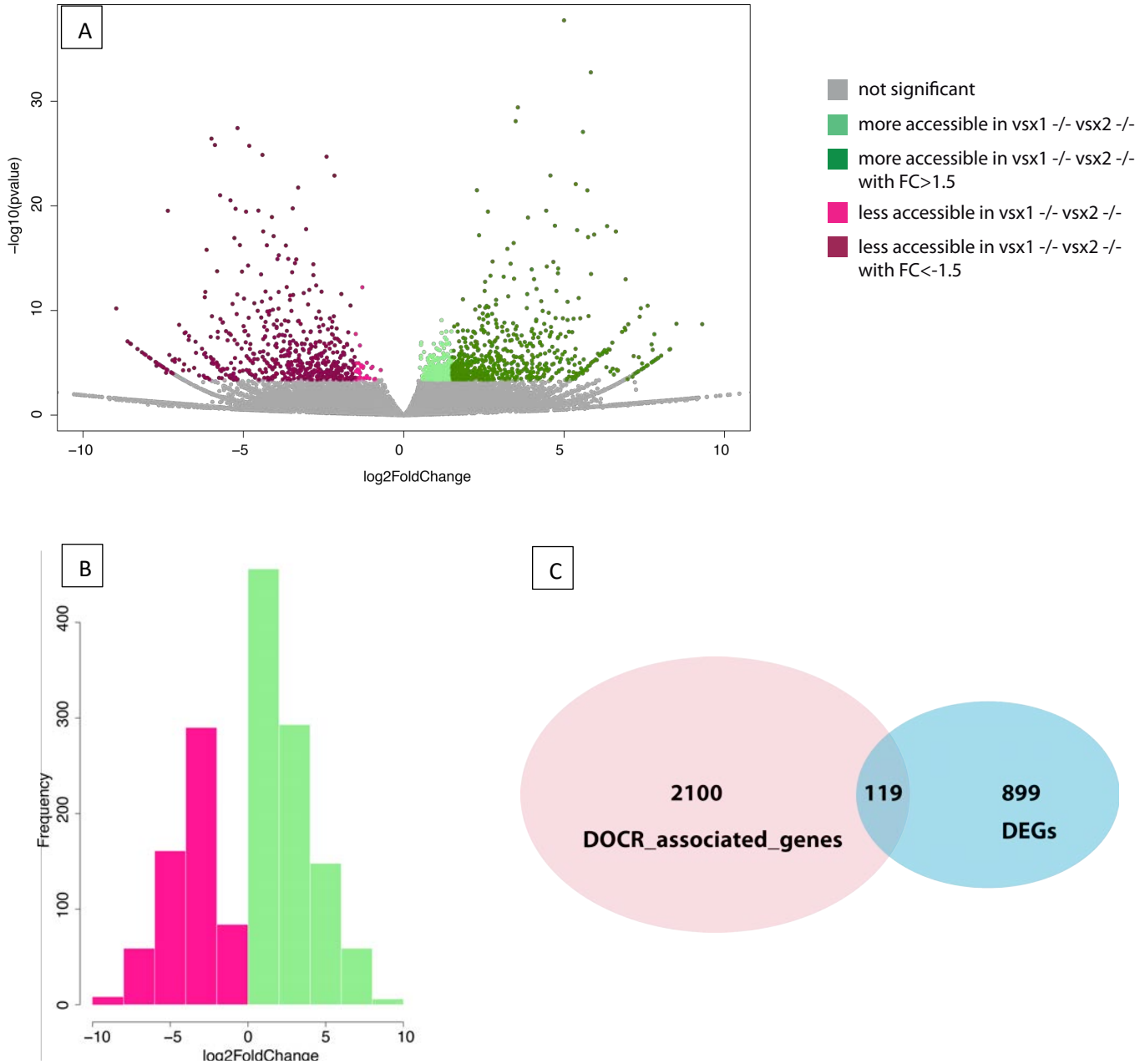

Figure 28. Vsx1 -/- vsx2 -/- ATAC-seq. (A) *Volcano plot illustrating the chromatin accessibility variations between WT and vsx1 -/- vsx2 -/- zebrafish embryo head at 18 hpf. (B) Distribution of chromatin variation fold change. (C) Correlation between genes associated with ATAC-seq DOCRs and RNA-seq DEGs*

Even if 2`219 genes could be associated with these DOCRs, only the 5.4% of them corresponded to DEGs from the RNA-seq (e.g. *lhx2b* and *sox21b*) (Fig 28 C). Nevertheless, when we analyzed the GO enrichment of the whole subset of genes associated with DOCRs. We detected many terms related to neurogenesis and eye differentiation among GO biological processes enriched with highest fold (Fig 29; complete GO enrichment analysis in Appendix XI). This observation indicates that though many cis-regulatory modules of the retinal GRN are modified in the absence of *vsx* function, yet this has a modest impact on the transcriptional program. Hence, most of the key TFs do not suffer an increase in expression, and when they do, like in the case of *lhx2b* and *sox21*, they present only a mild increment.

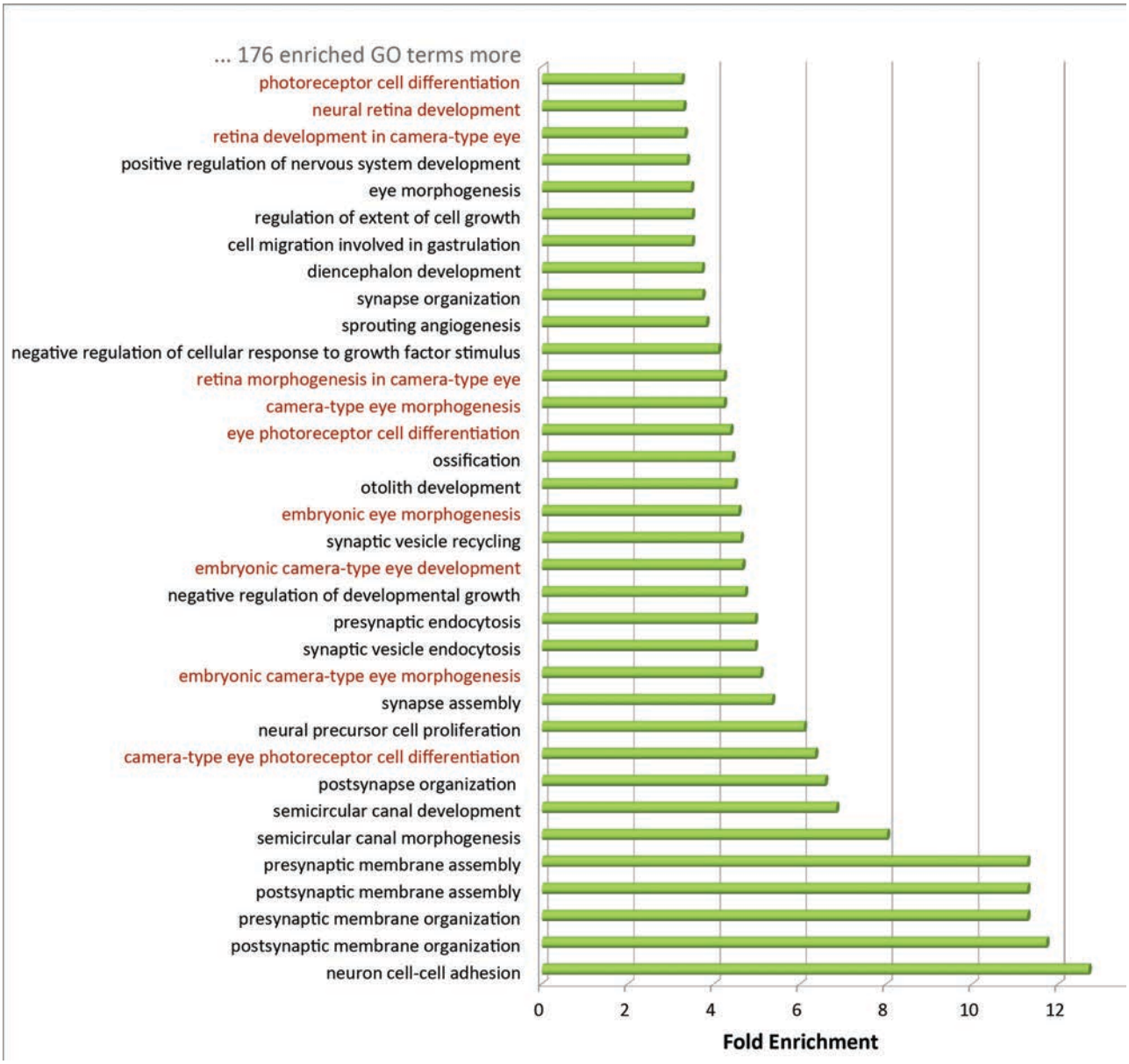

Figure 29. Vsx1 -/- vsx2 -/- DOCR GO. First 34 *biological process GO terms enriched in genes associated with a more accessible DOCR in the vsx1 -/- vsx2 -/- double mutants. The GO terms directly related with eye differentiation are highlighted in red.*

Considering together all our data, the most logical hypothesis is that gene redundancy, as provided by functionally related TFs able to bind similar motifs in the genome, is sufficient to maintain the architecture of the retinal GRN even in the absence of *vsx* gene function. Thus genetic robustness rather than genetic compensation may account for the absence of early morphogenetic defects in the zebrafish retina.

6. RPE regulatory wiring analysis

In RPE, motif enrichment analysis of the DOCRs highlighted a multiplicity of binding motifs, which correspond to the TFs identified as up-regulated in the RNA-seq analysis. First of all, the motif analysis showed a very considerable and significant enrichment of *tfap2a* and *tfap2c* binding motifs, in agreement with the early expression of these factors in the RPE. This considerable enrichment points to a prominent position for these factors within the regulatory hierarchy of the eye pigmented tissue. In addition, a very significant enrichment for *bHLH*, *tead* and *otx2* binding motifs was observed (FIG 30 A, complete RPE ME analysis in online Appendix XII). As it happened for the NR-specific homeobox domain (5'-TAATT-3'), also the bHLH motif (5'-CACGTG-3') can be bound by distinct TFs expressed in RPE, such as *mitfa*, *bHLHE40*, *bHLHE41*, *tfec* and *tcf12* (Fig 30 B).

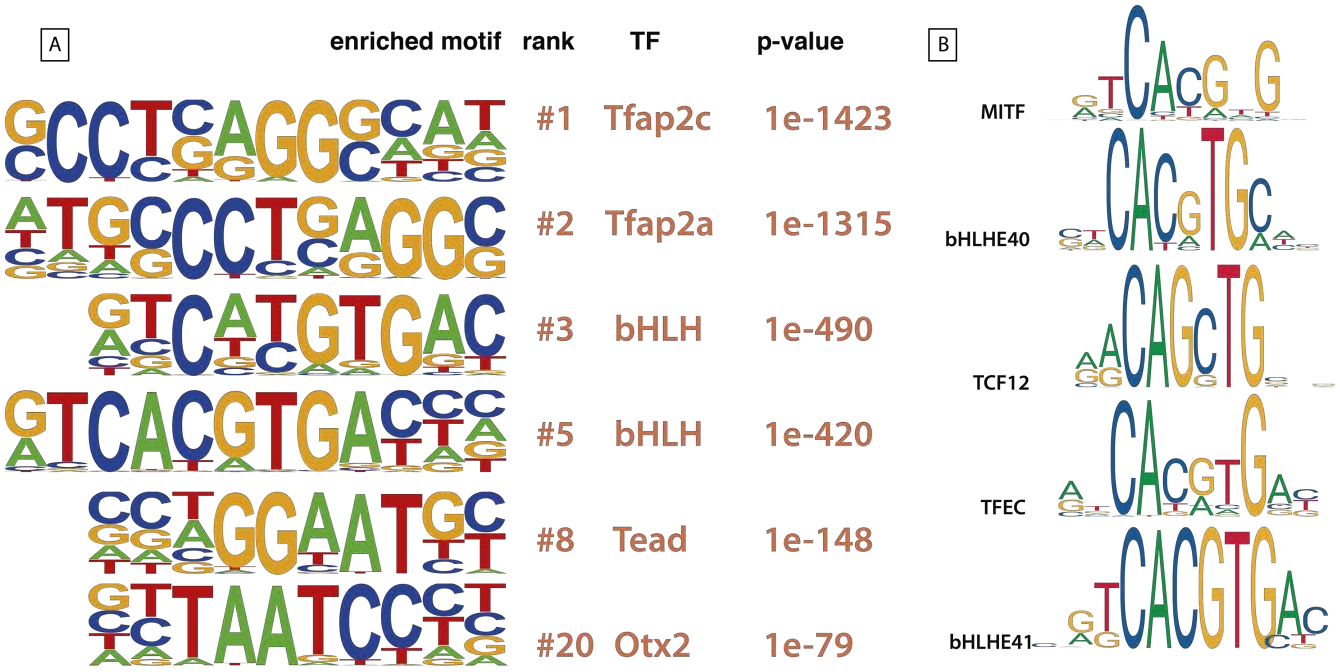

Figure 30. RPE motif enrichment analysis. *(A) Representative TF binding motifs enriched in RPE DOCRs. (B) Binding motif similarity among TFs of the bHLH family. Motifs from JASPAR database (http://jaspar.genereg.net). MITF, bHLHE40 and TCF12 are from mus musculus, whereas TFEC and bHLHE41 are from homo sapiens.*

As already done for the NR, we tried to dissect the interdependence among these TFs (Fig 31) The RPE GRN presented a discrete grade of inter-connectivity, but this effect was not as strong as in NR. While the average rate of co-occurrence of binding sites for two different TFs in distinct CREs regulating the same gene in RPE did not differ much from that found in NR, the rate of physical co-occurrence of different TFBS in the same CREs dropped from 29% in the NR to 11,7% in the RPE (Fig 31 C-D). Even if some RPE TFs show a high level of cooperation regulating the same gene from different CREs (e.g. *mitfa*, *tead*, *tfap2a*, *tfpa2c*), no RPE TF coupling reaches the 88% synergism rate of the NR *sox/homeobox* combination (data not shown).

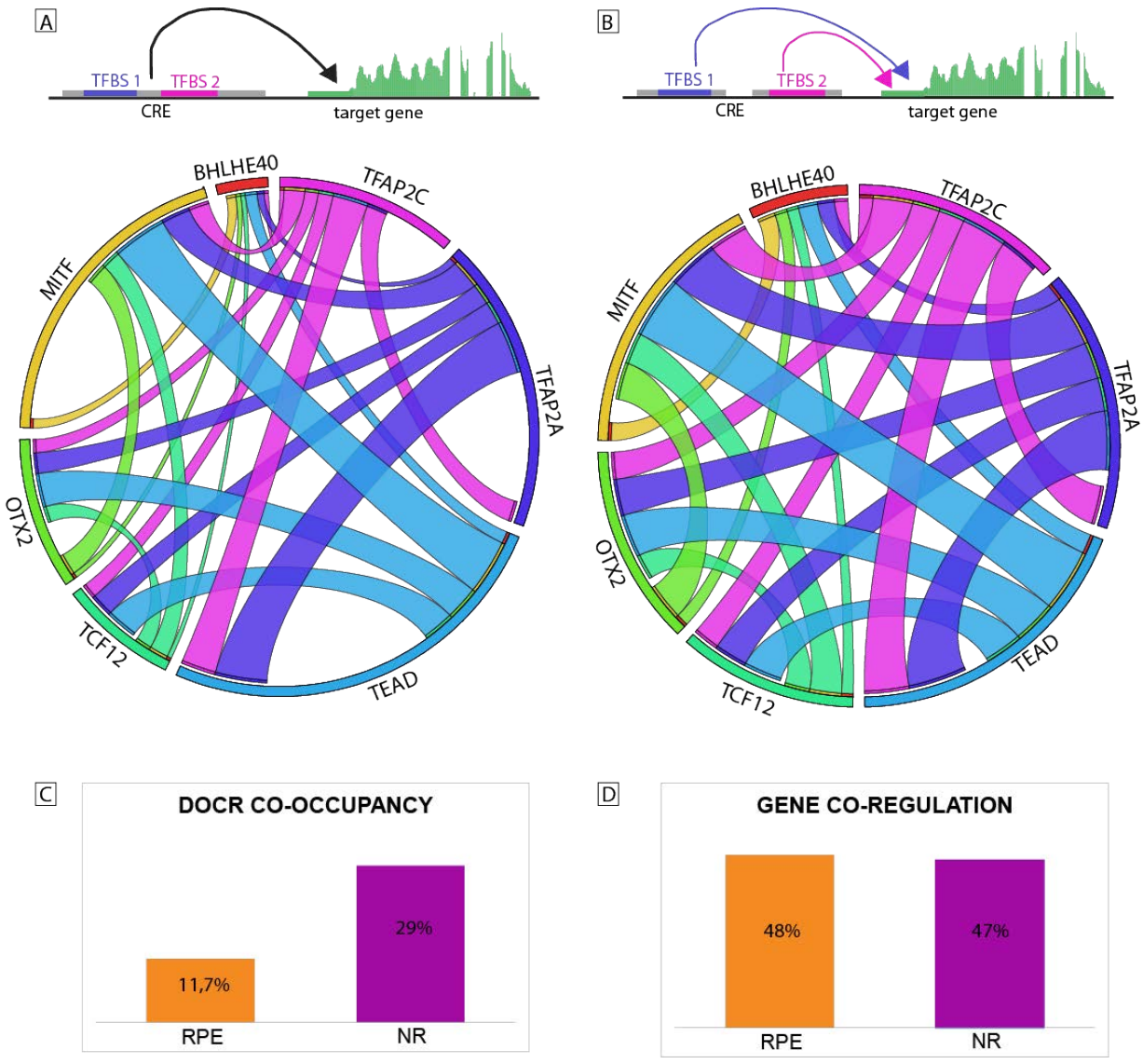

Figure 31. RPE TF cooperation. *(A) Circoplot illustrating the co-occupancy rate of TFBS for different TFs in the same DOCRs (B) Circoplot illustrating the degree of cooperation between TFs regulating the same gene from different DOCRs. (C) Average percentage of co-occupancy in the same DOCR for two different TF in RPE and NR. (D) Average percentage of two different TF regulating the same gene from different DOCRs in RPE and NR.*

Basically, the RPE network is less dependent on the interaction of the different TFs within the same CRE. In such a branched regulatory scenario, each TF is likely to trigger distinct and/or context-dependent transcriptional sub-programs within a broader developmental network. In this perspective, we assessed the ontology enrichment of the genes associated with DOCRs containing the different TFBS, disclosing different processes associated with particular TFs (or a sub-combination of particular TFs) (Fig 32).

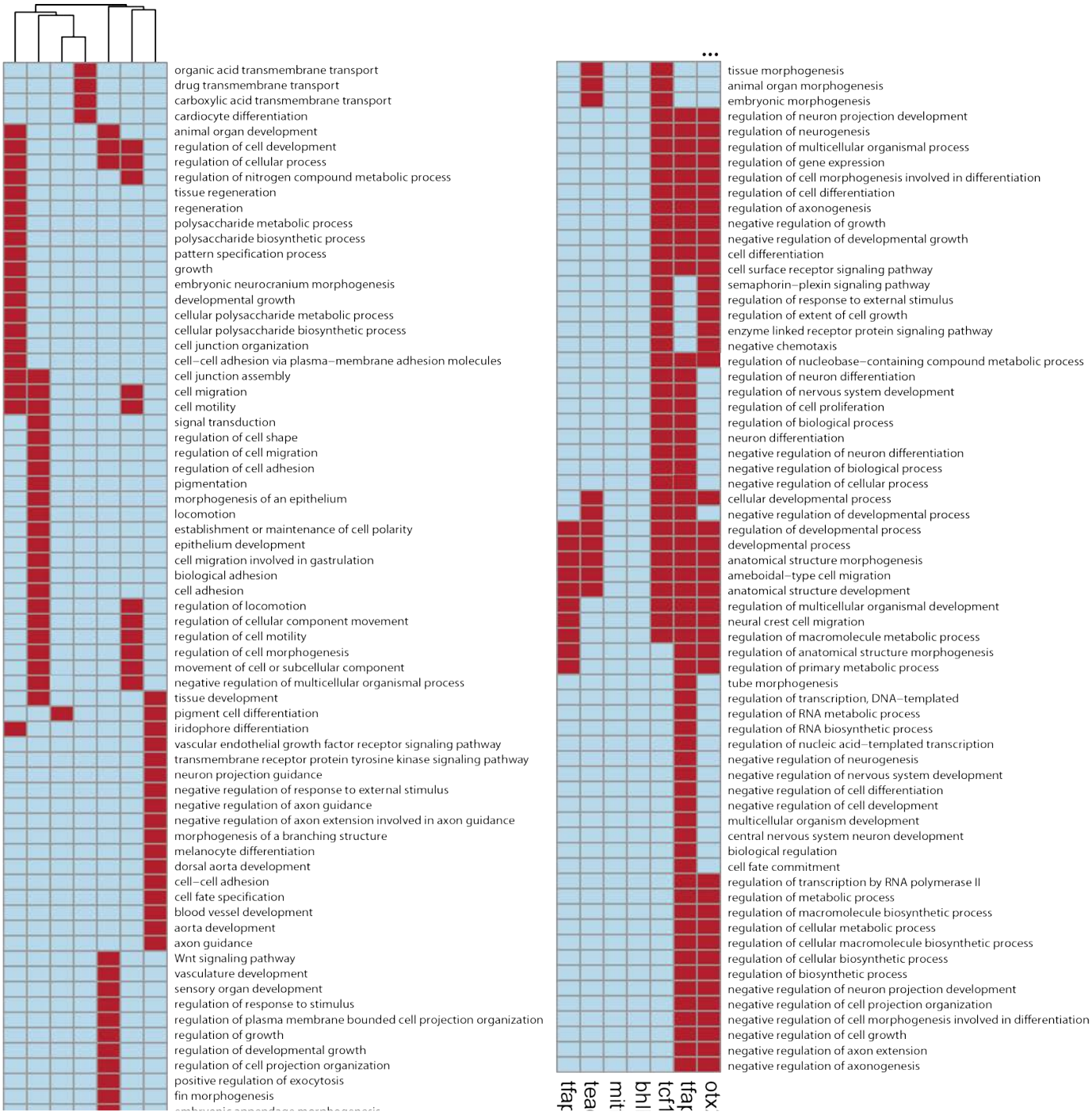

Figure 32. GO terms associated with RPE TFs. *Hierarchical cluster of the biological process GO terms enriched in genes associated with particular TFBS in RPE DOCRs. Different TFs trigger distinct cell features.*

While most of the TFBS under consideration resulted to be associated with genes involved in several GO processes, *mitfa* could be correlated only with pigment cell differentiation, together with *otx2*. This is in agreement with the data published by Martinez-Morales and colleagues in 2003 revealing a direct role for these factors in the transcriptional control of melanogenic genes (Martinez-Morales, 2003). However, unless *mitfa*, *otx2* binding sites are significantly associated with several more GO processes, alone, or often in association with either *tfap2c* or *tfap2c* and *tcf12* together. The GO terms associated to these three TFs, noteworthy clustering together, suggest that they may regulate transcription and metabolic processes while repressing the neuron differentiation and axonogenesis (presumably inhibiting the identity of NR). Interestingly, the analysis of GO terms linked to *tead* regulated genes points to a role in epithelium morphogenesis, controlling genes related to cell motility, regulation of cell shape, cell adhesion and also pigmentation.

Our ontology enrichment analysis revealed that *Tead* is associated almost exclusively with GO terms related to morphogenesis. On the other hand, our RNA-seq data highlighted the differential expression in the RPE of the intermediate filament machinery (Fig 14), suggesting a role in shaping of the RPE during optic cup folding. To gain insight into the regulation of these cytoskeletal components, we performed a motif enrichment analysis of the subset of DOCRs associated with IF and desmosome genes upregulated in the RPE (Fig 33 A, complete list of genes in online Appendix XIII). This analysis revealed that motifs for *tead* factors occupy the top positions of the ranking with a higher significance, being *tfap2a* and *tfap2c* binding sites enriched to a lesser extent (Fig 33 B). When compared to that of the entire set of DOCRs, the ratio *tead* binding motifs/DOCRs is 4.5 fold higher for the CREs specifically associated with components of the desmosome machinery,. This very same ratio does not increase for *tfap2a and tfpa2c*, on the contrary it decreases slightly (Fig 33 C). In the CREs associated with desmosome and IF, *Klf* factor binding motifs are also enriched (Fig 33 B). From our RNA-seq data, these factors resulted to be also upregulated at the earliest stage of RPE development (Fig 10).

The motif enrichment analysis of CREs associated to the desmosomal machinery points to a role of the *tead* family in the regulation of these cytoskeletal components. To investigate this link, we focused on the double mutant zebrafish embryos for the *tead* better-studied co-activators *yap* and *taz*, which display RPE defects (Miesfeld et al., 2015). We tested the mRNA levels of keratin and pigmentation genes in dissected heads of *yap -/- taz -/-* embryos at 18 hpf.. In the double mutant heads, the expression of keratin and pigmentation genes is severely compromised; on the other hand the expression of NR markers (*vsx2* and *six3a*) does not seem to be affected. This suggests that the optic cup molecular impairment caused by the inactivation of *tead* factors is RPE-specific and cannot be related to a general developmental problem of the eye (Fig 33 D). Furthermore, this observation confirms the direct role of *tead* factors in the transcriptional regulation of genes encoding for intermediate filaments and desmosome components.

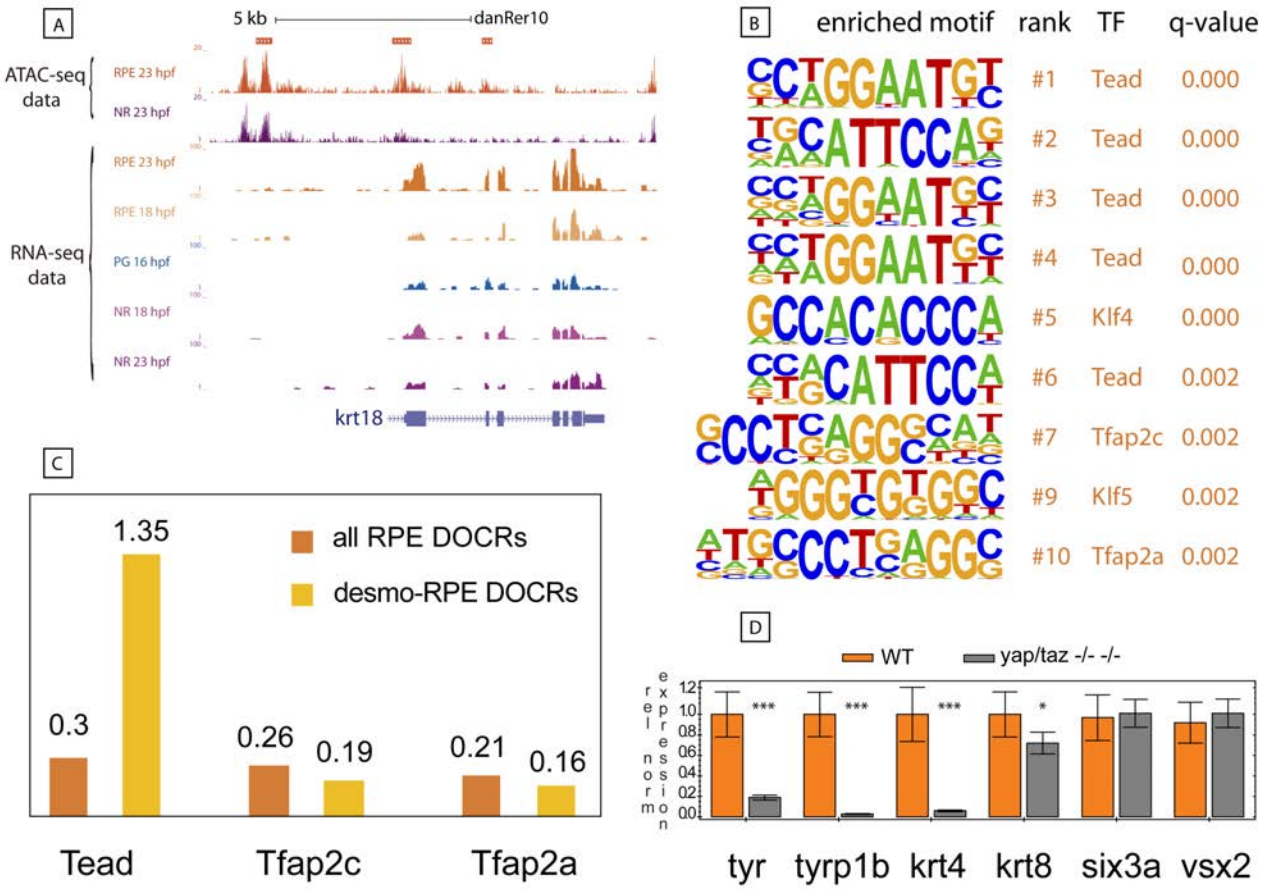

Figure 33. Tead role during RPE morphogenesis. *(A) Example of DOCRs more accessible in RPE associated with an intermediate filament gene (e. g. krt18). (B) Motif enrichment analysis of the DOCRs associated with intermediate filament or desmosome component genes. (C) TF binding motifs/DOCR ratio comparison between the all the DOCRs more accessible in RPE and the subset of DOCRs associated with intermediate filament or desmosome component genes.*

7. CRISPR/Cas9 F0 screen

We investigated *in vivo* the possible role of some candidate genes identified by our bioinformatics analyses as potentially important for the functionality of the eye GRNs. Due to its high efficiency, CRISPR/Cas9 technology opened the possibility of performing F0 mutagenesis screens in zebrafish (Shankaran, Dahlem, Bisgrove, Yost, & Tristani-Firouzi, 2017). We selected 21 candidate genes on the bases of their gene expression changes (Fig 34), CRE composition and/or dynamics, associated gene ontology terms, and number of paralogues to perform a CRISPR analysis at F0. We excluded from the screen those genes with multiple paralogues sharing a high homology of sequence in order to avoid possible compensation mechanisms (El-Brolosy et al., 2019). However, when it was experimentally justified, we targeted more than one paralogue by injecting different sgRNAs simultaneously in 1-cell stage embryos (see Method section for more details).

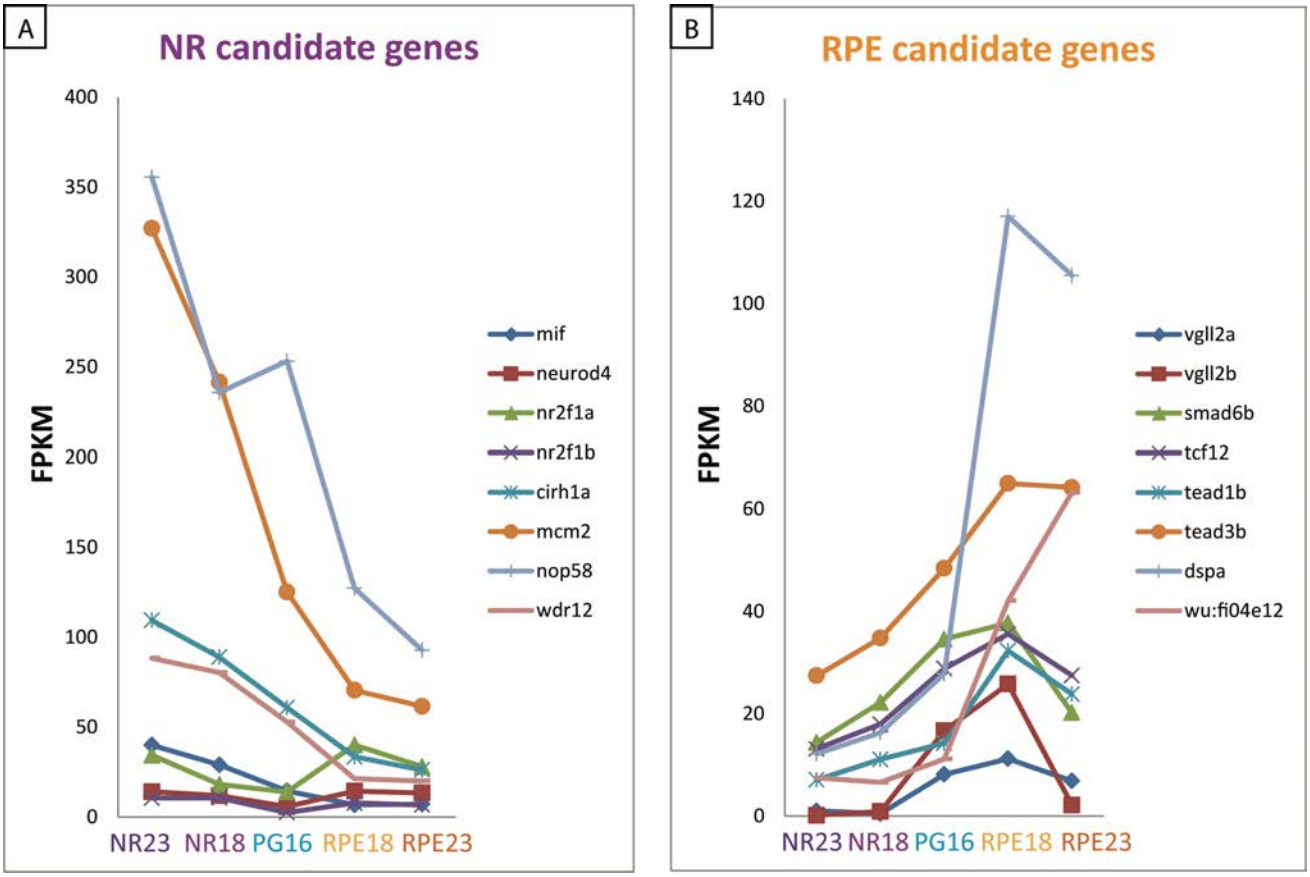

Figure 34. Gene expression level variations during optic cup development. *Expression levels of candidate genes producing an impaired eye phenotype when targeted in F0 with CRISPR/Cas9 system. (A) Expression levels of candidate genes upregulated in NR. Neurod4 and nr2f1 TFs are upregulated along also in RPE. This can underline a functional role for the development of the whole optic cup, not only NR. (B) Expression levels of candidate genes upregulated in RPE.*

For 12 candidate genes tested, a substantial percentage of sgRNA+Cas9 injected embryos displayed aberrant eye morphology, such as microphtalmia, eye fissure closure defects and/or hypopigmentation, thus confirming a role for the selected candidates on eye morphogenesis (Fig 35). Further details about candidate genes and resulting phenotype at 48 hpf are provided in the following Annex 1.

In conclusion, our CRISPR/Cas9 screens uncovered new genes necessary for eye development. This result indicates that biological investigations carried out with omics approaches are a suitable tool for the identification and validation of novel components of retinal GRNs.

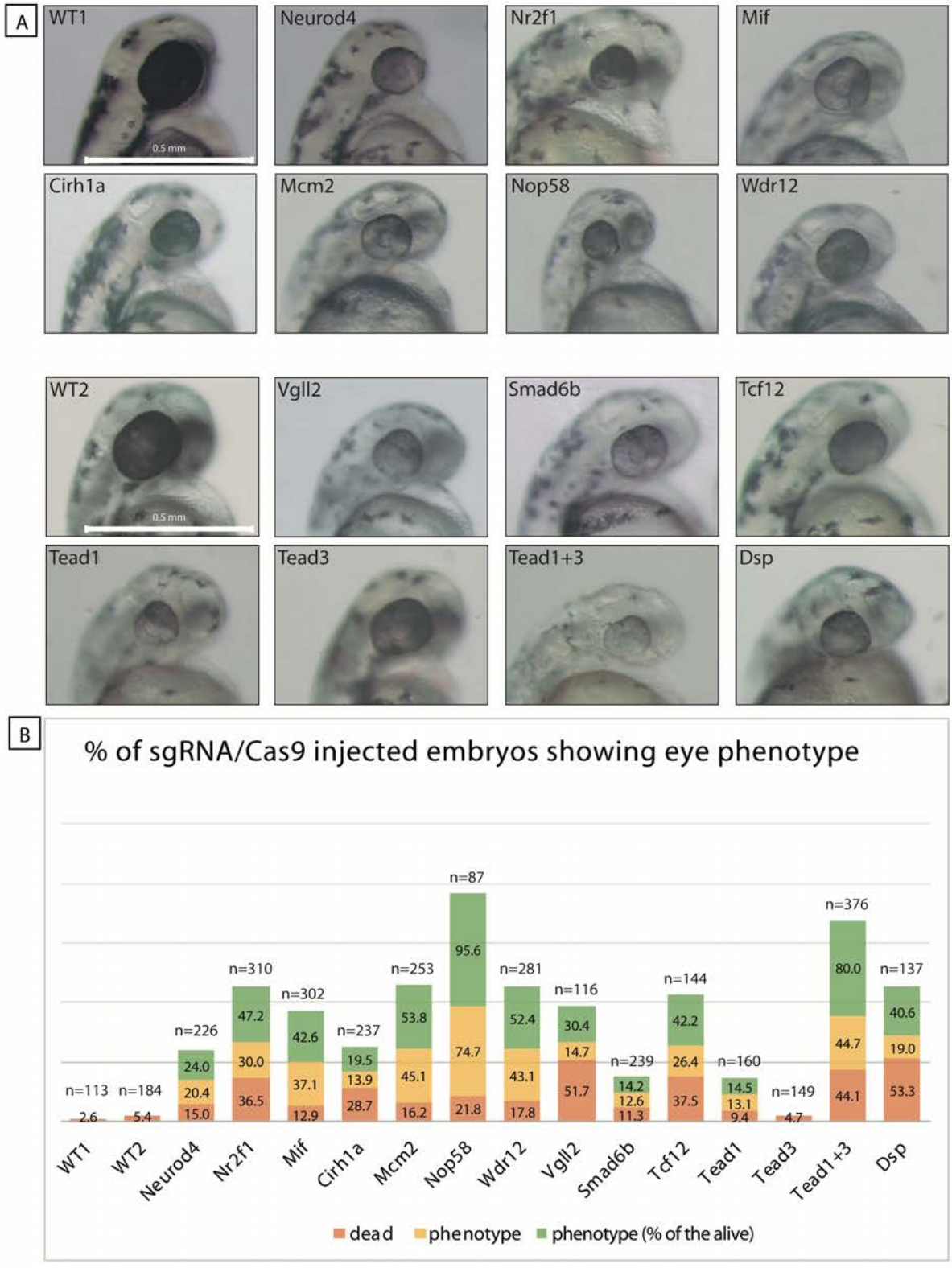

Figure 35. CRISPR/Cas9 F0 screening. *(A) Resulting eye phenotype upon the injection of Cas9 protein and sgRNAs for the targeted gene. (B) Table resuming the number of injected embryos showing an impaired eye phenotype upon the injection of Cas9/sgRNAs complex. The percentage of affected embryos is calculated both on the total number of embryos and on the number of embryos alive at 48 hpf.*

8. Gene expression analysis during hiPSCs-to-RPE differentiation

Ultimately, we are interested in ascertaining to which extend our findings on the architecture of the GRNs in zebrafish are conserved in human species. As previously discussed, deriving hiPSCs to RPE cells have important applications, both as a suitable model of RPE differentiation in basic research, as well as in cell replacement therapy for retinal degenerative diseases. In view of this, we followed the transcriptional changes occurring along the differentiation process from hiPSCs to RPE. We were interested in verifying not only whether the RPE TFs identified in zebrafish played a role in human RPE differentiation, but also whether or not the *consecutio temporum* of expression of the said TFs was preserved. We thank our collaborator Berta de la Cerda (CABIMER, Seville) for her invaluable work with hiPSCs-to-RPE cell culture system, which provided us the starting material for our molecular experiments. Several protocols for RPE cell differentiation have been described, but they are all quite time-consuming and take several weeks. The protocol we used (see Method section for further details) requires up to 100 days to obtain mature RPE cells suitable for surgical transplantation. At the end of this differentiation process, all the RPE cells should display proper pigmentation and morphology, cell type-specific marker expression, polarized membrane, vascular endothelial growth factor secretion and phagocytic activity. However, since we were interested in the early stages of RPE specification and development, we focused our analysis on the first 4 weeks of cell culture differentiation. While the hiPSC colonies displayed morphological features typical of pluripotent cells, such as a smooth surface and tightly packed cells with large nuclei (Fig 36 A). Between the second and third week of differentiation the cells start to acquire a pigmented shade and hexagonal shape (Fig 36 C-D). At week 4, clusters of lightly pigmented cells with typical RPE cobblestone appearance can be already appreciated (Fig 36 E).

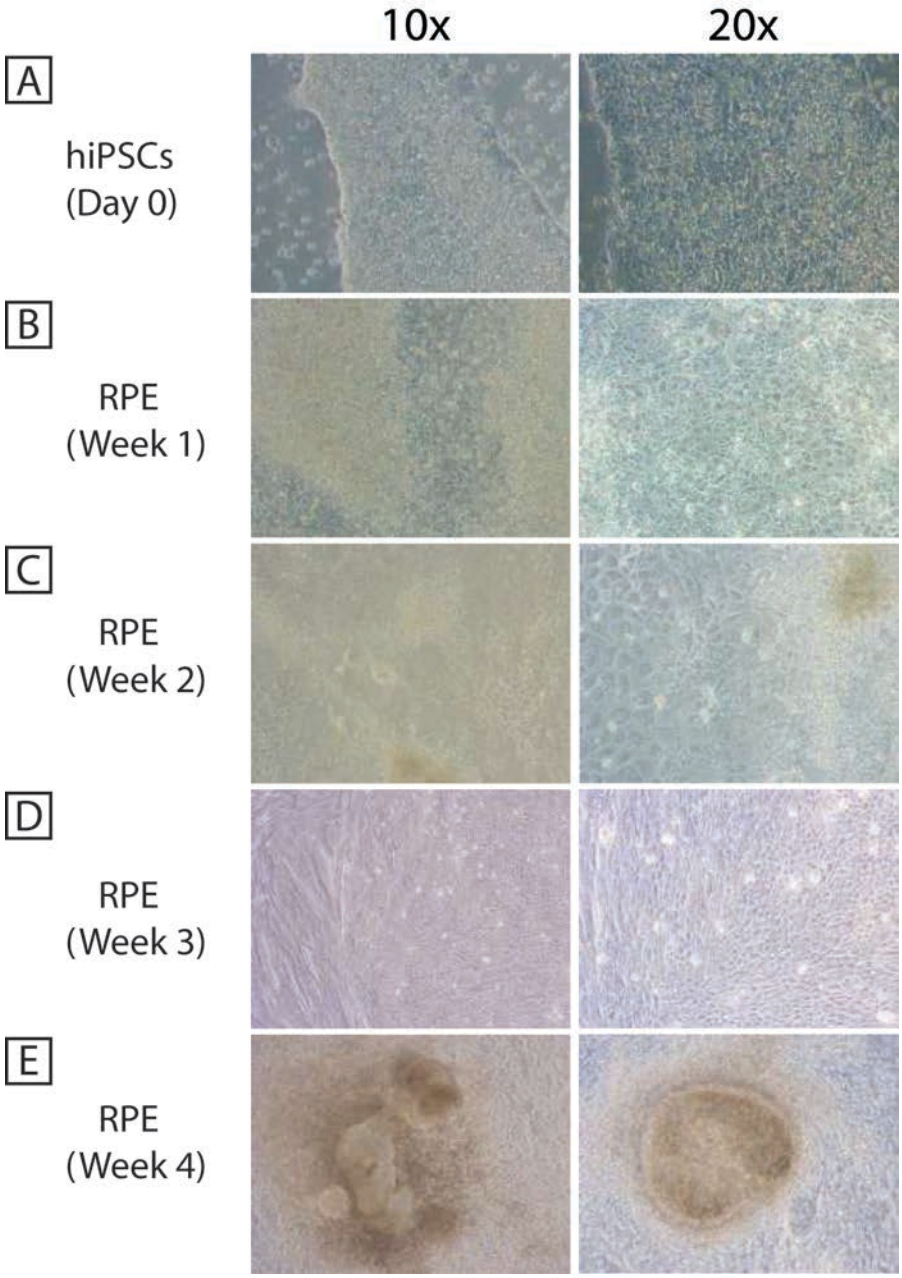

Figure 36. hiPSCs-to-RPE differentiation. *(A) hiPSCs prior differentiation. Compact colonies that have distinct borders, well-defined edges and a large nucleus with less cytoplasm. (B) Week 1 of RPE differentiation. Cells begin to acquire a more polygonal morphology. (C) Week 2 of RPE differentiation. Hexagonal cells starting to lightly pigment. (D) Week 3 of RPE differentiation. Cells start to appear like an epithelial sheet. (E) Week 4 of RPE differentiation. Evidently pigmented cells with cobblestone morphology.*

First of all, we tested by RT-qPCR the mRNA levels of stemness genes (NANOG and OCT4) and mature RPE markers (CRALBP, RPE65) as internal controls of our experimental system. As expected, the stemness

markers decreased rapidly after the first week of differentiation while CRALBP and RPE65 rose in the fourth week (Fig 38). Then we investigated the gene expression dynamics of the following candidate genes:

- *Genes already known to be involved in RPE early development:* MITF, OTX2, BHLHE40, TFEC, TYR;
- *Notch receptor genes:* NOTCH1, NOTCH2, NOTCH3. Our RNA-seq data highlighted *notch* genes as upregulated in the RPE. Notably, they peak at 18 hpf and then rapidly decrease, suggesting a possible involvement as transient early signalling pathway (Fig 37 A). In addition, they also are associated with a considerable number of DOCRs, both in NR and RPE, implying the need of a fine regulation *via* the combinatorial action of multiple CREs (Fig 37 B);

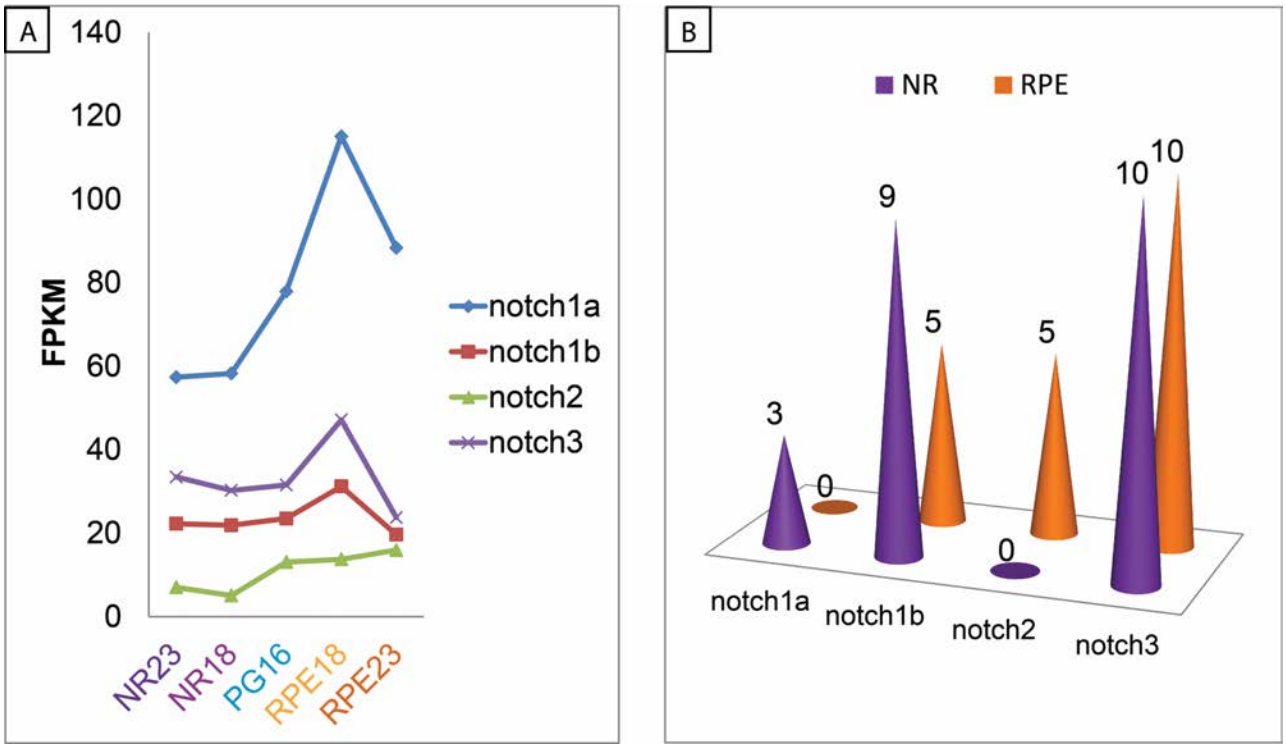

Figure 37. Notch regulation during optic cup development. *(A) Notch gene transcript levels in the distinct domains and stages of the optic cup examined. (B) Number of DOCRs associated with notch genes. In purple are reported the DOCRs more accessible in NR, whereas in orange the DOCRs more accessible in RPE.*

- Intermediate filament and desmosome genes: DSP, EVPL, KRT4, KRT5, KRT8;
- TFs identified in the first wave of activation: TCF12, SMAD6, TFAP2A, TFAP2C, VGLL2, TEAD1, TEAD2, TEAD3, TEAD4.

Except OTX2, rising very early after the induction of RPE differentiation, the other well-known specifiers and/or marker of RPE identity (MITF, BHLHE40, TFEC, TYR) only start to rise between the third and fourth week of differentiation. On the other hand, human orthologous TFs that in zebrafish belong to the earliest RPE cluster, such as TFAP2A, TFAP2C, TEAD2 and TEAD3, continued to be among the earliest genes to be

expressed after the initiation of RPE cell differentiation. Notably, VGLL2 rapidly rise and fall in the first week, following the same temporal expression pattern already seen in zebrafish. The only exceptions in the TF order of appearance between zebrafish and human are TCF12 and SMAD6. While in zebrafish the expression trend of these TFs resemble VGLL2's one, in human cells they start to be abundantly expressed only after the third week. Always according to our zebrafish *in vivo* data, also intermediate filament, desmosome and *notch* genes are upregulated during human RPE cell differentiation. Currently our data do not allow us to make functional hypotheses about the possible role of *notch* signalling on the differentiation of the RPE, but this observation would deserve attention in future studies. Nevertheless, this experiment confirms that the activation of intermediate filaments and desmosome is a conserved feature across evolution, which may play a crucial role for the morphogenesis of RPE cells. Furthermore, our observations indicate that the regulatory logic of the genetic networks specifying RPE cells is conserved among vertebrate species (Fig 38).

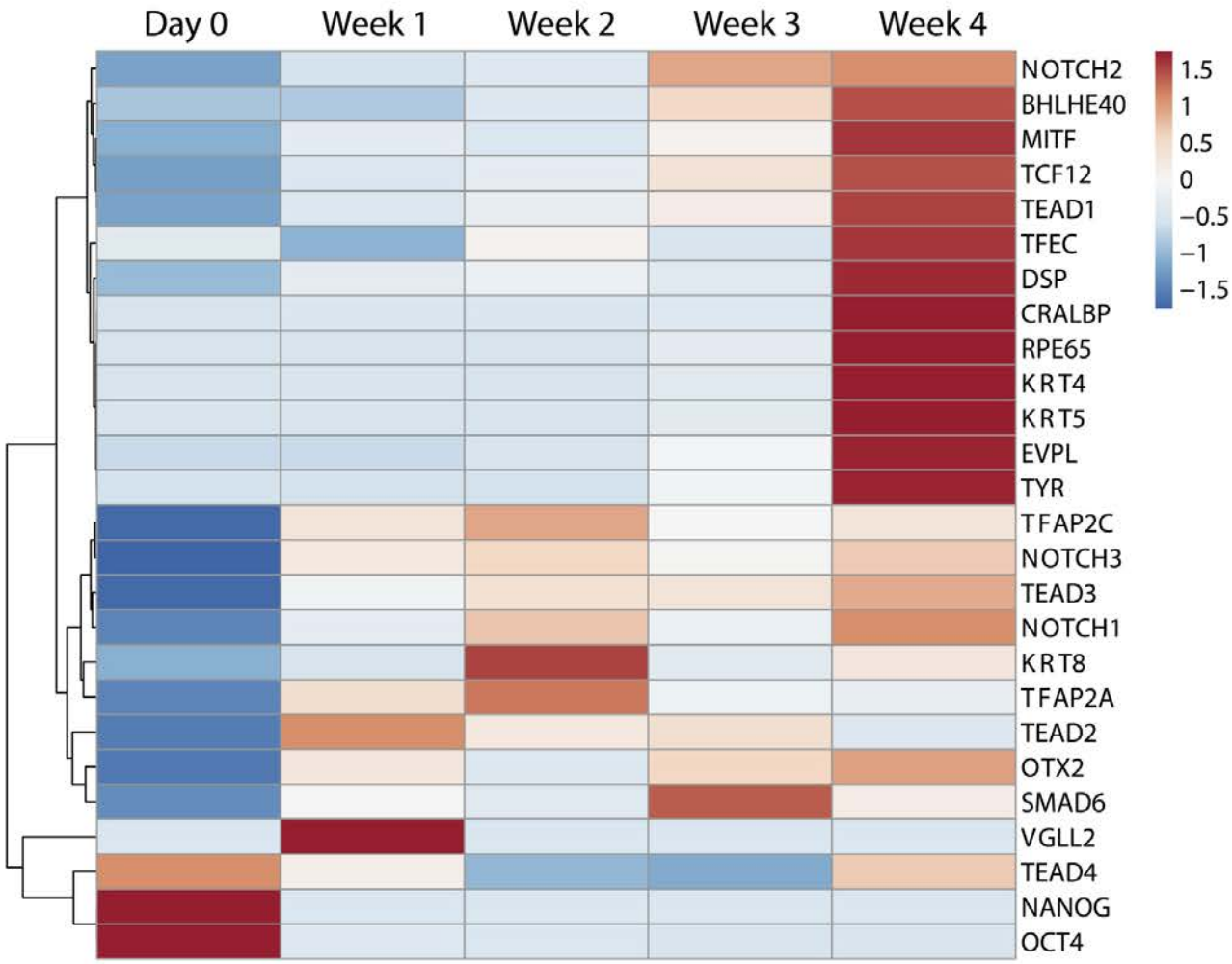

Figure 38. Gene expression during hiPSCs-to-RPE differentiation. *Hierarchical clustered heatmap showing gene expression level variations during the differentiation towards RPE starting from hiPSCs.The genes selected for this analysis were highlighted as possible pivotal during RPE development by our zebrafish omics datasets.*

Annex I

1. Description of CRISPR/Cas9 F0 screen phenotypes

Basing on their expression pattern, regulatory dynamics and ontology, we selected 21 candidate genes to be targeted with CRISPR/Cas9 mutagenesis tool. In the event that two close paralogues of the same candidate gene have been targeted at the same time, this is appropriately indicated in parentheses. The selected candidate genes are: *cirh1a, dhx3, dkc1, heart, hells, mcm2, mcm5, mif, nop58, tsr2, ttcf27, twistnb, wdr12, dsp (dspa + wu:fi04e12) , neurod4, nr2f1 (nr2f1a + nr2f1b), smad6b, tcf12, tead1 (tead1a + tead1b), tead3 (tead3a + tead3b), vgll2 (vgll2a + vgll2b).* The mutagenesis *of dhx3, dkc1, heart, hells, mcm5, tsr2, ttc27* and *twistnb* produced no reliable rate of consistent eye phenotype (data not shown). The description of aberrant eye phenotype resulted from the mutagenesis of other candidate genes is presented below.

neurod4*:* this gene belongs to the neurogenic differentiation factor family and encodes a *bHLH* TF expressed in the developing nervous system with high levels of expression in the brain, retina and cranial ganglions. Expression gradually becomes restricted to the NR. *Neurod4* also regulates amacrine cell fate determination (Geer et al., 2010). In our transcriptomic analyses, it belongs to the cluster 6 of TF heatmap (i.e. the cluster of genes particularly expressed in NR at 18 hpf)(Fig 8). However, this TF is also upregulated in RPE vs PG, suggesting a possible determining role in the initial differentiation of the whole optic cup (Fig 34 A). 24% of the crispant embryos displayed microphtalmia and hypopigmentation (Fig 35).

nr2f1 *(nr2f1a + nr2f1b):* the protein encoded by this gene is a nuclear hormone receptor and transcriptional regulator. Defects in this gene are associated with Bosch-Boonstra optic atrophy syndrome (C.-A. Chen et al., 2016; Geer et al., 2010). The two zebrafish orthologues of this gene are both upregulated in NR (Fig 34 A). *Nr2f1a* belongs to TF cluster 2 (genes particularly expressed in NR at 23 hpf), whereas *nr2f1b* belongs to cluster 6 (genes particularly expressed in NR at 18 hpf) (Fig 8). A large percentage of the injected embryos died before reaching 48 hpf. 47.2% of the survivor crispant embryos showed severe microphtalmia and an abnormal optic cup folding (Fig 35).

mif*:* this gene functions as an autocrine mediator of adhesion-depent signalling in cell cycle progression (Liao, Bucala, & Mitchell, 2003). *Mif* is upregulated in NR (Fig 34 A). 42.6% of the crispant embryos showed mild microphtalmia and hypopigmentation (Fig 35).

cirh1a*:* this gene encodes a ribosome biogenesis factor and may also acts as a transcriptional regulator (Prieto & McStay, 2007; Yu, Mitchell, & Richter, 2009). It is upregulated across the examined stages of NR

differentiation (Fig 34 A). The sgRNAs+Cas9 injected embryos suffered a noticeable rate of mortality. 19.5% of the survivor injected embryos showed marked microphtalmia (Fig 35).

mcm2*:* the protein encoded by this gene is one of the highly conserved mini-chromosome maintenance proteins that are involved in the initiation of eukaryotic genome replication. This protein has been shown to regulate the helicase activity of the complex (Geer et al., 2010). Our transcriptomic data detected this gene as strongly upregulated in NR (Fig 34 A). 53.8% of the crispant embryos exhibit abnormal eye development with microphtalmia, defects in eye fissure closure and hypopigmentation (Fig 35).

nop58*:* this gene encodes for a core component of box C/D small nucleolar ribonucleoproteins and it is required for 60S ribosomal subunit biogenesis (Geer et al., 2010). Its expression is considerably high in PG and NR, particularly increasing at 23 hpf. In parallel, it gradually decreases in RPE (Fig 34 A). 95.6% of the crispant embryos displayed a general impairment of the embryo morphology, with severe microphtalmia and disrupted shaping of the optic cup (Fig 35).

wdr12*:* this gene encodes for another protein involved in ribosomal biogenesis (Geer et al., 2010). It is highly expressed in PG and increase in NR at 18 hpf, remaning stable at 23 hpf, while decreasing gradually in RPE (Fig 34 A). The 52.4% of the survivor injected displayed reduced eye size (Fig 35).

vgll2 *(vgll2a + vgll2b):* these genes are members of the *vgll* family, which comprises transcriptional co-factors binding *tead* TFs to regulate events involved in embryonic patterning and cell fate determination. *Vgll* proteins are believed to mainly repress gene expression, regulating similar genes to those regulated by *yap* and *taz* (Figeac et al., 2019; Lin, Park, & Guan, 2017). However, the mechanisms that modulate *vgll2* interaction with *tead* factors remain poorly characterized. In our RNA-seq data both *a* and *b* zebrafish orthologues of *vgll*2 transiently peak in RPE at 18 hpf, then rapidly decrease at 23 hpf (Fig 34 B). They both belong to the TF cluster 3 (Fig 8). The injected embryos showed a very high level of mortality; more than half of the embryos do not reach 48 hpf. However, 30.4% of the embryos that managed to survive exhibits microphtalmia, slight defects of optic cup fissure closure and hypopigmentation (Fig 35).

smad6b*:* this gene belongs to the SMAD family proteins, which are signal transducers and transcriptional modulators that mediate multiple signalling pathways. *Smad6* is known to negative regulate BMP, TGFβ/activin and Wnt/β-catenin pathway (Xie et al., 2011). Our analysis of the optic cup transcriptome locates the zebrafish orthologue *smad6b* in the TF cluster 3 (Fig 8). It is robustly expressed in PG and RPE at 18 hpf, suggesting a pivotal role at the earliest phase of RPE differentiation (Fig 35 B). 14.2% of the embryos crispant for this gene displays reduced eye size and hypopigmentation (Fig 34).

tcf12*:* this gene encodes for a member of the *bHLH* family. It is expressed in many tissues and may participate in regulating lineage-specific gene expression through the formation of heterodimers with other *bHLH* proteins. *Tcf12* is an effector of the Wnt signalling pathway and can be related also with the TGFβ pathway. Indeed, the cooperation between these pathways may be important for the specification of cell fates during development (Brantjes, Barker, van Es, & Clevers, 2002; Geer et al., 2010; Letamendia, Labbé, & Attisano, 2001) and, therefore, RPE specification. *Tcf12* expression pattern traces *smad6b*'s one (Fig 34B). It also belongs to the TF cluster 3 (Fig 8). The embryos injected with Cas9 protein and sgRNAs targeting this gene exhibit a high rate of mortality; however the 42.2% of the survived embryos display coloboma, microphtalmia and slight defects in eye pigmentation (Fig 35).

tead1 *(tead1a + tead1b):* as already mentioned, members of the *tead* family of TF are well known as transcriptional effectors of the Hippo signaling pathway and are implicated in processes such as development, cell growth and proliferation, tissue homeostasis, and regeneration. The majority of our knowledge of *teads* is in the context of Hippo signalling as nuclear DNA binding proteins passively activated by *yap* and *taz*. However, recent studies demonstrated alternative Hippo-independent regulation of *teads,* for example *via vgll* factors (Lin et al., 2017). In zebrafish, *tead* family comprises four paralogues sharing a high sequence homology. Only two of the four paralogues resulted to be differentially regulated during the optic cup development, *tead1b* and *tead3b*, both upregulated in RPE and belonging to TF cluster 3 (Fig 8; Fig 34 B). However, given their high sequence homology, we targeted the four paralogue genes, first in pairs with their closest paralogue and then all together. 14.5% of the crispants for *tead1a* and *tead1b* showed severely reduced eye size and impaired morphology, defects of the optic fissure closure and pronounced hypopigmentation (Fig 35).

tead3 *(tead3a + tead3b):* double crispants for *tead3a* and *tead3b* exhibited no clear eye phenotype. Many embryos had a slightly reduced eye size, however this could be due to a little delay in development, also because later on the embryos continued to develop normally as wt-like (Fig 35).

tead1 + tead3 *(tead1a + tead1b + tead3a + tead3b):* the embryos injected with Cas9 endonuclease and sgRNAs targeting the four *tead* paralogues suffered a high rate of mortality. Although we cannot exclude that this mortality effect may be due to a toxicity effect produced by the injection of many sgRNAs, the total concentration of each sgRNA had been lowered to be comparable to the other CRISPR/Cas9 screen experiments performed (see Method section for more details). An alternative hypothesis for high lethality is related to the indispensable function of *teads* during development. Not surprisingly, also the *yap -/- taz -/-* zebrafish mutants die before 20 hpf. The "death escaper" crispants, likely to be genetic mosaics that

could bear the first days of embryonic development, showed a strong phenotype in 80% of the cases. Embryos dispaly abnormal morphology, severe microphtalmia, eye fissure closure defects and an almost total deficiency of pigmentation throughout the entire body (Fig 35).

dsp *(dspa + wu:fi04e12): desmoplakin* (*dsp*) is a structural constituent of cytoskeleton that anchors intermediate filaments to desmosomal plaques and forms an obligate component of functional desmosomes (Geer et al., 2010). In zebrafish, both *dspa* and its paralogue *wu:fi04e12* are significantly upregulated in the RPE (Fig 34 B). More than half of these embryos die before they reach 48 hpf. This was not unexpected because *desmoplakin* homozygous null mice die by embryonic day E6.5 due to instability of desmosomes and tissue integrity (Gallicano et al., 1998). Lethality phenotype rescue, by aggregation with wild-type tetraploid morulae, increases mouse embyronic survival but with noted major defects in heart muscle, epidermis and neuroepithelium (Gallicano, Bauer, & Fuchs, 2001). In zebrafish, 40.6% of survivor crispants exhibits aberrant embryo morphology, microphtalmia, coloboma and eye hypopigmentation (Fig 35).

Discussion

1. Optic cup GRNs

Mechanisms controlling the development of the vertebrate eye have intrigued the minds of developmental biologists for generations. Three embryonic tissues, the neural ectoderm, the surface ectoderm and the periocular mesenchyme, contribute to the formation of such a complex and fascinating organ. Hence, the developing eye has always represented an invaluable and accessible system for studying the interactions among cells, different inductive signals and, more recently, genes, in specifying multiple cell fates. In the last decade, the advent of NGS technologies produced a multitude of data inspecting the genomic and transcriptomic eye landscapes in different mutants and/or in different cell types. Unfortunately this omics exploration of the eye has been uneven, focusing mainly on later stages of retina development and, in particular, on the mechanisms underlying the differentiation of photoreceptors: a relevant topic in the context of retinal degenerative diseases. Much less has been investigated about the early steps of optic cup development, and very little on the main subject of this thesis: the primary GRN bifurcation of the optic vesicle into NR and RPE. We can consider the NR and the RPE as *different twins:* one will give rise to highly specialized neurons, the other to an epithelial sheet; one is composed of cuboidal cells undergoing basal constriction, the other is formed by polygonal cells flattening as the optic cup folds; eventually, one will detect visual stimuli and the other will pigment to absorb scattered light, recycle damaged membranes from and supply nutrient to the photoreceptors. However, both of them differentiate very quickly from the same kind of cells: the optic vesicle neuroepithelial progenitors. To date, the knowledge of regulatory logics leading to their different final shape and identity has remained fragmentary and unclear. The present work aimed to dissect the GRNs in charge of this cell-fate bifurcation investigating both transcriptional and chromatin accessibility changes during the differentiation of the two optic cup domains. Our datasets highlighted a higher number of DEGs and more accessible chromatin regions during the differentiation from PG towards RPE than towards NR. Further, RPE identity requires a transcriptional program with a strong repressive component against NR-specific genes. This is particularly true in case of TFs, since the number of repressed TFs exceeds the number of TFs activated. All these data together may suggest that the PG cell-identity is by default committed to a neural differentiation programme, whereas the RPE development not only requires chromatin remodelling to expose tissue-specific CREs, but also the complementary repression of neurogenic TFs.

2. Neural retina GRNs

The data here presented suggest that the neural differentiation programme is the default state in the uncommitted progenitors of the optic vesicle. The fact that a number of TFs, such as those belonging to the

her family, can be found associated to 15 hpf PG, and 18 hpf NR and RPE gene expression clusters, but are absent in the two optic cup domain clusters at 23 hpf, is in line with this hypothesis. Recent studies demonstrated that *her* genes play critical roles in maintaining the undifferentiated state of neural progenitors and regulating neurogenesis and gliogenesis (Cheng et al. 2015). If, as we argue, the identity of the optic vesicle progenitors is already primed towards neural differentiation, the expression of *her* genes would be necessary to prevent the imminent neurogenesis, allowing progenitor proliferation and an eventual epithelial switch. *Her* factors continue to be expressed in NR and RPE at 18 hpf and then decrease at 23 hpf in both tissues. Maybe in the first case the neurogenesis finally needs to start, whereas, in the latter one, there is no more need to inhibit neuronal differentiation since the RPE has already acquired an epithelial identity. In either way, our work is insufficient to clearly explain any possible role for the different *her* genes in the distinct eye domains. Another interesting aspect is that *her* gene activity is dependent on *notch* signalling, that can either activate or repress their expression (Cheng et al. 2015). Even if we have no data to directly link the expression of *her* factors to *notch* signalling in the RPE, we found *notch* proteins to be transiently expressed and tightly regulated in the pigmented eye tissue. *Notch* pathway is already well known to repress proneural gene expression (Engler, Zhang, and Taylor 2018) and a very recent work proposed that the RPE-derived *notch* signal could be critical for the fate determination of RPCs (Ha et al. 2017). Nevertheless, its potential role in RPE development has been only suggested but never investigated (Schouwey and Beermann 2008).

After the PG stage, NR development stands on a network pivoting on several TFs already well-known to be implicated in retina development. What we found is that this network is highly interconnected, based on the choral action of *sox* and *homeodomain* TFs. The *homeodomain* is a 60 amino acid DNA binding module composed of three alpha helices in a helix-turn-helix configuration, able to bind the *homeobox* DNA motif. *Homeodomain* proteins are among the most numerous TFs, however, they exhibit low sequence specificity or weak binding affinity and can function with high specificity *in vivo* only incorporating additional DNA binding domains or interacting with additional TFs (Zou and Levine 2012). Since our work detected several *homeodomain* TFs sharing a common binding motif and being co-expressed at the same stages of NR (e.g. *rx1, rx2, vsx1, vsx2, lhx2b*), we hypothesize that the most likely scenario is that they can virtually regulate the same gene batteries to control NR development cooperatively. Even if the presence of a TFBS in an ATAC-seq-detected-open chromatin region does not ensure that the TF is actually binding and functioning as transcriptional regulator, the *homeobox* sequences that we detected in NR DOCRs exhibit a high grade of cooperativity in virtually regulating the same gene. Additionally, in almost 90% of the cases, they regulate NR genes together with *sox* TFs.

In agreement with our interpretation, when we undermined NR regulatory network in teleost models by mutating both *vsx1* and *vsx2* nodes, neural retina was properly specified. Developmental defects were only observed at later stages when *vsx* loss of function resulted in a failure in the differentiation of

bipolar cells, leading to blindness. This unexpected outcome is in contrast to the phenotype associated to *Vsx2* mutation in mouse, which severely affected the whole retina development (Green, Stubbs, and Levine 2003). This could be due both to a simply different hierarchical weight that the same TF has in different animal models and to the genetic buffering capacity of each species in response to detrimental mutations. Anyhow, to further investigate the potential regulatory network changes in the *vsx1/vsx2* null zebrafish embryos, we interrogated both the transcriptomic and chromatin accessibility landscapes. Although our RNA-seq data determined a modest misregulation of few NR TFs, these transcriptomic results did not point out any strong evidence of transcriptional compensation to counterbalance the loss of *vsx* factors. In parallel, ATAC-seq of the double mutants revealed an increased accessibility of CREs that can be linked to neural genes. These data in overall appear cryptic and of ambiguous interpretation. A possible explanation may be that zebrafish embryos manage to countervail the loss of *vsx* with minimal transcriptome changes, thanks to the extreme redundancy and robustness of their regulatory network based on the *homeobox* factor cooperative action. Different *homeobox* factors seem to coordinate the expression of the same genes from different CREs. Hence an increased "chromatin relaxation" of CREs containing non-*vsx homeobox* factors would promote the binding efficiency (and therefore activity) of the above factors. This chromatin remodelling is indeed supposed to permit the expression of neural genes that otherwise, in absence of functional *vsx* regulators, would be restricted to become transcriptionally active.

Chromatin relaxation renders DNA structure more transcriptionally permissive, presumably exposing additional regulatory elements such as *shadow enhancers,* an expression that stands for "remote secondary enhancers mapping far from the target gene and mediating activities overlapping the primary enhancer"(Hong, Hendrix, and Levine 2008). Indeed, GRN robustness can be conferred not only by the expression of multiple genes that perform redundant tasks, but also through the presence of several individual enhancers driving similar expression patterns. The extent to which enhancer redundancy exists and can thereby have a major impact on developmental robustness remains unclear. However, recent studies in *Drosophila* estimated that 64% of the examined loci possess shadow enhancers (Cannavò et al. 2016). Thus, a possible molecular mechanism to explain GRN robustness in *vsx* double mutants is a readjustment of the CRE accessibility landscape to maintain the main regulatory architecture of the network. To describe this mechanism, momentarily exiting the scientific area and entering the world of literature, we can steal Tancredi's words in the famous Southern Italian novel *Il Gattopardo*: "everything needs to change so everything can stay the same" (Tomasi di Lampedusa 1958).

The failing of bipolar cell differentiation in *vsx* double mutants, can be explained by the existence of an independent set of CREs regulating on one side the fate of early NR domain and on the other the differentiation of bipolar cells later during development. A very recent study by Norrie and colleagues individuated a bipolar neuron-specific super enhancer upstream of Vsx2, whose deletion in mice led to the

loss of bipolar neurons (Norrie et al. 2019). This mouse phenotype resembles our results in zebrafish more than then the direct mutation of Vsx2 mouse gene. As we already hypothesized, during the initial development of NR, zebrafish embryos somehow compensate the lack of *vsx* factors. Later on, at the moment of the differentiation of bipolar cells, which are among the last retinal neurons to differentiate, the retina GRN is no longer capable to sustain the lack of *vsx*, resulting in the complete absence of bipolar neurons in a perfectly shaped eye. This role for *vsx* genes in bipolar cells specification is in line with previous observations in Drosophila, indicating an ancestral function for Vsx genes in the specification of retinal interneurons in all metazoans (Erclik et al. 2008).

3. RPE GRNs

While our data describe a redundant NR GRN established on just two TF families, the RPE rather seems to base its developmental program on the coordinated action of various TFs. Previous literature data recognized *otx2* and *mitfa* as the two main factors responsible for RPE development (Martinez-Morales et al. 2001; Nguyen and Arnheiter 2000). Nevertheless, in our analysis, the transcriptional levels of both TFs start to increase only at later stages of RPE morphogenesis. However, while *otx2,* before its transcriptional increase at 23 hpf, in optic vesicle PG and RPE at 18 hpf already presented considerable expression levels; *mitfa* is really poorly transcribed, with expression values close to the background. In addition, *otx2* binding sites resulted to be associated with genes linked to several developmental processes, whereas *mitfa* only resulted to be significantly related to genes involved in pigment cell differentiation together with *otx2*. Although this result is in agreement with previous data by Martinez-Morales et al. (Martinez-Morales 2003), which showed that the collaboration between these two TFs induces the expression of melanogenic genes, the discovery that *mitfa* function in RPE was restricted only to the transcriptional activation of pigmentation cascade was unexpected. This may be due either to the statistical limitations inherent to GO analyses, or to a less important hierarchical weight for *mitfa* in zebrafish than in other vertebrate species. An antecedent work demonstrated that, in zebrafish, *mitfa* is not even necessary for eye pigmentation, suggesting that its role could be replaced by other *bHLH* factors (Lane and Lister 2012). Our data also found a robust expression of several *bHLH* TFs in RPE (e.g. *bHLHE40, bHLHE41, tfec*). However, an alternative scenario also supported by our work is that the dispensability of *mitfa* in zebrafish RPE specification might be due to an actual secondary role in the RPE GRN, provided that at the beginning of RPE differentiation it is scarcely transcribed. To what extent this is a zebrafish-specific molecular mechanism or can also be valid in other species will be discussed in a following section (**3. GRN in human RPE in vitro model: from developmental biology to retinal diseases**). Apart from all the possible interpretations that can be given on the issue, our study highlighted an earlier wave of TFs expression before the peaking of *otx2* and *mitfa*. This

includes genes such as *tcf12*, *tead1b, tead3b, tfap2a* and *tfap2c*, which may actually play not only an earlier but also a more crucial role than *mitfa* in the specification of the zebrafish pigmented epithelium.

Tcf factors are the major effectors of *Wnt* pathway (Cadigan and Waterman 2012). Although *tcf12* role during RPE genesis has not been investigated, such an early expression may link *Wnt* signalling (i.e. already known to be involved in RPE specification) with the establishment of the RPE transcriptional program. Indeed, *tcf12* TFBS in RPE-more-accessible-DOCRs are associated precisely with genes involved in the regulation of the *Wnt* pathway and the negative regulation of neuron differentiation. These findings fit with our interpretation of the transcriptomic data, describing the initial necessity for progenitor cells to inhibit neuronal identity in order to differentiate into RPE. Also *tfap2* factors can be linked to negative regulation of neurogenesis, as well as to transcription regulation and developmental processes such as morphogenesis, motility and growth. *Tfap2* paralogues are known to regulate melanocyte differentiation together with *Mitf*. In particular, *Tfap2a* mutations have been associated with different pigmentation anomalies (Seberg et al. 2017) and and RPE trans-differentiation to NR (Bassett et al. 2007, 2010; Gestri et al. 2009; West-Mays et al. 1999). However, so far, *Tfap2* role during optic cup differentiation is scarcely understood, no molecular mechanisms have been proposed to explain these anomalies and no direct connection between *Tfap2* factors and other nodes of the RPE GRN has been proved or even postulated. Our work dissected for the first time regulatory circuits entailing *Tfap2* factors during optic cup development, determining their central role within the earliest stages of RPE development. Last, we focused on the function of *Tead* factors. So far it is still unclear if the activity of *Tead* factors in RPE is either linked to *Hippo* pathway or related to *Wnt/β-catenin* signalling, as observed in other contexts (Moreno-Marmol, Cavodeassi, and Bovolenta 2018; Totaro, Panciera, and Piccolo 2018). Miesfeld and colleagues linked *tead* activity in RPE to *yap/taz* complex (Miesfeld et al. 2015). In turn, our RPE data did not assessed any *yap/taz* gene expression increase, but a transient upregulation of *vgll2a* and *vgll2b.* Although the *Hippo* pathway modulators *Yap* and *Taz* are currently the better known and most extensively studied co-activators and regulators of *Tead* transcriptional activity, also *Vgll* co-factors have been identified as *Tead* binding partners (Lin, Park, and Guan 2017). There are still few studies describing the functional role of the *Vgll/Tead* complex, but several works showed that *Vgll* family proteins have binding sites on *Tead* that overlap with *Yap/Taz* binding sites. Thus *VGLL* proteins compete with *YAP/TAZ* for *TEAD* binding, promoting the transcription of target gene batteries that have been related to *Yap/Taz* independent signalling pathways, such as *Wnt* pathway (Jiao et al. 2014; Pobbati et al. 2012; W. Zhang et al. 2014). Though we are far from understanding the precise molecular mechanisms, our work implies that *Tead* factors play a pivotal role in the onset of RPE genetic program, and not only by regulating *yap/taz*-driven gene expression. Our data and literature data taken as a whole, cannot make us exclude neither the implication of the *Hippo* nor the *Wnt* pathway (nor other still unrevealed pathway) upstream of *Teads* during RPE

differentiation regulation. Probably the two paths act concurrently, cooperating to finely regulate the development of the pigmented tissue of the eye.

Ultimately, our work suggested *tead* factors to be the main responsible for the morphogenetic changes of the pigmented domain cells during the optic cup folding. The relations among transcriptional regulators, cytoskeletal elements and morphogenesis will be analysed further in the next section (**2. Cytoskeletal remodelling during optic cup morphogenesis**).

4. Cytoskeletal remodeling during optic cup morphogenesis

The acquisition of the NR and RPE molecular identity entails a profound remodelling of cell shape in each domain. One of the issues we wanted to explore with our work was the relations between cell morphology changes and transcriptional programs. NR upregulated cytoskeletal genes are enriched for genes participating in microtubule organization. This is in agreement with the elongation of apico-basal axis of columnar cells, where the microtubules are nucleated with uniform polarity to serve as substrate for the polarized transport of membrane vesicles within the cell. Further during development, microtubules are among of the major cytoskeletal components of neurons. Besides polarity, they are also essential for many fundamental cellular and developmental processes, such as neuronal migration, differentiation and maintenance of neuronal morphology, since they provide dynamic and mechanical functions and control local signalling events (Kapitein and Hoogenraad 2015; Meads and Schroer 1995). In contrast to the NR, the pigmented tissue exhibits a noticeable upregulation of genes encoding for desmosomes proteins, IFs and elements of the acto-myosin apparatus. Both actin and IF networks may act as a mechanical unit to connect adjacent through adherens junctions and desmosomes. IFs are highly flexible and can be considered “shock absorbers” that dissipate elastic energy when cells are subjected to external forces. The loss of contacts between the IFs of adjacent cells, primarily operated by desmosomes, leads to the loss of adhesion forces between the cells (Godsel, Hobbs, and Green 2008; Herrmann and Aebi 2004; Sanghvi-Shah and Weber 2017; Wang and Stamenović 2000). It is worth mentioning that, among others IFs’ elements, we registered a considerable increase of *krt8* and *krt18*, which were found to be specific for RPE cells by previous studies (Fuchs, Kivelä, and Tarkkanen 1991).

However, IFs are not just static cellular scaffolding, but they serve as highly sensitive mediators of cytoskeletal crosstalk with both microtubule and actin structures through signal transduction from the extracellular to the intracellular space (Chang and Goldman 2004). One transcriptional regulator functioning as mediator between cytoskeletal rearrangements and gene transcription is the *YAP/TAZ* complex, which can translocate to the nucleus and activating gene transcription in response to mechanical stimuli (Hatzfeld, Keil, and Magin 2017). *Yap* and *Taz* control gene expression through interaction with *Tead* factors (H. Zhang, Pasolli, and Fuchs 2011), which were among the earliest TFs that we found to be

expressed throughout RPE development. Further, our CRE analysis linked their activity to the transcriptional modification of cytoskeletal genes. Even if so far *YAP/TAZ/TEAD* action has been not directly linked to desmosomes, YAP was co-immunoprecipitated with plakoglobin, a desmosome component, in human heart. This finding suggests that there may be physical interactions between *YAP* and desmosomes that could modulate its activity (Hatzfeld, Keil, and Magin 2017). A large scale ChIP-seq analysis of *Tead4* target genes in endometrial cells identified desmosomal components as putative *Tead4* target genes (Liu et al. 2016). In addition, desmosome mutations in arrhythmogenic cardiomyopathy model were shown to affect Hippo pathway, suggesting a loop feedback mechanisms between desmosome and the *YAP/TAZ/TEAD* signalling (Chen et al. 2014). *Yap* and *Tead* were already known to be involved in RPE differentiation (Kim et al. 2016; Miesfeld et al. 2015). The expression of *Otx2* and other RPE markers is missing in the presumptive RPE of *Yap* mutants, indicating that *Yap* acts rather upstream in the regulatory network controlling RPE specification (Kim et al., 2016). This early requirement had made it difficult to determine *YAP/TEAD* possible implications in RPE cell flattening using classical genetic approaches (Moreno-Marmol, Cavodeassi, and Bovolenta 2018). Our omics approach not only confirms *tead* factors to be at a hierarchical top position among RPE specifiers, but it also suggests their activity may be linked to the morphogenetic phenomena. From this perspective, we can speculate that in RPE cell shaping is not just a passive adaptation to NR basal constriction, but a dynamic feedback/feedforward specification mechanism where cell morphogenesis influences gene transcription and *vice versa.* However, further functional experiments are still necessary to untangle all the potential mechanotransduction dynamics that are likely to modulate RPE gene expression and orchestrate the development of the eye as a whole.

5. GRN in human RPE in vitro model: from developmental biology to retinal diseases

Since the characterization of iPSCs in 2006, this technology has been applied to understand the mechanisms of disease and to develop therapeutic tools. The recent availability of patient-derived-iPSCs to differentiate retinal lineages is proving to be a valuable system to discover new disease-causing mutations, studying genotype-phenotype relationships, performing therapeutics-toxicity screenings and developing personalised cell therapy approaches for retinal diseases. However, the full potential is yet to be achieved because of the molecular and morphological complexity of retinal cells, which makes *in vitro* differentiation very challenging. So far, the implementation of retinal cell differentiation protocols from iPSCs has focused mainly on RPE cells; not only because their relatively simple morphology and symbiotic relationship with photoreceptors, but also for their crucial role in the onset of retinal degenerative diseases such as retinitis pigmentosa and AMD. Alterations in the cytoskeleton have already been linked to subnormal phagocytosis in stem-cell-derived RPE cells and this might imply anomalies of other cell functions (Gibbs, Kitamoto, and Williams 2003). Therefore, an indispensable pre-requisite for any RPE cell replacement therapy is the

detailed knowledge of cytoskeletal components involved in pigmented cell differentiation. Our work provides a detailed picture of the earliest components required for RPE differentiation both in zebrafish and human cells. Further, it links the assembly of RPE cytoskeleton to the activity of a precise group of TFs. This could be instrumental to improve the culturing and delivering of intact and functioning RPE cells into patients' retina.

As already mentioned above, this study highlighted an avant-garde wave of transcriptional regulators that could be essential for the specification and early differentiation of the RPE, such as *TEAD, VGLL2* and *TFAP2.* The pioneer expression of these TFs was found to be maintained also in human RPE cell differentiation model, anticipating the expression of *MITF.* This data places *TEAD* and *TFAP2* paralogues in a hierarchical top position within the RPE regulatory network. Their early function may have been maintained across evolution because of an actual indispensable role that these factors would play in the specification of pigmented eye tissue. In this perspective, the role of *MITF* would be relegated to a secondary function linked to pigmentation arousal, and therefore not necessary for the initial commitment of the optic vesicle progenitors to the RPE fate. Since timing continues to be a significant barrier to routine clinical use of the hiPSCs-to-RPE *in vitro* differentiation technology, our findings have enormous potential for exploring new and improved ways to induce RPE development, such as *in vivo* direct-lineage reprogramming starting from related cell-types.

In conclusion, this study dissected the transcriptomic landscapes and regulatory dynamics guiding the earliest development of the eye neuroepithelial derivatives. Further, we identified components of the machinery driving optic cup morphogenesis and integrated them into the specification networks defining the identity of the different domains. Our work not only represents a resource for the scientific community to expand our understanding of the genetic mechanisms underlying eye development, but also paved the way for future clinical investigations oriented towards the treatment of retinopathies.

Concluding Remarks

1. Transcriptomic landscapes of NR and RPE considerably diverge during development. The widest variation of the developmental programs occurs in first two hours since GRN bifurcation.

2. A greater number of upregulated genes and more accessible chromatin regions is involved during the differentiation towards RPE fate than towards NR fate.

3. Distal enhancers represent the most dynamic cis-regulatory elements during optic cup development.

4. The action of *mitfa* in RPE development is preceded by an early wave of TFs, including *tfap2a, tfap2c*, *tcf12* and *tead* factors.

5. NR cells shaping is associated with microtubule organization, whereas RPE morphogenesis requires the rearrangement of acto-myosin complex, desmosomes and intermediate filament machinery.

6. NR GRN is extremely robust and redundant. It is based on the synergic action of *homebox* and *sox* factors.

7. The mutation of *vsx1* and *vsx2* do not affect the morphogenesis of the optic cup in teleost model, but impairs the differentiation of bipolar neurons.

8. Transcriptomic landscape of *vsx1/vsx2* zebrafish mutants does not highlight evident signals of transcriptional compensation.

9. Chromatin accessibility landscape of of *vsx1/vsx2* zebrafish mutants reveals the rewiring of cis-regulatory elements influencing the expression of genes involved in retinal development.

10. RPE development requires the prior suppression of neural differentiation programs.

11. *Mitfa* could be associated only with RPE pigmentation, whereas other earliest TFs seem to be in charge of further developmental processes.

12. The expression of RPE cytoskeletal elements may be linked to *tead* transcriptional activity.

13. *Tead* activity during the earliest phases of RPE development may not be mediated exclusively by *Hippo* signalling pathway.

14. The used multi-omics approach helped to individuated novel components of the optic cup GRNs.

15. In the human model of RPE differentiation the *consecution temporum* of TF expression detected in zebrafish is conserved. The discovery of earlier specifiers of human RPE tissue represents valuable information for clinical applications.

References

Ach, Thomas et al. (2015). Lipofuscin Redistribution and Loss Accompanied by Cytoskeletal Stress in Retinal Pigment Epithelium of Eyes With Age-Related Macular Degeneration. Investigative Opthalmology & Visual Science 56(5): 3242. http://iovs.arvojournals.org/article.aspx?doi=10.1167/iovs.14-16274.

Adelmann, H. (1929). Experimental studies on the development of the eye. Journal of Experimental Zoology, 54, 291–317.

Adler, R., & Canto-Soler, M. V. (2007). Molecular mechanisms of optic vesicle development: Complexities, ambiguities and controversies. Developmental Biology, 305(1), 1–13. https://doi.org/10.1016/j.ydbio.2007.01.045

Aldiri, I., Xu, B., Wang, L., Chen, X., Hiler, D., Griffiths, L., … Dyer, M. A. (2017). The Dynamic Epigenetic Landscape of the Retina During Development, Reprogramming, and Tumorigenesis. Neuron, 94(3), 550-568.e10. https://doi.org/10.1016/j.neuron.2017.04.022

Anne K. Hennig, G.-H. P., & Chen, and S. (2009). Regulation of photoreceptor gene expression by Crx-associated transcription factor network. 114–133.

Arendt, D., Tessmar, K., Medeiros de Campos-Baptista, M. I., Dorresteijn, A., & Wittbrodt, J. (2002). Development of pigment-cup eyes in the polychaete Platynereis dumerilii and evolutionary conservation of larval eyes in bilateria. Development, 129(5), 1143–1154.

Arnheiter, H. (2010). The discovery of the microphthalmia locus and its gene, Mitf. Pigment Cell Melanoma Res, 46(4), 729–735. https://doi.org/10.1016/j.cortex.2009.08.003.Predictive

Barski, A., Cuddapah, S., Cui, K., Roh, T.-Y., Schones, D. E., Wang, Z., … Zhao, K. (2007). High-resolution profiling of histone methylations in the human genome. Cell, 129(4), 823–837. https://doi.org/10.1016/j.cell.2007.05.009

Bassett, Erin A. et al. (2010). AP-2α Knockout Mice Exhibit Optic Cup Patterning Defects and Failure of Optic Stalk Morphogenesis. Human Molecular Genetics 19(9): 1791–1804. https://academic.oup.com/hmg/article-lookup/doi/10.1093/hmg/ddq060.

Bassett, Erin A et al. (2007). Conditional Deletion of Activating Protein 2alpha (AP-2alpha) in the Developing Retina Demonstrates Non-Cell-Autonomous Roles for AP-2alpha in Optic Cup Development. Molecular and cellular biology 27(21): 7497–7510. http://www.ncbi.nlm.nih.gov/pubmed/17724084.

Bäumer, N., Marquardt, T., Stoykova, A., Spieler, D., Treichel, D., Ashery-Padan, R., & Gruss, P. (2003). Retinal pigmented epithelium determination requires the redundant activities of Pax2 and Pax6. Development, 130(13), 2903–2915. https://doi.org/10.1242/dev.00450

Behesti, H., Papaioannou, V., & Sowden, J. (2009). Loss of Tbx2 delays optic vesicle invagination leading to small optic cups. Developmental Biology, 333(2), 360–372. https://doi.org/10.1016/j.ydbio.2009.06.026.Loss

Berson. (1993). A randomized trial of vitamin A and vitamin E supplementation for retinitis pigmentosa. Archives of Ophthalmology, 111(6), 761–772.

Bertolotti, E., Neri, A., Camparini, M., Macaluso, C., & Marigo, V. (2014). Stem cells as source for retinal pigment epithelium transplantation. Progress in Retinal and Eye Research, 42, 130–144. https://doi.org/10.1016/j.preteyeres.2014.06.002

Bessa, J., Tena, J. J., De La Calle-Mustienes, E., Fernández-Miñán, A., Naranjo, S., Fernández, A., … Gómez-Skarmeta, J. L. (2009). Zebrafish Enhancer Detection (ZED) vector: A new tool to facilitate transgenesis and the functional analysis of cis-regulatory regions in zebrafish. Developmental Dynamics, 238(9), 2409–2417. https://doi.org/10.1002/dvdy.22051

Bharti, K., Gasper, M., Ou, J., Brucato, M., Clore-Gronenborn, K., Pickel, J., & Arnheiter, H. (2012). A regulatory loop involving PAX6, MITF, and WNT signaling controls retinal pigment epithelium development. PLoS Genetics, 8(7), 1–17. https://doi.org/10.1371/journal.pgen.1002757

Bharti, K., Liu, W., Csermely, T., Bertuzzi, S., & Arnheiter, H. (2008). Alternative promoter use in eye development: The complex role and regulation of the transcription factor MITF. Development, 135(6), 1169–1178. https://doi.org/10.1242/dev.014142

Binder, S., Krebs, I., Hilgers, R. D., Abri, A., Stolba, U., Assadoulina, A., … Feichtinger, H. (2004). Outcome of transplantation of autologous retinal pigment epithelium in age-related macular degeneration: A prospective trial. Investigative Ophthalmology and Visual Science, 45(11), 4151–4160. https://doi.org/10.1167/iovs.04-0118

Blackshaw, S., Fraioli, R. E., Furukawa, T., & Cepko, C. L. (2001). Comprehensive analysis of photoreceptor gene expression and the identification of candidate retinal disease genes. Cell, 107(5), 579–589. https://doi.org/10.1016/S0092-8674(01)00574-8

Bogdanović, O., Fernandez-Miñán, A., Tena, J. J., De La Calle-Mustienes, E., Hidalgo, C., Van Kruysbergen, I., … Gómez-Skarmeta, J. L. (2012). Dynamics of enhancer chromatin signatures mark the transition from pluripotency to cell specification during embryogenesis. Genome Research, 22(10), 2043–2053. https://doi.org/10.1101/gr.134833.111

Bonilha, V. L. (2014). Retinal pigment epithelium (RPE) cytoskeleton invivo and invitro. Experimental Eye Research, 126, 38–45. https://doi.org/10.1016/j.exer.2013.09.015

Bovolenta, P., Mallamaci, A., Briata, P., Corte, G., & Boncinelli, E. (1997). Implication of OTX2 in pigment epithelium determination and neural retina differentiation. Journal of Neuroscience, 17(11), 4243–4252. https://doi.org/10.1523/jneurosci.17-11-04243.1997

Brantjes, H., Barker, N., van Es, J., & Clevers, H. (2002). TCF: Lady Justice casting the final verdict on the outcome of Wnt signalling. Biological Chemistry, 383(2), 255–261. https://doi.org/10.1515/BC.2002.027

Brooks, M. J., Rajasimha, H. K., Roger, J. E., & Swaroop, A. (2011). Next-generation sequencing facilitates quantitative analysis of wild-type and Nrl retinal transcriptomes. (November), 3034–3054.

Buenrostro, J. D., Giresi, P. G., Zaba, L. C., Chang, H. Y., & Greenleaf, W. J. (2013). Transposition of native chromatin for fast and sensitive epigenomic profiling of open chromatin, DNA-binding proteins and nucleosome position. Nature Methods, 10(12), 1213–1218. https://doi.org/10.1038/nmeth.2688

Buenrostro, J. D., Wu, B., Litzenburger, U. M., Ruff, D., Gonzales, M. L., Snyder, M. P., … Greenleaf, W. J. (2015). Single-cell chromatin accessibility reveals principles of regulatory variation. https://doi.org/10.1038/nature14590

Buenrostro, J., Wu, B., Chang, H., & Greenleaf, W. (2015). ATAC-seq: A Method for Assaying Chromatin Accessibility Genome-Wide. 1–10. https://doi.org/10.1002/0471142727.mb2129s109.ATAC-seq

Bumsted, K. M., & Barnstable, C. J. (2000). Dorsal retinal pigment epithelium differentiates as neural retina in the Microphthalmia (mi/mi) mouse. Investigative Ophthalmology and Visual Science, 41(3), 903–908.

Burger, L., Gaidatzis, D., Schu, D., & Stadler, M. B. (2013). Identification of active regulatory regions from DNA methylation data. 41(16). https://doi.org/10.1093/nar/gkt599

Burmeister, M., Novak, J., Liang, M. Y., Basu, S., Ploder, L., Hawes, N. L., … McInnes, R. R. (1996). Ocular retardation mouse caused by Chx10 homeobox null allele: impaired retinal progenitor proliferation and bipolar cell differentiation. Nature Genetics, 12(4), 376–384. https://doi.org/10.1038/ng0496-376

Burnight, E. R., Gupta, M., Wiley, L. A., Anfinson, K. R., Tran, A., Triboulet, R., … Tucker, B. A. (2017). Using CRISPR-Cas9 to Generate Gene-Corrected Autologous iPSCs for the Treatment of Inherited Retinal Degeneration. Molecular Therapy, 25(9), 1999–2013. https://doi.org/10.1016/j.ymthe.2017.05.015

Cadigan, Ken M, and Marian L Waterman. (2012). TCF/LEFs and Wnt Signaling in the Nucleus. Cold Spring Harbor perspectives in biology 4(11). http://www.ncbi.nlm.nih.gov/pubmed/23024173.

Cai, H., Fields, M. A., Hoshino, R., & Priore, L. V. Del. (2012). Effects of aging and anatomic location on gene expression in human retina. 4(May), 1–20. https://doi.org/10.3389/fnagi.2012.00008

Cai, Z., Feng, G. S., & Zhang, X. (2010). Temporal requirement of the protein tyrosine phosphatase Shp2 in establishing the neuronal fate in early retinal development. Journal of Neuroscience, 30(11), 4110–4119. https://doi.org/10.1523/JNEUROSCI.4364-09.2010

Cannavò, Enrico et al. (2016). Shadow Enhancers Are Pervasive Features of Developmental Regulatory Networks. Current biology : CB 26(1): 38–51. http://www.ncbi.nlm.nih.gov/pubmed/26687625.

Carl, M., Loosli, F., & Wittbrodt, J. (2002). Six3 inactivation reveals its essential role for the formation and patterning of the vertebrate eye. Development, 129(17), 4057–4063.

Carlson, M. (2019). A set of annotation maps describing the entire Gene Ontology.

Carroll, S. B. (2008). Evo-Devo and an Expanding Evolutionary Synthesis: A Genetic Theory of Morphological Evolution. Cell, 134(1), 25–36. https://doi.org/10.1016/j.cell.2008.06.030

Cepko, C. (2014). Intrinsically different retinal progenitor cells produce specific types of progeny. Nature Reviews Neuroscience, 15(9), 615–627. https://doi.org/10.1038/nrn3767

Cepko, C. L., Austin, C. P., Yang, X., Alexiades, M., & Ezzeddine, D. (1996). Cell fate determination in the vertebrate retina. 93(January), 589–595. Retrieved from http://www.pnas.org/content/pnas/93/2/589.full.pdf

Chaitankar, V., Karakülah, G., Ratnapriya, R., Giuste, F. O., Brooks, M. J., & Swaroop, A. (2016). Next generation sequencing technology and genomewide data analysis: Perspectives for retinal research. Progress in Retinal and Eye Research, 55, 1–31. https://doi.org/10.1016/j.preteyeres.2016.06.001

Chang, Lynne, and Robert D Goldman. (2004). Intermediate Filaments Mediate Cytoskeletal Crosstalk. Nature reviews. Molecular cell biology 5(8): 601–13. http://www.ncbi.nlm.nih.gov/pubmed/15366704.

Chen, C.-A., Bosch, D. G. M., Cho, M. T., Rosenfeld, J. A., Shinawi, M., Lewis, R. A., … Schaaf, C. (2016). The expanding clinical phenotype of Bosch-Boonstra-Schaaf optic atrophy syndrome: 20 new cases and possible genotype-phenotype correlations. Genetics in Medicine : Official Journal of the American College of Medical Genetics, 18(11), 1143–1150. https://doi.org/10.1038/gim.2016.18

Chen, T., Saw, T. B., Mege, R. M., & Ladoux, B. (2018). Mechanical forces in cell monolayers. Journal of Cell Science, 131(24). https://doi.org/10.1242/jcs.218156

Chen, Suet Nee et al. (2014). The Hippo Pathway Is Activated and Is a Causal Mechanism for Adipogenesis in Arrhythmogenic Cardiomyopathy. Circulation research 114(3): 454–68. http://www.ncbi.nlm.nih.gov/pubmed/24276085.

Cheng, Yi-Chuan et al. (2015). The Transcription Factor Hairy/E(Spl)-Related 2 Induces Proliferation of Neural Progenitors and Regulates Neurogenesis and Gliogenesis. Developmental Biology 397(1): 116–28. https://linkinghub.elsevier.com/retrieve/pii/S0012160614005594.

Chow, R. L., Altmann, C. R., Lang, R. A., & Hemmati-Brivanlou, A. (1999). Pax6 induces ectopic eyes in a vertebrate. Development, 126(19), 4213–4222.

Chuang, A. T., Margo, C. E., & Greenberg, P. B. (2014). Retinal implants: A systematic review. British Journal of Ophthalmology, 98(7), 852–856. https://doi.org/10.1136/bjophthalmol-2013-303708

Chuang, J. C., & Raymond, P. A. (2002). Embryonic origin of the eyes in teleost fish. BioEssays, 24(6), 519–529. https://doi.org/10.1002/bies.10097

Clark, B. S., Stein-O'Brien, G. L., Shiau, F., Cannon, G. H., Davis-Marcisak, E., Sherman, T., … Blackshaw, S. (2019). Single-Cell RNA-Seq Analysis of Retinal Development Identifies NFI Factors as Regulating Mitotic Exit and Late-Born Cell Specification. Neuron, 102(6), 1111-1126.e5. https://doi.org/10.1016/j.neuron.2019.04.010

Cong, L., Ran, F. A., Cox, D., Lin, S., Barretto, R., Hsu, P. D., … Marraffini, L. a. (2013). Cong, L., Ran, F. A., Cox, D., Lin, S., Barretto, R., Habib, N., … Zhang, F. (2013). Multiplex Genome Engineering Using CRISPR/Cas Systems. Science (New York, N.Y.). Science (New York, N.Y.), 339(6121), 819–823. https://doi.org/10.1126/science.1231143.Multiplex

Consortium, E. P. (2012). An Integrated Encyclopedia of DNA Elements in the Human Genome. Nature, 9(37), 57–74. https://doi.org/10.1038/nature11247.An

Corbo, J. C., Lawrence, K. A., Karlstetter, M., Myers, C. A., Abdelaziz, M., Dirkes, W., … Langmann, T. (2010). CRX ChIP-seq reveals the cis-regulatory architecture of mouse photoreceptors. Genome Research, 20(11), 1512–1525. https://doi.org/10.1101/gr.109405.110

Coulombre, J. L., & Coulombre, A. J. (1965). Regeneration of neural retina from the pigmented epithelium in the chick embryo. Developmental Biology, 12(1), 79–92. https://doi.org/10.1016/0012-1606(65)90022-9

Cusanovich, D. A., Daza, R., Adey, A., Pliner, H. A., Christiansen, L., Gunderson, K. L., … Shendure, J. (2015). Multiplex single-cell profiling of chromatin accessibility by combinatorial cellular indexing. 348(6237).

D'Cruz, P. M. (2000). Mutation of the receptor tyrosine kinase gene Mertk in the retinal dystrophic RCS rat. Human Molecular Genetics, 9(4), 645–651. https://doi.org/10.1093/hmg/9.4.645

David E. Buchholz, S. T. H. (2009). E MBRYONIC S TEM C ELLS / I NDUCED P LURIPOTENT S TEM C ELLS Derivation of Functional Retinal Pigmented Epithelium from Induced. Stem Cells, 27, 2427–2434. https://doi.org/10.1002/July

Davidson, E. H. (2001). Genomic Regulatory Systems: In Development and Evolution. https://doi.org/https://doi.org/10.1016/B978-0-12-205351-1.X5000-9

Davidson, E. H., & Erwin, E. H. (2006). Response to Comment on "Gene Regulatory Networks and the Evolution of Animal Body Plans." Science, 313(5788), 761c-761c. https://doi.org/10.1126/science.1126765

Davidson, E. H., Rast, J. P., Oliveri, P., Ransick, A., Calestani, C., Yuh, C. H., … Bolouri, H. (2002). A genomic regulatory network for development. Science, 295(5560), 1669–1678. https://doi.org/10.1126/science.1069883

de Melo, J., Zibetti, C., Clark, B. S., Hwang, W., Miranda-Angulo, A. L., Qian, J., & Blackshaw, S. (2016). Lhx2 Is an Essential Factor for Retinal Gliogenesis and Notch Signaling. The Journal of Neuroscience, 36(8), 2391–2405. https://doi.org/10.1523/jneurosci.3145-15.2016

Decembrini, S., Koch, U., Radtke, F., Moulin, A., & Arsenijevic, Y. (2014). Derivation of traceable and transplantable photoreceptors from mouse embryonic stem cells. Stem Cell Reports, 2(6), 853–865. https://doi.org/10.1016/j.stemcr.2014.04.010

Del Rio-Tsonis, K., & Tsonis, P. A. (2003). Eye regeneration at the molecular age. Developmental Dynamics, 226(2), 211–224. https://doi.org/10.1002/dvdy.10224

den Hollander, A. (2009). A Homozygous Missense Mutation in the IRBP Gene (RBP3) Associated with Autosomal Recessive Retinitis Pigmentosa. 50(41864–1872), 1–7. https://doi.org/10.1038/jid.2014.371

D'Haeseleer, P. (2005). How does gene expression clustering work? Nature Biotechnology, Vol. 23, pp. 1499–1501. https://doi.org/10.1038/nbt1205-1499

Diacou, R., Zhao, Y., Zheng, D., Cvekl, A., & Liu, W. (2018). Six3 and Six6 Are Jointly Required for the Maintenance of Multipotent Retinal Progenitors through Both Positive and Negative Regulation. Cell Reports, 25(9), 2510-2523.e4. https://doi.org/10.1016/j.celrep.2018.10.106

Dimitra Athanasiou, Monica Aguilà, Dalila Bevilacqua, Sergey S. Novoselov, David A. Parfitt, and M. E. C. (2017). THE CELL STRESS MACHINERY AND RETINAL DEGENERATION. 587(13), 2008–2017. https://doi.org/10.1016/j.febslet.2013.05.020

Domınguez-Cejudo, M. A., & Casares, F. (2015). Anteroposterior patterning of Drosophila ocelli requires an anti-repressor mechanism within the hh pathway mediated by the Six3 gene Optix. Development (Cambridge), 142(16), 2801–2809. https://doi.org/10.1242/dev.125179

Eberhart, A., Feodorova, Y., Song, C., & Wanner, G. (2013). Epigenetics of eu- and heterochromatin in inverted and conventional nuclei from mouse retina. 535–554. https://doi.org/10.1007/s10577-013-9375-7

Eden, E., Navon, R., Steinfeld, I., Lipson, D., & Yakhini, Z. (2009). GOrilla: a tool for discovery and visualization of enriched GO terms in ranked gene lists. BMC Bioinformatics, 10, 48. https://doi.org/10.1186/1471-2105-10-48

Eiraku, M., Takata, N., Ishibashi, H., Kawada, M., Sakakura, E., Okuda, S., … Sasai, Y. (2011). Self-organizing optic-cup morphogenesis in three-dimensional culture. Nature, 472(7341), 51–58. https://doi.org/10.1038/nature09941

El-Brolosy, M. A., Kontarakis, Z., Rossi, A., Kuenne, C., Günther, S., Fukuda, N., … Stainier, D. Y. R. (2019). Genetic compensation triggered by mutant mRNA degradation. Nature, 568(7751), 193–197. https://doi.org/10.1038/s41586-019-1064-z

Engler, Anna, Runrui Zhang, and Verdon Taylor. (2018). Notch and Neurogenesis. In , 223–34. http://link.springer.com/10.1007/978-3-319-89512-3_11.

Erclik, Ted, Volker Hartenstein, Howard D Lipshitz, and Roderick R McInnes. (2008). Conserved Role of the Vsx Genes Supports a Monophyletic Origin for Bilaterian Visual Systems. Current biology : CB 18(17): 1278–87. http://www.ncbi.nlm.nih.gov/pubmed/18723351.

Falkner-Radler, C. I., Krebs, I., Glittenberg, C., Považay, B., Drexler, W., Graf, A., & Binder, S. (2011). Human retinal pigment epithelium (RPE) transplantation: Outcome after autologous RPE-choroid sheet and RPE cell-suspension in a randomised clinical study. British Journal of Ophthalmology, 95(3), 370–375. https://doi.org/10.1136/bjo.2009.176305

Farkas, M. H., Grant, G. R., White, J. A., Sousa, M. E., Consugar, M. B., & Pierce, E. A. (2013). Transcriptome analyses of the human retina identify unprecedented transcript diversity and 3 . 5 Mb of novel transcribed sequence via significant alternative splicing and novel genes. BMC Genomics, 14(1), 1. https://doi.org/10.1186/1471-2164-14-486

Ferrari, S., Di Iorio, E., Barbaro, V., Ponzin, D., S. Sorrentino, F., & Parmeggiani, F. (2011). Retinitis Pigmentosa: Genes and Disease Mechanisms. Current Genomics, 12(4), 238–249. https://doi.org/10.2174/138920211795860107

Ferreira, R. C., Popova, E. Y., James, J., Briones, M. R. S., Zhang, S. S., & Barnstable, X. C. J. (2017). Histone Deacetylase 1 Is Essential for Rod Photoreceptor Differentiation by Regulating Acetylation at Histone H3 Lysine 9 and Histone H4 Lysine 12 in the Mouse Retina * Edited by Joel Gottesfeld. The Journal of Biological Chemistry, 292(6), 2422–2440. https://doi.org/10.1074/jbc.M116.756643

Figeac, N., Mohamed, A. D., Sun, C., Schönfelder, M., Matallanas, D., Garcia-Munoz, A., … Wackerhage, H. (2019). VGLL3 operates via TEAD1, TEAD3 and TEAD4 to influence myogenesis in skeletal muscle. Journal of Cell Science, 132(13). https://doi.org/10.1242/jcs.225946

Fish, M. B., Nakayama, T., Fisher, M., Hirsch, N., Cox, A., Reeder, R., … Grainger, R. M. (2014). Xenopus mutant reveals necessity of rax for specifying the eye field which otherwise forms tissue with telencephalic and diencephalic character. Developmental Biology, 395(2), 317–330. https://doi.org/10.1016/j.ydbio.2014.09.004

Fitzpatrick, D. R., & Heyningen, V. Van. (2005). Developmental eye disorders. https://doi.org/10.1016/j.gde.2005.04.013

Fuchs, U, T Kivelä, and A Tarkkanen. (1991). Cytoskeleton in Normal and Reactive Human Retinal Pigment Epithelial Cells. Investigative ophthalmology & visual science 32(13): 3178–86. http://www.ncbi.nlm.nih.gov/pubmed/1748549.

Fuhrmann, S. (2010). Eye morphogenesis and patterning of the optic vesicle. In Current Topics in Developmental Biology (Vol. 93). https://doi.org/10.1016/B978-0-12-385044-7.00003-5

Fuhrmann, S., Zou, C., & Levine, E. M. (2014). Retinal pigment epithelium development, plasticity, and tissue homeostasis (Invited review for Experimental Eye Research). Experimental Eye Research, 0, 141–150. https://doi.org/10.1016/j.exer.2013.09.003

Fujimura, N., Taketo, M. M., Mori, M., Korinek, V., & Kozmik, Z. (2009). Spatial and temporal regulation of Wnt/β-catenin signaling is essential for development of the retinal pigment epithelium. Developmental Biology, 334(1), 31–45. https://doi.org/10.1016/j.ydbio.2009.07.002

Furukawa, T., Morrow, E. M., Li, T., Davis, F. C., & Cepko, C. L. (1999). Retinopathy and attenuated circadian entrainment in Crx-deficient mice. Nature Genetics, 23(4), 466–470. https://doi.org/10.1038/70591

Gago-rodrigues, I., Fernandez-Miñan, A., & Martinez-morales, J. R. (2015). Analysis of opo cis - regulatory landscape uncovers Vsx2 requirement in early eye morphogenesis. (May). https://doi.org/10.1038/ncomms8054

Gallicano, G. I., Bauer, C., & Fuchs, E. (2001). Rescuing desmoplakin function in extra-embryonic ectoderm reveals the importance of this protein in embryonic heart, neuroepithelium, skin and vasculature. Development (Cambridge, England), 128(6), 929–941. Retrieved from http://www.ncbi.nlm.nih.gov/pubmed/11222147

Gallicano, G. I., Kouklis, P., Bauer, C., Yin, M., Vasioukhin, V., Degenstein, L., & Fuchs, E. (1998). Desmoplakin is required early in development for assembly of desmosomes and cytoskeletal linkage. The Journal of Cell Biology, 143(7), 2009–2022. https://doi.org/10.1083/jcb.143.7.2009

Galy, A., Néron, B., Planque, N., Saule, S., & Eychène, A. (2002). Activated MAPK/ERK kinase (MEK-1) induces transdifferentiation of pigmented epithelium into neural retina. Developmental Biology, 248(2), 251–264. https://doi.org/10.1006/dbio.2002.0736

Gamsiz. (2013). Genome-wide transcriptome analysis in murine neural retina using high-throughput RNA sequencing. 99(1), 44–51. https://doi.org/10.1016/j.ygeno.2011.09.003.Genome-wide

Gao, Z., Mao, C. A., Pan, P., Mu, X., & Klein, W. H. (2014). Transcriptome of Atoh7 retinal progenitor cells identifies new Atoh7-dependent regulatory genes for retinal ganglion cell formation. Developmental Neurobiology, 74(11), 1123–1140. https://doi.org/10.1002/dneu.22188

Garber, M., Grabherr, M. G., Guttman, M., & Trapnell, C. (2011). Computational methods for transcriptome annotation and quantification using RNA-seq. Nature Methods, 8(6), 469–477. https://doi.org/10.1038/nmeth.1613

Gaudet, P., Livstone, M. S., Lewis, S. E., & Thomas, P. D. (2011). Phylogenetic-based propagation of functional annotations within the Gene Ontology consortium. 12(5). https://doi.org/10.1093/bib/bbr042

Geer, L. Y., Marchler-Bauer, A., Geer, R. C., Han, L., He, J., He, S., … Bryant, S. H. (2010). The NCBI BioSystems database. Nucleic Acids Research, 38(Database issue), D492-6. https://doi.org/10.1093/nar/gkp858

Gestri, Gaia et al. (2009). Reduced TFAP2A Function Causes Variable Optic Fissure Closure and Retinal Defects and Sensitizes Eye Development to Mutations in Other Morphogenetic Regulators. Human Genetics 126(6): 791–803. http://link.springer.com/10.1007/s00439-009-0730-x.

Gibbs, D., J. Kitamoto, and D. S. Williams. (2003). Abnormal Phagocytosis by Retinal Pigmented Epithelium That Lacks Myosin VIIa, the Usher Syndrome 1B Protein. Proceedings of the National Academy of Sciences 100(11): 6481–86. http://www.pnas.org/cgi/doi/10.1073/pnas.1130432100.

Gilfillan, G. D., Hughes, T., Sheng, Y., Hjorthaug, H. S., Straub, T., Gervin, K., … Lyle, R. (2012). Limitations and possibilities of low cell number. 1–13.

Goding, C. R. (2000). Mitf from neural crest to melanoma: Signal transduction and transcription in the melanocyte lineage. Genes and Development, 14(14), 1712–1728. https://doi.org/10.1101/gad.14.14.1712

Godsel, Lisa M., Ryan P. Hobbs, and Kathleen J. Green. (2008). Intermediate Filament Assembly: Dynamics to Disease. Trends in Cell Biology 18(1): 28–37. https://linkinghub.elsevier.com/retrieve/pii/S0962892407003017.

Goff, L., Trapnell, C., & Kelley, D. (2019). cummeRbund: Analysis, exploration, manipulation, and visualization of Cufflinks high-throughput sequencing data. https://doi.org/10.18129/B9.bioc.cummeRbund

Golson, M. L., & Kaestner, K. H. (2016). Fox transcription factors : from development to disease. 4558–4570. https://doi.org/10.1242/dev.112672

Gomes, F. L. A. F., Zhang, G., Carbonell, F., Correa, J. A., Harris, W. A., Simons, B. D., & Cayouette, M. (2011). Reconstruction of rat retinal progenitor cell lineages in vitro reveals a surprising degree of stochasticity in cell fate decisions. 235, 227–235. https://doi.org/10.1242/dev.059683

Gonzalez-Cordero, A., Kruczek, K., Naeem, A., Fernando, M., Kloc, M., Ribeiro, J., … Ali, R. R. (2017). Recapitulation of Human Retinal Development from Human Pluripotent Stem Cells Generates Transplantable Populations of Cone Photoreceptors. Stem Cell Reports, 9(3), 820–837. https://doi.org/10.1016/j.stemcr.2017.07.022

Grant, C. E., Bailey, T. L., & Noble, W. S. (2011). FIMO: Scanning for occurrences of a given motif. Bioinformatics, 27(7), 1017–1018. https://doi.org/10.1093/bioinformatics/btr064

Grant, G. R., Farkas, M. H., Pizarro, A. D., Lahens, N. F., Schug, J., Brunk, B. P., … Pierce, E. A. (2011). Comparative analysis of RNA-Seq alignment algorithms and the RNA-Seq unified mapper (RUM). 27(18), 2518–2528. https://doi.org/10.1093/bioinformatics/btr427

Gray, S., & Jolla, L. (1994). Short-range repression permits multiple enhancers to function autonomously within a complex promoter. 1829–1838.

Green, Eric S, Jennifer L Stubbs, and Edward M Levine. (2003). Genetic Rescue of Cell Number in a Mouse Model of Microphthalmia : Interactions between Chx10 and G1-Phase Cell Cycle Regulators. : 539–52.

Gregory-evans, C. Y., Wallace, V. A., & Gregory-evans, K. (2013). Progress in Retinal and Eye Research Gene networks : Dissecting pathways in retinal development and disease. Progress in Retinal and Eye Research, 33, 40–66. https://doi.org/10.1016/j.preteyeres.2012.10.003

Gregory-Evans, C. Y., Williams, M. J., Halford, S., & Gregory-Evans, K. (2004). Ocular coloboma: A reassessment in the age of molecular neuroscience. Journal of Medical Genetics, 41(12), 881–891. https://doi.org/10.1136/jmg.2004.025494

Gregory-Evans, K., & Bhattacharya, S. S. (1998). Genetic blindness: Current concepts in the pathogenesis of human outer retinal dystrophies. Trends in Genetics, 14(3), 103–108. https://doi.org/10.1016/S0168-9525(98)01402-4

Griffiths, J. A., Scialdone, A., & Marioni, J. C. (2018). Using single-cell genomics to understand developmental processes and cell fate decisions. 1–12. https://doi.org/10.15252/msb.20178046

Gu, S. (1997). Mutations in RPE65 cause autosomal recessive childhood-onset severe retinal dystrophy. Nature Genetics, 15, 57–61.

Guillemot, F., & Cepko, C. L. (1992). Retinal fate and ganglion cell differentiation are potentiated by acidic FGF in an in vitro assay of early retinal development. Development, 114(3), 743–754.

Ha, Taejeong et al. (2017). The Retinal Pigment Epithelium Is a Notch Signaling Niche in the Mouse Retina. Cell reports 19(2): 351–63. http://www.ncbi.nlm.nih.gov/pubmed/28402857.

Haghverdi, L., Büttner, M., Wolf, F. A., Buettner, F., & Theis, F. J. (2016). Diffusion pseudotime robustly reconstructs lineage branching. (August). https://doi.org/10.1038/nmeth.3971

Hanovice, N. J., Leach, L. L., Slater, K., Gabriel, A. E., Romanovicz, D., Shao, E., … Gross, J. M. (2019). Regeneration of the zebrafish retinal pigment epithelium after widespread genetic ablation. In PLoS Genetics (Vol. 15). https://doi.org/10.1371/journal.pgen.1007939

Hao, H., Kim, D. S., Klocke, B., Johnson, K. R., Cui, K., Gotoh, N., … Swaroop, A. (2012). Transcriptional regulation of rod photoreceptor homeostasis revealed by in vivo NRL targetome analysis. PLoS Genetics, 8(4). https://doi.org/10.1371/journal.pgen.1002649

Hartsock, A., & Nelson, W. J. (2008). Adherens and tight junctions: Structure, function and connections to the actin cytoskeleton. Biochimica et Biophysica Acta - Biomembranes, 1778(3), 660–669. https://doi.org/10.1016/j.bbamem.2007.07.012

Hatzfeld, M., Keil, R., & Magin, T. M. (2017). Desmosomes and intermediate filaments: Their consequences for tissue mechanics. Cold Spring Harbor Perspectives in Biology, 9(6), 1–20. https://doi.org/10.1101/cshperspect.a029157

Hazim, R. A., Karumbayaram, S., Jiang, M., Dimashkie, A., Lopes, V. S., Li, D., … Williams, D. S. (2017). Differentiation of RPE cells from integration-free iPS cells and their cell biological characterization. Stem Cell Research and Therapy, 8(1), 1–17. https://doi.org/10.1186/s13287-017-0652-9

He, J., Zhang, G., Almeida, A. D., Cayouette, M., Simons, B. D., & Harris, W. A. (2012). How Variable Clones Build an Invariant Retina. Neuron, 75(5), 786–798. https://doi.org/10.1016/j.neuron.2012.06.033

Herrmann, Harald, and Ueli Aebi. (2004). Intermediate Filaments: Molecular Structure, Assembly Mechanism, and Integration Into Functionally Distinct Intracellular Scaffolds. Annual Review of Biochemistry 73(1): 749–89. http://www.annualreviews.org/doi/10.1146/annurev.biochem.73.011303.073823.

Heermann, S., Schütz, L., Lemke, S., Krieglstein, K., & Wittbrodt, J. (2015). Eye morphogenesis driven by epithelial flow into the optic cup facilitated by modulation of bone morphogenetic protein. ELife, 2015(4), 1–17. https://doi.org/10.7554/eLife.05216

Heimberg, G., Bhatnagar, R., El-samad, H., Thomson, M., Heimberg, G., Bhatnagar, R., … Thomson, M. (2016). Low Dimensionality in Gene Expression Data Enables the Accurate Extraction of Transcriptional Programs from Shallow Sequencing Article Low Dimensionality in Gene Expression Data Enables the Accurate Extraction of Transcriptional Programs from Shallow Sequ. Cell Systems, 2(4), 239–250. https://doi.org/10.1016/j.cels.2016.04.001

Hill, R. E. (1991). Mouse small eye results from mutations in a paired-like homeobox-containing gene. Nature, 353, 412–414.

Hiller, M., Agarwal, S., Notwell, J. H., Parikh, R., Guturu, H., Wenger, A. M., & Bejerano, G. (2013). Computational methods to detect conserved non-genic elements in phylogenetically isolated genomes: Application to zebrafish. Nucleic Acids Research, 41(15). https://doi.org/10.1093/nar/gkt557

Hirami, Y., Osakada, F., Takahashi, K., Okita, K., Yamanaka, S., Ikeda, H., … Takahashi, M. (2009). Generation of retinal cells from mouse and human induced pluripotent stem cells. Neuroscience Letters, 458(3), 126–131. https://doi.org/10.1016/j.neulet.2009.04.035

Hodgkinson, C. A., Moore, K. J., Nakayama, A., Steingrímsson, E., Copeland, N. G., Jenkins, N. A., & Arnheiter, H. (1993). Mutations at the mouse microphthalmia locus are associated with defects in a gene encoding a novel basic-helix-loop-helix-zipper protein. Cell, 74(2), 395–404. https://doi.org/10.1016/0092-8674(93)90429-T

Holt, C. (1980). Cell movements in Xenopus eye development.

Holt, C. E., Bertsch, T. W., Ellis, H. M., & Harris, W. A. (1988). Cellular determination in the xenopus retina is independent of lineage and birth date. Neuron, 1(1), 15–26. https://doi.org/10.1016/0896-6273(88)90205-X

Hong, Joung-Woo, David A Hendrix, and Michael S Levine. (2008). Shadow Enhancers as a Source of Evolutionary Novelty. Science (New York, N.Y.) 321(5894): 1314. http://www.ncbi.nlm.nih.gov/pubmed/18772429.

Horsford, D. J., Nguyen, M. T. T., Sellar, G. C., Kothary, R., Arnheiter, H., & McInnes, R. R. (2005). Chx10 repression of Mitf is required for the maintenance of mammalian neuroretinal identity. Development, 132(1), 177–187. https://doi.org/10.1242/dev.01571

Howden, S. E., Maufort, J. P., Duffin, B. M., Elefanty, A. G., Stanley, E. G., & Thomson, J. A. (2015). Simultaneous Reprogramming and Gene Correction of Patient Fibroblasts. Stem Cell Reports, 5(6), 1109–1118. https://doi.org/10.1016/j.stemcr.2015.10.009

Hu, Y., Wang, X., Hu, B., Mao, Y., Chen, Y., Qiao, J., & Id, F. T. (2019). Dissecting the transcriptome landscape of the human fetal neural retina and retinal pigment epithelium by single-cell RNA-seq analysis. 1–26.

Huang, R., He, Y., Sun, B., & Liu, B. (2018). Bioinformatic analysis identifies three potentially key differentially expressed genes in peripheral blood mononuclear cells of patients with takayasu's arteritis. Cell Journal, 19(4), 647–653. https://doi.org/10.22074/cellj.2018.4991

Hughes, A. E. O., Enright, J. M., Myers, C. A., Shen, S. Q., & Corbo, J. C. (2017). Cell Type-Specific Epigenomic Analysis Reveals a Uniquely Closed Chromatin Architecture in Mouse Rod Photoreceptors. Scientific Reports, 7(January), 1–16. https://doi.org/10.1038/srep43184

Hyer, J., Kuhlman, J., Afif, E., & Mikawa, T. (2003). Optic cup morphogenesis requires pre-lens ectoderm but not lens differentiation. Developmental Biology, 259(2), 351–363. https://doi.org/10.1016/S0012-1606(03)00205-7

Hyer, J., Mima, T., & Mikawa, T. (1998). FGF1 patterns the optic vesicle by directing the placement of the neural retina domain. Development, 125(5), 869–877.

Iida, A., Iwagawa, T., Kuribayashi, H., Satoh, S., Mochizuki, Y., Baba, Y., … Watanabe, S. (2014). Histone demethylase Jmjd3 is required for the development of subsets of retinal bipolar cells. Proceedings of the National Academy of Sciences, 111(10), 3751–3756. https://doi.org/10.1073/pnas.1311480111

Isiegas, Carolina ; Marinich-Madzarevich, Jorge A.; Marchena, Miguel; Ruiz, José M.; Cano, María J.; Villa, Pedro de la; Hernández-Sánchez, Catalina ; De la Rosa, Enrique J. ; Pablo, F. de. (2016). Intravitreal injection of proinsulin-loaded microspheres delays photoreceptor cell death and vision loss in the rd10 mouse model of retinitis pigmentosa. Investigative Ophthalmology and Visual Science, 57, 3610–3618.

Iwamatsu, T. (2004). Stages of normal development in the medaka Oryzias latipes. Mechanisms of Development, 121(7–8), 605–618. https://doi.org/10.1016/j.mod.2004.03.012

Izadi. (2017). A comparative analytical assay of gene regulatory networks inferred using microarray and RNA-seq datasets. Bioinformation, 12(06), 340–341. https://doi.org/10.6026/97320630012340

Jaitin. (2014). Massively Parallel Single-Cell. (February).

Jiao, Shi et al. (2014). A Peptide Mimicking VGLL4 Function Acts as a YAP Antagonist Therapy against Gastric Cancer. Cancer cell 25(2): 166–80. http://www.ncbi.nlm.nih.gov/pubmed/24525233.

Jiao, S., Li, C., Miao, H., Zhang, L., Li, L., Zhou, Z.. (2017). VGLL4 Targets a TCF4-TEAD4 Complex to Coregulate Wnt and Hippo Signalling in Colorectal Cancer. Nature communications 8: 14058. http://www.ncbi.nlm.nih.gov/pubmed/28051067.

Johnson, D. S., Mortazavi, A., & Myers, R. M. (2007). Protein-DNA Interactions. (June), 1497–1503.

Jones. (2017). Cell-based therapeutic strategies for replacement and preservation in retinal degenerative diseases. Prog Retin Eye Res., 176(3), 139–148. https://doi.org/10.1016/j.physbeh.2017.03.040

Jorstad. (2017). Stimulation of functional neuronal regeneration from Müller glia in adult mice. 232(1), 103–107. https://doi.org/10.1530/JOE-16-0447.Hepatocyte-specific

Jothi, R., Cuddapah, S., Barski, A., Cui, K., & Zhao, K. (2008). Genome-wide identification of in vivo protein-DNA binding sites from ChIP-Seq data. Nucleic Acids Research, 36(16), 5221–5231. https://doi.org/10.1093/nar/gkn488

Kapitein, Lukas C, and Casper C Hoogenraad. (2015). Building the Neuronal Microtubule Cytoskeleton. Neuron 87(3): 492–506. http://www.ncbi.nlm.nih.gov/pubmed/26247859.

Kawakami, K. (2007). Tol2: A versatile gene transfer vector in vertebrates. Genome Biology, 8(SUPPL. 1), 1–10. https://doi.org/10.1186/gb-2007-8-s1-s7

Kennedy, N., Stearns, G. W., Smyth, V. A., Ramamurthy, V., Eeden, F. Van, Ankoudinova, I., … Brockerhoff, S. E. (2004). Zebrafish rx3 and mab21l2 are required during eye morphogenesis. 270, 336–349. https://doi.org/10.1016/j.ydbio.2004.02.026

Kim, J. W., Yang, H. J., Brooks, M. J., Zelinger, L., Karakülah, G., Gotoh, N., … Swaroop, A. (2016). NRL-Regulated Transcriptome Dynamics of Developing Rod Photoreceptors. Cell Reports, 17(9), 2460–2473. https://doi.org/10.1016/j.celrep.2016.10.074

Kim, Jin Young et al. (2016). Yap Is Essential for Retinal Progenitor Cell Cycle Progression and RPE Cell Fate Acquisition in the Developing Mouse Eye. Developmental biology 419(2): 336–47. http://www.ncbi.nlm.nih.gov/pubmed/27616714.

Kim, J. Y., Park, R., Lee, J. H. J., Shin, J., Nickas, J., Kim, S., & Cho, S. H. (2016). Yap is essential for retinal progenitor cell cycle progression and RPE cell fate acquisition in the developing mouse eye. Developmental Biology, 419(2), 336–347. https://doi.org/10.1016/j.ydbio.2016.09.001

Kimmel, C. B., Ballard, W. W., Kimmel, S. R., Ullmann, B., & Schilling, T. F. (1995). Stages of embryonic development of the zebrafish. Developmental Dynamics, 203(3), 253–310. https://doi.org/10.1002/aja.1002030302

Kimura, A., Namekata, K., Guo, X., Harada, C., & Harada, T. (2016). Neuroprotection, growth factors and BDNF-TRKB signalling in retinal degeneration. International Journal of Molecular Sciences, 17(9). https://doi.org/10.3390/ijms17091584

Kleinjan, D. A., Bancewicz, R. M., Gautier, P., Dahm, R., Schonthaler, H. B., Damante, G., … Coutinho, P. (2008). Subfunctionalization of duplicated zebrafish pax6 genes by cis-regulatory divergence. PLoS Genetics, 4(2). https://doi.org/10.1371/journal.pgen.0040029

Kolde, R. (2019). pheatmap: Pretty Heatmaps.

Kolodziejczyk, A. A., Kim, J. K., Svensson, V., Marioni, J. C., & Teichmann, S. A. (2015). Review The Technology and Biology of Single-Cell RNA Sequencing. Molecular Cell, 58(4), 610–620. https://doi.org/10.1016/j.molcel.2015.04.005

Kolomeyer, A. M., & Zarbin, M. A. (2014). Trophic factors in the pathogenesis and therapy for retinal degenerative diseases. Survey of Ophthalmology, 59(2), 134–165. https://doi.org/10.1016/j.survophthal.2013.09.004

Kouzarides, T. (2007). Chromatin Modifications and Their Function. 693–705. https://doi.org/10.1016/j.cell.2007.02.005

Kreis, Thomas E., and Walter Birchmeier. (1980). Stress Fiber Sarcomeres of Fibroblasts Are Contractile. Cell 22(2): 555–61. https://linkinghub.elsevier.com/retrieve/pii/0092867480903657.

Krishna, D., Karunakaran, P., Seesi, S. Al, Banday, A. R., Baumgartner, M., Olthof, A., … Kanadia, R. N. (2016). Network-based bioinformatics analysis of spatio-temporal RNA-Seq data reveals transcriptional programs underpinning normal and aberrant retinal development. https://doi.org/10.1186/s12864-016-2822-z

Krishnakumar. (2013). PARP-1 Regulates Chromatin Structure and Transcription Through a KDM5B-Dependent Pathway. 71(2), 233–236. https://doi.org/10.1038/mp.2011.182.doi

Krzywinski, M., Schein, J., Birol, I., Connors, J., Gascoyne, R., Horsman, D., … Marra, M. A. (2009). Circos : An information aesthetic for comparative genomics. Genome Research, 19(604), 1639–1645. https://doi.org/10.1101/gr.092759.109.19

Kumar, L., & Futschik, M. E. (2007). Mfuzz: A software package for soft clustering of microarray data. Bioinformation, 2(1), 5–7. https://doi.org/10.6026/97320630002005

Kwan, K. M., Fujimoto, E., Grabher, C., Mangum, B. D., Hardy, M. E., Campbell, D. S., … Chien, C. Bin. (2007). The Tol2kit: A multisite gateway-based construction Kit for Tol2 transposon transgenesis constructs. Developmental Dynamics, 236(11), 3088–3099. https://doi.org/10.1002/dvdy.21343

Kwan, K. M., Otsuna, H., Kidokoro, H., Carney, K. R., Saijoh, Y., & Chien, C. Bin. (2012). A complex choreography of cell movements shapes the vertebrate eye. Development, 139(2), 359–372. https://doi.org/10.1242/dev.071407

Lacalli, T. C. (2004). Sensory systems in amphioxus: A window on the ancestral chordate condition. Brain, Behavior and Evolution, 64(3), 148–162. https://doi.org/10.1159/000079744

Lagutin, O. (2003). A delimitation of the Paya area in Honduras and cerain stylistic resemblances found in Costa Rica and Honduras. Genes & Development 17:368–379 © 2003, 17, 368–379. https://doi.org/10.1101/gad.1059403.bera

Lagutin, O., Zhu, C. C., Furuta, Y., Rowitch, D. H., McMahon, A. P., & Oliver, G. (2001). Six3 promotes the formation of ectopic optic vesicle-like structures in mouse embryos. Developmental Dynamics, 221(3), 342–349. https://doi.org/10.1002/dvdy.1148

Lake, B. B., Chen, S., Sos, B. C., Fan, J., Kaeser, G. E., Yung, Y. C., … Zhang, K. (2018). Integrative single-cell analysis of transcriptional and epigenetic states in the human adult brain. 36(1). https://doi.org/10.1038/nbt.4038

Lane, B. M., & Lister, J. A. (2012). Otx but Not Mitf Transcription Factors Are Required for Zebrafish Retinal Pigment Epithelium Development. PLoS ONE, 7(11). https://doi.org/10.1371/journal.pone.0049357

Letamendia, A., Labbé, E., & Attisano, L. (2001). Transcriptional regulation by Smads: crosstalk between the TGF-beta and Wnt pathways. The Journal of Bone and Joint Surgery. American Volume, 83-A Suppl(Pt 1), S31-9. Retrieved from http://www.ncbi.nlm.nih.gov/pubmed/11263663

Letelier, J., Bovolenta, P., & Martínez-Morales, J. R. (2017). The pigmented epithelium, a bright partner against photoreceptor degeneration. Journal of Neurogenetics, 31(4), 203–215. https://doi.org/10.1080/01677063.2017.1395876

Li, L., & Turner, J. E. (1988). Inherited retinal dystrophy in the RCS rat: Prevention of photoreceptor degeneration by pigment epithelial cell transplantation. Experimental Eye Research, 47(6), 911–917. https://doi.org/10.1016/0014-4835(88)90073-5

Li, L., & Turner, J. E. (1991). Optimal conditions for long-term photoreceptor cell rescue in RCS rats: The necessity for healthy RPE transplants. Experimental Eye Research, 52(6), 669–679. https://doi.org/10.1016/0014-4835(91)90019-B

Li, M., Jia, C., Kazmierkiewicz, K. L., Bowman, A. S., Tian, L., Liu, Y., … Curcio, C. A. (2014). Comprehensive analysis of gene expression in human retina and supporting tissues. 23(15), 4001–4014. https://doi.org/10.1093/hmg/ddu114

Li, Z., Joseph, N. M., & Easter, S. S. (2000). The morphogenesis of the zebrafish eye, including a fate map of the optic vesicle. Developmental Dynamics, 218(1), 175–188. https://doi.org/10.1002/(SICI)1097-0177(200005)218:1<175::AID-DVDY15>3.0.CO;2-K

Liao, H., Bucala, R., & Mitchell, R. A. (2003). Adhesion-dependent signaling by macrophage migration inhibitory factor (MIF). The Journal of Biological Chemistry, 278(1), 76–81. https://doi.org/10.1074/jbc.M208820200

Lin, Kimberly C, Hyun Woo Park, and Kun-Liang Guan. (2017). Regulation of the Hippo Pathway Transcription Factor TEAD. Trends in biochemical sciences 42(11): 862–72. http://www.ncbi.nlm.nih.gov/pubmed/28964625.

Lin, K. C., Park, H. W., & Guan, K.-L. (2017). Regulation of the Hippo Pathway Transcription Factor TEAD. Trends in Biochemical Sciences, 42(11), 862–872. https://doi.org/10.1016/j.tibs.2017.09.003

Liu, I. S. C., Chen, J. de, Ploder, L., Vidgen, D., van der Kooy, D., Kalnins, V. I., & Mclnnes, R. R. (1994). Developmental expression of a novel murine homeobox gene (Chx10): Evidence for roles in determination of the neuroretina and inner nuclear layer. Neuron, 13(2), 377–393. https://doi.org/10.1016/0896-6273(94)90354-9

Liu, W., Lagutin, O., Swindell, E., Jamrich, M., & Oliver, G. (2010). Neuroretina specification in mouse embryos requires Six3-mediated suppression of Wnt8b in the anterior neural plate. October, 120(10). https://doi.org/10.1172/JCI43219DS1

Liu, Xiangfan et al. (2016). Tead and AP1 Coordinate Transcription and Motility. Cell reports 14(5): 1169–80. http://www.ncbi.nlm.nih.gov/pubmed/26832411.

Livesey, F. J., Furukawa, T., Steffen, M. A., Church, G. M., & Cepko, C. L. (2000). Microarray analysis of the transcriptional network controlled by the photoreceptor homeobox gene Crx. Current Biology, 10(6), 301–310. https://doi.org/10.1016/S0960-9822(00)00379-1

Lo Giudice, Q., Leleu, M., La Manno, G., & Fabre, P. J. (2019). Single-cell transcriptional logic of cell-fate specification and axon guidance in early-born retinal neurons. Development, 146(17), dev178103. https://doi.org/10.1242/dev.178103

Loosli, F., Winkler, S., Burgtorf, C., Wurmbach, E., Ansorge, W., Henrich, T., … Wittbrodt, J. (2001). Medaka eyeless is the key factor linking retinal determination and eye growth. Development, 128(20), 4035–4044.

Loosli, Felix, Staub, W., Finger-Baier, K. C., Ober, E. A., Verkade, H., Wittbrodt, J., & Baier, H. (2003). Loss of eyes in zebrafish caused by mutation of chokh/rx 3. EMBO Reports, 4(9), 894–899. https://doi.org/10.1038/sj.embor.embor919

Loosli, Felix, Winkler, S., & Wittbrodt, J. (1999). Six3 overexpression initiates the formation of ectopic retina. Genes and Development, 13(6), 649–654. https://doi.org/10.1101/gad.13.6.649

Lopashov, G. V, & Stroeva, O. G. (1964). Development of the eye: experimental studies. Jerusalem: Israel Program Fo Scientific Translation.

Love, M. I., Huber, W., & Anders, S. (2014). Moderated estimation of fold change and dispersion for RNA-seq data with DESeq2. Genome Biology, 15(12), 1–21. https://doi.org/10.1186/s13059-014-0550-8

Lowe, E. K., Cuomo, C., Voronov, D., & Arnone, M. I. (2019). Using ATAC-seq and RNA-seq to increase resolution in GRN connectivity. In Methods in Cell Biology (1st ed., Vol. 151). https://doi.org/10.1016/bs.mcb.2018.11.001

Lu, B., Malcuit, C., Wang, S., Girman, S., Francis, P., Lemieux, L., … Lund, R. (2009). Long-term safety and function of RPE from human embryonic stem cells in preclinical models of macular degeneration. Stem Cells, 27(9), 2126–2135. https://doi.org/10.1002/stem.149

Lukowski, S. W., Lo, C. Y., Sharov, A. A., Nguyen, Q., Fang, L., Hung, S. S. C., … Wong, R. C. B. (2019). A single - cell transcriptome atlas of the adult human retina The retina is a specialized neural tissue that senses light and initiates image. (August), 1–38.

Lund, R. D., Wang, S., Klimanskaya, I., Holmes, T., Ramos-Kelsey, R., Lu, B., … Lanza, R. (2006). Human embryonic stem cell-derived cells rescue visual function in dystrophic RCS rats. Cloning and Stem Cells, 8(3), 189–199. https://doi.org/10.1089/clo.2006.8.189

Luo, C., Keown, C. L., Kurihara, L., Zhou, J., He, Y., Li, J., … Ecker, J. R. (2017). Single-cell methylomes identify neuronal subtypes and regulatory elements in mammalian cortex Chongyuan. 604(August), 600–604.

Macosko, E. Z., Basu, A., Satija, R., Nemesh, J., Shekhar, K., Goldman, M., … McCarroll, S. A. (2015a). Highly Parallel Genome-wide Expression Profiling of Individual Cells Using Nanoliter Droplets. Cell, 161(5), 1202–1214. https://doi.org/10.1016/j.cell.2015.05.002

Macosko, E. Z., Basu, A., Satija, R., Nemesh, J., Shekhar, K., Goldman, M., … McCarroll, S. A. (2015b). Highly parallel genome-wide expression profiling of individual cells using nanoliter droplets. Cell, 161(5), 1202–1214. https://doi.org/10.1016/j.cell.2015.05.002

Malawista, Stephen E. (1975). MICROTUBULES AND THE MOBILIZATION OF LYSOSOMES IN PHAGOCYTIZING HUMAN LEUKOCYTES. Annals of the New York Academy of Sciences 253(1 The Biology o): 738–49. http://doi.wiley.com/10.1111/j.1749-6632.1975.tb19242.x.

Mandai, M., Watanabe, A., Kurimoto, Y., Hirami, Y., Morinaga, C., Daimon, T., … Takahashi, M. (2017). Autologous induced stem-cell-derived retinal cells for macular degeneration. New England Journal of Medicine, 376(11), 1038–1046. https://doi.org/10.1056/NEJMoa1608368

Marioni, J. C., Mason, C. E., Mane, S. M., Stephens, M., & Gilad, Y. (2008). RNA-seq : An assessment of technical reproducibility and comparison with gene expression arrays. 1509–1517. https://doi.org/10.1101/gr.079558.108.

Marlhens. (1997). Mutations in RPE65 cause Leber's congenital amaurosis. Nature Genetics, 15, 57–61.

Martinez-Mir, A. (1998). Retinitis pigmentosa caused by a homozygous mutation in the Stargardt disease gene ABCR. Nature Genetics, 18(3), 231–236. https://doi.org/10.1038/ng0598-51

Martinez-Morales. (2003). OTX2 Activates the Molecular Network Underlying Retina Pigment Epithelium Differentiation * ´ n Martı. 278(24), 21721–21731. https://doi.org/10.1074/jbc.M301708200

Martínez-Morales, J. R., Rodrigo, I., & Bovolenta, P. (2004). Eye development: A view from the retina pigmented epithelium. BioEssays, 26(7), 766–777. https://doi.org/10.1002/bies.20064

Martinez-Morales, J. R., Signore, M., Acampora, D., Simeone, A., & Bovolenta, P. (2001). Otx genes are required for tissue specification in the developing eye. Development, 128(11), 2019–2030.

Martinez-Morales, Juan Ramón. (2016). Vertebrate Eye Gene Regulatory Networks. In Organogenetic Gene Networks - Genetic Control of Organ Formation (pp. 259–274). Springer International Publishing.

Martinez-Morales, Juan Ramon, & Wittbrodt, J. (2009). Shaping the vertebrate eye. Current Opinion in Genetics and Development, 19(5), 511–517. https://doi.org/10.1016/j.gde.2009.08.003

Martinez-Morales, J. R., Rembold, M., Greger, K., Simpson, J. C., Brown, K. E., Quiring, R., … Wittbrodt, J. (2009). Ojoplano-mediated basal constriction is essential for optic cup morphogenesis. Development, 136(13), 2165–2175. https://doi.org/10.1242/dev.033563

Mathers, P. H., Grinberg, A., & Mahon, K. A. (1997). The Rx homeobox gene is essential for vertebrate eye development. 387(June), 603–607.

Matsuo, I., Kuratani, S., Kimura, C., Takeda, N., & Aizawa, S. (1995). Mouse Otx2 functions in the formation and patterning of rostral head. Genes and Development, 9(21), 2646–2658. https://doi.org/10.1101/gad.9.21.2646

Mccall, M. N. (2010). Estimation of Gene Regulatory Networks. Journal of Postdoctoral Research, 1(January 2013), 60–69.

McConnell, B. B., & Yang, V. W. (2010). Mammalian Krüppel-Like Factors in Health and Diseases Beth. 90(4), 1337–1381. https://doi.org/10.1152/physrev.00058.2009.Mammalian

Meads, T, and T A Schroer. (1995). Polarity and Nucleation of Microtubules in Polarized Epithelial Cells. Cell motility and the cytoskeleton 32(4): 273–88. http://www.ncbi.nlm.nih.gov/pubmed/8608606.

Mears, A. J., Kondo, M., Swain, P. K., Takada, Y., Bush, R. A., Saunders, T. L., … Swaroop, A. (2001). Nrl is required for rod photoreceptor development. Nature Genetics, 29(4), 447–452. https://doi.org/10.1038/ng774

Medina-Martinez, O., Amaya-Manzanares, F., Liu, C., Mendoza, M., Shah, R., Zhang, L., … Jamrich, M. (2009). Cell-autonomous requirement for Rx function in the mammalian retina and posterior pituitary. PLoS ONE, 4(2), 1–7. https://doi.org/10.1371/journal.pone.0004513

Metzker, M. L. (2010). Sequencing technologies the next generation. Nature Reviews Genetics, 11(1), 31–46. https://doi.org/10.1038/nrg2626

Mi, H., Muruganujan, A., Ebert, D., Huang, X., & Thomas, P. D. (2019). PANTHER version 14: more genomes, a new PANTHER GO-slim and improvements in enrichment analysis tools. Nucleic Acids Research, 47(D1), D419–D426. https://doi.org/10.1093/nar/gky1038

Mi, H., Muruganujan, A., Huang, X., Ebert, D., Mills, C., Guo, X., & Thomas, P. D. (2019). Protocol Update for large-scale genome and gene function analysis with the PANTHER classification system (v.14.0). Nature Protocols, 14(3), 703–721. https://doi.org/10.1038/s41596-019-0128-8

Miesfeld, J. B., Gestri, G., Clark, B. S., Flinn, M. A., Poole, R. J., Bader, J. R., … Link, B. A. (2015). Yap and Taz regulate retinal pigment epithelial cell fate. Development (Cambridge), 142(17), 3021–3032. https://doi.org/10.1242/dev.119008

Mo, A., Luo, C., Davis, F. P., Mukamel, E. A., Henry, G. L., Nery, J. R., … Nathans, J. (2016). Epigenomic landscapes of retinal rods and cones. ELife, 5, 1–29. https://doi.org/10.7554/elife.11613

Mochii, M., Ono, T., Matsubara, Y., & Eguchi, G. (1998). Spontaneous transdifferentiation of quail pigmented epithelial cell is accompanied by a mutation in the Mitf gene. Developmental Biology, 196(2), 145–159. https://doi.org/10.1006/dbio.1998.8864

Moignard, V., Woodhouse, S., Haghverdi, L., Lilly, A. J., Tanaka, Y., Wilkinson, A. C., … Göttgens, B. (2015). Decoding the regulatory network of early blood development from single-cell gene expression measurements. 33(3). https://doi.org/10.1038/nbt.3154

Moreno-Marmol, Tania, Florencia Cavodeassi, and Paola Bovolenta. (2018). Setting Eyes on the Retinal Pigment Epithelium. Frontiers in cell and developmental biology 6: 145. http://www.ncbi.nlm.nih.gov/pubmed/30406103.

Moreno-mateos, M. A., Vejnar, C. E., Beaudoin, J., Juan, P., Mis, E. K., Khokha, M. K., … Haven, N. (2016). CRISPRscan: designing highly efficient sgRNAs for CRISPR/ Cas9 targeting in vivo. 12(10), 982–988. https://doi.org/10.1038/nmeth.3543.CRISPRscan

Mortazavi, A., Williams, B. A., McCue, K., Schaeffer, L., & Wold, B. (2008). Mapping and quantifying mammalian transcriptomes by RNA-Seq. Nature Methods, 5(7), 621–628. https://doi.org/10.1038/nmeth.1226

Mu, X. (2001). Gene expression in the developing mouse retina by EST sequencing and microarray analysis. Nucleic Acids Research, 29(24), 4983–4993. https://doi.org/10.1093/nar/29.24.4983

Müller, F., Rohrer, H., & Vogel-Höpker, A. (2007). Bone morphogenetic proteins specify the retinal pigment epithelium in the chick embryo. Development, 134(19), 3483–3493. https://doi.org/10.1242/dev.02884

Murphy, D., Cieply, B., Carstens, R., Ramamurthy, V., & Stoilov, P. (2016). The Musashi 1 Controls the Splicing of Photoreceptor-Specific Exons in the Vertebrate Retina. PLoS Genetics, 12(8), 1–27. https://doi.org/10.1371/journal.pgen.1006256

Mustafi, D., Kevany, B. M., Genoud, C., Okano, K., Cideciyan, A. V, Sumaroka, A., … Palczewski, K. (2011). Defective photoreceptor phagocytosis in a mouse model of enhanced S-cone syndrome causes progressive retinal degeneration. 3157–3176. https://doi.org/10.1096/fj.11-186767

Nakayama, A., Nguyen, M. T. T., Chen, C. C., Opdecamp, K., Hodgkinson, C. A., & Arnheiter, H. (1998). Mutations in microphthalmia, the mouse homolog of the human deafness gene MITF, affect neuroepithelial and neural crest-derived melanocytes differently. Mechanisms of Development, 70(1–2), 155–166. https://doi.org/10.1016/S0925-4773(97)00188-3

Nakayama, T., Fish, M. B., Fisher, M., Oomen-Hajagos, J., Thomsen, G. H., & Grainger, R. M. (2015). Simple and efficient CRISPR/Cas9-mediated targeted mutagenesis in Xenopus tropicalis. 34(3), 474–476. https://doi.org/10.1161/ATVBAHA.114.303112.ApoA-I

Neuhauss, S. C. F., Biehlmaier, O., Seeliger, M. W., Das, T., Kohler, K., Harris, W. A., & Baier, H. (1999). Genetic disorders of vision revealed by a behavioral screen of 400 essential loci in zebrafish. Journal of Neuroscience, 19(19), 8603–8615. https://doi.org/10.1523/jneurosci.19-19-08603.1999

Nguyen, M. T. T., & Arnheiter, H. (2000). Signaling and transcriptional regulation in early mammalian eye development: A link between FGF and MITF. Development, 127(16), 3581–3591.

Nimwegen, E. Van. (2012). DNA-binding factors shape the mouse methylome at distal regulatory regions. https://doi.org/10.1038/nature10716

Nommiste, B., Fynes, K., Tovell, V. E., Ramsden, C., da Cruz, L., & Coffey, P. (2017). Stem cell-derived retinal pigment epithelium transplantation for treatment of retinal disease. In Progress in Brain Research (1st ed., Vol. 231). https://doi.org/10.1016/bs.pbr.2017.03.003

Norrie, J. L., Lupo, M. S., Xu, B., Al Diri, I., Valentine, M., Putnam, D., … Dyer, M. A. (2019). Nucleome Dynamics during Retinal Development. Neuron, 1–17. https://doi.org/10.1016/j.neuron.2019.08.002

Ogundijo, O. E., Elmas, A., & Wang, X. (2016). Reverse engineering gene regulatory networks from measurement with missing values. Eurasip Journal on Bioinformatics and Systems Biology, 2017(1). https://doi.org/10.1186/s13637-016-0055-8

Osakada, F., Jin, Z. B., Hirami, Y., Ikeda, H., Danjyo, T., Watanabe, K., … Takahashi, M. (2009). In vitro differentiation of retinal cells from human pluripotent stem cells by small-molecule induction. Journal of Cell Science, 122(17), 3169–3179. https://doi.org/10.1242/jcs.050393

Park, P. J. (2009). ChIP-seq: Advantages and challenges of a maturing technology. Nature Reviews Genetics, 10(10), 669–680. https://doi.org/10.1038/nrg2641

Peng, Y. R., Shekhar, K., Yan, W., Herrmann, D., Sappington, A., Bryman, G. S., … Sanes, J. R. (2019). Molecular Classification and Comparative Taxonomics of Foveal and Peripheral Cells in Primate Retina. Cell, 176(5), 1222-1237.e22. https://doi.org/10.1016/j.cell.2019.01.004

Perry, S. F., Ekker, M., Farrell, A. P., & Brauner, C. J. (2010). Zebrafish. Elsevier.

Phillips, M. J., Perez, E. T., Martin, J. M., Reshel, S. T., Wallace, K. A., Capowski, E. E., … Gamm, D. M. (2014). Modeling human retinal development with patient-specific iPS cells reveals multiple roles for VSX2. Stem Cells, 32(6), 1480–1492. https://doi.org/10.1126/scisignal.2001449.Engineering

Picker, A., Cavodeassi, F., Machate, A., Bernauer, S., Hans, S., Abe, G., … Brand, M. (2009). Dynamic coupling of pattern formation and morphogenesis in the developing vertebrate retina. PLoS Biology, 7(10). https://doi.org/10.1371/journal.pbio.1000214

Pinelli, M., Carissimo, A., Cutillo, L., Lai, C., Mutarelli, M., Moretti, M. N., … Bernardo, D. (2016). An atlas of gene expression and gene co-regulation in the human retina. 44(12), 5773–5784. https://doi.org/10.1093/nar/gkw486

Pittack, C., Jones, M., & Reh, T. A. (1991). Basic fibroblast growth factor induces retinal pigment epithelium to generate neural retina in vitro. Development, 113(2), 577–588.

Pittack, Catrin, Grunwald, G. B., & Reh, T. A. (1997). Fibroblast growth factors are necessary for neural retina but not pigmented epithelium differentiation in chick embryos. Development, 124(4), 805–816.

Planque, N., Turque, N., Opdecamp, K., Bailly, M., Martin, P., & Saule, S. (1999). Expression of the microphthalmia-associated basic helix-loop-helix leucine zipper transcription factor Mi in avian neuroretina cells induces a pigmented phenotype. Cell Growth and Differentiation, 10(7), 525–536.

Pobbati, Ajaybabu V et al. (2012). Structural and Functional Similarity between the Vgll1-TEAD and the YAP-TEAD Complexes. Structure (London, England : 1993) 20(7): 1135–40. http://www.ncbi.nlm.nih.gov/pubmed/22632831.

Polato, F., & Becerra, S. P. (2015). Retinal Degenerative Diseases: Mechanisms and Experimental Therapies. 699–706. https://doi.org/10.1007/978-3-319-17121-0

Pollen, A. A., Nowakowski, T. J., Shuga, J., Wang, X., Leyrat, A. A., Lui, J. H., … West, J. A. A. (2014). Low-coverage single-cell mRNA sequencing reveals cellular heterogeneity and activated signaling pathways in developing cerebral cortex. Nature Biotechnology, 32(10). https://doi.org/10.1038/nbt.2967

Popova, E. Y., Xu, X., DeWan, A. T., Salzberg, A. C., Berg, A., Hoh, J., … Barnstable, C. J. (2012). Stage and Gene Specific Signatures Defined by Histones H3K4me2 and H3K27me3 Accompany Mammalian Retina Maturation In Vivo. PLoS ONE, 7(10). https://doi.org/10.1371/journal.pone.0046867

Porges, Y., Gershoni-Baruch, R., Leibu, R., Goldscher, D., Zonis, S., Shapira, I., & Miller, B. (1992). Hereditary microphthalmia with colobomatous cyst. American Journal of Ophthalmology, 114(1), 30–34. https://doi.org/10.1016/S0002-9394(14)77409-4

Porter, F. D., Drago, J., Xu, Y., Cheema, S. S., Wassif, C., Huang, S. P., … Westphal, H. (1997). Lhx2, a LIM homeobox gene, is required for eye, forebrain, and definitive erythrocyte development. Development, 124(15), 2935–2944.

Preissl, S., Fang, R., Huang, H., Zhao, Y., Raviram, R., Gorkin, D. U., … Ren, B. (2018). in developing mouse forebrain reveals. Nature Neuroscience. https://doi.org/10.1038/s41593-018-0079-3

Prieto, J.-L., & McStay, B. (2007). Recruitment of factors linking transcription and processing of pre-rRNA to NOR chromatin is UBF-dependent and occurs independent of transcription in human cells. Genes & Development, 21(16), 2041–2054. https://doi.org/10.1101/gad.436707

Ramsden, C. M., Powner, M. B., Carr, A. J. F., Smart, M. J. K., da Cruz, L., & Coffey, P. J. (2013). Stem cells in retinal regeneration: Past, present and future. Development (Cambridge), 140(12), 2576–2585. https://doi.org/10.1242/dev.092270

Rembold, M., Loosli, F., Adams, R. J., & Wittbrodt, J. (2006). individual Cell Migration Serves as the Driving Force for Optic Vesicle Evagination. Science, (August), 1130–1135.

Rhode, B. (1992). Development and differentiation of the eye in Platynereis dumerilii (Annelida, Polychaeta). Journal of Morphology, 212(1), 71–85. https://doi.org/10.1002/jmor.1052120108

Rotty, Jeremy D, and James E Bear. (2015). Competition and Collaboration between Different Actin Assembly Pathways Allows for Homeostatic Control of the Actin Cytoskeleton. BioArchitecture 5(1–2): 27–34. https://www.tandfonline.com/doi/full/10.1080/19490992.2015.1090670.

Rowan, S., & Cepko, C. L. (2004). Genetic analysis of the homeodomain transcription factor Chx10 in the retina using a novel multifunctional BAC transgenic mouse reporter. Developmental Biology, 271(2), 388–402. https://doi.org/10.1016/j.ydbio.2004.03.039

Rowan, S., Chen, C.-M. A., Young, T. L., Fisher, D. E., & Cepko, C. L. (2004). Transdifferentiation of the retina into pigmented cells in ocular retardation mice defines a new function of the homeodomain gene Chx10. Development (Cambridge, England), 131(20), 5139–5152. https://doi.org/10.1242/dev.01300

Ruzycki, P. A., Zhang, X., & Chen, S. (2018). CRX directs photoreceptor differentiation by accelerating chromatin remodeling at specific target sites. Epigenetics and Chromatin, 11(1), 1–16. https://doi.org/10.1186/s13072-018-0212-2

Sahel, J.-A., & Roska, B. (2013). Gene Therapy for Blindness. Annual Review of Neuroscience, 36(1), 467–488. https://doi.org/10.1146/annurev-neuro-062012-170304

Samuel, A., Housset, M., Fant, B., & Lamonerie, T. (2014). Otx2 ChIP-seq reveals unique and redundant functions in the mature mouse retina. PLoS ONE, 9(2). https://doi.org/10.1371/journal.pone.0089110

Sanghvi-Shah, Rucha, and Gregory F. Weber. (2017). Intermediate Filaments at the Junction of Mechanotransduction, Migration, and Development. Frontiers in Cell and Developmental Biology 5. http://journal.frontiersin.org/article/10.3389/fcell.2017.00081/full.

Santos-Pereira, J. M., Gallardo-Fuentes, L., Neto, A., Acemel, R. D., & Tena, J. J. (2019). Pioneer and repressive functions of p63 during zebrafish embryonic ectoderm specification. Nature Communications, 10(1), 3049. https://doi.org/10.1038/s41467-019-11121-z

Schouwey, Karine, and Friedrich Beermann. (2008). The Notch Pathway: Hair Graying and Pigment Cell Homeostasis. Histology and histopathology 23(5): 609–19. http://www.ncbi.nlm.nih.gov/pubmed/18283646.

Schulte, D., Furukawa, T., Peters, M. A., Kozak, C. A., & Cepko, C. L. (1999). Misexpression of the Emx-Related Homeobox Genes cVax and mVax2 Ventralizes the Retina and Perturbs the Retinotectal Map. 24, 541–553.

Schwartz, S. D., Hubschman, J. P., Heilwell, G., Franco-Cardenas, V., Pan, C. K., Ostrick, R. M., … Lanza, R. (2012). Embryonic stem cell trials for macular degeneration: A preliminary report. The Lancet, 379(9817), 713–720. https://doi.org/10.1016/S0140-6736(12)60028-2

Schwartz, S. D., Regillo, C. D., Lam, B. L., Eliott, D., Rosenfeld, P. J., Gregori, N. Z., … Lanza, R. (2015). Human embryonic stem cell-derived retinal pigment epithelium in patients with age-related macular degeneration and Stargardt's macular dystrophy: Follow-up of two open-label phase 1/2 studies. The Lancet, 385(9967), 509–516. https://doi.org/10.1016/S0140-6736(14)61376-3

Schwarz, M., Cecconi, F., Bernier, G., Andrejewski, N., Kammandel, B., Wagner, M., & Gruss, P. (2000). Spatial specification of mammalian eye territories by reciprocal transcriptional repression of Pax2 and Pax6. Development, 127(20), 4325–4334.

Seberg, Hannah E. et al. (2017). TFAP2 Paralogs Regulate Melanocyte Differentiation in Parallel with MITF ed. Gregory S. Barsh. PLOS Genetics 13(3): e1006636. https://dx.plos.org/10.1371/journal.pgen.1006636.

Secombe, J., & Eisenman, R. N. (2007). The function and regulation of the JARID1 family of histone H3 lysine 4 demethylases: The Myc connection. Cell Cycle, 6(11), 1324–1328. https://doi.org/10.4161/cc.6.11.4269

Seth, A., Culverwell, J., Walkowicz, M., Toro, S., Rick, J. M., Neuhauss, S. C. F., … Karlstrom, R. O. (2006). Erratum: Belladonna/(lhx2) is required for neural patterning and midline axon guidance in the zebrafish

forebrain (Development vol. 133 (725-735)). Development, 133(9), 1856. https://doi.org/10.1242/dev.02390

Shankaran, S. S., Dahlem, T. J., Bisgrove, B. W., Yost, H. J., & Tristani-Firouzi, M. (2017). CRISPR/Cas9-Directed Gene Editing for the Generation of Loss-of-Function Mutants in High-Throughput Zebrafish F0 Screens. Current Protocols in Molecular Biology, 119, 31.9.1-31.9.22. https://doi.org/10.1002/cpmb.42

Shapiro, E., Biezuner, T., & Linnarsson, S. (2013). technologies will revolutionize whole-organism science. Nature Publishing Group, (July), 1–13. https://doi.org/10.1038/nrg3542

Sharon, D., Blackshaw, S., Cepko, C. L., & Dryja, T. P. (2002). Profile of the genes expressed in the human peripheral retina, macula, and retinal pigment epithelium determined through serial analysis of gene expression (SAGE). Proceedings of the National Academy of Sciences, 99(1), 315–320. https://doi.org/10.1073/pnas.012582799

Shekhar, K., Lapan, S. W., Whitney, I. E., Cepko, C. L., Regev, A., Sanes, J. R., … Macosko, E. Z. (2016). Comprehensive Classification of Retinal Bipolar Neurons by Single-Cell Transcriptomics Resource Comprehensive Classification of Retinal Bipolar Neurons by Single-Cell Transcriptomics. Cell, 166(5), 1308-1323.e30. https://doi.org/10.1016/j.cell.2016.07.054

Sidhaye, J., & Norden, C. (2017). Concerted action of neuroepithelial basal shrinkage and active epithelial migration ensures efficient optic cup morphogenesis. ELife, 6, 1–29. https://doi.org/10.7554/elife.22689

Simson, J V, and S S Spicer. (1973). Activities of Specific Cell Constituents in Phagocytosis (Endocytosis). International review of experimental pathology 12: 79–118. http://www.ncbi.nlm.nih.gov/pubmed/4573098.

Sinn, R., & Wittbrodt, J. (2013). An eye on eye development. Mechanisms of Development, 130(6–8), 347–358. https://doi.org/10.1016/j.mod.2013.05.001

Small, S., & Blair, A. (1992). Regulation of even-skipped stripe 2 in the Drosophila embryo. 1(1), 4047–4057. https://doi.org/10.1002/j.1460-2075.1992.tb05498.x

Smedley, D., Haider, S., Durinck, S., Pandini, L., Provero, P., Allen, J., … Kasprzyk, A. (2015). The BioMart community portal: An innovative alternative to large, centralized data repositories. Nucleic Acids Research, 43(W1), W589–W598. https://doi.org/10.1093/nar/gkv350

Solovei, I., Kreysing, M., & Lancto, C. (2009). Nuclear Architecture of Rod Photoreceptor Cells Adapts to Vision in Mammalian Evolution. 356–368. https://doi.org/10.1016/j.cell.2009.01.052

Song, W. K., Park, K. M., Kim, H. J., Lee, J. H., Choi, J., Chong, S. Y., … Lanza, R. (2015). Treatment of macular degeneration using embryonic stem cell-derived retinal pigment epithelium: Preliminary results in Asian patients. Stem Cell Reports, 4(5), 860–872. https://doi.org/10.1016/j.stemcr.2015.04.005

Sprague, J., Clements, D., Conlin, T., Edwards, P., Frazer, K., Schaper, K., … Westerfield, M. (2003). The Zebrafish Information Network (ZFIN): The zebrafish model organism database. Nucleic Acids Research, 31(1), 241–243. https://doi.org/10.1093/nar/gkg027

Steinfeld, J., Steinfeld, I., Bausch, A., Coronato, N., Hampel, M. L., Depner, H., … Vogel-Höpker, A. (2017). BMP-induced reprogramming of the neural retina into retinal pigment epithelium requires Wnt signalling. Biology Open, 6(7), 979–992. https://doi.org/10.1242/bio.018739

Steinfeld, J., Steinfeld, I., Coronato, N., Hampel, M. L., Layer, P. G., Araki, M., & Vogel-Höpker, A. (2013). RPE specification in the chick is mediated by surface ectoderm-derived BMP and Wnt signalling. Development (Cambridge), 140(24), 4959–4969. https://doi.org/10.1242/dev.096990

Steingrímsson, E., Copeland, N. G., & Jenkins, N. A. (2004). Melanocytes and the Microphthalmia Transcription Factor Network . Annual Review of Genetics, 38(1), 365–411. https://doi.org/10.1146/annurev.genet.38.072902.092717

Stossel, Thomas P. (1974). Phagocytosis. New England Journal of Medicine 290(13): 717–23. http://www.nejm.org/doi/abs/10.1056/NEJM197403282901306.

Strauss, O. (2005). The retinal pigment epithelium in visual function. Physiological Reviews, 85(3), 845–881. https://doi.org/10.1152/physrev.00021.2004

Suzuki, K. I. T., Isoyama, Y., Kashiwagi, K., Sakuma, T., Ochiai, H., Sakamoto, N., … Yamamoto, T. (2013). High efficiency TALENs enable F0 functional analysis by targeted gene disruption in Xenopus laevis embryos. Biology Open, 2(5), 448–452. https://doi.org/10.1242/bio.20133855

Sven, H., Christopher, B., Nathanael, S., Eric, B., Yin C., L., Laslo, P., … Glass, C. K. (2010). Simple combinations of lineage-determining transcription factors prime cis-regulatory elements required for macrophage and B cell identities. Molecular Cell, 38(4), 576–589. https://doi.org/10.1016/j.molcel.2010.05.004.Simple

Svensson, V., Natarajan, K. N., Ly, L., Miragaia, R. J., Labalette, C., Macaulay, I. C., … Teichmann, S. A. (2017). Power analysis of single-cell RNA-sequencing experiments. Nature Publishing Group, (March). https://doi.org/10.1038/nmeth.4220

Takahashi, K., & Yamanaka, S. (2006). Induction of Pluripotent Stem Cells from Mouse Embryonic and Adult Fibroblast Cultures by Defined Factors. Cell, 126(4), 663–676. https://doi.org/10.1016/j.cell.2006.07.024

Tarau, Ioana-Sandra, Andreas Berlin, Christine A Curcio, and Thomas Ach. (2019). The Cytoskeleton of the Retinal Pigment Epithelium: From Normal Aging to Age-Related Macular Degeneration. International journal of molecular sciences 20(14). http://www.ncbi.nlm.nih.gov/pubmed/31336621.

Tétreault, N., Champagne, M., & Bernier, G. (2009). The LIM homeobox transcription factor Lhx2 is required to specify the retina fi eld and synergistically cooperates with Pax6 for Six6 trans-activation. Developmental Biology, 327(2), 541–550. https://doi.org/10.1016/j.ydbio.2008.12.022

Thompson, D. A., Li, Y., McHenry, C. L., Carlson, T. J., Ding, X., Sieving, P. A., … Gal, A. (2001). Mutations in the gene encoding lecithin retinol acyltransferase are associated with early-onset severe retinal dystrophy. Nature Genetics, 28(2), 123–124. https://doi.org/10.1038/88828

Thurman, R. E., Rynes, E., Humbert, R., Vierstra, J., Maurano, M. T., Haugen, E., … Stamatoyannopoulos, J. A. (2012). The accessible chromatin landscape of the human genome. Nature, 489(7414), 75–82. https://doi.org/10.1038/nature11232

Tomasi di Lampedusa, Giuseppe. (1958). Il Gattopardo.

Totaro, A., Panciera, T., & Piccolo, S. (2019). YAP / TAZ upstream signals and downstream responses. 20(8), 888–899. https://doi.org/10.1038/s41556-018-0142-z.YAP/TAZ

Toy, J., Yang, J. M., Leppert, G. S., & Sundin, O. H. (1998). The Optx2 homeobox gene is expressed in early precursors of the eye and activates retina-specific genes. Proceedings of the National Academy of Sciences of the United States of America, 95(18), 10643–10648. https://doi.org/10.1073/pnas.95.18.10643

Trapnell, C., Cacchiarelli, D., Grimsby, J., Pokharel, P., Li, S., Morse, M., … Rinn, J. L. (2014). The dynamics and regulators of cell fate decisions are revealed by pseudotemporal ordering of single cells. Nature Biotechnology, 32(4), 381–386. https://doi.org/10.1038/nbt.2859

Trapnell, C., Roberts, A., Goff, L., Pertea, G., Kim, D., Kelley, D. R., … Patcher, L. (2013). DE analysis | RNA-SEQ With CuffLinks and TopHat. Nature Protocols, 7(3), 562–578. https://doi.org/10.1038/nprot.2012.016.Differential

Turner. (1987). A common progenitor for neurons and glia persists in rat retina late in development.

Turner, D., Snyder, E. Y., & Cepko, C. (1990). Lineage-Independent Determination in the Embryonic Mouse Retina of Cell Type. 4.

Turque, N., Denhez, F., Martin, P., Planque, N., Bailly, M., Bègue, A., … Saule, S. (1996). Characterization of a new melanocyte-specific gene (QNR-71) expressed in v-myc-transformed quail neuroretina. The EMBO Journal, 15(13), 3338–3350. https://doi.org/10.1002/j.1460-2075.1996.tb00699.x

Ueki, Y., Wilken, M. S., Cox, K. E., Chipman, L. B., Bermingham-mcdonogh, O., & Reh, T. A. (2015). A transient wave of BMP signaling in the retina is necessary for Mu¨ ller glial differentiation. 533–543. https://doi.org/10.1242/dev.118745

Ueno, K., Iwagawa, T., Kuribayashi, H., Baba, Y., Nakauchi, H., Murakami, A., … Watanabe, S. (2016). Transition of differential histone H3 methylation in photoreceptors and other retinal cells during retinal differentiation. Scientific Reports, 6(August 2015), 1–12. https://doi.org/10.1038/srep29264

Ueno, K., Iwagawa, T., Ochiai, G., Koso, H., Nakauchi, H., Nagasaki, M., … Watanabe, S. (2017). Analysis of Müller glia specific genes and their histone modification using Hes1-promoter driven EGFP expressing mouse. Scientific Reports, 7(1), 1–12. https://doi.org/10.1038/s41598-017-03874-8

Van Zeeburg, E. J. T., Maaijwee, K. J. M., Missotten, T. O. A. R., Heimann, H., & Van Meurs, J. C. (2012). A free retinal pigment epitheliumchoroid graft in patients with exudative age-related macular degeneration: Results up to 7 years. American Journal of Ophthalmology, 153(1), 120-127.e2. https://doi.org/10.1016/j.ajo.2011.06.007

Vejnar, C. E., Moreno-Mateos, M. A., Cifuentes, D., Bazzini, A. A., & Giraldez, A. J. (2016). Optimization strategies for the CRISPR-Cas9 genome-editing system. Cold Spring Harbor Protocols, 2016(10), 829–832. https://doi.org/10.1101/pdb.top090894

Viczian, A. S., Solessio, E. C., Lyou, Y., & Zuber, M. E. (2009). Generation of functional eyes from pluripotent cells. PLoS Biology, 7(8). https://doi.org/10.1371/journal.pbio.1000174

Vogel-Höpker, A., Momose, T., Rohrer, H., Yasuda, K., Ishihara, L., & Rapaport, D. H. (2000). Multiple functions of fibroblast growth factor-8 (FGF-8) in chick eye development. Mechanisms of Development, 94(1–2), 25–36. https://doi.org/10.1016/S0925-4773(00)00320-8

Voronina, V. A., Kozhemyakina, E. A., Kernick, C. M. O., Kahn, N. D., Wenger, S. L., Linberg, J. V, … Mathers, P. H. (2004). Mutations in the human RAX homeobox gene in a patient with anophthalmia and sclerocornea. 13(3), 315–322. https://doi.org/10.1093/hmg/ddh025

Wagner, G. P. (2007). The Developmental Genetics of Homology. Nature Genetics, 8(June), 473–479. https://doi.org/10.1002/9780470319390.ch13

Wallis, D. E., Roessler, E., Hehr, U., Nanni, L., Wiltshire, T., Richieri-Costa, A., … Muenke, M. (1999). Mutations in the homeodomain of the human SIX3 gene cause holoprosencephaly. Nature Genetics, 22(2), 196–198. https://doi.org/10.1038/9718

Wang, B., Yang, W., McKittrick, J., & Meyers, M. A. (2016). Keratin: Structure, mechanical properties, occurrence in biological organisms, and efforts at bioinspiration. Progress in Materials Science, 76, 229–318. https://doi.org/10.1016/j.pmatsci.2015.06.001

Wang, S., Sengel, C., Emerson, M. M., & Cepko, C. L. (2014). A Gene Regulatory Network Controls the Binary Fate Decision of Rod and Bipolar Cells in the Vertebrate Retina. Developmental Cell, 30(5), 513–527. https://doi.org/10.1016/j.devcel.2014.07.018

Wang, Ning, and Dimitrije Stamenović. (2000). Contribution of Intermediate Filaments to Cell Stiffness, Stiffening, and Growth. American Journal of Physiology-Cell Physiology 279(1): C188–94. https://www.physiology.org/doi/10.1152/ajpcell.2000.279.1.C188.

Wang, Z., Gerstein, M., & Snyder, M. (2009). RNA-Seq: a revolutionary tool for transcriptomics.

Watanabe, S., & Murakami, A. (2016). Regulation of Retinal Development via the Epigenetic Modification of Histone H3. Spinal Degenerative Disease, 635–641. https://doi.org/10.1016/c2013-0-06451-1

Wei, T., & Simko, V. (2017). R package “corrplot”: Visualization of a Correlation Matrix.

Weirauch, M. T., Yang, A., Albu, M., Cote, A. G., Montenegro-Montero, A., Drewe, P., … Hughes, T. R. (2014). Determination and inference of eukaryotic transcription factor sequence specificity. Cell, 158(6), 1431–1443. https://doi.org/10.1016/j.cell.2014.08.009

Weissmann, Gerald, Ira Goldstein, Sylvia Hoffstein, and Pi-Kwang Tsung. (1975). RECIPROCAL EFFECTS OF CAMP AND CGMP ON MICROTUBULE-DEPENDENT RELEASE OF LYSOSOMAL ENZYMES. Annals of the New York Academy of Sciences 253(1 The Biology o): 750–62. http://doi.wiley.com/10.1111/j.1749-6632.1975.tb19243.x.

West-Mays, J A et al. (1999). AP-2alpha Transcription Factor Is Required for Early Morphogenesis of the Lens Vesicle. Developmental biology 206(1): 46–62. http://www.ncbi.nlm.nih.gov/pubmed/9918694.

Westenskow, P., Piccolo, S., & Fuhrmann, S. (2009). β-catenin controls differentiation of the retinal pigment epithelium in the mouse optic cup by regulating Mitf and Otx2 expression. Development, 136(15), 2505–2510. https://doi.org/10.1242/dev.032136

Wijesena, N., Simmons, D. K., & Martindale, M. Q. (2017). Antagonistic BMP-cWNT signaling in the cnidarian Nematostella vectensis reveals insight into the evolution of mesoderm. Proceedings of the National Academy of Sciences of the United States of America, 114(28), E5608–E5615. https://doi.org/10.1073/pnas.1701607114

Wilson, S. W., & Houart, C. (2009). Early Steps in the Development of the Forebrain The Structure, Origins, and Morphogenesis of the Forebrain. 6(2), 167–181.

Wright, A. F., Chakarova, C. F., Abd El-Aziz, M. M., & Bhattacharya, S. S. (2010). Photoreceptor degeneration: Genetic and mechanistic dissection of a complex trait. Nature Reviews Genetics, 11(4), 273–284. https://doi.org/10.1038/nrg2717

Xie, Z., Chen, Y., Li, Z., Bai, G., Zhu, Y., Yan, R., … Jing, N. (2011). Smad6 promotes neuronal differentiation in the intermediate zone of the dorsal neural tube by inhibition of the Wnt/beta-catenin pathway. Proceedings of the National Academy of Sciences of the United States of America, 108(29), 12119–12124. https://doi.org/10.1073/pnas.1100160108

Yamada, K., & Miyamoto, K. (2005). BASIC HELIX-LOOP-HELIX TRANSCRIPTION FACTORS, BHLHB2 AND BHLHB3; THEIR GENE EXPRESSIONS ARE REGULATED BY MULTIPLE EXTRACELLULAR STIMULI. Frontiers in Bioscience, 3151–3171.

Yang, H. J., Ratnapriya, R., Cogliati, T., Kim, J. W., & Swaroop, A. (2015). Vision from next generation sequencing: Multi-dimensional genome-wide analysis for producing gene regulatory networks underlying retinal development, aging and disease. Progress in Retinal and Eye Research, 46, 1–30. https://doi.org/10.1016/j.preteyeres.2015.01.005

Yao, J., Wang, L., Chen, L., Zhang, S., Zhao, Q., Jia, W., & Xue, J. (2006). Cloning and developmental expression of the DEC1 ortholog gene in zebrafish. 6, 919–927. https://doi.org/10.1016/j.modgep.2006.03.006

Yin, J., Morrissey, M. E., Shine, L., Kennedy, C., Higgins, D. G., & Kennedy, B. N. (2014). Genes and signaling networks regulated during zebrafish optic vesicle morphogenesis.

Yoshida, S., Yashar, B. M., Hiriyanna, S., & Swaroop, A. (2002). Microarray Analysis of Gene Expression in the Aging Human Retina AND. 43(8), 2554–2560.

Young, R. W., & Bok, D. (1969). Participation of the retinal pigment epithelium in the rod outer segment renewal process. The Journal of Cell Biology, 42(2), 392–403. https://doi.org/10.1083/jcb.42.2.392

Yu, J., Farjo, R., MacNee, S. P., Baehr, W., Stambolian, D. E., & Swaroop, A. (2003). Annotation and analysis of 10,000 expressed sequence tags from developing mouse eye and adult retina. Genome Biol, 4(10), R65. Retrieved from http://www.ncbi.nlm.nih.gov/entrez/query.fcgi?cmd=Retrieve&db=PubMed&dopt=Citation&list_uids=14519200

Yu, B., Mitchell, G. A., & Richter, A. (2009). Cirhin up-regulates a canonical NF-kappaB element through strong interaction with Cirip/HIVEP1. Experimental Cell Research, 315(18), 3086–3098. https://doi.org/10.1016/j.yexcr.2009.08.017

Yu, W., Mookherjee, S., Chaitankar, V., Hiriyanna, S., Kim, J. W., Brooks, M., … Wu, Z. (2017). Nrl knockdown by AAV-delivered CRISPR/Cas9 prevents retinal degeneration in mice. Nature Communications, 8, 1–15. https://doi.org/10.1038/ncomms14716

Yu, G., Wang, L.-G., & He, Q.-Y. (2015). ChIPseeker: an R/Bioconductor package for ChIP peak annotation, comparison and visualization. Bioinformatics (Oxford, England), 31(14), 2382–2383. https://doi.org/10.1093/bioinformatics/btv145

Yvon, C., Ramsden, C. M., Lane, A., Powner, M. B., Da Cruz, L., Coffey, P. J., & Carr, A. J. F. (2015). Using Stem Cells to Model Diseases of the Outer Retina. Computational and Structural Biotechnology Journal, 13, 382–389. https://doi.org/10.1016/j.csbj.2015.05.001

Zelinger, L., & Swaroop, A. (2019). RNA Biology in Retinal Development and Disease. 34(5), 341–351. https://doi.org/10.1016/j.tig.2018.01.002.RNA

Zhang, L., Mathers, P. H., & Jamrich, M. (2000). Function of Rx, but not Pax6, is essential for the formation of retinal progenitor cells in mice. Genesis, 28(3–4), 135–142. https://doi.org/10.1002/1526-968X(200011/12)28:3/4<135::AID-GENE70>3.0.CO;2-P

Zhang, Y., Liu, T., Meyer, C. A., Eeckhoute, J., Johnson, D. S., Bernstein, B. E., … Shirley, X. S. (2008). Model-based analysis of ChIP-Seq (MACS). Genome Biology, 9(9). https://doi.org/10.1186/gb-2008-9-9-r137

Zhang, Haiying, H Amalia Pasolli, and Elaine Fuchs. (2011). Yes-Associated Protein (YAP) Transcriptional Coactivator Functions in Balancing Growth and Differentiation in Skin. Proceedings of the National Academy of Sciences of the United States of America 108(6): 2270–75. http://www.ncbi.nlm.nih.gov/pubmed/21262812.

Zhang, Wenjing et al. (2014). VGLL4 Functions as a New Tumor Suppressor in Lung Cancer by Negatively Regulating the YAP-TEAD Transcriptional Complex. Cell research 24(3): 331–43. http://www.ncbi.nlm.nih.gov/pubmed/24458094.

Zhao, S., Hung, F. C., Colvin, J. S., White, A., Dai, W., Lovicu, F. J., … Overbeek, P. A. (2001). Patterning the optic neuroepithelium by FGF signaling and Ras activation. Development, 128(24), 5051–5060.

Zhong, X., Gutierrez, C., Xue, T., Hampton, C., Natalia, M., Cao, L., … Cell, S. (2015). Generation of three dimensional retinal tissue with functional photoreceptors from human iPSCs. 1–31. https://doi.org/10.1038/ncomms5047.Generation

Zibetti, C., Liu, S., Wan, J., Qian, J., & Blackshaw, S. (2019). Epigenomic profiling of retinal progenitors reveals LHX2 is required for developmental regulation of open chromatin. Communications Biology, 2(1), 142. https://doi.org/10.1038/s42003-019-0375-9

Zou, C., & Levine, E. M. (2012). Vsx2 Controls Eye Organogenesis and Retinal Progenitor Identity Via Homeodomain and Non-Homeodomain Residues Required for High Affinity DNA Binding. PLoS Genetics, 8(9). https://doi.org/10.1371/journal.pgen.1002924

Zuber, M. E., Gestri, G., Viczian, A. S., Barsacchi, G., & Harris, W. A. (2003). Specification of the vertebrate eye by a network of eye field transcription factors. 5155–5167. https://doi.org/10.1242/dev.00723

Zuber, M. E., Perron, M., Philpott, A., Bang, A., & Harris, W. A. (1999). Giant eyes in Xenopus laevis by overexpression of XOptx2. Cell, 98(3), 341–352. https://doi.org/10.1016/S0092-8674(00)81963-7